SUPPORTING INFORMATION

Table of Contents

List of Figures Cited in Main Text....2
List of Figures Cited Only Here....3
Table S1. Alphanumeric list of lunar meteorites from Africa and some of their properties (2019 December 31)....4
Key and Abbreviations....24
Plot Symbols....25
Table S2 References....27
Table S2. INAA data for subsamples, weighted means with 95% confidence limits, analytical uncertainties, sources of samples, and miscellaneous sample data.....29
Table S3a. Results of INAA: Mass-weighted mean concentrations of stones....30
Table S3b. Results of INAA: Mass-weighted mean concentrations of clans....37
Table S4. Results of EPMA of fused beads: Major-element data....39
Table S5. Mean composition of typical feldspathic lunar meteorites....45
Table S6. Results of regression analysis of Ni, Ir, and Au against Co for some metal-rich meteorites....47
Table S7. Estimated number of lunar meteorites and launch craters....48
Figures Cited in Main Text....64
Figures Cited Only Here....148
INAA Procedures and Uncertainties....168
Procedures....168
NWA 5000 Sawdust and INAA Uncertainty and Error....168
Table S8. Results of INAA for NWA 5000 sawdust....171
Systematic Error with Time....174
Light Rare Earth Element Variability in NWA 5000 Sawdust....178
References....179

List of Figures Cited in Main Text

S1 Photos of 12 INAA samples, as received ... 64
S2 Photos of INAA subsampling ... 65
S3 Stone mean (a) and launch-crater (b) data for Th vs. FeO_T ... 66
S4 Stone mean data for Cr/Sc vs. Sc ... 68
S5 Stone mean data for Na_2O vs. Sc ... 69
S6 Stone mean data for Na/Eu vs. Sc ... 70
S7 Stone mean data for La/Sm and Lu/Sm vs Sc ... 71
S8 Chondrite-normalized REE in typical feldspathic meteorites ... 73
S9 Chondrite-normalized REE in atypical feldspathic meteorites ... 76
S10 Chondrite-normalized REE in Apollo-16-like feldspathic meteorites ... 78
S11 Chondrite-normalized REE in troctolitic meteorites ... 79
S12 Chondrite-normalized REE in anorthositic-noritic meteorites ... 80
S13 Chondrite-normalized REE in mafic meteorites (basaltic breccias) ... 83
S14 Chondrite-normalized REE in mare basaltic meteorites ... 84
S15 Stone mean data for Sm/Th vs. Sc and Sm ... 86
S16 Stone mean data for Eu vs. Sc ... 87
S17 Subsample data for Sm vs. Sc in typical feldspathic meteorites ... 88
S18 Subsample data for Cr/Sc, La/Sm, and Lu/Sm vs. Sc in typical feldspathic meteorites ... 90
S19 Subsample data for Sm/Th, Na_2O, and Na/Eu in typical feldspathic meteorites ... 91
S20 Subsample data for Co, Ni, and Ni/Co in typical feldspathic meteorites ... 92
S21 Subsample data for Sr, Ba, and Ba/Sr in typical feldspathic meteorites ... 93
S22 Comparison of subsample data for the DaG 262 and DaG 400 clans, and similar ... 94
S23 Subsample data for the NWA 8222 clan ... 95
S24 Subsample data for 22 stones of the large NWA 8046 clan ... 96
S25 Subsample data for atypical feldspathic lunar meteorites ... 98
S26 Subsample data for the NWA 8641 clan ... 100
S27 Photo of a large sawn slab of NWA 5000 ... 102
S28 Photo of large metal grains in NWA 5000 ... 102
S29 Subsample data for NWA 5000 and comparison to NWA 8641 ... 103
S30 Subsample data for of anorthositic troctolite NWA 5744 ... 104
S31 Stone mean data for SiO_2 vs. Al_2O_3 ... 106
S32 Stone mean data for TiO_2 vs. Sc ... 107
S33 Subsample data for paired stones NWA 4472 and NWA 4485 ... 108
S34 Subsample data for NWA 7022 and comparison to MIL 090036 ... 109
S35 Stone-mean data for meteorites similar in composition to Apollo 16 soil ... 110
S36 Stone-mean data for Ni vs. Ir ... 112
S37 Subsample data for Sc and Ir in the NWA 4936 clan and comparison to Apollo 16 soil ... 113
S38 Subsample data for Sm-rich NWA 6687 ... 114
S39 Subsample data for meteorites rich in incompatible elements ... 115
S40 Subsample and REE data for NEA 003 ... 116
S41 Subsample data for basaltic breccias with low Sm ... 117
S42 Subsample data for launch pairs NWA 4884, NWA 7611 clan, DEW 12007, QUE 94281, and Y-793274/981031 ... 118
S43 Stone mean data for Eu/Sm vs. Sc ... 120
S44 Stone mean data for FeO/Sc vs. Sc ... 121
S45 Subsample data for the NWA 3163 clan and stone mean for meteorites of similar composition ... 122
S46 Subsample data for "anorthositic-noritic and basalt-bearing feldspathic" meteorites at the high end of the Sm concentration range ... 123
S47 Subsample data for the 11 stones of the NWA 2995 clan ... 125

S48 Comparison of stone-mean data for the NWA 2995, NWA 7611, and NWA 7834 clans..... 127
S49 Subsample data for the 25 stones of the NWA 7834 clan 129
S50 Subsample data for the 13 stones of the NWA 8673 clan 130
S51 Stone mean data for Cr/Sc vs. TiO_2 in mare basalts and gabbros..... 131
S52 Subsample data for mare basalts..... 132
S53 Subsample data of 16 stones of the NWA 773 clan..... 133
S54 Subsample data for Ni, Ir, and Au vs. Co in metal-rich NWA 5000 and NWA 8673..... 134
S55 Estimated CM-chondrite normalized Ni/Co, Ir/Co, and Au/Co ratios in metal in metal-rich meteorites..... 136
S56 Subsample data for Au vs. Ir 137
S57 Photo of a large slice of NEA 001 138
S58 Stone-mean data for K_2O and P_2O_5..... 139
S59 Comparison of U vs. Th data in typical feldspathic meteorites (stone-means) and DaG 262 (subsamples) 139
S60 Subsample data for La/Sm vs. U in the DaG 262 clan 141
S61 Stone-mean data for As and Br vs. Sc 142
S62 Subsample data for 4 pieces of NWA 8701..... 143
S63 Magnitude of Ce anomalies in NWA lunar meteorites having significant anomalies..... 144
S64 Stone-mean data for Eu vs. Na_2O in Kalahari 008 and Kalahari 009 and comparison to other meteorites..... 145
S65 Subsample data Sc and Co vs. FeO in Kalahari 008 and Kalahari 009 145
S66 Subsample data for Lynch 002 and Calcalong Creek..... 146

List of Figures Cited Only Here

S67 Stone mean data for Ba vs. Sc and Ba index definition..... 148
S68 Subsample data for paired stones NWA 2998 and NWA 7262 and comparison to DaG 400 clan .. 149
S69 Subsample data for meteorites of Fig. S35 (Apollo-16-like)..... 151
S70 Comparison of subsample data for NEA 001 to stone means of other meteorites of similar composition..... 152
S71 Subsample data for low-Sc, low-Sm anorthositic norites..... 153
S72 Subsample data for 4 different pieces of NWA 10495 155
S73 Subsample data for paired stones NWA 10509 and NWA 10798..... 157
S74 Comparison of the NWA 10141 clan to NWA 11077, with photos 159
S75 Meteorites at the high-Sm end of the range of typical feldspathic lunar meteorites..... 161
S76 Subsample data for 4 different pieces of NWA 7493..... 162
S77 Subsample data for 5 different pieces of NWA 10309..... 163
S78 Comparison of subsample data for NWA 4932 and SaU 300 (Oman)..... 164
S79 Comparison of subsample data for Dhofar 1428 (Oman) and MAC 88104/5 (Antarctica) 165
S80 Subsample data for Dho1436/1443, MIL 07006, and PCA 02007 with comparison to stone means of the NWA 10509 and 10626 clans 166
S81 Correlation of Eu and Na for 27 samples of NWA 5000 sawdust..... 169
S82 Correlation of Sc with Eu and Na for 27 samples of NWA 5000 sawdust..... 170
S83 INAA data vs. irradiation number for 27 samples of NWA 5000 sawdust 175
S84 Data for Sm vs. La and Ce in 27 samples of NWA 5000 sawdust 178

Table S1. Alphanumeric list of lunar meteorites from Africa and some of their properties (2019 December 31)

Plot	Stone Name	Mass (g)	Pcs.	**Terrestrially,** or possibly launch paired with:	FeO %	Sc µg/g	Sm µg/g	SEI	BaI	UI	*N*	Petrographic and compositional features from MetBull and [peer-reviewed references]
C	Anoual	5.92	5	773 & pairs	21.	42	4.8	0	1		3 98	**P:** FrBr; LiCl: Bas & OlGab; We **C:** low Na & Eu (Fig. S53)
}	Aridal 017	590.	1	**10608?** (found nearby)	5.1	8	2.2	5	3	6	3 3	**P:** PoBr, fg; LiCl: none; $Fo_{73\text{-}90}$; FeNi **C:** high Cr/Sc (Fig. S4), apparent troctolitic precursor
2	Dar al Gani 262	513.	1	**DaG 996, 1042, & 1048**	4.4	8	1.0	7	3	3	2 19	**P:** RgBr, fg; LiCl: An, IMBr, GlSph, FeNi; ShM, We [B01,C01,K01] **C:** typFLM (Figs. S17–S21); high U/Th, high La/Sm (Figs. S22, S59, & S60), moderately high Br (Fig. S61)
4	Dar al Gani 400	1425.	1	**DaG 1058**	3.1	6	0.7	5	3	7	17 23	**P:** RgBr; LiCl: An, IMBr, GrBr, Nor, Sph; ShM, We [C01,J02,K01,W01] **C:** feldspathic extreme of typFLM (Figs. S17–S21 & S68), mod high Na/Eu (Fig. S6), high U/Th and P/Th (Fig. S59 and S58)
2	Dar al Gani 996	12.31	1	**262 & pairs**	4.3	8	1.2	6	4		9 19	**P:** RgBr, fg; LiCl: IMBr; ShM, Sn; Ves, We **C:** typFLM; like Dag 262 (Fig. S22), moderately high Br (Fig. S61); high P/Th (Fig. S58)
2	Dar al Gani 1042	801.	1	**262 & pairs**	4.3	8	1.1	7	4		8 19	**P:** RgBr; LiCl: An, IMBr, GrBr; Sph, ShM, We **C:** typFLM; like Dag 262 (Fig. S22)
2	Dar al Gani 1048	0.801	1	**262 & pairs**	n.a.	n.a.	n.a.	n.a.	n.a.		0 19	**P:** IMBr; LiCl: Gab, Ba, Sph, Ves, Me **C:** no INAA data
4	Dar al Gani 1058	1815.	1	**400**	3.0	5	0.6	5	6		6 23	**P:** RgBr, fg; LiCl: An; We **C:** typFLM; like DaG 400 but higher La/Sm (S22), much higher U/Th (Fig. S59), moderately high Br (Fig. S61)
n.a.	Errachidia	156.	1	?	feld	n.a.	n.a.	n.a.	n.a.	n.a.	n.a.	**P:** RgBr, fg; LiCl: An, Me; GlSph **C:** no INAA data
®	Galb Inal	4050.	2	**7834 & pairs**	9.9	21	3.5	7	3		8 133	**P:** RgBr; LiCl: An, Tro, Nor, Me; ShM, GlSph **C:** like NWA 10149 (Fig. S49)
8	Kalahari 008	598.	1	**Kalahari 009**	4.7	11	0.7	4	1	6	9 17	**P:** RgBr; LiCl: IMBr, GrBr [S02] **C:** high Na (Fig. S5), v high Na/Eu (Fig. S6), high Eu/Sm (Figs. S43 & S64), high Lu/Sm (Fig. S7), high SiO_2 (Fig. S31); high K/Th and P/Th (Fig. S58)
9	Kalahari 009	13,500.	1	**Kalahari 008**	16.4	53	0.6	1	1	7	8 17	**P:** monomict FrBr; LiCl: Bas; Mask; [S02]; nonmare Bas? [W02] **C:** low Ca/Al (Fig. 18), low Ti/Sc (Fig. S32), v low ITEs (Fig. 6); v high Lu/Sm (S7), high Na (Fig. S5) & v high Na/Eu (Figs. S6 & S64), high SiO_2 (Fig. S31); high K/Th and P/Th (Fig. S58)
±	La'gad	337.74	3	**NWA 8455 & pairs**	7.1	12	8.7	8	6		5 76	**P:** PoBr; LiCl: none; We **C:** Most similar to 8455 clan but most mafic (Sc: 1.15×) and richest in ITEs (1.15×) (Figs. S35 & S69), moderately high Br (Fig. S61)
Ñ	La'gad 003	27,249.	many	**10509 & pairs**	5.7	12	1.0	5	9		19 41	**P:** PoBr, fg; LiCl: rare Bas, Gl; We **C:** like NWA 10509 but 7 different pieces vary considerably (Fig. S73); allegedly found near NWA 10509, all have high Ba
n.a.	Lahmada 020	12,168.	sev	**046? 047?**	feld	n.a.	n.a.	n.a.	n.a.	n.a.	n.a.	**P:** PoBr; LiCl: none; ves **C:** no INAA data
n.a.	Lahmada 046	71.24	1	**020? 047?**	feld	n.a.	n.a.	n.a.	n.a.	n.a.	n.a.	**P:** PoBr; LiCl: none; Ves, FeNi **C:** no INAA data

Plot	Stone Name	Mass (g)	Pcs.	**Terrestrially,** or possibly launch paired with:		FeO %	Sc µg/g	Sm µg/g	SEI	BaI	UI	*N*	Petrographic and compositional features from MetBull and [peer-reviewed references]
n.a.	Lahmada 047	182.	many	**020? 046**		feld	n.a.	n.a.	n.a.	n.a.	n.a.	n.a.	**P:** PoBr; LiCl: none; Ves, FeNi **C:** no INAA data
1	NEA 001	262.	1	**unique**		5.3	11	0.8	4	3	7	26 26	**P:** RgBr; LiCl: An, IMBr, Bas, Gab; Gl, Sph; We (photo: Fig. S1a) [S01] **C:** heterogeneous (Figs. **7** & S70), high Lu/Sm (Fig. S7), INAA data for 6-mg sample of calcite-gypsum is richer in U (0.65 µg/g) than whole rock (0.17 µg/g; photo: Fig. S57)
3	NEA 003	124.	2	**unique**	basalt	20.6	47	1.6	0	4	7	7 12	**P:** large MBas clast [H01,H02]; Mask **C:** 1.7% TiO_2 (Fig. S51), low ITEs (Figs. 6 & S52), v high Lu/Sm (Fig. S7)
3					breccia	24.9	53	3.7	1	2	9	5 12	**P:** PoBr with large MBas clast [H01,H02]; LiCl: Bas **C:** 1.8% TiO_2; more mafic than the basalt, and not otherwise compositionally similar (Figs. S51 & S40), high Lu/Sm (Fig. S7), low Na (Fig. S5)
A	NWA 032	300.	1	**479**; LaPaz Icefield basalts		22.1	56	6.6	0	2	3	12 18	**P:** MBas, olivine phyric [F02] **C:** 3.0% TiO_2, similar to some A12 & A15 low-Ti basalts (Fig. S51) and NWA 4734 (Fig. S52)
A	NWA 479	156.	1	**032**		22.4	57	6.6	0	3		6 18	**P:** MBas, olivine phyric **C:** indistinguishable from NWA 032 (Fig. S52)
B	NWA 482	1015.	1	**unique**		3.8	7	0.8	6	0	4	13 13	**P:** IMBr; LiCl: An, Tro; ShM, FeNi [D01,K01,W01] **C:** typFLM (Figs. S17–S21); low La/Sm (Fig. S7), high Na/Eu (Fig. S6)
C	NWA 773	633.	3	Anoual, 2700, 2727, 2977, 3160, 3170, 3333, 6950, 7007, 8127, 10656, 10985, 11616, 11703, & 11767		19.0	30	5.3	0	1	8	10 98	**P:** FrBr; LiCl (many large): Bas & Gab; Ves, We [F01,J01,V01,Z02] **C:** low Na & Eu (Figs. S51, S52, & S53) [V01]
C	773 pair	*(?)*	?	773 & pairs		18.6	24	3.7	0	0		2 98	**P:** OlGab **C:** like NWA 773, 2977, 3333, 6950, & 8127 OlGab (Fig. S53)
D	NWA 2200	552.	1	**unique**		3.9	7	1.1	6	1	3	10 10	**P:** PoBr, fg; LiCl: An, Bas **C:** typFLM (Figs. S17–S21)
n.a.	NWA 2402	500.	1	**7611 pair?**		12.	n.a.	n.a.	n.a.	n.a.	n.a.	n.a.	**P:** PoBr, LiCl: Bas **C:** No INAA data; 18% Al_2O_3 [P. Warren, MetBull]
n.a.	NWA 2420	395	1	?		~4	n.a.	0.9	n.a.	n.a.	n.a.	n.a.	**P:** PoBr, fg; LiCl: IM spheroids **C:** No INAA data; 31% Al_2O_3 [P. Warren, MetBull]
n.a.	NWA 2425	810.	1	**8046 & pairs?**		~6	n.a.	n.a.	n.a.	n.a.	n.a.	n.a.	**P:** PoBr, fg: LiCl: none; Sph **C:** No INAA data; 27.1% Al_2O_3 [P. Warren, MetBull]
C	NWA 2700	31.7	1	773 & pairs		19.4	37	5.3	0	1		1 98	**P:** RgBr; LiCl: Bas & OlGab; Mask, Sph, We **C:** Fig. S53
C	NWA 2727	191.2	4	773 & pairs		19.7	35	5.2	0	1		15 98	**P:** PoBr; LiCl: Bas & OlGab; Mask, ShM, We [V01] **C:** Fig. S53
C	NWA 2977	233.	1	773 & pairs		18.6	26	3.1	0	0		6 98	**P:** OlGab; Mask, ShM **C:** Fig. S53

Plot	Stone Name	Mass (g)	Pcs.	**Terrestrially,** or possibly launch paired with:	FeO %	Sc µg/g	Sm µg/g	SEI	BaI	UI	*N*	Petrographic and compositional features from MetBull and [peer-reviewed references]
E	NWA 2995	538.	1	**2996, 3190, 4503, 5151, 5152, 6252, 6554, & 6555**	9.8	19	4.7	6	1	7	8 71	**P:** PoBr; LiCl: An, Nor, Tro, Bas, Gab, Gl, GrBr, KP; ShM, FeNi [M01] **C:** Heterogeneous; subchondritic Ir/Ni (Fig. S36b); overlaps with 7834 clan but has less terrestrial Ba and slightly (1.1×) greater Na & Eu, on average (Figs. S46 & S47); mod. high K/Th and P/Th (Fig. S58) [K03]
E	2995 pair	*(691.)*	?	**2995 & pairs**	11.7	22	4.6	5	2		6 71	**P:** none **C:** like NWA 2995 (Fig. S47)
E	2995 pair	*(168.)*	?	**2995 & pairs**	10.8	22	4.0	6	1		6 71	**P:** none **C:** like NWA 2995 (Fig. S47)
E	NWA 2996	968.	1	**2995 & pairs**	9.7	18	4.6	6	2		8 71	**P:** RgBr; LiCl: An, Nor, Tro, Gab, Gl; Ves (photo: Fig. S1i) [M01] **C:** like NWA 2995 (Fig. S47); mod. high K/Th and P/Th (Fig. S58)
F	NWA 2998	163.	1	**7262?**	2.7	5	0.4	4	0	6	8 15	**P:** FrBr, fg; LiCl: An, Nor, Tro; ShM, Mask (photo: Fig. S1a) **C:** feldspathic extreme of typFLM (Figs. S17–S21 & S68); high Eu/Sm (Fig. S43)
G	NWA 3136	95.1	1	**unique**	15.4	47	3.9	6	5	4	8 8	**P:** RgBr, fg; LiCl: Bas, An, GlBr, Ves **C:** one of the most basaltic of breccias: 15% FeO, 1.2% TiO_2 (Figs. 6, 10, & S41), moderately high As (Fig. S61)
C	NWA 3160	34.	3	773 & pairs	20.9	40	6.9	0	0		16 98	**P:** FrBr; LiCl: Bas [V01] **C:** Fig. S53
H	NWA 3163	1634.	1	**4483, 4881, 6275**	5.8	13	0.5	3	0	6	10 32	**P:** GrBr, poikiloblastic recrystallized breccia; LiCl: none; Mask **C:** ferroan, low Sm/Sc (Fig. 6), high Eu/Sm (Fig. S43), low La/Sm & high Lu/Sm (Fig. S7), low SE (0.2 ng/g Ir, Fig. 12), low TiO_2, (0.2%), high Sm/Th (Figs. S15 & S45)
C	NWA 3170	60.	1	773 & pairs	20.7	40	11.2	0	0		3 98	**P:** PoBr; LiCl: Bas; ShM **C:** Fig. S53 [V01]
E	NWA 3190	40.7	1	**2995 & pairs**	9.2	18	3.8	6	2		8 71	**P:** PoBr; LiCl: An, Nor, Gab, Bas **C:** like NWA 2995 (Fig. S47)
C	NWA 3333	33.	1	773 & pairs	20.9	33	4.5	0	0		15 98	**P:** FrBr; LiCl: Bas & OlGab; ShM **C:** Fig. S53
I	NWA 4472	64.3	1	**4485**	9.2	21	19.5	5	3	5	9 23	**P:** RgBr; LiCl: IMBr, Bas, SpTro, KpBas, Granite, Alkali An, GrBr; Sph, Gl, FeNi [J03] **C:** KREEP-bearing (Fig. 6), MBas-bearing with high Ti/Sc (Fig. S32), low Sm/Th (Fig. S15), 2 REE-rich subsamples (Fig. S33), high Br (Fig. S61)
H	NWA 4483	208.	12	**3163 & pairs**	5.0	11	0.5	3	1		10 32	**P:** GrBr, fg; LiCl: none; Mask, FeNi **C:** like NWA 3163 (Fig. S45)
I	NWA 4485	188.	1	**4472**	9.5	21	13.8	8	2		14 23	**P:** RgBr; LiCl: Bas; Sph **C:** like NWA 4472, light clast contains FeNi grain (Fig. S33)
E	NWA 4503	70.	1	**2995 & pairs**	9.4	18	5.2	6	1		6 71	**P:** PoBr; LiCl: An, KP; ShM, Ves **C:** like NWA 2995 (Fig. S47), high Sb
J	NWA 4734	1372.	2	**10597**; 032 & 479; LAP	21.8	60	7.4	0	0	5	12 14	**P:** MBas, olivine phyric; Mask [C04,E01,W03,Z01] **C:** 2.8% TiO_2 (Fig. S51), similar to some A12 & A15 low-Ti basalts and NWA 032 (Fig. S52)
N	NWA 4819	234.	1	**unique**	7.0	13	3.4	7	2	4	9 9	**P:** RgBr, fg; LiCl: An, ShM, Sph **C:** high Cr/Sc (Figs. S4, S71), moderately high Br (Fig. S61)
H	NWA 4881	606.	1	**3163 & pairs**	6.0	15	0.5	4	2		9 32	**P:** GrBr, poikiloblastic recrystallized breccia; LiCl: none; Mask, FeNi **C:** most mafic of the 3163 clan (Fig. S45)

Plot	Stone Name	Mass (g)	Pcs.	**Terrestrially,** or possibly launch paired with:	FeO %	Sc µg/g	Sm µg/g	SEI	BaI	UI	*N*	Petrographic and compositional features from MetBull and [peer-reviewed references]
L	NWA 4884	42.	1	7611 & pairs; DEW 12007, EET 87/96, QUE 94281, Y-79/98	13.7	30	3.1	5	0	4	9 9	**P:** GlBr: LiCl: Bas, An, Tro; Ves; Bas Br with some An **C:** compare with 2995 & 7834 clans (Fig. S51), less Ba than 7611 clan but probably launch paired (Figs. S42 & S41); 0.6% TiO_2
M	NWA 4898	137.	1	**unique**	17.2	65	4.6	0	0	2	6 6	**P:** MBas; Mask **C:** 2.5% TiO_2, high-alumina (12.4% Al_2O_3); "depleted" light REE (Figs. S14d & S7; lowest Fe/Sc of meteorites studied here (Fig. S44); v high Sm/Th (Fig 13)
K	NWA 4932	93.3	1	**unique;** not SaU 300 [K03]	8.6	20	1.2	8	5	3	8 8	**P:** PoBr, fg; LiCl: Gab, Tro; FeNi (photo: Fig. S1b) **C:** low Sm/Sc, low Na, low Sm/Th, high SEs (Fig. S71); like 8673 clan but lower La/Sm, much higher Lu/Sm (Fig. S7), moderately high Br (Fig. S61)
O	NWA 4936	179.	2	**5406, 6221, 6355, 6470, 6570, 7190, 7986, & 8181**	5.9	9	6.1	8	0	6	10 54	**P:** GlBr, fg; LiCl: sparse, Bas, Tro; FeNi **C:** like A16 regolith but higher Na & Eu (Figs. S35 & S69); 0.7% TiO_2 (Fig. S32); high SEs (Fig. 12)
P	NWA 5000	11,528.	1	8641 & pairs?	5.8	10	1.5	8	3	8	20 20	**P:** FrBr; LiCl: Gab, IMBr, GlBr; FeNi (photos: Figs. S33 & S28) **C:** low Ir/Ni (Fig. S54); may be related to NWA 8641 (Figs. S26 & S29)
E	NWA 5151	289.	1	**2995 & pairs**	8.5	17	4.8	6	2		6 71	**P:** FrBr; LiCl: An, Tro, Bas, Gb, IMBr; ShM, FeNi **C:** feldspathic extreme of NWA 2995 clan (Fig. S47); high La/Sm (Fig. S7) and Ce/Ce* (Fig. S60)
E	NWA 5152	38.	1	**2995 & pairs**	9.0	17	3.9	7	2		6 71	**P:** PoBr; LiCl: An, GrBr, Bas; Ves **C: f**eldspathic extreme of NWA 2995 clan 2995 (Fig. S47)
Q	NWA 5153	50.4	1	**unique (2995 & pairs?)**	12.7	26	4.6	5	0	6	6 6	**P:** FrBr; LiCl: An, Bas, Gab **C:** like NWA 2995 clan but higher Sc (Fig. S46)
R	NWA 5207	101.	1	**unique (2995 & pairs?)**	7.6	16	3.9	7	1	6	8 8	**P:** FrBr; LiCl: An, Bas, Gab, IMBr, Gl **C:** like NWA 2995 clan but lower Sc & low Cr/Sc (Fig. S46)
O	NWA 5406	281.	6	**4936 & pairs**	5.8	9	6.3	8	0		6 54	**P:** GlBr, fg; LiCl: sparse, Bas, Tro; FeNi **C:** like NWA 4936 (Figs. S35 & S69)
S	NWA 5744	170.	1	**8599, 8687, 10140, 10178, 10318, 10401, 11252, & 12997**	6.0	9	0.4	4	2	6	8 47	**P:** GrBr, AnTro (Fig. 8); LiCl: none; Fo_{79} olivine. **C:** high *Mg'* (80; Fig. 5), high Cr/Sc (Fig. S3), low IEs (Fig. 6), high Lu/Sm (Fig. S7), low TiO_2/Sc (Fig. S36)
S	5744 pair	*(745.)*	?	**5744 & pairs**	6.3	10	0.5	4	3		2 47	**P:** none **C:** like 5744 (Fig. S30)
S	5744 pair	*(1052.)*	?	**5744 & pairs**	5.9	9	0.4	3	4		5 47	**P:** none **C:** like 5744 (Fig. S30), slight positive Ce anomaly (Fig. S63)
S	5744 pair	*(?)*	?	**5744 & pairs**	5.7	8	0.4	4	2		4 47	**P:** none **C:** like 5744 (Fig. S30)
O	NWA 6221	109.4	1	**4936 & pairs**	6.6	10	5.7	8	2		6 54	**P:** GlBr, fg; LiCl: sparse lithic **C:** like NWA 4936 (Figs. S35 & S69)
E	NWA 6252	113.	1	**2995 & pairs**	12.9	27	3.9	8	2		3 71	**P:** PoBr; LiCl: An, Nor, Gab, Bas, Tro, GrBr, KP **C:** mafic extreme of NWA 2995 clan (Fig. S47); high La/Sm and Ce/Ce* (Fig. S63)
H	NWA 6275	1.3	5	**3163 & pairs**	3.4	7	0.4	1	0		3 32	**P:** GrBr; LiCl: none; Mask, FeNi; (photo: Fig. S1j) **C:** most feldspathic stone of the NWA 3163 clan (Fig. S45); small sample, likely rich in a feldspathic clast
O	NWA 6355	760.	1	**4936 & pairs**	5.8	10	6.1	8	0		6 54	**P:** GlBr, fg; LiCl: sparse lithic, GabNor; FeNi, Ves **C:** like NWA 4936 (Figs. S35 & S69)

Plot	Stone Name	Mass (g)	Pcs.	**Terrestrially,** or possibly launch paired with:	FeO %	Sc µg/g	Sm µg/g	SEI	BaI	UI	*N*	Petrographic and compositional features from MetBull and [peer-reviewed references]
O	NWA 6470	96.	1	**4936 & pairs**	5.6	10	5.0	8	2		6 54	**P:** GlBr, fg; LiCl: sparse lithic, GabNor; FeNi; Ves **C:** like NWA 4936 (Figs. S35 & S69)
T	NWA 6481	13.7	1	**unique**	4.7	9	1.6	6	4	5	8 8	**P:** FrBr, fg; LiCl: sparse; Gl (photo: Fig. S1e) **C:** high Na compared to typFLM (Fig. S25), high Eu/Sm (Fig. S43)
E	NWA 6554	138.	1	**2995 & pairs**	11.3	20	4.1	7	1		7 71	**P:** PoBr; LiCl: An, Nor, Gab, Bas, Tro, GrBr, KP **C:** like NWA 2995 (Fig. S47); greater SE & Cr/Sc than other NWA 2995 pairs (Fig. S47)
E	NWA 6555	29.72	1	**2995 & pairs**	12.3	26	3.8	9	1		7 71	**P:** PoBr; LiCl: An, Nor, Gab, Bas, Tro, GrBr, KP, IMBr **C:** mafic extreme of NWA 2995 clan, low Cr/Sc (Fig. S47)
O	NWA 6570	415.	1	**4936 & pairs**	5.8	9	6.6	8	0		4 54	**P:** GlBr, fg; LiCl: sparse lithic, An; FeNi, Ves **C:** like NWA 4936 (Figs. S35 & S69)
U	NWA 6578	1638.	1	**unique**	4.2	8	1.1	5	1	1	8 8	**P:** PoBr, fg; LiCl: sparse; ShM, FeNi **C:** typFLM; low *Mg´* (62.5, Table S4); much like NWA 7493 but far less scatter (Figs. S17–S21, S74, & S79)
V,v	NWA 6687	42.4	2	**unique**	16.3	38	17.5	4	5	4	8 8	**P:** PoBr: LiCl: sparse; Ves (photo: Fig. S1d) **C:** Unique. Highest IEs among lunar meteorites from northern Africa (19 µg/g Sm, Fig. 6). Norm (wt%, NWA 6678c of Table S4): 35% plagioclase, 2.5% orthoclase, 15% diopside, 33% hypersthene, 6.5 % olivine, 7.5 % ilmenite, 1.0% apatite, 0.13% zircon, and 0.35% chromite. Compositionally, a mixture of KREEP & mare basalt, similar to Apollo 12 soils (Figs. S38b, S39). High terrestrial Ca (Fig. S38a), v low (sub KREEP) Na/Eu (Fig. S6), highest TiO_2 among lunar meteorites (3.8% TiO_2, Fig. S32), low SiO_2 (Fig. S31), moderately high As and Br (Fig. S61)
W	NWA 6721	181.	12	**unique**	5.0	10	1.5	6	6	4	11 11	**P:** FrBr, fg; LiCl: “ophitic textured;” FeNi **C:** high Na (terrestrial) compared to typFLM (Fig. S5); v high Na/Eu (Fig. S6), largest positive Ce anomaly (Ce/Ce* = 1.23, Fig. S63), moderately high Br (Fig. S61)
n.a.	NWA 6831	20.	1	?	feld	n.a.	n.a.	n.a.	n.a.	n.a.	n.a.	**P:** FrBr: LiCl: IMBr, Bas; Ves **C:** No INAA data
X	NWA 6888	208.	1	**unique**	5.7	13	2.1	5	9	5	8 8	**P:** RgBr, fg; LiCl: IMBr, GrBr, An, Gab, GabNor, Tro, Bas; Sph, FeNi **C:** Distinct from others of similar composition in Sc-Sm space (Fig. S71a), high Na & Na/Eu (Figs. S5 & S6); high K/Th and P/Th (Fig. S58)
C	NWA 6950	1649.	1	773 & pairs	19.4	25	3.4	0	2		6 98	**P:** OlGab; ShM **C:** like NWA 2977 (Fig. S53)
C	NWA 7007	91.	1	773 & pairs	19.2	39	7.4	0	2		6 98	**P:** PoBr: LiCl: Bas & OlGab; Ves **C:** like NWA 773 (Fig. S53), moderately high Br (Fig. S61) [V01]

Plot	Stone Name	Mass (g)	Pcs.	**Terrestrially,** or possibly launch paired with:		FeO %	Sc µg/g	Sm µg/g	SEI	BaI	UI	*N*	Petrographic and compositional features from MetBull and [peer-reviewed references]
Y	NWA 7022	444.	1	MIL 090036? (Fig. S34)	matrix	5.3	10	5.6	7	0	6	5 11	**P:** FrBr; LiCl: one large IMBr clast (4 cm, ⅓ of stone; MetBull); Plag: $An_{91–95}$. **C:** like 4936 clan (Figs. S35a–d & S69), including high TiO_2/Sc (Fig. S32), but distinctly lower Cr/Sc ("Y" point at (10,65) on Fig. S4), high Na (Fig. S5), lower SEs and more nearly chondritic Ir/Ni (Fig. S35e,f)
					clast	6.3	14	9.2	6	0	3	6 11	**P:** IMBr clast **C:** clast is more mafic than the breccia (Fig. S34) with higher IEs (Fig. S69), v low Cr/Sc (Figs. S4 & S34c); highest Na_2O (0.74%) of NWA meteorites (Fig. S5)
O	NWA 7190	5.28	3	**4936 & pairs**		6.0	9	6.4	8	1		4 54	**P:** GlBr, fg; LiCl: sparse, GabNor; FeNi **C:** like NWA 4936 (Figs. S35 & S69)
f	NWA 7262	413.	5	**2998?**		3.1	6	0.6	4	0	5	7 15	**P:** FrBr, fg; LiCl: An; FeNi **C:** typFLM; like NWA 2998 but more mafic (Fig. S68)
Z	NWA 7274	372.6	1	**unique**		6.1	12	4.8	8	5	4	9 9	**P:** FrBr, fg; LiCl: none; FeNi **C:** high Sm/Sc, moderately high SEs (Fig. S46), low Na/Eu and Eu/Sm compared to otherwise similar anorthositic norites (Figs. S6 & S43), moderately high Br (Fig. S61)
[	NWA 7493	503.	6	**unique**		4.4	8	0.9	5	2	8	24 24	**P:** FrBr; LiCl: IMBr; ShM, FeNi (photo: Fig. S1e) **C:** typFLM most like NWA 8046, NWA 8222, & Sueilila 005 but much greater scatter (Figs. S17–S21 & S76), low Cr/Sc vs. 8046 (Fig. S18a), low Ni (Fig. S20b) & lower Ni/Co than NWA 8222 (Fig. S20c)
L	NWA 7611	916.	1	**2402?, 8277, 10480, & 10566;** 4884, DEW 12007, EET 87/96, QUE 94281, Y-79/98		12.1	27	3.1	6	3	5	11 31	**P:** RgBr; LiCl: Gab **C:** basaltic breccia with some anorthosite; compare with 2995 & 7834 clans (Fig. S51); greater Ba than NWA 4811 but probably launch paired (Figs. S42 & S41); 0.6% TiO_2
L	7611 pair	*(332.)*	?	**7611 & pairs**		15.4	33	3.1	5	1		3 31	**P:** none **C:** like NWA 7611 (Fig. S42)
®	NWA 7834	905.	1	**Galb Inal, 7948, 8306, 10149, 10172, 10203, 10253, 10258, 10263, 10272, 10291, 10317, 10376, 10546, 10599, 10644, 10782, 10810, 10989, 11109, 11185, 11249, & 11563**		10.1	20	3.7	6	4	9	12 133	**P:** GlBr; LiCl: Bas; FeNi **C:** Basalt bearing; 0.6% TiO_2, like 2995 clan but lower Sc & Na, higher Ba (Figs. S46 & S49), high Cr/Sc (Fig. S4), subchondritic Ir/Ni (Fig. S36)
®	7834 pair	*(?)*	1	**7834 & pairs**		10.4	20	4.1	6	5		3 133	**P:** none **C:** like NWA 7834 (Fig. S49)
#	NWA 7931	5.92	1	**unique**		7.5	18	1.9	7	3	1	6 6	**P:** PoBr; LiCl: none; FeNi **C:** 4:1 mix of typFLM & low-Ti basalt; higher Eu/Sm, lower Cr/Sc, and higher Sm/Th than otherwise similar NWA 8673 clan (Figs. S43 & S71)
®	NWA 7948	59.8	1	**7834 & pairs**		9.6	18	3.2	6	3		7 133	**P:** PoBr, fg; LiCl: some; VesShM, FeNi **C:** like NWA 7834 (Fig. S49)
©	NWA 7959	156.	1	**unique**		3.3	5	1.2	7	7	4	8 8	**P:** PoBr; LiCl: none; FeNi **C:** typFLM; mod high *Mg´* (72; Table S4), low SiO_2 (Fig. S31); moderately high Br (Fig. S61), high terrestrial Ba (Figs. S17–S21)

Plot	Stone Name	Mass (g)	Pcs.	**Terrestrially,** or possibly launch paired with:	FeO %	Sc µg/g	Sm µg/g	SEI	BaI	UI	*N*	Petrographic and compositional features from MetBull and [peer-reviewed references]
O	NWA 7986	12.2	1	**4936 & pairs**	5.7	9	6.2	8	1		4 54	**P:** GlBr, fg; LiCl: sparse, An; FeNi **C:** like NWA 4936 (Figs. S35 & S69)
@	NWA 8001	23.4	1	**unique**	4.7	9	3.5	7	5	4	8 8	**P:** RgBr: LiCl: Bas; Sph **C:** atypFLM; moderately high IEs (Fig. S25)
/	NWA 8010	58.	1	**unique**	5.8	11	6.4	7	6	6	7 13	**P:** GlBr; LiCl: An, Gab; VesShM, Sph **C:** like A16 regolith; most like NWA 8455 clan (Fig. S35) but lower Na & Eu (Figs. S5 & S16), even lower Ir/Ni than Apollo 16 (Figs. S35 & S36), high Ti/Sc (Fig. S32); high As & Br (Fig. S61,; high K/Th and P/Th (Fig. S58)
$	NWA 8022	1226.	1	**10082**	3.7	5	1.1	8	1	4	7 10	**P:** FrBr, v fg; LiCl: none; FeNi **C:** atypFLM; one of the most unusual compositions: high Sm/Sc (Fig. 6), high Na & Eu (Figs. S5, S16, & S25b), high Eu/Sm (Fig. S43), high SEs (Fig. 12), high La/Sm & Lu/Sm (Fig. S7,S9f), low Sm/Th (Figs. S15 & S25)
%	NWA 8046	47.3	1	**8046, 10309, 10461, 10609, 10643, 10649, 10756, 10822, 10901, 11029, 11266, 11269, 11273, 11303, 11379, 11428, 11460, 11479, 11515, 12691, 12760, & possibly-to-probably 2425, 11331, 11407, 11421, 11444, 11517, 11532, 11695, 11787, 11789, 11898, 11966, 11968, 12630, 12695, 12765 , & 12966**	4.5	8	0.7	7	4	5	6 86	**P:** FrBr, fg; LiCl: none; FeNi **C:** typFLM; high Cr/Sc, low Na & Na/Eu (Figs. S17–S21), some subsamples contain mare basalt (Fig. S24)
%	8046 pair	*(?)*	?	**8046 & pairs**	4.4	8	0.7	5	5		3 86	**P:** none **C:** typFLM; like NWA 8046 (Fig. S24)
%	8046 pair	*(?)*	?	**8046 & pairs**	4.8	8	0.9	6	4		2 86	**P:** none **C:** typFLM; like NWA 8046 (Fig. S24)
%	8046 pair	*(?)*	?	**8046 & pairs**	5.3	9	0.9	6	0		5 86	**P:** none **C:** typFLM; like other NWA 8046 clan but higher Sc, Cr, Fe, Co, IEs, Sm/Eu, low Ba (Fig. S24)
&	NWA 8055	98.	1	**unique**	6.4	16	1.0	5	6	5	8 8	**P:** FrBr, fg; LiCl: Bas; FeNi **C:** low *Mg'* (58, Fig. 10), low Sm/Sc, low Cr/Sc (Fig. S4), high Sm/Th (Fig. S15), low Ni (Fig. S71), low La/Sm & high Lu/Sm (Fig. S7), high Eu/Sm (Fig. S43), high As (Fig. S61)
C	NWA 8127	529.	1	773 & pairs	18.2	29	2.6	0	0		3 98	**P:** OlGab; ShM, Mask **C:** like 773 OlGab (Fig. S53)
O	NWA 8181	18.2	1	**4936 & pairs**	6.7	10	7.7	8	1		4 54	**P:** GlBr, fg; LiCl: sparse, An; FeNi, Ves **C:** like NWA 4936 (Figs. S35 & S69)

Plot	Stone Name	Mass (g)	Pcs.	**Terrestrially,** or possibly launch paired with:	FeO %	Sc µg/g	Sm µg/g	SEI	BaI	UI	*N*	Petrographic and compositional features from MetBull and [peer-reviewed references]
½	NWA 8182	15.6	1	**unique**	10.6	20	7.1	6	0	7	6 6	**P:** PoBr; LiCl: none; VesShM **C:** most like 2995 clan but higher IEs & Na (Fig. S46), MBas-bearing with high Ti/Sc (Fig. S32); low Ba
£	NWA 8222	208.6	1	**10823, 11212, 11237, Rabt Sbayta 002, 004, 005?, 006?**	3.4	7	0.6	5	4	5	8 37	**P:** FrBr, fg; LiCl: none; Ves **C:** typFLM; large Sc variation, low Sm, high Lu/Sm, high Sm/Th, low Cr/Sc, low SEs (Figs. S4, S17–S21, & S23), some subsamples have high U/Th (Fig. S59)
£	8222 pair	*(35.)*	?	**8222 & pairs**	3.6	7	0.7	5	4		5 37	**P:** none **C:** like NWA 8222 (Fig. S23)
£	8222 pair	*(600.)*	?	**8222 & pairs**	3.5	7	0.9	4	4		3 37	**P:** none **C:** like NWA 8222; highest IEs (1.2–1.6×) (Fig. S23)
L	NWA 8277	773.	1	**7611 & pairs**	14.5	32	3.1	5	3		10 31	**P:** FrBr; basaltic breccia with some anorthosite; LiCl: none **C:** like NWA 7611 (Fig. S42)
®	NWA 8306	1389.	1	**7834 & pairs**	8.9	17	3.3	6	5		8 133	**P:** PoBr; LiCl: Bas; FeNi **C:** like NWA 7834 (Fig. S49)
±	NWA 8455	2814.	1	**8607?, 8609, 8651, 8668, 8727, 8783, 10130, 10228, 10621, 10953, La'gad;** Dho 1627 & 1980	6.0	10	7.4	8	6	5	7 76	**P:** FrBr; LiCl: Gab, ShM; FeNi **C:** like A16 regolith but higher Na (Fig. S35); like NWA 4936 clan but higher Sm/Eu & much higher Ba (Fig. S69), high SEs (Fig. 12) with subchondritic Ir/Ni (Figs. 15 & S36)
±	8455 pair	*(117.)*	?	**8455 & pairs**	5.9	10	7.1	8	5		3 76	**P:** none **C:** like NWA 8455 (Figs. S35 & S69)
±	8455 pair	*(598.)*	?	**8455 & pairs**	6.8	11	7	8	4		3 76	**P:** none **C:** like NWA 8455 (Figs. S35 & S69)
±	8455 pair	*(192.)*	?	**8455 & pairs**	6.0	10	6.2	8	4		3 76	**P:** none **C:** like NWA 8455 but lowest IEs of clan (Figs. S35 & S69)
¼	NWA 8586	704.5	1	**unique**	4.0	8	1.2	4	1	8	8 8	**P:** FrBr; LiCl: An, Bas; FeNi **C:** typFLM but highly variable Sc, Fe, & IEs, low Sm/Th, low Ni (Figs. S17–S21), high HREE (Fig. S8k,S7), moderately high U/Th (S59)
S	NWA 8599	36.5	1	**5744 & pairs**	5.4	7	0.4	5	4		6 47	**P:** GrBr, troctolitic; LiCl: An; Fo_{77} olivine. **C:** like NWA 5744 (Fig. S30)
n.a.	NWA 8607	261.	1	**8455 & pairs?**	n.a.	n.a.	n.a.	n.a.	n.a.	n.a.	n.a.	**P:** PoBr; LiCl: OlGabNor, OlGabAn; ShM **C:** no INAA data; ShM: 24±5% Al_2O_3, 7±3% FeO, 7±2% MgO [C. Agee & N. Muttik in MetBull]
±	NWA 8609	45.	1	**8455 & pairs**	6.0	10	9.0	8	6		8 76	**P:** FrBr; LiCl: An, IMBr, Gab; FeNi **C:** like NWA 8455; highest IEs & Na of clan (Figs. S35 & S69)
§	NWA 8632	23.8	1	**unique**	22.8	51	4.7	0	6	4	5 5	**P:** MBas, porphyritic **C:** 2.5% TiO_2 (Figs. S51 & S52); most similar to NWA 032/479
¿	NWA 8641	5895.	1	**8682, 10049, 10077, 10133;** 5000?	5.0	11	2.6	6	4	7	8 45	**P:** PoBr; LiCl: An; FeNi **C:** atypFLM; moderately rich in IEs, high Na, low Cr/Sc (Figs. S25 & S26)
¿	8641 pair	*(140.)*	?	**8641 & pairs**	5.1	10	2.9	7	6		4 45	**P:** none **C:** like NWA 8641 (Fig. S26)

Plot	Stone Name	Mass (g)	Pcs.	**Terrestrially,** or possibly launch paired with:	FeO %	Sc µg/g	Sm µg/g	SEI	BaI	UI	*N*	Petrographic and compositional features from MetBull and [peer-reviewed references]
±	NWA 8651	598.	1	**8455 & pairs**	6.1	10	7.7	8	4		4 76	**P:** PoBr; LiCl: none; stone is dominated by one large GrBr or IMBr clast **C:** like NWA 8455 (Figs. S35 & S69)
±	NWA 8668	166.3	1	**8455 & pairs**	5.6	9	6.6	8	4		7 76	**P:** PoBr; LiCl: none; FeNi **C:** like NWA 8455 (Figs. S35 & S69)
{	NWA 8673	263.	1	**8733, 8746, 10048, 10065, 10123, 10902, 10964, 11110, 11193, 11216, 11228, 11788;** Dho 925 & SaU 449	7.3	16	1.8	9	6	6	8 65	**P:** FrBr, fg; Bas; FeNi **C:** compared to otherwise similar NWA 2995 clan & NWA 7834 clan, lower IEs, Na, Eu, Sm/Th, & higher SEs (Fig. S46), lower Fe_T/Sc (Fig. S44), higher SEs (Figs. 12 & S46f), moderately high As (Fig. S61); Dhofar connection: see Fig. S50
{	8673 pair	*(?)*	?	**8673 & pairs**	7.2	16	2.4	9	8		3 65	**P:** none **C:** like NWA 8673 (Fig. S50); highest Sr (1.8×) & Ba (5.2×)
¿	NWA 8682	82	sev	**8641 & pairs**	4.9	9	2.5	6	6		12 45	**P:** PoBr; LiCl: Bas; Ves, FeNi **C:** like NWA 8641 (Fig. S26)
S	NWA 8687	562.5	5	**5744 & pairs**	6.4	8	0.3	5	3		4 47	**P:** MoBr, AnTro; LiCl: none; Fo_{78} olivine, VesShM (photo: Fig. S1f) **C:** like NWA 5744 (Fig. S30); one Cr-rich subsample (9800 µg/g, spinel), v high U, high REE, Ce/Ce* = 1.19 (Fig. S63)
\	NWA 8701	72.	1	**unique**	6.5	18	4.6	5	2	9	12 20	**P:** FrBr; LiCl: none; FeNi **C:** v low Cr/Sc, Fe/Sc, v low Sm/Th (Figs. S4 & S46), high La/Sm & Lu/Sm (Fig. S7), high Na/Eu (Fig.S6), high As, and As correlates with Sc & Sm (R^2 = 0.91 & 0.88); sample A is more mafic and anomalously high in As, Rb, & Cs (Figs. S61 & S62)
\	8701 pair	*(?)*	?	**8701**	6.6	19	3.6	5	2		8 20	**P:** none **C:** like NWA 8701 (Fig. S62)
±	NWA 8727	2436.3	1	**8455 & pairs**	6.4	11	8.3	9	3		6 76	**P:** MoBr "olivine leuco-gabbro" (C. Agee in MetBull); ShM, FeNi **C:** like NWA 8455 but low-end of Na range (Figs. S35 & S69)
{	NWA 8733	51.	6	**8673 & pairs**	8.3	18	2.5	9	4		8 65	**P:** PoBr; LiCl: An, Bas; FeNi **C:** like NWA 8673 (Fig. S50)
{	NWA 8746	69.9	1	**8673 & pairs**	8.2	18	2.5	9	4		7 65	**P:** FrBr, fg; LiCl: Bas, Gl; FeNi **C:** like NWA 8673 (Fig. S50)
)	NWA 8753	1345.	1	**unique**	3.1	5	0.9	4	1	5	11 11	**P:** FrBr; LiCl: none; Gl, FeNi **C:** typFLM; high Sm/Sc, Cr/Sc; v low Ba (Figs. S17–S21), moderately high Br (Fig. S61)
±	NWA 8783	27.5	24	**8455 & pairs**	5.9	10	7.4	9	5		10 76	**P:** PoBr; LiCl: Bas; VesShM, FeNi **C:** like NWA 8455 (Figs. S35 & S69)
{	NWA 10048	352.3	61	**8673 & pairs**	8.0	18	2.3	9	5		8 65	**P:** PoBr, fg; LiCl: none; VesShM **C:** like NWA 8673 (Fig. S50)
¿	NWA 10049	56.	1	**8641 & pairs**	5.1	10	2.9	6	6		8 45	**P:** RgBr; LiCl: IMBr, Gab, agglutinates; ShM, FeNi, We **C:** like NWA 8641 (Fig. S26)
{	NWA 10065	282.8	1	**8673 & pairs**	7.9	18	2.3	9	6		4 65	**P:** RgBr, fg; LiCl: Sph; Ves, FeNi **C:** like NWA 8673 (Fig. S50)

Plot	Stone Name	Mass (g)	Pcs.	**Terrestrially,** or possibly launch paired with:	FeO %	Sc µg/g	Sm µg/g	SEI	BaI	UI	*N*	Petrographic and compositional features from MetBull and [peer-reviewed references]
b	NWA 10073	64.	1	**unique**	3.7	7	1.4	6	0	4	6 9	**P:** FrBr; LiCl: none; ShM, FeNi (photo: Fig. S1k) **C:** typFLM; high Na and low Ba (Fig. S74), largest negative Ce anomaly (Ce/Ce*: 0.66, Fig. S63), high U/Th (S59), high Sb
b	10073 pair	249.	?	**10073**	3.9	8	1.5	6	3		3 9	**P:** PoBr; LiCl: none; ShM, FeNi **C:** typFLM; like NWA 10073 (Fig. S74)
¿	NWA 10077	5.27	1	**8641 & pairs**	5.2	10	2.7	7	6		4 45	**P:** PoBr; LiCl: none; Ves **C:** like NWA 8641
$	NWA 10082	5.20	3	**8022**	3.5	5	1.2	8	3		7 10	**P:** GrBr; LiCl: none; FeNi **C:** atypFLM; identical to NWA 8022
{	NWA 10123	149.5	1	**8673 & pairs?**	7.0	15	1.2	9	6		7 65	**P:** FrBr, fg; LiCl: none; FeNi **C:** like NWA 8673 (Fig. S50) but lowest Sc & IEs
±	NWA 10130	191	1	**8455 & pairs**	6.7	10	7.4	8	5		6 76	**P:** PoBr; LiCl: Bas; ShM **C:** like NWA 8455 but high Na like NWA 8609 & high SEs (Figs. S35 & S69)
¿	NWA 10133	54.2	many	**8641 & pairs**	5.6	11	3.9	7	6		9 45	**P:** PoBr; LiCl: Bas rare; Ves, FeNi, We **C:** like NWA 8641; 3 pieces analyzed, one richer in Sc than other 2 (Fig. S26)
S	NWA 10140	68.	1	**5744 & pairs**	5.1	6	0.3	4	1		1 47	**P:** GrBr, AnTro; LiCl: none; Fo_{77} olivine, VesShM. **C:** like NWA 5744 (Fig. S30)
=	NWA 10141	39.	1	**10142?, 10415, 11111; 11077?**	3.9	7	1.2	6	5	4	6 19	**P:** PoBr; LiCl: none; VesShM; An_{97}; in photographs, up to 5-mm spherical and ovoid clasts (Fig. S75) **C:** typFLM; low Na, low Lu/Sm (Figs. S17–S21, S74, & S79)
n.a.	NWA 10142	102.	1	**10141 & pairs?**	feld	n.a.	n.a.	n.a.	n.a.	n.a.	n.a.	**P:** PoBr; LiCl: none; VesShM **C:** no INAA data; ShM: 32±2% Al_2O_3, 3.0±1.3% FeO, 3.3±1.7% MgO consistent with that of 101410 [C. Agee & N. Muttik in MetBull]
®	NWA 10149	1815.	1	**7834 & pairs**	9.6	21	3.6	7	5	6	5 133	**P:** FrBr, fg; LiCl: none; Gl **C:** low Fe/Sc, Cr/Sc, Co/Sc range of clan (Fig. S49)
®	NWA 10172	788.	sev	**7834 & pairs**	11.1	25	3.5	6	5		5 133	**P:** FrBr, fg; LiCl: none; Me, ShM **C:** like NWA 10149 (Fig. S49)
S	NWA 10178	1279.3	3	**5744 & pairs**	4.3	7	0.3	3	3		6 47	**P:** GrBr, AnTro; LiCl: none; Fo_{77} olivine, VesShM, Mask **C:** like NWA 5744 (Fig. S30); 2 plagioclase-rich subsamples
®	NWA 10203	3300.	27	**7834 & pairs**	7.8	16	4.0	7	5		6 133	**P:** FrBr; LiCl: OlGab, AnGab, Gab; VesShM, FeNi **C:** like NWA 10149 (Fig. S49)
±	NWA 10228	19.4	1	**8455 & pairs**	6.4	10	7.6	8	5		6 76	**P:** IMBr, fg; LiCl: none but like NWA 8651 the stone is dominated by one large GrBr or IMBr clast **C:** like NWA 8455 (Figs. S35 & S69)
®	NWA 10253	6674.1	sev	**7834 & pairs**	9.9	19	3.7	6	3		6 16	**P:** FrBr; LiCl: Gab, mafic; ShM; We **C:** like NWA 7834 (Fig. S49)
®	NWA 10258	58.	1	**7834 & pairs**	8.6	17	4.1	7	4		10 16	**P:** PoBr, fg; LiCl: An; VesShM **C:** like NWA 7834 (Fig. S49)
®	NWA 10263	1015.	2	**7834 & pairs**	11.8	23	3.8	6	5		6 133	**P:** FrBr, fg; LiCl: none; FeNi **C:** like NWA 7834 (Fig. S49)

Plot	Stone Name	Mass (g)	Pcs.	**Terrestrially,** or possibly launch paired with:	FeO %	Sc µg/g	Sm µg/g	SEI	BaI	UI	*N*	Petrographic and compositional features from MetBull and [peer-reviewed references]
®	NWA 10272	74.25	1	**7834 & pairs**	11.9	25	4.0	6	3		6 133	**P:** FrBr, fg; LiCl none **C:** like NWA 10149 (Fig. S49)
®	NWA 10291	10.01	3	**7834 & pairs**	10.4	25	4.7	6	4		5 133	**P:** FrBr, fg; LiCl: rare Bas; Ves (photo: Fig. S1l) **C:** like NWA 10149 (Fig. S49)
%	NWA 10309	16,518.	sev	**8046 & pairs**	5.0	9	0.7	6	4		14 81	**P:** PoBr, fg; LiCl: none; FeNi **C:** typFLM; like NWA 8046 (Fig. S24), some subsamples contain mare basalt (Figs. S24 & S77)
®	NWA 10317	11.	1	**7834 & pairs**	10.5	19	3.4	6	3		4 133	**P:** PoBr, fg; LiCl: An, IMBr GrBr **C:** like NWA 7834 (Fig. S49)
S	NWA 10318	31.0	1	**5744 & pairs?**	6.3	10	0.6	4	3		4 47	**P:** MoBr, olivine-bearing AnNor; LiCl: none; Fo_{74} olivine, Mask **C:** like NWA 5744 (Fig. S30) but highest Sc (consistent with noritic mineralogy), Ce/Ce*: 0.89 (Fig. S63)
®	NWA 10376	20.	1	**7834 & pairs**	10.3	19	3.2	6	6		4 133	**P:** PoBr, fg; LiCl: Bas, Gab **C:** like NWA 7834 (Fig. S49)
S	NWA 10401	354.	2	**5744 & pairs**	5.9	8	0.4	4	2		6 47	**P:** GrBr, AnTro; LiCl: none; Fo_{81} olivine **C:** like NWA 5744 (Fig. S30)
h	NWA 10404	229.	1	**unique**	3.7	7	1.8	6	0	7	6 6	**P:** RgBr; LiCl: An, Gl **C:** atypFLM; on average slightly higher IEs than typFLM; 3.5× range in Sm at nearly constant Sc (Fig. S25)
=	NWA 10415	164.	3	**10141**	4.1	8	1.2	6	8		7 10	**P:** FrBr; LiCl: none; VesShM; in photographs, up to 5-mm spherical and ovoid clasts (Fig. S75) **C:** typFLM; like NWA 10141 (Figs. S17–S21, S74, & S79)
µ	NWA 10447	21.73	1	**unique**	15.2	30	2.6	5	5	4	5 5	**P:** FrBr, fg; LiCl: none **C:** like NWA 7611 clan but lower Sm, Na, & Eu, higher Cr/Sc & Co (Fig. S16 & S41)
%	NWA 10461	285.75	2	**8046 & pairs**	4.5	8	0.7	4	4		2 81	**P:** PoBr; LiCl: Gab; ShM **C:** typFLM; like NWA 8046 (Fig. S24)
L	NWA 10480	33.	1	**7611 & pairs**	13.8	31	3.0	5	3		3 31	**P:** PoBr, fg; LiCl: Gab, Bas, IMBr; ShM (photo: Fig. S1g) **C:** like NWA 7611 (Fig. S42)
f	NWA 10495	15,600.	sev	**Sueilila 005?**	5.4	14	0.9	3	8	8	15 21	**P:** FrBr; LiCl: An **C:** heterogeneous (Fig. S72), low Cr/Sc, high Sm/Th, low Ni, v high Ba (Fig. S71), low Fe/Sc (Fig. S44), low La/Sm & high Lu/Sm (Fig. S7), high Eu/Sm (Fig. S43), low Ni/Co, high As (Fig. S61)
Ñ	NWA 10509	660.	1	**10798, 10986, & La′gad 003;** 10626?	5.5	12	1.5	5	9	6	6 41	**P:** PoBr, fg; LiCl: none **C:** low Sm/Sc (Fig. 6), v high Ba (Figs. S71, S73e)
Ñ	10509 pair?	499.	?	**10509 & pairs**	7.4	18	1.2	4	7		5 41	**P:** none **C:** like NWA 10509; (Fig. S73); allegedly found near NWA 10509; all have high Ba
Ñ	10509 pair?	1051.	?	**10509 & pairs?**	5.7	13	1.3	5	9		5 41	**P:** none **C:** like NWA 10509 but higher Sc, lower Na_2O & Cr/Sc (Fig. S73), Ce/Ce* = 1.19; allegedly found near NWA 10509; all have high Ba

Plot	Stone Name	Mass (g)	Pcs.	**Terrestrially,** or possibly launch paired with:	FeO %	Sc µg/g	Sm µg/g	SEI	BaI	UI	*N*	Petrographic and compositional features from MetBull and [peer-reviewed references]
®	NWA 10546	43.35	1	**7834 & pairs**	10.1	20	3.5	6	5		3 133	**P:** FrBr, fg; LiCl: none; Ves **C:** like NWA 7834 (Fig. S49)
L	NWA 10566	130.	1	**7611 & pairs**	13.9	30	3.2	6	4		4 31	**P:** FrBr; LiCl: Gl **C:** like NWA 7611 (Fig. S42)
J	NWA 10597	350.	1	**4734**	22.5	58	7.0	0	0		2 14	**P:** MBas [C04,E01,W03,Z01] **C:** indistinguishable from NWA 4734 (Fig. S52)
®	NWA 10599	77.8	1	**7834 & pairs**	12.2	22	3.4	7	5		4 133	**P:** FrBr; LiCl: some; ShM, Ves **C:** like NWA 7834 (Fig. S49)
n.a.	NWA 10608	2014.	1	**Aridal 017?**	feld	n.a.	n.a.	n.a.	n.a.	n.a.	n.a.	**P:** FrBr; LiCl: some, IMBr **C:** no INAA data; found nearby Aridal 017
%	NWA 10609	43.02	1	**8046 & pairs**	4.6	9	0.7	6	5		6 81	**P:** FrBr; LiCl: some, IMBr; Ves **C:** typFLM; like NWA 8046, among lowest La/Sm of NWA 8046 clan (Fig. S24)
±	NWA 10621	22.	2	**8455 & pairs**	6.7	10	7.2	8	5		2 76	**P:** PoBr, fg; LiCl: none; FeNi **C:** like NWA 8455 (Figs. S35 & S69)
¢	NWA 10626	1849.	1	**unique;** 10509?	5.9	13	1.0	6	1	4	6 8	**P:** FrBr; LiCl: An, Bas; Ves **C:** like NWA 10509 but less scatter and much lower As & Ba (Figs. S71, S80)
¢	10626 pair	*(515.)*	?	10626	5.6	12	1.0	4	5		2 8	**P:** none **C:** like NWA 10626
%	NWA 10643	43.56	1	**8046 & pairs**	4.9	8	0.8	5	5		2 81	**P:** PoBr; LiCl: An; VesShM **C:** typFLM; like NWA 8046 (Fig. S24)
®	NWA 10644	166.	1	**7834 & pairs**	9.6	18	3.8	7	5		6 133	**P:** FrBr, fg; LiCl: none; VesShM **C:** like NWA 7834 (Fig. S49)
%	NWA 10649	41.3	1	**8046 & pairs**	4.5	8	0.6	5	4		4 73	**P:** FrBr, fg; LiCl: some **C:** typFLM; like NWA 8046 (Fig. S24)
C	NWA 10656	262.5	1	773 & pairs	19.7	34	5.9	0	0		1 98	**P:** Diab **C:** see Fig. S53 [V01]
Ø	NWA 10665	24.73	1	**unique**	3.7	6	1.1	7	3	3	6 6	**P:** PoBr, fg; LiCl: none; Gl, FeNi **C:** typFLM; like NWA 7959 but less Ba, higher Lu/Sm, lower Cr/Sc, less subsample scatter (Figs. S17–S21), high Zn (35 µg/g)
Ç	NWA 10678	49.15	1	**unique**	3.8	7	2.4	6	7	5	6 6	**P:** PoBr, fg, LiCl: An; FeNi **C:** distinct Sm/Sc & Cr/Sc (Fig. S25)
Ç	10678 pair	*(515.)*	?	10678	4.0	8	1.5	5	4	8	4 4	**P:** none **C:** like NWA 10678
n.a.	NWA 10713	60.2	1	?	feld	n.a.	n.a.	n.a.	n.a.	n.a.	n.a.	**P:** GrBr, fg: LiCl: none **C:** no INAA data
%	NWA 10756	125.	1	**8046 & pairs**	4.4	7	0.7	6	4		4 81	**P:** PoBr, fg; LiCl: Gab, Gl; Ves **C:** typFLM; like NWA 8046 (Fig. S24)
®	NWA 10782	39.	1	**7834 & pairs**	10.2	23	4.3	6	5		2 133	**P:** RgBr, fg; LiCl: IMBr, An; Ves, FeNi **C:** like NWA 10149 (Fig. S49)

Plot	Stone Name	Mass (g)	Pcs.	**Terrestrially,** or possibly launch paired with:		FeO %	Sc µg/g	Sm µg/g	SEI	BaI	UI	*N*	Petrographic and compositional features from MetBull and [peer-reviewed references]
¶	NWA 10783	22.	1	**unique;** 8641?		5.9	11	3.4	9	4	4	6 6	**P:** PoBr dominated (>95%) by large IMBr clast **C:** most like NWA 8641 clan (Fig. S25) but significantly greater FeO (1.15×), As (2.0×), Br (1.8×; Fig. S61), and Sm/Th (1.1×), Ni/Co (1.2×); lower Cr/Sc (0.9×) and Ba (0.3×). Ni and Ir are ~2× greater in NWA 10783
Ñ	NWA 10798	318.6	many	**10509 & pairs**		5.6	12	0.9	5	7		6 41	**P:** PoBr, fg; LiCl: GabAn, rare Bas, Ves, We **C:** like NWA 10509 but lower Sm & Ba (Fig. S73)
®	NWA 10810	402.4	2	**7834 & pairs**		11.2	20	3.6	6	4		4 133	**P:** RgBr; LiCl: Gab, Tro, GrBr, IMBr; Ves **C:** like NWA 7834 (Fig. S49)
%	NWA 10822	56.	1	**8046 & pairs**		4.3	7	0.6	5	0		4 81	**P:** PoBr; LiCl: none **C:** typFLM; like NWA 8046 but among lowest IEs, Eu, La/Sm & Ba of NWA 8046 clan (Fig. S24)
£	NWA 10823	202.	2	**8222**		3.9	8	0.7	5	3		5 37	**P:** PoBr; LiCl: An; VesShM **C:** typFLM (Fig. S17–S21); most mafic of NWA 8222 clan (Fig. S23)
%	NWA 10901	68.04	1	**8046 & pairs**		4.3	7	0.6	5	4		2 81	**P:** PoBr; LiCl: An; ShM, FeNi **C:** typFLM; like NWA 8046 (Fig. S24)
{	NWA 10902	36.28	2	**8673 & pairs**		7.7	18	2.5	9	7		2 65	**P:** PoBr; LiCl: An, Bas; ShM **C:** like NWA 8673 (Fig. S50)
±	NWA 10953	55.	1	**8455 & pairs**		6.5	10	8.4	8	6		6 76	**P:** FrBr; LiCl: scarce; FeNi, We, Ves **C:** like NWA 8455 but low Na & Eu (Figs. S35 & S69)
{	NWA 10964	26.	4	**8673 & pairs**		7.9	19	2.5	9	7		2 65	**P:** PoBr; LiCl: "igneous" [Z. Guo, MetBull]; FeNi **C:** like NWA 8673 (Fig. S50)
Ê	NWA 10973	25.	1	**unique**		6.1	11	7.2	9	5	6	6 13	**P:** PoBr; LiCl: none; FeNi, Ves **C:** like A16 regolith; most like NWA 8010 but higher Sm/Sc, Cr/Sc, Na/Eu, Sm/Th, SEs, Ir/Ni (Fig. S35), lower Br (0.13×) & As (0.22×), different subsample data trends (Fig. S69)
C	NWA 10985	250.	1	773 & pairs (11616 basalt)		18.4	49	4.1	0	5		4 98	**P:** Gab; ShM **C:** higher Sc (1.24×), lower Co (0.7×), & much higher Na (2.0×) & Eu (1.6×) than olivine-phyric basalt of NWA 773 clan (Fig. S53); high Ba
n.a.	NWA 10986	108.2	sev	**10509 & pairs**		6.0	15	0.9	n.a.	8	n.a.		**P:** GlBr; LiCl: An, Nor, AnNor, GabNor, Tro, TrAn, Bas [R01] **C:** no INAA data but see [R01]; v high Ba
®	NWA 10989	14.4	1	**7834 & pairs**		12.6	25	3.5	6	5		3 133	**P:** FrBr, fg; LiCl: Am, Bas; Mask, FeNi, Ves **C:** like NWA 7834 (Fig. S49)
¦	NWA 11006	2245	1	**unique**		3.7	6	1.2	4	3	3	4 4	**P:** IMBr; LiCl: IMBr, An, Gab, Nor, Tro; Ves **C:** typFLM; most like NWA 10665 but higher La/Sm, lower SEs, & Zn (Figs. S17–S21)
%	NWA 11029	75.	1	8046 & pairs		4.0	7	0.6	5	5		3 81	**P:** FrBr, fg; LiCl: none; FeNi **C:** typFLM; most like NWA 8046 (Fig. S24) but lowest Sc & distinctly lower Ba (Fig. S24)
~	NWA 11061	1040.	1	**unique**	matrix	3.3	6	0.8	5	0	5	5	**P:** PoBr, fg; LiCl: An; Ves **C:** typFLM; low Na, moderately low Cr/Sc, low Sr & Ba (Figs. S17–S21)
					FAN clast	0.4	1.1	0.17	0	0	7	3	

Plot	Stone Name	Mass (g)	Pcs.	**Terrestrially,** or possibly launch paired with:		FeO %	Sc µg/g	Sm µg/g	SEI	BaI	UI	*N*	Petrographic and compositional features from MetBull and [peer-reviewed references]
Þ	NWA 11077	1139.7	1	**10141 & pair?**		3.9	7	1.1	6	5	2	7 7	**P:** PoBr, v fg; LiCl: sparse IMBr; FeNi (photo: Fig. S75) **C:** typFLM; very similar to 10141 clan but totally different texture (Fig. S75) and significantly different light REE (0.9×) and Sm/Eu (Figs. S17–S21, S74, & S79)
®	NWA 11109	77.	10	**7834 & pairs**		10.8	18	3.4	7	5		3 133	**P:** PoBr; LiCl: An, Gab, Nor; VesShM **C:** like NWA 7834 (Fig. S49)
{	NWA 11110	62.	10	**8673 & pairs**		8.0	19	2.5	9	5		3 62	**P:** PoBr, fg; LiCl: scarce; ShM **C:** like NWA 8673 (Fig. S50)
=	NWA 11111	111.	2	**10141 & pairs**		3.9	7	1.3	5	7		6 19	**P:** PoBr; LiCl: none; ShM (photo: Fig. S75) **C:** typFLM (Figs. S17–S21); like NWA 10141 but higher La/Sm (Fig. S8n), lower Sm/Th (Figs. S17–S21, S74, & S79)
Û	NWA 11127	474.6	1	**unique**		6.1	14	1.7	5	4	6	6 6	**P:** PoBr, fg; LiCl: IMBr; ShM, Ves **C:** Most like NWA 8673 clan but lower Sc, Cr/Sc, SEs, & Ba (Fig. S71)
n.a.	NWA 11159	10.7	1	?		feld	n.a.	n.a.	n.a.	n.a.	n.a.	n.a.	**P:** FrBr; LiCl: Gab, Bas, IMBr; VesShM **C:** no INAA data
~	NWA 11182	60.	1	**unique**	matrix	3.7	7	0.6	2	7	3	3 8	**P:** FrBr; LiCl: An, Gab; VesShM (photo: Fig. S1h) [B02] **C:** typFLM; matrix most like NWA 8222 clan but much higher Sm/Th, lower SEs, higher Ba (Figs. S17–S21), Ce/Ce* = 0.82 in matrix and 0.73 mafic clast (Fig. S63); clast has high Cr/Sc, suggesting anorthositic troctolite but Sc is in the anorthositic norite range (Fig. S4).
					FAN clast	0.4	1.1	0.17	0	0	7	3	
®	NWA 11185	94.02	4	**7834 & pairs**		10.1	18	4.0	7	4		9 133	**P:** PoBr, fg; LiCl: IMBr; FeNi **C:** like NWA 7834 (Fig. S49)
{	NWA 11193	155.	1	**8673 & pairs**		7.9	18	2.4	9	7		4 65	**P:** PoBr, fg; LiCl: none; FeNi **C:** like NWA 8673 (Fig. S50) but highest Na (1.2×) and lowest Sm/Th (0.9×)
£	NWA 11212	197.5	sev	**8222 & pairs**		3.5	7	0.7	5	5		2 37	**P:** PoBr; LiCl: An; VesShM **C:** typFLM; like NWA 8222 (Fig. S23)
{	NWA 11216	222.34	many	**8673 & pairs**		10	17	3.4	9	4		6 65	**P:** PoBr, fg; LiCl: An; Ves; FeNi **C:** like NWA 8673 but highest IEs & high Na (Fig. S50), negative Ce anomaly (Fig. S63)
Ë	NWA 11223	28.	1	**11809**		4.4	9	1.3	6	8	5	5 5	**P:** GlBr; LiCl: An, Nor, OlNor **C:** enriched in light REE and Eu with negative Ce anomaly (Ce/Ce*: 0.66) from terrestrial alteration, high Eu, low Na/Eu (Figs. S15, S25, S63)
{	NWA 11228	140.	many	**8673 & pairs**		7.9	18	2.3	9	4		2 65	**P:** FrBr, fg; LiCl: Gab; ShM **C:** like NWA 8673 (Fig. S50)
£	NWA 11237	583.	1	**8222 & pairs**		3.7	7	0.6	5	3		4 37	**P:** PoBr; An; Gl, Ves **C:** typFLM; like NWA 8222 (Fig. S23)
k	NWA 11243	80.	1	**unique**		5.9	13	3.8	5	7	5	5 10	**P:** PoBr; LiCl: OlNor rare; FeNi, We **C:** distinct from otherwise similar in Fig. S46, high As (Fig. S61)
k	11243 pair	*(?)*	1	**11243**		5.6	12	3.3	6	6		5 10	**P:** none **C:** like NWA 11243

Plot	Stone Name	Mass (g)	Pcs.	**Terrestrially,** or possibly launch paired with:	FeO %	Sc µg/g	Sm µg/g	SEI	BaI	UI	*N*	Petrographic and compositional features from MetBull and [peer-reviewed references]
?	NWA 11249	73.6	1	**7834 & pairs**	9.1	22	3.6	9	6		3 133	**P:** FrBr, fg; LiCl: none; Sph, Ves **C:** like NWA 10149 (Fig. S49); high As (Fig. S61)
S	NWA 11252	22.9	1	**5744 & pairs**	4.7	7	0.7	3	3		1 47	**P:** GrBr, AnTro; LiCl: none; ShM, FeNi **C:** like NWA 5744 (Fig. S30)
%	NWA 11266	1017.	many	**8046 & pairs**	4.6	8	0.8	5	4		3 81	**P:** PoBr, fg; LiCl: none; Ves, FeNi **C:** typFLM; like NWA 8046 but high La/Sm (Fig. S24), Ce/Ce*: 0.86 (Fig. S63)
%	NWA 11269	220.	1	**8046 & pairs**	4.5	8	0.6	6	3		3 81	**P:** PoBr, fg; LiCl: none; Ves, FeNi **C:** typFLM; like NWA 8046 (Fig. S24)
%	NWA 11273	2808.	many	**8046 & pairs**	4.7	8	0.6	6	2		2 81	**P:** PoBr, fg; LiCl: Gl, rare Bas; Ves, FeNi **C:** typFLM; like NWA 8046 (Fig. S24)
%	NWA 11303	6000.	sev	**8046 & pairs**	4.5	8	0.6	5	5		2 81	**P:** PoBr, fg; LiCl: An; FeNi **C:** typFLM; like NWA 8046 (Fig. S24)
n.a.	NWA 11331	318.	sev	8046 & pairs?	feld	n.a.	n.a.	n.a.	n.a.	n.a.	n.a.	**P:** PoBr, fg; LiCl: none; Ves, Sph **C:** no INAA data
Â	NWA 11352	74.5	1	**unique**	4.2	8	1.2	9	2	2	5 5	**P:** PoBr; LiCl: An, Gab, Nor; Ves **C:** typFLM but high SEs, Ir, Sm/Th, Cr/Sc (Figs. S17–S21, S74, & S79)
n.a.	NWA 11367	305.	2	?	feld	n.a.	n.a.	n.a.	n.a.	n.a.	n.a.	**P:** PoBr; LiCl: OlNor; FeNi **C:** no INAA data
%	NWA1 1379	150.87	1	**8046 & pairs**	4.7	8	0.9	5	5		3 81	**P:** PoBr, fg; LiCl: An; Ves, FeNi **C:** typFLM; like NWA 8046 (Fig. S24)
n.a.	NWA 11407	700.	sev	8046 & pairs?	feld	n.a.	n.a.	n.a.	n.a.	n.a.	n.a.	**P:** PoBr, fg; LiCl: An; ShM, FeNi **C:** no INAA data
n.a.	NWA 11421	912.	many	8046 & pairs?	feld	n.a.	n.a.	n.a.	n.a.	n.a.	n.a.	**P:** PoBr; LiCl: An; ShM, FeNi **C:** no INAA data
%	NWA 11428	783.39	sev	**8046 & pairs**	4.9	9	0.7	6	3		2 81	**P:** PoBr; LiCl: An; ShM, FeNi **C:** typFLM; like NWA 8046 (Fig. S24)
n.a.	NWA 11444	1323.	~200	8046 & pairs?	n.a.	n.a.	n.a.	n.a.	n.a.	n.a.	n.a.	**P:** GlBr, GlBr; LiCl: Bas, Gab, Gl; VesShM, FeNi **C:** no INAA data
n.a.	NWA 11457	273.	7	?	feld	n.a.	n.a.	n.a.	n.a.	n.a.	n.a.	**P:** PoBr; LiCl: An; FeNi **C:** no INAA data
%	NWA 11460	286.	sev	**8046 & pairs**	3.9	7	0.8	5	3		2 81	**P:** PoBr; LiCl: Bas, Gab; FeNi **C:** typFLM; like NWA 8046 but high La/Sm & least mafic of 8046 clan (Fig. S24), Ce/Ce*: 0.82 (Fig. S63)
n.a.	NWA 11472	840.	1	?	n.a.	n.a.	n.a.	n.a.	n.a.	n.a.	n.a.	**P:** PoBr; LiCl: An; FeNi **C:** no INAA data
n.a.	NWA 11474	586.	many	?	feld	n.a.	n.a.	n.a.	n.a.	n.a.	n.a.	**P:** FrBr; LiCl: An; ShM **C:** no INAA data; ShM: 27.5±1.1% Al_2O_3, 4.2±1.3% FeO, 5.7±1.4% MgO [C. Agee in MetBull]
%	NWA 11479	504.	1	**8046 & pairs**	4.7	8	0.7	6	6		3 81	**P:** PoBr, fg; LiCl: An; Mask, FeNi **C:** typFLM; like NWA 8046 (Fig. S24)

Plot	Stone Name	Mass (g)	Pcs.	**Terrestrially,** or possibly launch paired with:		FeO %	Sc µg/g	Sm µg/g	SEI	BaI	UI	*N*	Petrographic and compositional features from MetBull and [peer-reviewed references]
%	NWA 11515	330.	many	**8046 & pairs**		4.6	8	0.6	5	5		3 81	**P:** PoBr; LiCl: Bas, Nor, Gab; FeNi **C:** typFLM; like NWA 8046 (Fig. S24)
n.a.	NWA 11517	88.	4	8046 & pairs?		feld	n.a.	n.a.	n.a.	n.a.	n.a.	n.a.	**P:** PoBr; LiCl: An, Gab, IMBr, Bas; VesShM, FeNi **C:** no INAA data
n.a.	NWA 11523	3362.	1	?		feld	n.a.	n.a.	n.a.	n.a.	n.a.	n.a.	**P:** FrBr; LiCl: none; FeNi **C:** no INAA data
n.a.	NWA 11524	820.	1	**Unique;** not 773; no other NWA breccia has 3% TiO_2 & 11% Al_2O_3		~19	n.a.	n.a.	n.a.	n.a.	n.a.	n.a.	**P:** PoBr with large clasts of Bas; ShM **C:** no INAA data; ShM: 3.2±0.6% TiO_2, 11±3% Al_2O_3, 18.9±1.1% FeO, 6.9±1.9% MgO [C. Agee in MetBull]
n.a.	NWA 11532	70.	sev	8046 & pairs?		feld	n.a.	n.a.	n.a.	n.a.	n.a.	n.a.	**P:** PoBr; LiCl: An; IMBr; Mask, FeNi **C:** no INAA data
®	NWA 11563	54.5	1	**7834 & pairs**		9.2	19	4.8	7	4		2 133	**P:** PoBr, fg; LiCl: none; Ves, FeNi **C:** like NWA 10149 (Fig. S49)
~	NWA 11616	2550.8	1	773 & pairs (10985 basalt)	matrix	19.0	41	6.5	0	0		3 98	**P:** PoBr; LiCl: OlGab & 1 large bas **C:** like other NWA-773-clan breccias (Fig. S53)
					FAN clast	0.4	1.1	0.17	0	0	7	3	
n.a.	NWA 11695	350.	many	8046 & pairs?		feld	n.a.	n.a.	n.a.	n.a.	n.a.	n.a.	**P:** PoBr; LiCl: An; ShM **C:** no INAA data; ShM: 28.9±0.1% Al_2O_3, 4.1±0.1% FeO, 6.2±0.0% MgO [C. Agee in MetBull]
C	NWA 11703	5309.1	1	773 & pairs		19.5	25	4.2	0	0	n.a.	1 98	**P:** OlGab; mask, ShM **C:** like NWA 773 & NWA 2977 OlGab; sawdust sample (Fig. S53)
C	NWA 11767	15.	many	773 & pairs?		n.a.	n.a.	n.a.	n.a.	n.a.	n.a.	n.a.	**P:** OlGab Br; ShM **C:** no INAA data
n.a.	NWA 11783	65.	sev	?		feld	n.a.	n.a.	n.a.	n.a.	n.a.	n.a.	**P:** FrBr, fg; LiCl: An; VesShM **C:** no INAA data; ShM: 28.0±0.5% Al_2O_3, 4.7±0.2% FeO, 6.0±0.2% MgO [C. Agee in MetBull]
n.a.	NWA 11787	23,500.	many	8046 & pairs?		feld	n.a.	n.a.	n.a.	n.a.	n.a.	n.a.	**P:** FrBr; LiCl: An, mafic, Tro; VesShM **C:** no INAA data; ShM: 31±4% Al_2O_3, 3±2% FeO, 5±3% MgO [C. Agee in MetBull]
n.a.	NWA 11788	10,441.	many	8673 & pairs		feld	n.a.	n.a.	n.a.	n.a.	n.a.	n.a.	**P:** FrBr, fg; LiCl: An; VesShM, FeNi **C:** no INAA data; ShM: 24±4% Al_2O_3, 8±3% FeO, 8±1% MgO [C. Agee in MetBull]
n.a.	NWA 11789	5492.	9	8046 & pairs?		feld	n.a.	n.a.	n.a.	n.a.	n.a.	n.a.	**P:** FrBr; LiCl: some, mafic; VesShM **C:** no INAA data; ShM: 28±4% Al_2O_3, 4±3% FeO, 7±4% MgO [C. Agee in MetBull]
n.a.	NWA 11801	67.05	1	?		n.a.	n.a.	n.a.	n.a.	n.a.	n.a.	n.a.	**P:** RgBr, fg; LiCl: An, Gab, Tro, IMBr, Gl; Sph, FeNi **C:** no INAA data
Ë	NWA 11809	67.	1	**11223**		4.0	8	1.2	4	9	4	3 3	**P:** PoBr, fg; LiCl: none **C:** like NWA 11223; high As (Fig. S61), negative Ce anomaly (Ce/Ce* = 0.70)
n.a.	NWA 11828	5340.	sev	?		feld	n.a.	n.a.	n.a.	n.a.	n.a.	n.a.	**P:** RgBr; LiCl: An, IMBr, GlBr, GrBr, Nor, GabNor, TroAn; Gl, Sph; FeNi; We **C:** no INAA data

Plot	Stone Name	Mass (g)	Pcs.	**Terrestrially,** or possibly launch paired with:	FeO %	Sc µg/g	Sm µg/g	SEI	BaI	UI	*N*	Petrographic and compositional features from MetBull and [peer-reviewed references]
d	NWA 11851	227.	1	**unique**	5.8	8	2.3	7	6	1	3 3	**P:** PoBr, fg; LiCl: Gab, IMBr; Fo_{76-82}; FeNi **C:** high Cr/Sc (137, Fig. S4), likely troctolitic precursor, Sc = 8.5 µg/g, like NWA 5744 clan but Sm = 2.3 µg/g, 5–6× higher (Fig. 6)
n.a.	NWA 11871	21.9	1	?	feld	n.a.	n.a.	n.a.	n.a.	n.a.	n.a.	**P:** PoBr; LiCl: none; FeNi, Ves **C:** no INAA data
Î	NWA 11886	36.	1	**unique**	21.2	67	16.5	1	0	2	3 3	**P:** FrBr; LiCl: none; FeNi **C:** high-Sm basaltic breccia (Fig. 6), high Eu (Fig. S16), lowest Na/Eu (Fig. S6), lowest Cr/Sc (Fig. S4), light REE "depletion" (Fig. S13f)
n.a.	NWA 11898	767.8	sev	8046 & pairs?	feld	n.a.	n.a.	n.a.	n.a.	n.a.	n.a.	**P:** FrBr; LiCl: none; FeNi, ves **C:** no INAA data; ShM: 31.3±1.2% Al_2O_3, 2.5±0.5% FeO, 2.0±0.5% MgO [C. Agee in MetBull]
n.a.	NWA 11962	85.8	1	?	bas?	n.a.	n.a.	n.a.	n.a.	n.a.	n.a.	**P:** RgBr, basaltic?; LiCl: Bas, Gab, Br; Sph, VesShM, FeNi **C:** no INAA data
n.a.	NWA 11966	157.13	1	8046 & pairs?	feld	n.a.	n.a.	n.a.	n.a.	n.a.	n.a.	**P:** FrBr; LiCl: none; VesShM, FeNi **C:** no INAA data; ShM: 31.0±1.2% Al_2O_3, 3.6±0.8% FeO, 3.0±0.6% MgO [C. Agee in MetBull]
n.a.	NWA 11968	427.8	1	8046 & pairs?	feld	n.a.	n.a.	n.a.	n.a.	n.a.	n.a.	**P:** FrBr, fg; LiCl: none; FeNi **C:** no INAA data; ShM: 30.7±3.6% Al_2O_3, 4.6±2.4% FeO, 4.0±2.2% MgO [C. Agee in MetBull]
n.a.	NWA 12008	577.	1	**unique?** 032/479, 4734/10597, LAP (NNL)	22.7 [C03]	53. [C03]	6.4 [C03]	n.a.	n.a.	n.a.	n.a.	**P:** Bas; distinct from NWA 032/479, NWA 4734/10597, and LAP stones [C03] **C:** no INAA data; compositionally [C03] indistinguishable from NNL launch-pair group (Fig. 13)
n.a.	NWA 12216	34.4	1	?	feld	n.a.	n.a.	n.a.	n.a.	n.a.	n.a.	**P:** PoBr; LiCl: none; Ves, FeNi **C:** no INAA data
n.a.	NWA 12248	37.3	1	?	feld	n.a.	n.a.	n.a.	n.a.	n.a.	n.a.	**P:** PoBr, fg; LiCl: none **C:** no INAA data
n.a.	NWA 12270	1300	6	?	feld	n.a.	n.a.	n.a.	n.a.	n.a.	n.a.	**P:** FrBr; LiCl: none; ShM **C:** no INAA data; ShM: 26.0±3.9% Al_2O_3, 5.9±1.7% FeO, 5.0±2.2% MgO [C. Agee in MetBull]
n.a.	NWA 12279	1830	1	?	feld	n.a.	n.a.	n.a.	n.a.	n.a.	n.a.	**P:** IMBr, fg; LiCl: An, OlGab, Gab, Gl; Ves **C:** no INAA data
n.a.	NWA 12368	1868	1	?	feld	n.a.	n.a.	n.a.	n.a.	n.a.	n.a.	**P:** FrBr; LiCl: "feldspathic and mafic" [C. Agee in MetBull]; ShM, FeNi **C:** no INAA data; ShM: 28.8±4.2% Al_2O_3, 4.2±2.1% FeO, 4.1±1.8% MgO [C. Agee in MetBull]
n.a.	NWA 12384	244.	2	**unique?**	bas	20.4 [C02]	n.a.	n.a.	n.a.	n.a.	n.a.	**P:** MBasBr; LiCl: MBas **C:** no INAA data; 2.0% TiO_2, high *Mg'* (55 [C02])
n.a.	NWA 12393	1267.1	1	**unique?** not 733 clan; plag is too anorthitic	bas	n.a.	n.a.	n.a.	n.a.	n.a.	n.a.	**P:** FrBr of OlGabNor mineralogy **C:** no INAA data; An_{96} vs. $An_{91–92}$ in NWA 773 clan [V01]
n.a.	NWA 12422	42.8	2	?	feld	n.a.	n.a.	n.a.	n.a.	n.a.	n.a.	**P:** PoBr; LiCl: none; Ves **C:** no INAA data

Plot	Stone Name	Mass (g)	Pcs.	**Terrestrially,** or possibly launch paired with:	FeO %	Sc µg/g	Sm µg/g	SEI	BaI	UI	*N*	Petrographic and compositional features from MetBull and [peer-reviewed references]
n.a.	NWA 12427	3469.	1	?	feld	n.a.	n.a.	n.a.	n.a.	n.a.	n.a.	**P:** FrBr; LiCl: anorthositic OlGab; VesShM **C:** no INAA data; ShM: 27.9±6.3% Al_2O_3, 5.5±3.2% FeO, 5.2±3.4% MgO [C. Agee in MetBull]
n.a.	NWA 12428	2070.	1	?	feld	n.a.	n.a.	n.a.	n.a.	n.a.	n.a.	**P:** FrBr; LiCl: "diverse;" VesShM **C:** no INAA data; ShM: 24.3±2.5% Al_2O_3, 6.3±2.7% FeO, 9.6±2.9% MgO [C. Agee in MetBull]
n.a.	NWA 12592	1420.	1	?	bas?	n.a.	n.a.	n.a.	n.a.	n.a.	n.a.	**P:** FrBr; LiCl: Bas; Ves **C:** no INAA data
n.a.	NWA 12593	332.8	1	12592?	feld	n.a.	n.a.	n.a.	n.a.	n.a.	n.a.	**P:** FrBr; LiCl: Bas; GrBr, IMBr; Ves, FeNi **C:** no INAA data
n.a.	NWA 12603	47.	4	?	feld	n.a.	n.a.	n.a.	n.a.	n.a.	n.a.	**P:** RgBr; LiCl: An, IMBr; Sph **C:** no INAA data
×	NWA 12604	631.	1	**unique**	6.0	13	3.	7	8	2	3 3	**P:** RgBr, GlBr, fg; LiCl: An, Gl, IMBr, Bas; Mask, ShM, Sph **C:** low Na, mod high Ni, low Cr/Sc (compare with NWA 4819), v high Ba (Fig. S46)
n.a.	NWA 12630	233.	2	8046 & pairs?	feld	n.a.	n.a.	n.a.	n.a.	n.a.	n.a.	**P:** PoBr; LiCl: none **C:** no INAA data
n.a.	NWA 12643	2602.	1	?	feld	n.a.	n.a.	n.a.	n.a.	n.a.	n.a.	**P:** PoBr; LiCl: none **C:** no INAA data
%	NWA 12691	103,770.	many	**8046 & pairs**	4.6	8	0.7	6	6		4 81	**P:** PoBr; LiCl: quench textured; VesShM; FeNi **C:** typFLM; like NWA 8046 (Fig. S24)
n.a.	NWA 12695	224.	1	?	feld	n.a.	n.a.	n.a.	n.a.	n.a.	n.a.	**P:** PoBr; LiCl: An **C:** no INAA data
n.a.	NWA 12697	140.	many	?	feld	n.a.	n.a.	n.a.	n.a.	n.a.	n.a.	**P:** FrBr; LiCl: An, IMBr, MBas; FeNi **C:** no INAA data
%	NWA 12760	58,090.	1	**8046 & pairs**	4.6	8	0.7	5	6		2 81	**P:** PoBr; LiCl: none; VesShM **C:** typFLM; like NWA 8046 (Fig. S24)
n.a.	NWA 12765	15,949.	1	8046 & pairs?	feld	n.a.	n.a.	n.a.	n.a.	n.a.	n.a.	**P:** PoBr; LiCl: none **C:** no INAA data
n.a.	NWA 12826	25.	many	?	feld	n.a.	n.a.	n.a.	n.a.	n.a.	n.a.	**P:** PoBr; LiCl: IMBr, MBas; FeNi **C:** no INAA data
n.a.	NWA 12830	232.	1	?	feld	n.a.	n.a.	n.a.	n.a.	n.a.	n.a.	**P:** IMBr; LiCl: none; FeNi **C:** no INAA data
n.a.	NWA 12831	150.8	9	?	feld	n.a.	n.a.	n.a.	n.a.	n.a.	n.a.	**P:** PoBr; LiCl: none **C:** no INAA data
n.a.	NWA 12839	68.75.	1	**unique?** 032/479, 4734/10597, LAP (NNL)	bas	23.0 [B03]	n.a.	n.a.	n.a.	n.a.	n.a.	**P:** diabase, distinct from NNL launch-pair clan **C:** no INAA data; but data of [B03] largely indistinguishable from NNL launch pair group
n.a.	NWA 12870	30.07	1	8046 & pairs?	feld	n.a.	n.a.	n.a.	n.a.	n.a.	n.a.	**P:** FrBr, fg; LiCl: none **C:** no INAA data

Plot	Stone Name	Mass (g)	Pcs.	**Terrestrially,** or possibly launch paired with:	FeO %	Sc µg/g	Sm µg/g	SEI	BaI	UI	*N*	Petrographic and compositional features from MetBull and [peer-reviewed references]
n.a.	NWA 12909	2742.	1	**unique?**	feld	n.a.	n.a.	n.a.	n.a.	n.a.	n.a.	**P:** FrBr; LiCl: An; noritic troctolite mineralogy **C:** no INAA data
n.a.	NWA 12952	808.	1	?	feld	n.a.	n.a.	n.a.	n.a.	n.a.	n.a.	**P:** PoBr, fg; LiCl: none **C:** no INAA data
n.a.	NWA 12966	1.39	1	8046 & pairs?	feld	n.a.	n.a.	n.a.	n.a.	n.a.	n.a.	**P:** PoBr; LiCl: none; FeNi **C:** no INAA data
n.a.	NWA 12971	280.	1	**unique?**	tro	n.a.	n.a.	n.a.	n.a.	n.a.	n.a.	**P:** IMBr, AnTro; LiCl: none; $Fo_{64.5–75}$,< that of NWA 773 clan; different color and texture **C:** no INAA data
n.a.	NWA 12980	1300.	1	?	n.a.	n.a.	n.a.	n.a.	n.a.	n.a.	n.a.	**P:** IMBr; LiCl: An **C:** no INAA data
n.a.	NWA 12985	33.	1	?	feld	n.a.	n.a.	n.a.	n.a.	n.a.	n.a.	**P:** FrBr; LiCl: none **C:** no INAA data
n.a.	NWA 12997	60.	many	5744 & pairs?	tro	n.a.	n.a.	n.a.	n.a.	n.a.	n.a.	**P:** Tro, IMBr **C:** no INAA data
5	Oued Awlitis 001	432.5	2	**unique?**	3.4	6	0.7	4	0	4	8 8	**P:** IMBr, LiCl: An; ShM, FeNi **C:** typFLM but with v low *Mg'* & Cr/Sc, high Eu/Sm (Figs. S17–S21)
£	Rabt Sbayta 002	6371.9	1	**8222 & pairs**	3.5	7	0.6	5	2		6 37	**P:** FrBr or RgBr, fg; LiCl: rare quench-textured; Ves **C:** typFLM; like NWA 8222 (Fig. S23)
£	Rabt Sbayta 004	15464.	1	**8222 & pairs**	3.5	7	0.7	5	3		4 37	**P:** FrBr or RgBr, fg; LiCl: none; Ves **C:** typFLM; like NWA 8222 (Fig. S23)
n.a.	Rabt Sbayta 005	20.78	4	**8222 & pairs?**	n.a.	n.a.	n.a.	n.a.	n.a.	n.a.	n.a.	**P:** FrBr or RgBr, fg; LiCl: none; Ves **C:** no INAA data
n.a.	Rabt Sbayta 006	4810.	2(4?)	**8222 & pairs?**	n.a.	n.a.	n.a.	n.a.	n.a.	n.a.	n.a.	**P:** FrBr; LiCl: none; ShM **C:** no INAA data; ShM: 33.2±1.9% Al_2O_3, 2.8±1.4% FeO, 2.1±1.2% MgO [C. Agee in MetBull]
Đ	Rabt Sbayta 007	4432.	1	**unique**	4.8	9	1.8	6	2	6	7 9	**P:** FrBr; LiCl: Br; FeNi **C:** mod. high Cr/Sc (Fig. S25), high Lu/Sm (Fig. S7)
Đ	Rabt Sbayta 007 pair	*(391.2)*	?	**Rabt Sbayta 007**	5.1	10	1.5	6	5		2 9	**P:** none **C:** like Rabt Sbayta 007 but slightly lower Sm & higher Cr/Sc (Fig. S25)
Æ	Rabt Sbayta 008	229.	1	**unique**	6.6	12	0.8	2	6	5	6 6	**P:** FrBr; LiCl: none; FeNi **C:** low Na & Eu (Fig. S5,S16), low La/Sm (Fig. S7), v low SEs (Fig. 12)
ƒ	Sueilila 005	282.	?	**10495?**	4.0	8	0.7	3	6		6 21	**P:** PoBr; LiCl: GabAn, Dun **C:** typFLM; highly feldspathic (Figs. S17–S21); allegedly found in the NWA 10495 strewn field, which may account for the high Ba, but Sm/Th is much lower (Fig. S72)
n.a.	Swayyah 001	4602.	6	?	bas	n.a.	n.a.	n.a.	n.a.	n.a.	n.a.	**P:** Gab **C:** no INAA data
!	Talhat Lihoudi	61.5	1	**unique**	5.3	10	2.4	5	8	3	6 6	**P:** RgBr; LiCl: none **C:** ~high Cr/Sc, low Sm/Th, low Ni, mod high Ba (Figs. S25 & S46)

Plot	Stone Name	Mass (g)	Pcs.	**Terrestrially,** or possibly launch paired with:	FeO %	Sc µg/g	Sm µg/g	SEI	BaI	UI	*N*	Petrographic and compositional features from MetBull and [peer-reviewed references]
ß	Tichiya	9354.	2	**unique**	6.1	14	4.7	6	8	6	7 7	**P:** FrBr, fg; LiCl: Bas, Gl **C:** high Eu (Fig. S16), high Sm/Th (Fig. S15), low Na/Eu (Fig. S6), Ce/Ce*: 0.74 (Fig. S63), high As (Fig. S61)
Samples with lunar-like compositions and petrography provided to us by meteorite dealers and collectors who claimed the parent rock to be from NWA												
]	rock 65	*(442.)*	?	in detail, unlike any lunar meteorite	4.7	6	0.8	9	0	5	5 5	**P:** none **C:** like typFLM but high very SEs, e.g., 30 ng/g Ir, and nonchondritic SE ratios (Fig. Figs. S44, S55)
¥	rock 87	*(158.)*	?	in detail, unlike any lunar meteorite	4.0	7	1.3	6	2	4	5 5	**P:** none **C:** like typFLM; most like NWA 10073 but different Sm/Sc slope, lower Na, lower Cr/Sc, higher Sm/Th (Figs. S74 & S79)
7	rock 142	*(169.)*	?	in detail, unlike any lunar meteorite	5.6	10	0.7	3	4	n.a.	2 2	**P:** none **C:** like typFLM but v low Cr/Sc (Fig. S4) and high Sm/Th (Fig. S15)
¾	rock 133	*(4185.)*	?	in detail, unlike any lunar meteorite	5.5	12	2.5	6	5	6	4 4	**P:** none **C:** low Na, low Ni (Fig. S46); Ce/Ce*: 1.17 (Fig. S12z**,** S63)
t	rock 4	*(26.)*	?	in detail, unlike any lunar meteorite	11.5	36	1.7	5	0	n.a.	2 2	**P:** none **C:** mafic but low Th Fig. S3, low La/Sm, high Lu/Sm (Figs. S7 & S13e), high Eu/Sm (Fig. S43), low Ti/Sc (Fig. S32), low Fe/Sc (Fig. S44), low Ba, high SiO_2 (Fig. S31)

Key and Abbreviations

Meteoritical Bulletin cutoff date: 31 December 2019

A16	Apollo 16, etc.
An	"anorthosites," anorthositic or feldspathic lithologies, including cataclastic anorthosites, noritic, gabbroic, troctolitic anorthosites, and their brecciated equivalents
BaI	Ba index: relative degree of Ba contamination using the scale of Fig. S67. Each increment represents a factor-of-2 higher concentration of Ba.
Bold	for stone name, indicates that the stone is compositionally unique or first-named stone of presumed pair group
bas	for meteorites with no composition data, described petrographically as basalt, diabase, or gabbro
Bas	(mare) basalt; for lithic clasts, may include nonmare rocks or crystalline impact-melt rocks of basaltic mineralogy and texture
Br	Breccia
Diab	diabase
Dun	dunite
feld	for meteorites with no composition data, described petrographically as "feldspathic"
fg	for breccias, matrix or groundmass described as "fine-grained" or "finer-grained"
FLM	feldspathic lunar meteorite
FrBr	fragmental breccia (Stöffler et al., 1980)
Gab	Gabbro or gabbro lithic clast(s) in breccias
Gl	glassy fragments, perhaps devitrified
GlBr	glassy-matrix (impact-melt) breccia, including some designated as regolith breccias but for which no regolith components are identified or described
GrBr	granulitic or granoblastic breccia, "granulite," recrystallized matrix
GabNor	gabbronorite
IMBr	impact-melt breccia or rock, "melt-matrix" breccia
ITEs	incompatible trace elements (K, P, Zr, REE (rare earth elements), Hf, Ta, Th, & U)
LAP	the 6 LaPaz Icefield (Antarctica) lunar meteorite stones
LiCl:	major lithic clasts include…; "none" = none are mentioned or described in the MetBull description
KP	KREEP norite, basalt, or glass
FeNi	FeNi metal observed (kamacite, taenite)
Mask	maskelynite observed
MBas	mare basalt
MetBull	the Meteoritical Bulletin Database < https://www.lpi.usra.edu/meteor/metbull.php >
Mg´	Whole-rock mole % MgO/(MgO+FeO_T)
MoBr	monomict or nearly monomict breccia
n.a.	not analyzed
N	number of subsamples of named stone; *bottom*: number of subsamples from which UI was calculated
none	no lithic clasts reported
Nor	norite or anorthositic norite
Oph	ophitic textured lithic clast
OlGab	olivine gabbro (NWA 773 clan)
Pcs.	number of "pieces" reported in MetBull
Plag	plagioclase
PoBr	polymict breccia, not unambiguously subclassified as FrBr, GlBr, GrBr, IMBr, or RgBr
RgBr	regolith breccia: described as having spherules (including devitrified), agglutinates, or glassy matrix containing vesicles presumably from solar-wind implanted ions
SE	siderophile elements (mainly, Ni and Ir)
Sev	several
ShM	shock-melt veins or "pockets" observed
Sn	schlieren observed
Sph	spherules (glassy or devitrified, including broken) observed
SpTro	spinel troctolite

tro	for meteorites with no composition data, described petrographically as troctolitic
Tro	troctolite or anorthositic troctolite
typFLM	typical FLM: mean composition for pair group is <11 µg/g Sc (Figs. 6 & S17), <1.5 µg/g Sm (Figs. 6 & S17), Cr/Sc < 110 (unless only 1–2 anomalously high subsamples (Figs. S18b & S4), 0.3–0.4% Na_2O (Figs. S5b & S19b), and 0.6–0.9 µg/g Eu (Fig. S16). Atypical FLMs are richer in incompatible elements (Sm, Th) or Na_2O (Fig. S25).
UI	lithophile-element uniformity index (all subsamples of pair group): 1 = compositionally uniform, 9 = heterogeneous, see text
v	very
Ves	vesicles in melt matrix
VesShM	shock-melt veins contain vesicles
We	described as weathered or containing weathering products (calcite, etc.)

Plot Symbols

symbol	meteorite or clan
1	NEA 001
2	DaG 262, 996, & 1042
3	NEA 003
4	DaG 400 & 1058
5	Oued Awlitis 001
7	rock 142
8	Kalahari 008
9	Kalahari 009
A	NWA 032 & 0479
Â	NWA 11352
Æ	Rabt Sbayta 008
B	NWA 482
b	NWA 10073 & 1 pair
ß	Tichiya
C	NWA 773, 2700, 2727, 2977, 3160, 3170, 3333, 6950, 7007, 8127, 10656, 10985, 11616, 11703, 11767, Anoual, & 1 pair
Ç	NWA 10678 & 1 pair
D	NWA 2200
Đ	Rabt Sbayta 007 & 1 pair
d	NWA 11851
E	NWA 2995, 2996, 3190, 4503, 5151, 5152, 6252, 6554, 6555, & 2 pairs
Ê	NWA 10973
Ë	NWA 11223, 11809
F	NWA 2998
f	NWA 7262
ƒ	NWA 10495, Sueilila 005
G	NWA 3136
H	NWA 3163, 4483, 4881, & 6275
h	NWA 10404
I	NWA 4472 & 4485
Î	NWA 11886
J	NWA 4734 & 10597
K	NWA 4932
k	NWA 11243 & 1 pair
L	NWA 4884, 7611, 8277, 10480, 10566, & 1 pair
M	NWA 4898
µ	NWA 10447
N	NWA 4819
Ñ	NWA 10509,10798, La'gad 003, & 2 possible pairs
O	NWA 4936, 5406, 6221, 6355, 6470, 6570, 7190, 7986, & 8181
Ø	NWA 10665
P	NWA 5000
Q	NWA 5153

symbol	meteorite or clan
R	NWA 5207
S	NWA 5744, 8599, 8687, 10140, 10178, 10318, 10401, 11252, & 3 pairs
T	NWA 6481
t	rock 004
U	NWA 6578
Û	NWA 11127
V,v	NWA 6687 (V = CaO corrected, v = raw)
W	NWA 6721
X	NWA 6888
Y	NWA 7022
Z	NWA 7274
@	NWA 8001
#	NWA 7931
¿	NWA 8641, 8682, 10049, 10077, 10133, & 1 pair
$	NWA 8022 & 10082
¢	NWA 10626 & 1 pair
¥	rock 087
£	NWA 8222, 10823, 11212, 11237, Rabt Sbayta 002, 004, & 2 pairs
%	NWA 8046, 10309, 10461, 10609, 10643, 10649, 10756, 10822, 10901, 11029, 11266, 11269, 11273, 11303, 11379, 11428, 11460, 11479, 11515, 12691, 12760, & 2 pairs
&	NWA 8055
/	NWA 8010
\	NWA 8701 & 1 pair
¦	NWA 11006
)	NWA 8753
[	NWA 7493
]	rock 065
{	NWA 8673, 8733, 8746, 10048, 10065, 10123, 10902, 10964, 11110, 11193, 11216, 11228, 11788, & 1 pair
}	Aridal 017
±	NWA 8455, 8609, 8651, 8668, 8727, 8783, 10130, 10228, 10621, 10953, La'gad & 3 pairs
×	NWA 12604
÷	NWA 11182
=	NWA 10141, 10415, & 11111
~	NWA 11061
¼	NWA 8586
½	NWA 8182
¾	rock 133
!	Talhat Lihoudi
§	NWA 8632
©	NWA 7959
®	NWA 7834, 7948, 8306, 10149, 10172, 10203, 10253, 10258, 10263, 10272, 10291, 10317, 10376, 10546, 10599, 10644, 10782, 10810, 10989, 11109, 11185, 11249, 11563, Galb Inal, & 1 pair
Þ	NWA 11077
¶	NWA 10783

Table S2 References

B01. Bischoff A., Weber D., Clayton R. N., Faestermann T., Franchi I. A., Herpers U., Knie K., Korschinek G., Kubik P. W., Mayeda T. K., Merchel S., Michel R., Neumann S., Palme H., Pillinger C. T., Schultz L., Sexton A. S., Spettel B., Verchovsky A. B., Weber H. W., Weckwerth G., and Wolf D. 1998. Petrology, chemistry, and isotopic compositions of the lunar highland regolith breccia Dar al Gani 262. *Meteoritics & Planetary Science* 33:1243–1257.

B02. Boyle S, Gross J, and Prissel T. C. 2018. Understanding the magnesium-suite lithology and lunar highlands terrain through a detailed investigation of lunar meteorites Northwest Africa (NWA) 10291 and 11182 (abstract #2346). 49th Lunar and Planetary Science Conference.

BO3. Burney D., Neal C. R., Irving A. J., Carpenter P. K., Tepper J. H., and Hoefnagels B. 2020. Petrology and chemical composition of lunar mare diabase Northwest Africa 12839: Comparisons with Apollo basalts (abstract #2613). 51st Lunar and Planetary Science Conference.

C01. Cahill J. T., Floss C., Anand M., Taylor L. A., Nazarov M. A., and Cohen B. A. 2004. Petrogenesis of lunar highlands meteorites: Dhofar 025, Dhofar 081; Dar al Gani 262, and Dar al Gani 400. *Meteoritics & Planetary Science* 39:503–530.

C02. Carpenter P. K., Jolliff B. L., Korotev R. L., Tepper J. H., Irving A. J., and Labenne L. 2019) Petrology and bulk composition of lunar mare basalt breccia Northwest Africa 12384 (abstract 2125). 50th Lunar and Planetary Science Conference.

C03.Cohen M. E., Kuehner S. M., Tepper J. H., Burney D. C., Neal C. R., Irving A. J., Korotev R. L., and B. Hoefnagels. 2019. Mineralogy and bulk composition of lunar mare basalt Northwest Africa 12008 (abstract 2508). 50th Lunar and Planetary Science Conference.

C04. Chen J., Jolliff B. L., Wang A., Korotev R. L., Wang K., Carpenter P. K., Chen H., Ling Z., Fu X., Ni Y., Cao H., and Huang Y. 2019. Petrogenesis and shock metamorphism of basaltic lunar meteorites Northwest Africa 4734 and 10597. *Journal of Geophysical Research: Planets.* DOI:10.1029/2019JE006084

D01. Daubar I. J., Kring D. A., Swindle T. D., and Jull A. J. T. 2002. Northwest Africa 482: A crystalline impact-melt breccia from the lunar highlands. *Meteoritics & Planetary Science* 37:1797–1814.

E01 Elardo S. M., Shearer C. K. Jr., Fagan A. L., Borg L. E., Gaffney A. M., Burger P. V., Neal C. R., Fernandes V. A., and McCubbin F. M. 2013. The origin of young mare basalts inferred from lunar meteorites Northwest Africa 4734, 032, and LaPaz Icefield 02205. *Meteoritics & Planetary Science* 49:261–291

F01. Fagan T. J., Taylor J. G., Keil K., Hicks T. L., Killgore M., Bunch T. E., Wittke J. H., Mittlefehldt D. W., Clayton R. N., Mayeda T. K., Eugster O., Lorenzetti S., and Norman M. D. 2003. Northwest Africa 773: Lunar origin and iron-enrichment trend. *Meteoritics & Planetary Science* 38:529–554.

F02. Fagan T. J., Taylor G. J., Keil K., Bunch T. E., Wittke J. H., Korotev R. L., Jolliff B. L., Gillis J. J., Haskin L. A., Jarosewich E., Clayton R. N., Mayeda T. K., Fernandes V. A., Burgess R., Turner G., Eugster O., and Lorenzetti S. 2002. Northwest Africa 032: Product of lunar volcanism. *Meteoritics & Planetary Science* 37:371–394.

H01. Haloda J., Týcová P., Jakeš P., Gabzdyl P., and Kosler J. 2006. Lunar meteorite Northeast Africa 003-B: A new lunar mare basaltic breccia (abstract #2311). 37th Lunar and Planetary Science Conference. CD-ROM

H02. Haloda J., Týcová P., Korotev R. L., Fernandes V. A., Burgess R., Thöni M., Jelenc M., Jakeš P., Gabzdyl P., and Košler J. 2009. Petrology, geochemistry, and age of low-Ti mare-basalt meteorite Northeast Africa 003-A: A possible member of the Apollo 15 mare basaltic suite. *Geochimica et Cosmochimica Acta* 73:3450–3470.

J01. Jolliff B. L., Korotev R. L., Zeigler R. A., Floss C., and Haskin L. A. 2003. Northwest Africa 773: Lunar mare breccia with a shallow-formed olivine-cumulate component, very-low-Ti (VLT) heritage, and a KREEP connection. *Geochimica et Cosmochimica Acta* 67:4857–4879.

J02. Joy K. H., Crawford I. A., Russell S. S., and Kearsley A. T. 2010. Lunar meteorite regolith breccias: An in situ study of impact melt composition using LA-ICP-MS with implications for the composition of the lunar crust. *Meteoritics & Planetary Scie*nce 45:917–946.

J03. Joy K. H., Burgess R., Hinton R., Fernandes V. A., Crawford I. A., Kearsley A. T., and Irving A. J. 2011. Petrogenesis and chronology of lunar meteorite Northwest Africa 4472: A KREEPy regolith breccia from the Moon. *Geochimica et Cosmochimica Acta* 75, 2420–2452.

K01. Korotev R. L., Jolliff B. L., Zeigler R. A., Gillis J. J., and Haskin L. A. (2003) Feldspathic lunar meteorites and their implications for compositional remote sensing of the lunar surface and the composition of the lunar crust. *Geochimica et Cosmochimica Acta* 67:4895–4923.

K03. Korotev R. L, Zeigler R. A., Jolliff B. L., Irving A. J., and Bunch T. E. 2009. Compositional and lithological diversity among brecciated lunar meteorites of intermediate iron composition. *Meteoritics & Planetary Science* 44:1287–1322.

M01. Mercer C. N., Treiman A. H., and Joy K. H. 2013. New lunar meteorite Northwest Africa 2996: A window into farside lithologies and petrogenesis. *Meteoritics & Planetary Science* 48:289–315.

R01. Roberts S. E., McCanta M. C., Jean M. M., and Taylor L. A. 2019. New lunar meteorite NWA 10986: A mingled impact melt breccia from the highlands—A complete cross section of the lunar crust. *Meteoritics & Planetary Science* 54, 3018–3035.

S01. Snape J. F., Joy K. H., and Crawford I. A. 2011. Characterization of multiple lithologies within the lunar feldspathic regolith breccia meteorite Northeast Africa 001. *Meteoritics & Planetary Science* 46:1288–1312.

S02. Sokol A. K., V. A. Fernandes, T. Schulz, A. Bischoff, R. Burgess, R. N. Clayton, C. Münker, K. Nishiizumi, H. Palme, L. Schultz, G. Weckwerth, K. Mezger, and M. Horstmannaan 2008. Geochemistry, petrology and ages of the lunar meteorites Kalahari 008 and 009: New constraints on early lunar evolution. *Geochimica et Cosmochimica Acta* 72:4845–4873.

V01. Valencia S. N., Jolliff B. L., and Korotev R. L. 2019. Petrography, relationships, and petrogenesis of the gabbroic lithologies in Northwest Africa 773 clan members Northwest Africa 773, 2727, 3160, 3170, 7007, and 10656. *Meteoritics & Planetary Science* 54:2083–2115.

W01. Warren P. H., Ulff-Møller F., and Kallemeyn G. W. 2005. "New" lunar meteorites: Impact melt and regolith breccias and large-scale heterogeneities of the upper lunar crust. *Meteoritics & Planetary Science* 40:989–1014.

W02. Warren P. H. and Taylor G. J. 2014. The Moon, *Treatise on Geochemistry (2nd Edition), Planets, Asteroids, Comets and The Solar System*, edited by Davis A. M. New York: Elsevier. pp. 213–250.

W03 Wang Y., Hsu W., Guan Y., Li X., Li Q., Liu Y., and Tang G. (2012) Petrogenesis of the Northwest Africa 4734 basaltic lunar meteorite. Geochimica et Cosmochimica Acta 92, 329-344.

Z01. Zeigler R. A., Korotev R. L., Jolliff B. L., and Haskin L. A. 2005. Petrology and geochemistry of the LaPaz icefield basaltic lunar meteorite and source-crater pairing with Northwest Africa 032. *Meteoritics & Planetary Science* 40:1073-1102

Z02. Zhang A.-C., Hsu W.-B., Floss C., Li X.-H., Qiu-Li Li, Liu Y. and Taylor L. A. 2010. Petrogenesis of lunar meteorite Northwest Africa 2977: Constraints from in situ microprobe results. *Meteoritics & Planetary Science* 45:1929–1947.

Table S2. INAA data for subsamples, weighted means with 95% confidence limits, analytical uncertainties, sources of samples, and miscellaneous sample data.

Table S2 is provided as XLS and CSV files (Table_S2_INAA_subsamples.xls and Table_S2_INAA_subsamples.csv).

Table S3a. Results of INAA: Mass-weighted mean concentrations of stones

meteorite	note	Na_2O	CaO	Sc	Cr	FeO_T	Co	Ni	Sr	Zr	Ba	La	Ce	Nd	Sm	Eu	Tb	Yb	Lu	Hf	Ta	Ir	Au	Th	U	mass
		%	%	μg/g	μg/g	%	μg/g	μg/g	μg/g	μg/g	μg/g	μg/g	μg/g	μg/g	μg/g	μg/g	μg/g	μg/g	ppm	μg/g	μg/g	ng/g	ng/g	μg/g	μg/g	mg
Anoual		0.192	n.a.	41.8	3190	21.0	59.7	<400	<200	<400	157	10.26	27.0	17.7	4.85	0.577	0.99	3.24	0.456	3.66	0.43	<15	*27*	1.58	0.38	101
Aridal 017		0.319	13.5	7.84	1015	5.12	19.4	110	158	92	188	4.67	11.6	7.8	2.17	0.746	0.47	1.71	0.240	1.71	0.19	2.7	1.7	0.84	0.30	177
DaG 262		0.349	16.7	7.67	640	4.38	20.1	240	202	27	150	2.21	5.8	3.2	1.02	0.749	0.21	0.82	0.121	0.74	0.10	10.5	*62*	0.36	0.18	47
DaG 400	all	0.349	*18.5*	5.58	452	3.09	11.3	110	263	<35	104	1.46	3.8	2.3	0.71	0.720	0.15	0.57	0.081	0.51	0.06	3.9	2.6	0.22	0.18	533
DaG 400	n.c.	0.349	*18.1*	6.09	498	3.38	12.2	120	270	<40	113	1.59	4.1	2.4	0.77	0.721	0.16	0.62	0.088	0.56	0.07	4.2	2.6	0.24	0.19	415
DaG 996		0.357	16.0	7.81	618	4.25	17.9	190	247	<60	306	3.06	7.3	4.2	1.21	0.776	0.24	0.91	0.128	0.88	0.11	8.5	4.6	0.44	0.42	234
DaG 1042		0.342	*17.6*	7.69	643	4.31	22.5	290	236	<80	263	2.71	6.7	3.8	1.12	0.738	0.23	0.87	0.125	0.84	0.12	11.9	4.2	0.45	0.44	204
DaG 1058		0.327	*18.2*	5.12	421	2.98	10.8	79	356	<50	683	1.40	3.7	2.2	0.60	0.693	0.13	0.48	0.067	0.40	0.05	4.1	<4	0.21	0.60	212
Galb Inal		0.450	15.1	21.2	1453	9.86	33.9	220	198	110	223	7.36	19.1	11.7	3.45	0.928	0.70	2.48	0.347	2.81	0.30	8.0	7.6	1.06	0.41	232
La'gad		0.450	14.6	11.80	956	7.08	38.2	480	368	300	1150	19.14	49.7	30.3	8.73	1.326	1.70	5.86	0.833	6.88	0.77	12.5	*660*	3.05	1.01	139
La'gad 003		0.336	14.1	13.0	894	5.72	17.1	130	198	36	5210	2.08	5.0	3.4	0.95	0.736	0.20	0.81	0.119	0.62	0.09	3.9	2.0	0.33	0.12	574
NEA 001		0.337	17.0	11.42	831	5.29	13.4	78	224	<80	147	1.71	4.5	2.5	0.80	0.741	0.19	0.76	0.109	0.58	0.08	2.7	1.8	0.25	0.17	630
NEA 003	m.b.	0.288	10.5	46.8	3720	20.6	51.5	72	147	<40	251	3.18	7.3	5.1	1.62	0.625	0.43	1.90	0.280	1.14	0.19	<5	<7	0.46	0.38	170
NEA 003	br.	0.201	11.4	53.2	3480	24.9	56.9	42	118	380	176	5.84	15.0	12.1	3.74	0.666	0.95	3.60	0.512	2.56	0.34	<12	<15	0.87	0.45	158
NWA 032		0.347	12.3	55.7	2740	22.1	41.8	50	142	170	n.a.	11.24	29.7	20.7	6.61	1.098	1.56	5.79	0.802	5.00	0.62	n.a.	n.a.	1.90	0.45	184
NWA 479		0.336	12.3	57.1	2720	22.4	43.1	75	127	<500	296	11.53	30.4	19.7	6.63	1.128	1.62	5.90	0.846	5.05	0.64	<15	<13	1.88	0.50	214
NWA 482		0.377	17.1	6.93	519	3.76	13.2	140	171	<40	30	1.52	4.0	2.5	0.79	0.750	0.16	0.63	0.090	0.58	0.07	5.3	3.4	0.24	0.08	334
NWA 773		0.186	9.0	29.8	3210	19.0	72.2	160	75	170	162	11.74	30.6	17.7	5.30	0.464	1.07	3.65	0.500	4.02	0.48	<7	<9	1.82	0.46	212
NWA 2200		0.330	16.8	6.95	504	3.95	15.3	170	169	30	65	2.43	6.3	4.1	1.09	0.796	0.23	0.87	0.122	0.79	0.10	7.6	*8.5*	0.40	0.10	298
NWA 2700		0.260	n.a.	37.3	3870	19.4	60.8	110	80	190	175	11.09	28.9	22.0	5.27	0.641	1.19	4.11	0.587	4.51	0.55	<15	*130*	1.75	0.44	25
NWA 2727		0.231	10.0	34.3	3420	19.9	68.4	130	<160	170	170	11.07	29.3	17.9	5.34	0.508	1.10	3.86	0.539	4.17	0.51	<9	<7	1.74	0.47	377
NWA 2977		0.113	n.a.	25.7	3560	18.6	81.4	190	<90	98	82	6.28	16.2	10.3	3.15	0.234	0.68	2.45	0.344	2.39	0.23	<15	<15	0.86	0.28	142
NWA 2977	pair	0.131	5.4	24.1	2730	18.6	85.0	210	71	120	64	8.09	20.2	13.0	3.69	0.257	0.76	2.56	0.369	2.61	0.29	<4	0.7	1.27	0.40	57
NWA 2995		0.467	13.9	19.3	1560	9.80	34.0	220	166	150	159	10.11	26.6	15.3	4.66	1.045	0.94	3.26	0.454	3.90	0.47	6.6	<10	1.90	0.54	246
NWA 2995	pair	0.463	13.8	22.0	1920	11.66	40.8	160	158	120	191	10.27	26.8	14.7	4.58	1.053	0.87	3.01	0.411	2.99	0.40	4.0	<7	1.51	0.39	148
NWA 2995	pair	0.435	14.2	21.6	1730	10.76	38.9	240	146	100	126	8.72	22.8	13.2	3.96	0.986	0.79	2.73	0.379	2.83	0.34	6.2	<8	1.30	0.36	180
NWA 2996		0.475	14.7	18.3	1580	9.70	34.2	180	162	120	187	10.38	28.0	16.2	4.63	1.097	0.90	3.07	0.425	3.32	0.38	5.4	<14	1.57	0.46	253
NWA 2998		0.344	17.4	4.89	356	2.67	7.7	60	192	<40	29	0.85	2.2	1.5	0.42	0.761	0.09	0.36	0.052	0.28	0.04	3.0	<4	0.13	0.03	224
NWA 3136		0.295	12.4	46.6	2860	15.36	35.6	160	152	100	645	7.67	20.6	12.4	3.86	0.935	0.82	3.37	0.476	2.93	0.34	6.0	<9	1.29	0.37	230
NWA 3160		0.153	n.a.	40.2	3560	20.9	64.4	110	<140	190	163	14.75	38.9	24.0	6.86	0.611	1.35	4.14	0.559	4.92	0.62	<10	<10	2.18	0.60	316
NWA 3163		0.288	15.8	12.63	1025	5.84	13.1	38	137	<80	17	0.79	2.2	<5	0.49	0.658	0.12	0.55	0.081	0.33	0.04	<4	<4	0.10	<0.2	304
NWA 3170		0.260	n.a.	39.6	2820	20.7	55.9	110	<170	<570	244	24.29	64.8	34.6	11.19	0.756	2.27	8.14	1.152	10.18	0.96	n.a.	n.a.	4.29	1.15	42
NWA 3190		0.451	14.1	18.00	1454	9.24	33.0	190	152	97	171	8.62	23.3	12.7	3.75	1.047	0.73	2.54	0.352	2.46	0.33	6.2	*22*	1.33	0.33	217
NWA 3333		0.154	n.a.	32.7	3600	20.9	78.1	150	<130	140	133	10.21	24.6	14.7	4.48	0.409	0.92	3.19	0.445	3.61	0.42	<10	*21*	1.43	0.38	584
NWA 4472	all	0.604	12.5	20.8	1550	9.19	22.6	130	215	440	601	44.66	116.	70.	19.51	1.50	4.00	13.4	1.82	11.1	1.60	3.3	<10	7.49	2.02	323
NWA 4472	REE	0.600	12.6	20.9	1540	9.20	22.5	120	217	440	606	32.12	83.	50.	14.22	1.45	2.99	11.2	1.55	11.0	1.57	3.4	<9	6.70	1.97	249
NWA 4483		0.292	16.2	11.20	889	5.01	12.6	54	143	<80	40	0.92	2.5	<7	0.53	0.682	0.13	0.57	0.084	0.34	0.05	1.5	<4	0.12	<0.2	314
NWA 4485		0.573	12.3	21.1	1590	9.51	36.8	260	209	420	430	30.76	79.8	47.0	13.77	1.431	2.88	10.77	1.501	11.01	1.44	16.6	<14	6.24	1.84	427
NWA 4503		0.497	14.0	17.76	1570	9.44	33.8	230	158	200	157	11.29	29.4	17.4	5.15	1.110	1.00	3.48	0.483	4.87	0.41	6.4	2.9	1.62	0.43	168
NWA 4734		0.377	13.1	59.5	2240	21.8	37.4	23	<300	<400	148	12.33	32.1	20.9	7.36	1.184	1.73	6.26	0.880	5.32	0.66	<14	<13	2.06	0.59	278
NWA 4819		0.363	14.9	13.01	1421	7.03	27.8	290	203	100	158	7.52	19.5	11.4	3.36	0.824	0.71	2.65	0.366	2.76	0.34	11.9	4.1	1.51	0.46	275
NWA 4881		0.283	15.9	14.61	1327	6.00	14.5	57	138	<100	86	0.91	2.5	<6	0.53	0.638	0.13	0.59	0.086	0.33	<0.9	<3	<3	0.11	<0.3	311
NWA 4884		0.366	13.9	29.9	2050	13.72	43.8	150	115	<210	88	6.29	16.4	10.1	3.07	0.786	0.64	2.35	0.326	2.25	0.26	<10	<10	0.93	0.26	266
NWA 4898		0.296	13.4	65.4	3020	17.17	24.8	18	<240	<390	72	4.71	14.8	12.2	4.56	0.997	1.06	4.00	0.570	4.45	0.24	<14	<10	0.44	<0.8	133
NWA 4932		0.307	13.5	19.72	1500	8.55	44.3	600	254	<120	447	2.34	6.3	<10	1.16	0.637	0.28	1.26	0.181	0.89	0.14	27.4	8.0	0.54	0.16	210
NWA 4936		0.512	14.4	8.89	777	5.94	42.5	600	198	180	172	13.26	35.0	20.5	6.14	1.394	1.17	3.96	0.547	4.71	0.59	19.1	12.1	1.95	0.48	294
NWA 5000	chips	0.411	15.3	9.94	861	5.76	37.2	530	181	<90	197	3.26	8.6	5.1	1.50	0.915	0.31	1.17	0.163	1.10	0.14	23.8	9.2	0.49	0.20	633
NWA 5000	dust	0.440	14.8	10.26	772	5.70	30.1	748	189	74	120	4.91	12.5	7.3	2.21	0.976	0.43	1.57	0.220	1.68	0.20	18.0	27.9	0.709	0.233	886
NWA 5151		0.478	14.3	16.71	1440	8.52	31.7	170	156	120	183	11.53	33.0	16.9	4.84	1.143	0.91	2.99	0.417	3.07	0.36	5.2	61	1.76	0.44	185

Table S3a, continued

meteorite	Note	Na_2O	CaO	Sc	Cr	FeO_T	Co	Ni	Sr	Zr	Ba	La	Ce	Nd	Sm	Eu	Tb	Yb	Lu	Hf	Ta	Ir	Au	Th	U	mass
		%	%	μg/g	μg/g	%	μg/g	μg/g	μg/g	μg/g	μg/g	μg/g	μg/g	μg/g	μg/g	μg/g	μg/g	μg/g	ppm	μg/g	μg/g	ng/g	ng/g	μg/g	μg/g	mg
NWA 5152		0.461	14.1	16.75	1460	9.03	34.4	210	165	110	146	8.65	22.9	13.6	3.93	1.037	0.77	2.66	0.369	2.84	0.37	8.4	3.4	1.30	0.33	166
NWA 5153		0.476	13.6	25.6	1960	12.72	42.4	150	132	120	127	9.94	26.2	14.8	4.61	0.993	0.90	3.15	0.431	3.27	0.40	3.6	<7	1.54	0.43	185
NWA 5207		0.484	14.9	15.52	1065	7.56	26.7	230	165	110	123	8.39	21.9	12.4	3.92	1.121	0.77	2.71	0.376	2.87	0.36	7.2	4.3	1.26	0.35	255
NWA 5406		0.546	14.4	9.08	768	5.82	34.6	520	198	200	159	13.65	35.7	21.5	6.35	1.442	1.25	4.15	0.573	4.92	0.62	12.4	11.8	1.97	0.52	178
NWA 5744		0.244	13.9	8.50	1079	5.97	22.6	100	126	<40	63	0.91	2.4	<7	0.45	0.567	0.10	0.42	0.062	0.28	0.04	<5	<6	0.12	<0.3	416
NWA 5744	pair	0.245	13.1	8.70	1208	5.91	21.5	76	142	14	254	0.80	2.2	1.7	0.42	0.572	0.09	0.41	0.057	0.24	0.04	1.1	2.6	0.08	<0.13	172
NWA 5744	pair	0.256	13.0	9.76	1289	6.27	21.5	86	113	<30	111	0.86	2.3	1.8	0.46	0.568	0.10	0.44	0.065	0.25	0.03	1.6	2.2	0.10	0.12	61
NWA 5744	pair	0.238	12.6	7.77	1249	5.67	24.5	110	132	<40	89	0.76	1.9	2.1	0.39	0.542	0.09	0.38	0.053	0.24	0.03	1.6	<3	0.08	<0.17	125
NWA 6221		0.519	14.6	9.74	776	6.61	81.8	1190	209	160	204	12.18	32.3	19.0	5.69	1.347	1.08	3.64	0.505	4.22	0.54	40.5	24	1.69	0.49	179
NWA 6252		0.386	13.7	27.2	2140	12.95	46.2	150		100	162	9.16	25.9	13.9	3.85	0.907	0.73	2.59	0.359	2.56	0.31	52.5	3.7	1.40	0.37	78
NWA 6275		0.312	17.5	7.35	500	3.40	8.1	27	147	<60	31	0.89	2.4	<6	0.42	0.707	0.09	0.37	0.054	0.22	<1.5	<4	<4	0.12	<0.2	101
NWA 6355		0.520	14.8	10.04	856	5.83	31.1	440	195	180	175	13.05	34.1	20.6	6.13	1.413	1.18	3.95	0.545	4.60	0.59	11.8	9.4	1.87	0.47	176
NWA 6470		0.510	15.0	9.59	885	5.59	27.5	380	191	150	194	11.07	28.5	17.2	4.97	1.318	0.97	3.24	0.446	3.80	0.47	10.6	8.1	1.63	0.43	177
NWA 6481		0.479	15.9	9.15	737	4.74	17.6	210	206	<90	285	3.52	9.1	5.4	1.63	1.017	0.34	1.32	0.187	1.19	0.16	7.3	2.5	0.60	0.23	231
NWA 6554		0.442	13.8	19.6	2120	11.32	46.6	320	144	150	134	9.01	24.5	13.1	4.11	0.967	0.80	2.77	0.390	3.68	0.34	10.9	3.6	1.38	0.36	174
NWA 6555		0.386	14.1	25.5	1760	12.32	62.7	560	123	89	121	8.13	22.3	12.7	3.80	0.913	0.77	2.66	0.373	2.65	0.33	23.4	11.5	1.18	0.32	196
NWA 6570		0.519	14.5	9.16	778	5.83	33.9	480	196	200	164	14.13	37.2	21.9	6.63	1.419	1.29	4.27	0.591	5.02	0.66	11.2	9.5	2.05	0.53	105
NWA 6578		0.324	16.9	8.12	599	4.18	12.8	120	198	<70	51	2.18	5.9	3.7	1.08	0.759	0.24	0.90	0.126	0.81	0.11	5.0	<5	0.36	0.14	232
NWA 6687	raw	0.515	*17.6*	37.7	1520	16.30	29.9	79	472	690	1090	33.8	89.	57.	17.5	2.00	3.50	12.3	1.69	17.5	1.44	<12	*33*	6.19	1.87	197
NWA 6687	cor.	0.568	n.a.	41.5	1680	17.96	32.9	87	521	759	1200	37.2	98.	63.	19.3	2.200	3.85	13.5	1.87	19.3	1.58	<12	*36*	6.82	2.06	179
NWA 6721		0.457	15.6	10.42	729	4.96	17.7	180	241	<80	1250	3.30	9.8	4.9	1.51	0.857	0.31	1.21	0.169	1.06	0.14	7.1	3.0	0.54	0.23	319
NWA 6888		0.460	14.2	12.97	901	5.66	18.0	130	303	52	6140	4.78	12.1	6.9	2.15	0.925	0.45	1.69	0.236	1.60	0.19	4.7	<7	0.67	0.23	233
NWA 6950		0.133	7.7	24.7	3070	19.4	84.7	190	<190	<270	142	6.55	18.2	11.7	3.35	0.270	0.70	2.63	0.374	2.52	0.28	<10	<10	0.95	0.37	147
NWA 7007		0.246	n.a.	39.2	3040	19.2	58.5	140	<205	200	268	15.45	41.6	23.5	7.40	0.599	1.48	4.94	0.695	5.24	0.63	<10	<10	2.40	0.68	120
NWA 7022	br.	0.603	15.2	10.33	676	5.31	18.8	210	200	170	143	12.59	32.9	18.8	5.61	1.390	1.08	3.51	0.480	4.14	0.49	9.4	4.2	2.07	0.53	156
NWA 7022	cl.	0.711	15.0	13.67	733	6.29	16.1	140	204	270	225	20.17	53.0	31.3	9.22	1.602	1.76	5.69	0.783	6.68	0.82	6.1	4.7	3.07	0.85	167
NWA 7190		0.520	14.5	9.41	808	5.95	33.6	470	196	190	200	14.46	38.2	20.6	6.35	1.420	1.23	4.13	0.569	4.84	0.63	12.4	11.0	2.06	0.56	111
NWA 7262		0.347	17.0	5.65	402	3.13	9.1	67	163	12	27	1.32	3.3	1.9	0.58	0.766	0.12	0.47	0.069	0.41	0.06	2.7	<4	0.22	0.07	242
NWA 7274		0.368	15.0	11.78	1047	6.07	28.4	310	207	140	742	10.62	27.4	15.9	4.84	0.937	0.96	3.56	0.494	3.54	0.43	12.8	3.8	1.93	0.66	232
NWA 7493		0.336	16.5	8.40	580	4.37	12.3	84	188	<60	97	1.96	5.2	3.2	0.94	0.763	0.20	0.75	0.106	0.60	0.09	3.6	2.3	0.28	0.14	743
NWA 7611		0.398	13.8	26.5	1760	12.11	38.9	170	160	84	183	6.38	16.5	10.5	3.09	0.867	0.63	2.33	0.329	2.24	0.27	5.0	3.7	0.97	0.42	320
NWA 7611	pair	0.338	11.2	32.8	2200	15.38	46.8	120	136	120	119	6.38	16.4	11.6	3.14	0.751	0.65	2.28	0.331	2.40	0.26	4.0	<5	0.88	0.54	103
NWA 7834		0.399	14.1	19.6	1600	9.86	38.3	230	173	100	260	8.00	20.9	12.4	3.58	0.966	0.71	2.47	0.343	2.58	0.31	6.0	3.0	1.15	0.42	326
NWA 7834	pair	0.427	12.9	20.1	1760	10.39	39.0	250	191	130	440	8.90	23.2	15.1	4.10	1.011	0.82	2.82	0.401	2.87	0.36	5.8	5.6	1.36	0.54	99
NWA 7931		0.336	14.8	18.4	1183	7.54	28.0	300	159	53	206	3.90	10.3	7.0	1.88	0.759	0.40	1.58	0.222	1.34	0.16	12.6	7.5	0.60	0.27	158
NWA 7948		0.400	13.2	17.81	1600	9.56	37.6	200	240	82	182	6.96	18.2	11.1	3.23	0.922	0.66	2.31	0.321	2.41	0.32	6.3	3.0	1.02	0.32	233
NWA 7959		0.336	16.7	5.49	475	3.35	18.2	210	241	24	1560	2.57	6.8	4.4	1.17	0.792	0.23	0.81	0.114	0.74	0.10	9.2	3.4	0.42	0.25	247
NWA 7986		0.514	14.7	9.09	742	5.65	30.7	430	178	180	185	13.26	34.4	19.3	6.23	1.410	1.20	3.99	0.553	4.65	0.64	10.3	10.2	1.90	0.42	104
NWA 8001		0.393	15.9	9.04	653	4.74	22.2	280	304	97	529	7.58	19.7	12.3	3.54	0.950	0.71	2.56	0.353	2.70	0.32	10.6	2.8	1.30	0.38	243
NWA 8010		0.476	15.0	11.32	854	5.83	36.7	380	269	170	1020	14.32	36.0	21.3	6.42	1.118	1.28	4.47	0.609	5.08	0.65	7.5	6.5	2.19	0.52	223
NWA 8022		0.458	16.4	5.31	477	3.71	31.7	520	207	29	66	2.72	6.8	4.2	1.14	0.986	0.25	1.11	0.158	0.95	0.16	24.5	8.2	0.70	0.20	223
NWA 8046		0.315	15.5	7.79	689	4.53	19.8	210	169	<40	242	1.69	4.4	2.3	0.73	0.755	0.15	0.57	0.084	0.44	0.06	10.7	2.6	0.21	0.07	152
NWA 8046	pair	0.326	15.7	7.78	698	4.43	16.1	130	203	25	343	1.69	4.1	2.5	0.75	0.766	0.15	0.57	0.085	0.43	0.06	4.4	2.0	0.21	0.15	90
NWA 8046	pair	0.356	14.8	8.32	750	4.79	17.9	170	175	44	222	2.05	4.6	4.0	0.88	0.813	0.18	0.63	0.096	0.53	0.08	5.3	2.5	0.28	0.10	61
NWA 8046	pair	0.318	14.8	8.95	864	5.35	21.1	190	149	36	38	1.89	5.0	3.2	0.91	0.682	0.19	0.74	0.107	0.63	0.08	6.2	4.0	0.28	0.11	165
NWA 8055		0.419	15.0	15.75	904	6.41	15.6	70	245	<80	1130	1.83	4.3	2.8	0.95	0.914	0.22	1.01	0.147	0.69	0.08	4.4	1.6	0.20	0.18	234
NWA 8127		0.111	n.a.	29.4	3690	18.2	78.9	130	<20	<90	69	4.76	13.1	4.8	2.61	0.230	0.58	2.25	0.326	1.87	0.10	<10	<10	0.64	0.20	72
NWA 8181		0.540	13.9	10.30	862	6.67	40.8	610	209	230	229	16.83	41.9	27.1	7.72	1.563	1.50	4.99	0.694	5.97	0.75	16.6	14.1	2.40	0.68	249
NWA 8182		0.530	12.4	19.9	1730	10.64	36.1	170	153	200	201	16.60	41.5	26.1	7.26	1.171	1.43	4.67	0.642	5.52	0.96	6.4	<8	2.25	0.70	176

Table S3a, continued

meteorite	note	Na_2O	CaO	Sc	Cr	FeO_T	Co	Ni	Sr	Zr	Ba	La	Ce	Nd	Sm	Eu	Tb	Yb	Lu	Hf	Ta	Ir	Au	Th	U	mass
		%	%	µg/g	µg/g	%	µg/g	µg/g	µg/g	µg/g	µg/g	µg/g	µg/g	µg/g	µg/g	µg/g	µg/g	µg/g	ppm	µg/g	µg/g	ng/g	ng/g	µg/g	µg/g	mg
NWA 8222		0.367	17.1	6.93	458	3.37	10.5	97	229	<40	228	1.36	3.4	2.6	0.61	0.812	0.13	0.53	0.075	0.41	0.05	4.3	1.8	0.20	0.13	250
NWA 8222	pair	0.362	17.5	6.86	476	3.54	9.2	79	201	42	309	2.01	5.2	3.5	0.90	0.812	0.19	0.74	0.105	0.59	0.07	3.2	2.3	0.35	0.17	108
NWA 8222	pair	0.361	17.7	7.18	481	3.57	10.9	120	229	29	263	1.64	3.9	2.7	0.75	0.814	0.15	0.54	0.079	0.42	0.06	4.4	1.8	0.32	0.26	161
NWA 8277		0.352	12.5	31.8	2220	14.54	45.5	160	161	77	207	6.25	15.9	11.5	3.06	0.780	0.65	2.28	0.327	2.21	0.24	3.9	4.6	0.87	0.38	340
NWA 8306		0.408	14.9	17.14	1540	8.86	34.4	230	202	81	519	7.27	18.1	12.5	3.30	0.921	0.67	2.29	0.317	2.37	0.32	6.0	3.5	1.01	0.45	242
NWA 8455		0.502	14.6	10.12	787	5.97	35.3	490	262	210	1070	16.23	40.3	25.3	7.44	1.322	1.43	4.91	0.668	5.61	0.68	12.3	11.5	2.44	0.70	196
NWA 8455	pair	0.557	13.6	10.20	843	5.88	31.9	460	222	230	508	15.66	38.9	25.8	7.06	1.319	1.40	4.86	0.667	5.42	0.63	13.1	10.7	2.47	0.77	96
NWA 8455	pair	0.509	13.1	10.58	900	6.84	46.4	690	219	270	529	17.83	44.7	28.4	8.24	1.393	1.63	5.62	0.769	6.62	0.79	19.5	15.6	2.89	0.81	74
NWA 8455	pair	0.545	14.6	10.46	855	6.04	31.8	450	232	200	360	13.71	35.3	21.6	6.23	1.325	1.21	4.19	0.580	4.73	0.56	13.6	12.5	2.13	0.73	92
NWA 8586		0.382	16.2	8.36	580	3.96	10.6	62	185	30	56	2.62	6.5	4.2	1.15	0.781	0.26	1.09	0.153	0.92	0.14	2.3	<3	0.65	0.39	233
NWA 8599		0.231	12.7	7.21	1292	5.41	22.8	110	139	<40	318	0.69	1.8	2.0	0.36	0.531	0.08	0.33	0.049	0.20	0.04	2.9	1.4	0.08	0.06	194
NWA 8609		0.633	14.6	10.12	944	5.99	41.4	770	313	270	938	19.92	51.2	30.7	8.98	1.311	1.78	6.11	0.832	6.74	0.80	20.2	17.2	3.19	1.24	262
NWA 8632		0.267	9.5	51.0	3360	22.8	49.4	72	171	110	933	7.64	20.3	14.5	4.66	0.799	1.11	4.05	0.567	3.48	0.41	<6	<10	1.34	<2	113
NWA 8641		0.469	15.6	10.57	726	5.03	15.6	170	216	70	290	5.72	14.2	9.4	2.56	1.049	0.51	1.82	0.251	2.11	0.24	7.7	3.7	0.83	0.32	226
NWA 8641	pair	0.503	15.3	10.07	730	5.08	20.5	230	242	83	1180	6.45	16.2	11.0	2.93	1.097	0.57	1.97	0.273	1.92	0.23	10.1	5.3	0.90	0.31	120
NWA 8651		0.489	13.6	10.23	817	6.09	35.1	480	229	250	491	17.10	44.1	26.4	7.70	1.420	1.51	5.06	0.699	5.99	0.71	12.8	9.7	2.69	0.83	139
NWA 8668		0.493	15.2	9.39	778	5.61	33.5	460	251	200	370	14.53	35.4	22.6	6.61	1.311	1.29	4.45	0.603	5.06	0.60	12.9	10.2	2.16	0.75	220
NWA 8673		0.311	13.6	15.53	1300	7.31	38.7	470	172	50	750	4.07	10.1	7.0	1.82	0.720	0.39	1.64	0.231	1.37	0.18	17.0	9.5	0.82	0.37	292
NWA 8673	pair	0.318	16.9	16.01	1249	7.17	36.2	410	353	91	4660	5.98	15.0	8.7	2.41	0.673	0.48	1.91	0.273	1.92	0.24	19.0	7.0	1.22	0.71	75
NWA 8682		0.476	15.3	9.48	737	4.90	17.3	200	255	71	1140	5.51	13.7	8.8	2.48	1.052	0.49	1.70	0.237	1.77	0.21	7.2	5.6	0.80	0.29	365
NWA 8687		0.210	11.6	7.24	3850	6.06	26.8	130	256	16	184	0.64	1.9	<4	0.32	0.471	0.08	0.31	0.047	0.18	0.03	2.5	2.4	0.09	0.83	140
NWA 8701		0.485	15.4	18.4	943	6.51	14.0	110	214	140	171	11.84	28.5	16.2	4.57	0.902	0.99	4.35	0.614	3.94	0.62	4.0	3.0	3.75	1.67	359
NWA 8701	pair	0.411	15.4	19.0	981	6.62	13.1	93	307	100	174	8.92	21.4	13.6	3.64	0.882	0.79	3.47	0.485	3.05	0.45	4.7	2.6	2.48	1.03	273
NWA 8727		0.486	13.5	10.63	860	6.40	36.6	500	289	250	361	18.12	45.9	28.1	8.32	1.473	1.63	5.47	0.752	6.43	0.80	13.0	15.4	2.73	0.72	211
NWA 8733		0.323	13.5	18.3	1485	8.27	44.3	580	181	82	314	5.55	13.9	8.9	2.54	0.720	0.54	2.17	0.311	1.92	0.25	26.2	9.8	1.11	0.45	268
NWA 8746		0.329	13.4	18.3	1459	8.17	39.0	460	175	72	352	5.77	14.5	9.5	2.54	0.740	0.53	2.13	0.303	1.90	0.25	21.6	7.7	1.14	0.40	207
NWA 8753		0.353	16.0	5.01	495	3.09	11.0	87	172	31	49	1.82	4.7	3.1	0.86	0.764	0.17	0.64	0.092	0.61	0.07	2.7	2.2	0.27	0.10	351
NWA 8783		0.527	13.9	9.83	823	5.90	33.4	490	240	220	556	16.21	41.4	25.0	7.36	1.350	1.44	4.97	0.680	5.88	0.65	13.8	11.2	2.58	0.89	315
NWA 10048		0.319	14.4	18.1	1472	7.99	38.8	510	219	66	546	4.97	12.8	8.2	2.30	0.705	0.50	1.98	0.286	1.76	0.22	21.0	8.8	0.99	0.60	257
NWA 10049		0.471	15.8	10.46	750	5.08	15.3	190	258	110	1136	6.38	16.2	11.1	2.86	1.053	0.56	1.91	0.270	2.35	0.23	6.6	4.7	0.93	0.34	276
NWA 10065		0.323	14.0	17.61	1393	7.92	40.3	470	223	68	1228	5.14	13.2	8.4	2.31	0.733	0.48	1.96	0.279	1.75	0.25	19.2	7.0	1.07	0.49	118
NWA 10073		0.395	16.2	7.42	625	3.72	14.8	160	183	49	39	3.07	7.8	5.5	1.44	0.804	0.29	1.08	0.152	1.05	0.12	8.0	2.5	0.56	0.39	189
NWA 10073	pair	0.376	16.5	7.57	619	3.88	14.6	160	320	48	132	3.32	8.5	5.5	1.50	0.793	0.30	1.13	0.160	1.09	0.15	6.2	2.8	0.61	0.50	96
NWA 10077		0.484	15.4	10.09	801	5.19	20.9	260	236	88	1130	5.83	14.6	9.3	2.67	1.063	0.52	1.82	0.252	1.87	0.23	10.2	6.6	0.86	0.28	111
NWA 10082		0.455	16.8	5.17	447	3.47	30.1	490	218	48	114	2.80	6.9	4.0	1.15	0.972	0.24	1.07	0.150	0.97	0.15	23.1	7.0	0.70	0.24	67
NWA 10123		0.305	13.3	15.13	1211	7.05	38.1	520	201	53	1040	2.72	6.8	4.2	1.21	0.694	0.26	1.13	0.163	0.91	0.13	23.2	7.9	0.56	0.30	211
NWA 10130		0.627	13.8	9.98	890	6.67	52.4	890	242	210	560	16.60	41.5	25.9	7.43	1.299	1.47	5.14	0.712	5.62	0.64	28.9	22	2.59	0.95	197
NWA 10133		0.492	13.7	10.93	845	5.62	20.6	240	260	120	871	8.35	20.9	13.6	3.86	1.131	0.74	2.60	0.363	3.04	0.35	7.6	5.4	1.28	0.40	253
NWA 10140		0.248	14.0	6.24	814	5.13	17.7	46	123	18	31	0.53	1.4	1.0	0.30	0.584	0.07	0.32	0.047	0.23	0.03	2.5	0.4	0.06	0.02	39
NWA 10141		0.313	16.7	7.35	567	3.95	13.6	140	253	52	469	2.60	6.8	4.9	1.25	0.726	0.26	0.94	0.135	0.90	0.13	5.4	2.3	0.43	0.20	203
NWA 10149		0.424	13.7	20.6	1384	9.55	36.0	300	204	120	505	7.96	20.6	13.5	3.61	0.956	0.74	2.53	0.362	2.73	0.34	9.9	5.0	1.30	0.51	149
NWA 10172		0.384	12.6	24.8	1810	11.06	36.7	200	188	120	460	7.68	19.8	12.6	3.55	0.893	0.73	2.55	0.369	2.53	0.31	5.5	3.2	1.16	0.48	168
NWA 10178		0.278	14.8	6.66	901	4.26	15.1	72	140	18	182	0.54	1.4	1.2	0.27	0.600	0.06	0.25	0.039	0.14	0.02	1.1	<1.3	0.06	0.04	191
NWA 10203		0.422	15.3	16.22	1185	7.78	28.6	220	221	180	625	8.95	23.2	13.9	3.97	1.028	0.80	2.80	0.395	4.34	0.33	7.8	4.4	1.30	0.48	203
NWA 10228		0.422	15.3	16.22	1185	7.78	28.6	220	221	180	625	8.95	23.2	13.9	3.97	1.028	0.80	2.80	0.395	4.34	0.33	7.8	4.4	1.30	0.48	203
NWA 10253		0.407	13.5	18.8	1640	9.93	35.8	190	186	140	200	7.83	20.1	12.9	3.69	0.928	0.72	2.53	0.359	2.87	0.34	4.8	4.2	1.17	0.45	198
NWA 10258		0.425	14.1	16.57	1397	8.62	34.7	260	188	140	403	8.90	22.7	14.0	4.08	1.011	0.80	2.79	0.392	3.27	0.35	7.3	21	1.33	0.53	303
NWA 10263		0.409	12.3	23.0	1740	11.79	44.3	240	190	140	457	8.30	20.9	14.2	3.80	0.935	0.77	2.62	0.379	2.90	0.26	5.9	4.4	1.25	0.51	206
NWA 10272		0.409	12.2	24.6	1780	11.91	41.8	220	155	150	261	8.59	21.8	13.6	3.98	0.944	0.79	2.78	0.392	3.05	0.48	5.7	3.4	1.32	0.48	160

Table S3a, continued

meteorite	note	Na_2O	CaO	Sc	Cr	FeO_T	Co	Ni	Sr	Zr	Ba	La	Ce	Nd	Sm	Eu	Tb	Yb	Lu	Hf	Ta	Ir	Au	Th	U	mass
		%	%	µg/g	µg/g	%	µg/g	µg/g	µg/g	µg/g	µg/g	µg/g	µg/g	µg/g	µg/g	µg/g	µg/g	µg/g	ppm	µg/g	µg/g	ng/g	ng/g	µg/g	µg/g	mg
NWA 10291		0.460	14.2	24.9	1560	10.39	32.7	170	172	150	408	10.28	26.1	16.2	4.68	1.041	0.93	3.10	0.434	3.25	0.38	5.9	2.9	1.56	0.61	160
NWA 10309		0.330	15.7	8.54	757	4.98	19.8	200	176	34	204	1.64	4.0	2.9	0.71	0.755	0.15	0.56	0.083	0.41	0.06	7.4	2.8	0.20	0.13	467
NWA 10317		0.395	12.5	19.3	1920	10.48	40.6	240	176	97	245	7.26	18.6	11.9	3.36	0.905	0.69	2.31	0.334	2.31	0.27	5.8	4.8	1.07	0.42	136
NWA 10318		0.254	12.7	9.79	1325	6.30	22.2	110	143	35	174	1.56	3.2	2.3	0.61	0.589	0.12	0.50	0.074	0.55	0.05	1.9	1.9	0.24	0.10	143
NWA 10376		0.380	13.8	19.4	1780	10.32	40.4	240	169	150	795	6.93	17.9	11.5	3.23	0.859	0.65	2.28	0.331	2.93	0.27	5.6	4.3	1.06	0.49	134
NWA 10401		0.236	12.6	7.91	1141	5.89	21.8	99	124	16	79	0.66	1.8	1.5	0.37	0.541	0.08	0.35	0.052	0.21	0.03	1.5	0.6	0.07	0.05	202
NWA 10404		0.359	16.6	6.61	520	3.72	14.3	150	173	68	62	3.82	9.8	6.3	1.79	0.822	0.35	1.32	0.185	1.35	0.17	6.3	3.3	0.66	0.22	206
NWA 10415		0.313	15.8	7.52	625	4.14	14.8	150	393	51	3110	2.59	6.6	4.4	1.20	0.729	0.25	0.91	0.132	0.90	0.11	6.3	2.5	0.41	0.19	238
NWA 10447		0.304	11.1	29.7	2730	15.15	53.4	140	170	67	497	5.27	13.8	10.3	2.59	0.672	0.55	1.92	0.281	1.88	0.23	6.1	2.9	0.79	0.46	169
NWA 10461		0.317	15.2	8.23	716	4.54	14.9	90	184	24	237	1.55	3.8	2.8	0.73	0.738	0.15	0.59	0.086	0.41	0.05	2.6	7.0	0.22	0.09	69
NWA 10480		0.359	13.0	31.0	1840	13.77	40.2	140	300	86	198	6.10	15.7	11.1	2.99	0.803	0.64	2.25	0.330	2.21	0.22	<6	3.0	0.89	0.84	97
NWA 10495		0.374	15.5	13.53	809	5.36	11.6	58	281	40	4380	1.74	3.7	3.2	0.87	0.887	0.19	0.79	0.117	0.53	0.07	1.8	1.3	0.15	0.11	492
NWA 10509		0.331	14.0	12.24	862	5.46	19.2	120	260	52	6670	3.31	8.5	5.6	1.46	0.755	0.30	1.11	0.162	0.99	0.11	4.4	2.2	0.46	0.19	200
NWA 10509?	pair	0.309	14.0	17.67	1059	7.49	21.5	95	196	55	1910	3.34	7.7	5.5	1.19	0.761	0.24	0.93	0.143	0.62	0.09	5.0	2.2	0.47	0.26	156
NWA 10509?	pair	0.346	14.1	12.61	901	5.67	17.4	110	284	41	5300	2.63	7.2	4.3	1.23	0.799	0.26	0.99	0.141	0.81	0.11	3.6	2.2	0.45	0.16	168
NWA 10546		0.414	13.3	20.0	1700	10.06	37.5	220	230	130	665	7.89	20.1	12.6	3.51	0.953	0.71	2.46	0.350	2.89	0.33	6.5	3.8	1.17	0.51	100
NWA 10566		0.414	11.9	30.2	1920	13.86	42.3	190	210	90	344	6.76	16.5	12.1	3.20	0.888	0.65	2.30	0.324	2.20	0.30	5.1	3.3	0.93	0.29	137
NWA 10597		0.354	10.2	58.5	2330	22.5	40.0	84	155	190	144	12.02	30.6	21.6	6.99	1.115	1.71	6.04	0.852	5.22	0.64	<8	<8	1.98	0.66	44
NWA 10599		0.409	11.1	21.8	2290	12.25	49.6	270	167	110	593	7.41	18.0	12.4	3.39	0.899	0.67	2.30	0.323	2.51	0.29	6.6	*7.2*	1.03	0.44	134
NWA 10606		0.328	15.9	8.85	755	4.60	16.9	160	191	31	345	1.30	3.3	2.3	0.70	0.735	0.16	0.58	0.085	0.62	0.13	5.1	2.0	0.18	0.15	214
NWA 10621		0.503	13.3	9.87	860	6.67	39.6	590	254	250	603	15.73	39.8	24.6	7.21	1.491	1.38	4.72	0.652	5.75	0.69	14.7	11.0	2.37	0.83	67
NWA 10626		0.336	15.5	13.15	963	5.89	20.6	200	156	43	63	1.99	5.2	3.4	1.01	0.760	0.22	0.90	0.133	0.74	0.09	3.5	2.8	0.31	0.12	197
NWA 10626	pair	0.332	16.0	12.44	857	5.63	14.2	68	176	23	475	2.21	5.5	3.6	1.00	0.774	0.21	0.85	0.124	0.65	0.09	2.5	1.5	0.32	0.10	67
NWA 10643		0.321	14.6	8.39	754	4.86	17.5	130	198	24	443	1.90	4.6	3.4	0.79	0.751	0.15	0.61	0.092	0.56	0.06	4.7	2.7	0.26	0.18	67
NWA 10644		0.418	12.7	17.81	1620	9.62	37.0	260	180	150	536	8.43	21.1	13.1	3.77	0.969	0.75	2.57	0.366	3.35	0.34	6.2	*12.3*	1.31	0.50	207
NWA 10649		0.317	15.3	7.59	702	4.50	16.2	120	165	26	244	1.52	3.5	2.4	0.64	0.735	0.13	0.52	0.077	0.39	0.05	4.3	1.2	0.19	0.13	115
NWA 10656		0.184	7.6	34.3	3190	19.71	69.1	130	56	180	150	12.36	32.1	20.5	5.91	.433	1.20	4.02	0.585	4.31	0.43	<4	*6.6*	1.87	0.57	20
NWA 10665		0.361	16.7	6.35	523	3.73	18.0	240	182	46	138	2.32	5.9	3.8	1.09	0.801	0.22	0.82	0.117	0.78	0.10	11.1	4.2	0.36	0.33	203
NWA 10678		0.385	16.2	7.05	493	3.76	13.7	140	253	92	1390	5.36	12.9	8.8	2.37	0.886	0.46	1.57	0.219	1.86	0.20	6.7	2.3	0.78	0.27	208
NWA 10678	pair	0.389	16.4	7.67	532	3.99	13.0	120	214	55	348	3.38	7.6	6.3	1.54	0.867	0.29	1.03	0.145	0.95	0.125	5.1	4.6	0.45	0.18	102
NWA 10756		0.316	15.8	7.39	724	4.45	17.4	140	189	27	285	1.70	4.1	2.5	0.69	0.743	0.14	0.53	0.078	0.41	0.06	5.8	3.0	0.21	0.20	135
NWA 10782		0.414	14.2	23.2	1540	10.20	35.3	210	224	120	653	8.97	22.7	15.0	4.28	0.952	0.84	2.87	0.399	2.84	0.32	5.9	4.5	1.28	0.56	68
NWA 10783		0.492	14.9	10.85	727	5.92	28.9	400	233	120	298	7.36	18.7	11.1	3.41	1.132	0.67	2.35	0.327	2.37	0.27	16.4	*17.3*	1.02	0.50	205
NWA 10798		0.334	14.9	12.22	866	5.61	15.1	96	202	35	2530	1.86	4.7	3.3	0.90	0.749	0.20	0.82	0.119	0.65	0.09	4.3	1.7	0.29	0.11	176
NWA 10810		0.405	12.4	19.9	1860	11.22	43.7	220	188	120	342	7.83	20.1	12.0	3.57	0.888	0.72	2.44	0.349	2.57	0.30	5.6	3.6	1.18	0.52	129
NWA 10822		0.312	16.2	7.16	705	4.32	15.3	120	157	29	33	1.00	2.6	2.0	0.55	0.706	0.12	0.48	0.072	0.38	0.06	3.7	1.3	0.17	0.08	118
NWA 10823		0.361	17.3	8.06	492	3.93	10.5	92	190	41	156	1.49	3.9	2.3	0.72	0.824	0.15	0.61	0.089	0.44	0.07	4.3	4.3	0.21	0.16	169
NWA 10901		0.315	15.4	7.34	684	4.34	15.1	110	167	35	185	1.33	3.5	2.5	0.81	0.727	0.13	0.54	0.077	0.43	0.05	3.1	0.9	0.17	0.09	65
NWA 10902		0.315	13.8	17.91	1379	7.71	32.7	390	205	92	1560	5.41	13.8	8.5	2.46	0.733	0.51	2.05	0.301	1.87	0.25	17.4	5.8	1.07	0.49	68
NWA 10953		0.435	14.3	10.18	875	6.48	45.2	720	226	290	902	18.81	47.5	29.8	8.43	1.175	1.66	5.86	0.802	6.49	0.72	19.0	15.8	3.08	0.93	175
NWA 10964		0.305	12.7	18.6	1427	7.94	34.2	380	255	95	2320	5.51	14.1	8.5	2.49	0.715	0.51	2.13	0.304	1.94	0.26	17.0	5.9	1.12	0.56	62
NWA 10973		0.487	14.3	11.15	961	6.11	29.5	440	284	220	809	15.41	40.4	24.9	7.19	1.012	1.43	4.80	0.657	4.98	0.49	12.8	11.2	2.18	0.75	180
NWA 10985		0.324	9.4	48.7	4200	18.4	48.8	32	145	140	590	6.97	17.8	13.3	4.07	0.833	0.93	3.47	0.501	2.92	0.45	<6	*19*	1.11	0.32	107
NWA 10989		0.382	12.1	25.5	2150	12.61	44.8	190	181	120	649	7.89	18.4	11.8	3.46	0.865	0.70	2.39	0.339	2.52	0.27	4.3	*8.4*	1.04	0.55	91
NWA 11006		0.352	16.8	6.07	506	3.71	10.7	68	181	50	186	3.13	7.2	4.3	1.23	0.805	0.24	0.88	0.125	0.87	0.11	2.7	1.6	0.53	0.27	139
NWA 11029		0.319	16.2	6.91	679	4.05	14.2	110	193	26	393	1.35	3.3	2.2	0.62	0.732	0.13	0.49	0.072	0.39	0.05	3.2	1.3	0.18	0.13	82
NWA 11061		0.329	17.0	6.36	425	3.34	11.0	99	165	35	23	1.79	4.5	3.0	0.84	0.773	0.17	0.65	0.092	0.63	0.07	4.1	1.6	0.29	0.08	156
NWA 11077		0.316	17.4	7.41	594	3.94	13.5	130	198	55	638	2.39	6.1	3.9	1.15	0.731	0.23	0.87	0.125	0.85	0.10	5.6	2.1	0.39	0.17	208
NWA 11109		0.375	13.6	18.2	1570	10.80	43.8	230	271	110	618	7.46	18.9	12.2	3.36	0.838	0.67	2.25	0.316	2.32	0.27	7.7	2.3	1.06	0.55	103

Table S3a, continued

meteorite	note	Na_2O %	CaO %	Sc µg/g	Cr µg/g	FeO_T %	Co µg/g	Ni µg/g	Sr µg/g	Zr µg/g	Ba µg/g	La µg/g	Ce µg/g	Nd µg/g	Sm µg/g	Eu µg/g	Tb µg/g	Yb µg/g	Lu ppm	Hf µg/g	Ta µg/g	Ir ng/g	Au ng/g	Th µg/g	U µg/g	mass mg
NWA 11110		0.334	13.8	19.1	1510	7.99	33.0	390	198	96	650	5.64	13.9	8.3	2.53	0.715	0.53	2.13	0.304	1.94	0.25	15.3	5.8	1.08	0.70	101
NWA 11111		0.313	17.2	7.28	550	3.86	13.4	120	206	51	1720	3.04	7.1	4.4	1.26	0.745	0.24	0.89	0.128	0.86	0.11	5.1	2.0	0.48	0.22	193
NWA 11127		0.348	15.7	14.48	958	6.09	14.9	87	158	62	229	4.13	10.1	6.1	1.73	0.762	0.36	1.48	0.211	1.32	0.19	3.2	2.8	0.89	0.29	193
NWA 11182	br.	0.339	16.7	7.14	495	3.67	7.2	33	211	29	1500	1.19	2.4	2.0	0.58	0.814	0.11	0.45	0.066	0.31	0.05	1.0	3.7	0.10	0.07	82
NWA 11182	cl.	0.326	11.9	18.2	2210	10.06	25.0	85	222	34	2160	2.07	3.7	3.5	1.00	0.812	0.20	0.81	0.123	0.46	0.05	1.5	1.6	0.12	0.15	171
NWA 11185		0.428	12.9	19.0	1590	10.08	38.4	250	198	150	359	8.52	21.7	13.8	3.97	0.975	0.79	2.70	0.381	2.93	0.33	6.6	4.0	1.27	0.53	275
NWA 11193		0.383	12.5	17.58	1401	7.86	33.4	400	214	90	1580	5.68	14.0	8.6	2.38	0.754	0.50	1.98	0.285	1.92	0.25	17.2	6.9	1.22	0.47	139
NWA 11212		0.376	17.0	7.21	460	3.48	9.7	88	243	30	518	1.42	3.5	2.3	0.66	0.835	0.14	0.54	0.078	0.38	0.06	3.7	2.0	0.19	0.11	65
NWA 11216		0.350	13.8	17.46	1386	9.99	111.9	1570	222	120	334	6.75	17.2	10.6	3.06	0.739	0.63	2.44	0.348	2.33	0.32	54.5	29.0	1.23	0.79	161
NWA 11223		0.390	14.9	8.81	695	4.42	11.9	120	281	34	2950	2.75	4.4	6.0	1.35	1.054	0.22	0.67	0.098	0.38	0.06	6.8	1.8	0.14	0.07	172
NWA 11228		0.331	13.2	18.2	1456	7.94	33.9	410	199	100	293	5.45	13.9	7.4	2.34	0.758	0.49	2.03	0.290	1.85	0.24	20.0	6.3	1.12	0.46	128
NWA 11237		0.359	17.3	7.33	453	3.76	9.7	79	192	26	141	1.07	2.8	2.2	0.55	0.786	0.12	0.49	0.072	0.35	0.05	3.4	1.1	0.15	0.16	141
NWA 11243		0.439	14.2	13.29	956	5.88	19.2	130	236	140	2040	7.99	20.2	13.1	3.84	1.059	0.77	2.78	0.398	2.93	0.34	3.4	3.3	1.36	0.53	172
NWA 11243	pair	0.454	14.7	12.45	878	5.64	16.9	170	249	97	1120	6.64	16.0	11.3	3.28	1.072	0.64	2.30	0.323	2.17	0.26	5.1	3.7	1.06	0.36	150
NWA 11249		0.352	11.9	22.1	1740	9.11	35.4	400	254	120	1180	7.82	19.4	12.4	3.60	0.737	0.73	2.82	0.403	2.73	0.36	15.9	6.5	1.51	0.78	90
NWA 11252	dust	0.271	14.0	7.35	917	4.70	15.6	67	141	36	104	1.43	3.6	2.4	0.70	0.709	0.14	0.55	0.081	0.48	0.08	1.4	3.0	0.19	0.07	26
NWA 11266		0.320	15.9	7.77	748	4.46	16.3	130	184	39	247	1.96	4.2	3.0	0.79	0.741	0.16	0.59	0.087	0.45	0.06	4.0	1.7	0.23	0.16	104
NWA 11269		0.317	16.3	7.87	718	4.51	18.1	190	198	42	171	1.18	3.1	2.3	0.63	0.715	0.14	0.55	0.081	0.42	0.07	7.8	1.5	0.17	0.05	107
NWA 11273		0.313	16.1	8.13	727	4.74	17.7	150	162	<40	83	1.17	3.1	2.1	0.62	0.738	0.14	0.56	0.081	0.44	0.07	7.0	2.5	0.16	0.09	73
NWA 11303		0.322	15.8	7.98	720	4.48	15.0	120	199	40	601	1.32	3.4	2.0	0.64	0.711	0.13	0.55	0.082	0.42	0.08	3.9	7.7	0.20	0.05	70
NWA 11352		0.372	16.4	7.57	605	4.20	20.9	300	203	47	74	2.44	6.2	4.3	1.19	0.834	0.24	0.89	0.127	0.81	0.10	14.5	4.6	0.37	0.14	172
NWA 11379		0.327	15.1	8.41	755	4.71	17.7	140	171	34	349	2.03	4.8	2.7	0.88	0.813	0.17	0.64	0.094	0.46	0.07	4.6	4.7	0.26	0.11	98
NWA 11428		0.321	15.9	9.10	775	4.90	16.6	130	165	33	137	1.55	3.4	2.3	0.74	0.781	0.15	0.63	0.092	0.48	0.07	5.3	2.9	0.22	0.07	69
NWA 11460		0.309	16.8	6.69	691	3.91	14.0	110	153	30	105	2.58	4.7	3.1	0.81	0.772	0.14	0.52	0.079	0.49	0.06	3.1	*8.5*	0.34	0.20	113
NWA 11479		0.317	15.6	7.81	841	4.68	19.7	230	197	46	695	1.69	4.5	2.6	0.71	0.749	0.16	0.59	0.086	0.53	0.07	6.6	2.9	0.27	0.10	192
NWA 11515		0.311	15.7	8.43	770	4.64	16.4	130	182	22	468	1.29	3.3	2.2	0.63	0.713	0.14	0.56	0.081	0.43	0.07	4.6	1.6	0.18	0.05	194
NWA 11563		0.437	13.3	19.2	1392	9.16	33.7	250	202	160	431	10.46	26.1	15.1	4.77	1.023	0.91	3.02	0.417	3.09	0.36	8.8	*14.7*	1.37	0.48	74
NWA 11616	br.	0.247	8.8	41.5	3100	19.0	58.5	140	88	240	171	13.10	32.9	21.9	6.55	0.575	1.32	4.64	0.649	5.10	0.55	<7	<6	2.03	0.67	99
NWA 11616	m.b.	0.360	10.1	46.1	3200	18.8	43.1	24	114	220	90	7.80	21.2	14.7	4.92	0.915	1.16	4.27	0.608	4.10	0.62	<6	<6	1.38	0.39	66
NWA 11703	dust	0.132	5.7	24.9	2930	19.5	85.2	200	67	120	93	8.80	23.1	14.7	4.16	0.290	0.85	2.84	0.417	3.04	0.33	<3	4.6	1.33	0.57	29
NWA 11809		0.403	15.9	8.01	766	3.99	13.1	80	357	39	5760	2.94	4.9	5.3	1.25	1.052	0.20	0.67	0.097	0.43	0.05	3.2	1.9	0.17	0.20	187
NWA 11851		0.338	12.4	8.47	1159	5.85	30.0	220	239	110	1030	5.37	13.6	7.6	2.26	0.832	0.50	2.23	0.317	2.12	0.29	14.0	3.5	1.49	0.50	183
NWA 11886	.	0.561	8.9	67.2	2280	21.2	30.4	30	248	450	249	20.64	56.3	46.1	16.52	2.38	4.02	14.95	2.090	13.12	2.42	<4	<10	2.73	1.14	66
NWA 12691		0.323	16.7	7.89	664	4.71	19.4	170	256	36	1037	1.58	3.6	3.2	0.67	0.768	0.134	0.50	0.074	0.43	0.06	6.1	2.4	0.25	0.13	139
NWA 12760		0.322	16.1	7.98	702	4.43	16.0	120	223	33	763	1.29	3.3	2.6	0.65	0.742	0.139	0.58	0.085	0.45	0.08	5.1	0.8	0.21	0.18	71
OA 001		0.361	17.2	6.41	408	3.45	8.5	51	168	20	23	1.55	3.9	2.9	0.75	0.824	0.16	0.60	0.085	0.53	0.10	2.3	1.4	0.21	0.08	236
Rabt Sbayta 002		0.368	17.2	7.13	440	3.49	9.3	81	213	26	76	1.09	2.8	2.0	0.57	0.806	0.12	0.49	0.071	0.36	0.05	3.5	1.9	0.15	0.07	204
Rabt Sbayta 004		0.373	17.4	7.00	458	3.48	9.8	93	196	30	159	1.80	4.1	2.8	0.74	0.854	0.15	0.55	0.080	0.40	0.05	5.3	2.0	0.22	0.22	137
Rabt Sbayta 007		0.372	15.3	9.40	751	4.82	16.0	140	206	65	101	3.86	9.6	5.9	1.81	0.852	0.37	1.38	0.196	1.33	0.16	5.3	3.6	0.62	0.33	233
Rabt Sbayta 007	pair	0.339	15.7	9.97	887	5.09	17.7	170	175	57	461	3.49	7.7	5.8	1.55	0.827	0.33	1.19	0.171	1.10	0.14	7.0	2.6	0.57	0.19	123
Rabt Sbayta 008		0.286	14.5	12.46	885	6.57	17.1	54	177	25	739	1.41	3.8	2.6	0.77	0.660	0.16	0.68	0.101	0.37	0.05	<2	<2	0.21	0.10	185
Sueilila 005		0.316	16.0	7.61	491	4.01	8.5	36	200	24	1040	1.58	3.8	2.6	0.71	0.709	0.140	0.53	0.079	0.41	0.06	1.4	1.1	0.21	0.12	200
Talhat Lihoudi		0.373	15.1	10.17	988	5.32	13.5	100	280	98	3290	5.40	13.8	8.3	2.44	0.876	0.49	1.91	0.270	1.95	0.26	3.0	1.4	1.08	0.38	198
Tichiya		0.415	14.1	14.03	948	6.07	20.4	160	293	120	4710	10.69	19.0	17.0	4.68	1.351	0.83	2.67	0.369	2.49	0.29	4.5	3.7	1.10	0.42	222
rock 004		0.322	13.9	35.6	2000	11.49	21.0	100	101	<190	60	3.76	9.5	6.1	1.69	0.664	0.38	1.92	0.284	1.36	0.19	3.0	*240*	0.76	0.20	47
rock 065		0.329	16.8	6.18	496	4.68	41.5	740	172	18	33	1.81	4.5	3.0	0.84	0.786	0.17	0.67	0.093	0.60	0.08	39.8	8.2	0.30	0.15	146
rock 087		0.363	16.6	7.30	544	3.96	15.1	170	176	51	82	2.87	7.6	4.6	1.34	0.810	0.28	1.03	0.148	1.01	0.12	7.5	3.2	0.49	0.15	167

Table S3a, continued

	note	Na_2O %	CaO %	Sc µg/g	Cr µg/g	FeO_T %	Co µg/g	Ni µg/g	Sr µg/g	Zr µg/g	Ba µg/g	La µg/g	Ce µg/g	Nd µg/g	Sm µg/g	Eu µg/g	Tb µg/g	Yb µg/g	Lu ppm	Hf µg/g	Ta µg/g	Ir ng/g	Au ng/g	Th µg/g	U µg/g	mass mg
rock 133		0.325	13.8	11.60	888	5.52	20.5	140	227	76	602	5.99	16.7	9.2	2.53	0.902	0.46	1.60	0.230	1.62	0.24	6.8	2.9	0.96	0.32	119
rock 142		0.310	14.7	9.64	537	5.64	13.5	39	190	34	308	1.52	3.7	2.4	0.75	0.728	0.16	0.64	0.095	0.46	0.06	1.9	1.3	0.17	0.12	119
Not from northern Africa																										
Calcalong Creek		0.434	13.6	22.3	1262	9.66	25.9	110	121	250	208	19.0	49.	29.0	8.59	1.06	1.76	6.71	0.920	6.77	0.90	3.4	3.1	3.95	1.10	208
EET 87521		0.403	12.8	34.2	1830	16.64	45.7	<200	103	98	70	6.96	18.0	12.0	3.41	0.839	0.718	2.55	0.350	2.57	0.30	<9	<11	1.00	0.28	373
EET 96008		0.387	11.9	37.2	1950	18.7	48.9	<170	97	100	69	7.06	18.5	11.0	3.43	0.799	0.722	2.60	0.363	2.62	0.30	0.1	0.2	0.90	0.21	504
GRA 6157		0.359	15.3	5.45	548	3.55	13.4	96	159	15	24	1.37	3.6	2.1	0.66	0.845	0.142	0.58	0.081	0.45	0.066	3.2	<4	0.23	0.07	57
Kalahari 008		0.561	15.4	10.89	710	4.67	10.8	61	200	<75	46	1.48	3.6	2.4	0.75	1.01	0.183	0.75	0.108	0.53	0.070	1.8	<3	0.17	0.11	278
Kalahari 009		0.485	11.6	53.2	2880	16.43	26.3	<250	117	<350	<130	0.95	2.4	<20	0.60	0.48	0.202	1.25	0.190	0.40	<0.3	<13	<12	<0.4	<1.1	265
LAP 02205		0.393	12.5	59.0	1960	22.3	36.3	<150	144	199	147	14.36	37.	24.	8.28	1.31	1.88	6.93	0.951	5.84	0.74	<3	<3	2.08	0.54	240
LAP 02224		0.370	12.8	58.6	2110	22.1	37.1	<150	135	200	152	13.06	35.	23.	7.75	1.24	1.82	6.65	0.921	5.70	0.72	<3	<3	2.18	0.57	189
LAP 02226		0.369	13.2	59.5	2060	21.8	35.7	<150	126	186	148	12.24	34.	22.	7.42	1.21	1.74	6.44	0.893	5.53	0.71	<3	<3	2.05	0.53	190
LAP 02436		0.354	12.9	60.7	2430	21.9	39.8	<150	121	170	132	11.35	31.	21.	6.80	1.13	1.63	5.90	0.821	4.90	0.61	<3	<3	1.83	0.45	191
LAP 03632		0.379	13.2	59.3	2040	22.2	36.3	<150	122	188	148	12.76	35.	23.	7.63	1.24	1.77	6.60	0.926	5.62	0.71	<3	<3	2.10	0.55	211
LAP 04841		0.379	12.8	58.5	2220	21.8	37.2	<150	130	194	151	12.52	33.	23.	7.18	1.21	1.73	6.31	0.907	5.43	0.66	<3	<3	2.05	0.54	250
LAR 06638		0.339	16.1	6.69	557	3.90	21.1	280	153	30	34	2.63	6.5	4.0	1.20	0.825	0.246	0.95	0.134	0.86	0.115	12.	3.7	0.42	0.22	282
Lynch 002	cont.	0.382	12.7	18.7	1583	8.98	46.3	270	168	180	784	35.1	121.	43	10.08	1.81	1.57	4.98	0.678	4.69	0.61	11.	5	5.08	0.72	232
MAC 88104/5		0.401	13.8	18.45	1500	9.35	34.7	222	212	147	274	7.38	18.8	11.9	3.39	0.921	0.679	2.36	0.333	2.62	0.30	6.8	*5.6*	1.10	0.438	4737
MET 01210		0.304	14.7	53.7	1620	16.03	26.6	180	147	89	79	5.39	14.6	9.8	3.60	1.03	0.852	3.36	0.474	2.66	0.37	7.1	<8	0.85	0.23	240
MIL 05035		0.295	13.2	92.6	1630	21.1	22.2	<400	<400	87	<160	3.13	8.2	<30	2.79	0.993	0.760	3.27	0.502	2.14	0.30	<5	<10	0.46	<0.9	423
MIL 07006		0.348	15.7	12.00	843	5.54	17.6	170	147	<70	31	2.21	5.7	3.5	1.12	0.801	0.249	0.99	0.140	0.84	0.102	6.6	<5	0.36	0.10	153
MIL 090034		0.372	16.7	6.62	474	3.40	8.1	45	159	24	26	1.80	4.7	3.0	0.86	0.839	0.183	0.70	0.099	0.62	0.076	1.9	<2	0.28	0.07	481
MIL 090036		0.618	15.5	9.77	658	5.01	17.8	220	198	150	131	11.11	29.	17.2	5.04	1.38	0.976	3.25	0.449	3.86	0.44	8.7	1.8	1.65	0.46	556
MIL 090070		0.374	16.7	6.29	433	3.26	8.1	43	161	27	27	2.15	5.4	3.3	0.98	0.860	0.202	0.78	0.110	0.66	0.082	2.4	<0.4	0.32	0.13	318
MIL 090075		0.388	16.6	6.90	520	3.70	11.1	83	162	94	78	6.78	17.2	10.4	3.02	0.941	0.613	2.22	0.305	2.31	0.26	3.0	<2.1	1.11	0.33	326
MIL 13317		0.603	12.4	22.4	1334	9.91	16.4	110	174	350	257	22.1	56.	34.	9.92	1.14	1.97	7.29	0.991	8.14	1.03	3.5	2.0	4.65	1.45	266
DEW 12007		0.407	12.2	26.0	1670	12.04	36.9	200	156	130	75	6.46	16.7	11.4	3.16	0.893	0.658	2.38	0.343	2.60	0.30	5.5	5.2	1.03	0.36	163
PCA02007		0.333	15.1	12.65	1074	6.26	29.2	350	147	36	34	2.55	6.9	4.2	1.27	0.763	0.282	1.12	0.157	0.94	0.135	17.	6.7	0.41	0.11	494
QUE 93069		0.344	16.3	7.60	595	4.38	22.6	310	158	42	40	3.19	8.3	5.0	1.50	0.819	0.317	1.16	0.163	1.12	0.142	13.	4.7	0.52	0.13	115
QUE 94281		0.396	12.7	28.9	1780	13.30	45.6	290	116	97	76	6.66	17.8	10.1	3.17	0.839	0.678	2.44	0.341	2.51	0.32	11.	2.9	1.02	0.26	464
Yamato 791197		0.328	15.2	12.91	914	5.91	19.1	180	149	41	31	2.35	6.1	3.7	1.16	0.757	0.270	1.01	0.147	0.86	0.11	6.6	2.1	0.32	0.11	138.
Yamato 82192		0.475	15.4	10.00	707	5.15	14.1	93	174	<80	23	1.12	2.9	1.9	0.61	0.972	0.145	0.69	0.100	0.43	0.056	2.9	<5	0.15	<0.4	101
Yamato 82193		0.429	15.4	8.37	703	4.36	15.4	160	166	<70	23	1.27	3.3	1.8	0.64	0.889	0.140	0.59	0.085	0.44	0.062	5.2	<5	0.20	<0.4	133
Yamato 86032		0.430	15.4	10.32	874	5.02	16.9	160	165	<70	23	1.28	3.4	2.1	0.66	0.889	0.148	0.68	0.098	0.49	0.068	5.6	<5	0.20	<0.3	263
Yamato 981031		0.416	13.0	24.8	1920	12.14	39.6	150	124	110	85	7.04	19.	11.9	3.37	0.907	0.692	2.53	0.353	2.63	0.37	3.4	<9	1.11	0.30	204
Yamato 983885		0.365	13.8	19.4	1493	8.56	40.3	530	130	120	116	9.32	24.	13.6	4.15	0.831	0.911	3.67	0.511	3.36	0.46	23.	8.1	2.10	0.55	107

Notes and Abbreviations

Except where noted (n.c. and REE), this summary table presents mass-weighted-mean concentration data determined by INAA for all analyzed subsamples of a stone. Data for individual subsamples, analytical and sampling uncertainties, elements determined imprecisely (Zn, As, Br, Ag, and Sb), number of subsamples, and sources of samples are presented in Table S2.

all	mean of all analyzed subsamples
br.	breccia lithology
ch.	chip samples
cl.	clast
cont.	severely contaminated by terrestrial weathering products
cor.	corrected for terrestrial calcite by assuming CaO/Al_2O_3 =0.819, the same as Apollo 12 regolith
dust	sawing "dust;" see Table S8 for all NWA 5000 sawdust data
FeO_T	total Fe as FeO
italic	contaminated with terrestrial Au and, for DaG 400/1058 and NWA 6687, Ca
m.b.	mare basalt lithology
n.a.	not analyzed
n.c.	exclude subsamples dominated by large feldspathic clasts
OA	Oued Awlitis
pair	pairing assumed based on similar composition and appearence
raw	raw data for NWA 6687, which is strongly contaminated with terrestrial calcite
REE	excludes 2 (of 9) subsamples that are rich in phosphate
R.S.	Rabt Sbayta
Tal. Lih.	Talhat Lihoudi

Table S3a is also provided as Table_S3a_INAA_stone_means.xls

Table S3b. Results of INAA: Mass-weighted mean concentrations of clans

clan	Na_2O	CaO	Sc	Cr	FeO_T	Co	Ni	Sr	Zr	Ba	La	Ce	Nd	Sm	Eu	Tb	Yb	Lu	Hf	Ta	Ir	Au	Th	U	mass	*N*
	%	%	μg/g	μg/g	%	μg/g	μg/g	mg/g	μg/g	μg/g	μg/g	μg/g	μg/g	μg/g	μg/g	μg/g	μg/g	μg/g	μg/g	μg/g	ng/g	ng/g	μg/g	μg/g	mg	
DaG 262	0.350	16.8	7.75	630	4.29	20.1	240	240	33	270	2.8	6.9	3.9	1.15	0.758	0.233	0.88	0.126	0.85	0.11	10.1	10	0.44	0.41	484	19
s	0.010	0.8	0.14	60	0.09	4.5	90	20	10	130	0.6	1.0	0.6	0.11	0.023	0.015	0.04	0.006	0.16	0.01	3.2	17	0.08	0.16		
95%	0.005	0.4	0.07	30	0.04	2.2	40	10	5	60	0.3	0.5	0.3	0.05	0.011	0.007	0.02	0.003	0.08	0.01	1.5	8	0.04	0.08		
DaG 400	0.343	18.4	5.5	440	3.1	11.2	100	290	17	270	1.44	3.8	2.3	0.68	0.713	0.142	0.55	0.077	0.48	0.061	3.9	2.1	0.22	0.30	744	23
s	0.022	1.2	1.0	90	0.6	2.0	30	60	5	280	0.33	0.8	0.5	0.15	0.039	0.033	0.12	0.017	0.12	0.014	1.6	1.1	0.05	0.22		
95%	0.010	0.5	0.4	40	0.3	0.9	10	30	2	120	0.14	0.3	0.2	0.07	0.017	0.014	0.05	0.008	0.05	0.006	0.7	0.5	0.02	0.09		
NWA 032	0.341	12.3	56.5	2730	22.3	42.5	60	130	192	270	11.4	30.1	20.1	6.62	1.11	1.60	5.85	0.825	5.03	0.63	<2	<11	1.89	0.48	398	18
s	0.016	0.8	2.7	320	0.5	3.3	30	20	23	80	0.5	1.3	2.1	0.28	0.06	0.07	0.24	0.037	0.23	0.04	0.5	2.6	0.11	0.08		
95%	0.008	0.4	1.4	160	0.3	1.6	20	10	11	40	0.3	0.7	1.0	0.14	0.03	0.04	0.12	0.018	0.11	0.02	0.5	1.3	0.05	0.04		
NWA 773	0.188	9.5	34.7	3420	19.9	70	140	70	159	170	10.8	28	17	5.1	0.49	1.05	3.6	0.50	3.9	0.47	0.5	9	1.6	0.46	2503	98
s	0.069	2.0	7.6	860	1.5	13	50	30	101	110	7.0	18	11	3.0	0.21	0.55	1.6	0.23	2.3	0.28	1.0	22	1.1	0.31		
95%	0.014	0.4	1.5	170	0.3	3	10	10	20	20	1.4	4	2	0.6	0.04	0.11	0.3	0.05	0.5	0.06	0.2	4	0.2	0.06		
NWA 2995	0.453	14.1	19.8	1660	10.2	39	240	150	124	160	9.7	26.0	14.6	4.3	1.04	0.84	2.91	0.40	3.2	0.37	10	12	1.49	0.40	2012	71
s	0.053	0.8	4.9	420	2.3	14	180	20	64	50	2.5	7.1	3.7	1.1	0.12	0.20	0.67	0.09	1.4	0.10	21	23	0.46	0.13		
95%	0.012	0.2	1.2	100	0.5	3	40	10	15	10	0.6	1.7	0.9	0.3	0.03	0.05	0.16	0.02	0.3	0.02	5	5	0.11	0.03		
NWA 2998	0.345	17.2	5.3	380	2.91	8.5	60	180	11	30	1.10	2.8	1.7	0.50	0.764	0.104	0.42	0.061	0.35	0.05	2.8	1.1	0.17	0.052	466	15
s	0.007	0.3	0.7	60	0.37	0.9	10	20	4	10	0.31	0.7	0.6	0.11	0.010	0.018	0.07	0.011	0.09	0.02	0.9	0.7	0.06	0.027		
95%	0.004	0.2	0.4	30	0.20	0.5	10	10	2	0	0.17	0.4	0.3	0.06	0.006	0.010	0.04	0.006	0.05	0.01	0.5	0.4	0.03	0.015		
NWA 3163	0.290	16.1	12.3	1020	5.4	12.9	50	140	14	50	0.88	2.38	1.3	0.51	0.664	0.122	0.55	0.081	0.32	0.039	1.7	0.7	0.109	0.042	1030	32
s	0.013	0.8	2.9	380	1.1	2.1	20	10	11	50	0.13	0.26	0.8	0.05	0.041	0.015	0.08	0.012	0.05	0.012	1.8	1.0	0.021	0.031		
95%	0.005	0.3	1.0	140	0.4	0.8	10	0	4	20	0.05	0.09	0.3	0.02	0.015	0.005	0.03	0.004	0.02	0.004	0.6	0.3	0.007	0.011		
NWA 4472	0.586	12.4	21.0	1570	9.4	31	200	210	429	500	37	95	57	16	1.46	3.4	11.9	1.64	11.0	1.50	11	2	6.8	1.92	750	23
s	0.041	0.6	1.5	70	0.7	47	450	40	43	160	21	56	33	9	0.10	1.7	3.7	0.44	0.8	0.17	46	7	1.3	0.24		
95%	0.018	0.2	0.6	30	0.3	20	190	20	19	70	9	24	14	4	0.04	0.7	1.6	0.19	0.4	0.07	20	3	0.6	0.10		
NWA 4936	0.52	14.5	9.5	810	6.0	41	590	200	187	190	13.6	35.3	21.2	6.3	1.42	1.21	4.06	0.56	4.8	0.61	17	13	1.96	0.52	1573	54
s	0.02	0.5	0.8	120	0.7	36	550	20	31	30	2.0	4.8	3.4	0.9	0.10	0.18	0.59	0.08	0.8	0.10	22	10	0.29	0.10		
95%	0.006	0.1	0.2	30	0.2	10	150	10	9	10	0.5	1.3	0.9	0.3	0.03	0.05	0.16	0.02	0.2	0.03	6	3	0.08	0.03		
NWA 5744	0.244	13.2	8.0	1380	5.7	21.8	100	140	16	150	0.82	2.14	1.73	0.40	0.559	0.090	0.38	0.056	0.26	0.04	1.7	1.3	0.10	0.12	1708	47
s	0.026	1.2	1.2	1300	1.0	4.8	30	40	10	110	0.31	0.61	0.63	0.11	0.049	0.021	0.08	0.012	0.15	0.01	1.0	1.2	0.06	0.27		
95%	0.008	0.4	0.4	380	0.3	1.4	10	10	3	30	0.09	0.18	0.18	0.03	0.014	0.006	0.02	0.004	0.04	0.00	0.3	0.4	0.02	0.08		
NWA 7611	0.375	12.7	29.9	1990	13.7	42.5	160	180	87	210	6.4	16.2	11.2	3.09	0.82	0.643	2.30	0.328	2.24	0.26	4.3	3.7	0.91	0.44	997	31
s	0.032	1.1	3.3	330	1.5	4.6	40	60	29	80	0.6	1.7	1.9	0.26	0.07	0.060	0.16	0.021	0.29	0.04	2.0	2.5	0.10	0.17		
95%	0.012	0.4	1.2	120	0.6	1.7	20	20	11	30	0.2	0.6	0.7	0.10	0.02	0.022	0.06	0.008	0.11	0.02	0.8	0.9	0.04	0.06		
NWA 7834	0.412	13.4	20.0	1630	10.1	37.7	230	200	127	430	8.1	20.7	13.0	3.71	0.943	0.742	2.57	0.363	2.86	0.324	6.7	6.1	1.20	0.48	4219	133
s	0.037	1.3	3.9	340	1.7	7.0	60	40	48	220	1.5	3.8	2.4	0.64	0.097	0.116	0.36	0.050	0.94	0.080	2.6	7.5	0.24	0.12		
95%	0.006	0.2	0.7	60	0.3	1.2	10	10	8	40	0.3	0.6	0.4	0.11	0.017	0.020	0.06	0.009	0.16	0.014	0.5	1.3	0.04	0.02		
NWA 8022	0.458	16.5	5.3	470	3.7	31	510	210	33	80	2.74	6.8	4.2	1.15	0.982	0.244	1.10	0.156	0.95	0.16	24	7.9	0.70	0.21	290	10
s	0.009	0.6	0.5	50	0.3	7	120	10	10	30	0.28	0.7	0.6	0.12	0.015	0.027	0.12	0.017	0.07	0.02	8	2.1	0.07	0.04		
95%	0.007	0.4	0.4	40	0.2	5	80	10	7	20	0.20	0.5	0.4	0.09	0.011	0.019	0.09	0.012	0.05	0.01	5	1.5	0.05	0.03		
NWA 8046	0.321	15.79	8.0	740	4.60	17.5	160	180	31	340	1.59	3.83	2.62	0.700	0.747	0.145	0.562	0.083	0.45	0.10	5.6	2.8	0.213	0.119	2865	81
s	0.012	0.75	1.2	70	0.49	4.0	100	30	11	240	0.39	0.74	0.71	0.103	0.031	0.019	0.059	0.009	0.11	0.27	5.9	2.4	0.058	0.056		
95%	0.003	0.17	0.3	20	0.11	0.9	20	10	2	50	0.09	0.16	0.16	0.023	0.007	0.004	0.013	0.002	0.02	0.06	1.3	0.5	0.013	0.012		
NWA 8222	0.365	17.32	7.2	460	3.60	10.0	90	210	28	200	1.44	3.6	2.5	0.67	0.816	0.141	0.55	0.080	0.41	0.056	4.1	2.2	0.22	0.15	1235	37
s	0.008	0.30	0.7	50	0.28	1.1	20	20	11	120	0.39	0.9	0.7	0.14	0.022	0.029	0.10	0.015	0.10	0.014	1.1	1.1	0.10	0.07		
95%	0.003	0.10	0.2	20	0.09	0.4	10	10	4	40	0.13	0.3	0.2	0.05	0.007	0.010	0.03	0.005	0.03	0.005	0.4	0.4	0.03	0.02		
NWA 8455	0.523	14.06	10.18	850	6.22	38.5	580	260	249	660	17.0	43.1	26.6	7.7	1.35	1.51	5.22	0.72	6.2	0.70	15.9	52	2.65	0.87	2378	76
s	0.064	0.72	0.65	80	0.55	8.7	190	50	89	290	2.1	5.8	3.3	0.9	0.09	0.19	0.65	0.09	1.8	0.09	6.6	182	0.38	0.18		
95%	0.015	0.17	0.15	20	0.12	2.0	40	10	20	70	0.5	1.3	0.8	0.2	0.02	0.04	0.15	0.02	0.4	0.02	1.5	42	0.09	0.04		

Table S3b, continued

clan	Na_2O	CaO	Sc	Cr	FeO_T	Co	Ni	Sr	Zr	Ba	La	Ce	Nd	Sm	Eu	Tb	Yb	Lu	Hf	Ta	Ir	Au	Th	U	mass	*N*
	%	%	μg/g	μg/g	%	μg/g	μg/g	mg/g	μg/g	μg/g	μg/g	μg/g	μg/g	μg/g	μg/g	μg/g	μg/g	μg/g	μg/g	μg/g	ng/g	ng/g	μg/g	μg/g	mg	
NWA 8641	0.480	15.2	10.24	760	5.13	17.8	210	250	91	950	6.37	16.0	10.5	2.88	1.072	0.565	1.97	0.274	2.21	0.25	7.7	5.1	0.93	0.32	1351	45
s	0.019	1.7	1.42	80	0.46	5.1	80	30	37	450	1.66	4.2	2.9	0.78	0.051	0.145	0.49	0.068	0.81	0.07	4.4	2.9	0.26	0.09		
95%	0.006	0.5	0.43	20	0.14	1.5	30	10	11	130	0.50	1.3	0.9	0.23	0.015	0.044	0.15	0.020	0.24	0.02	1.3	0.9	0.08	0.03		
NWA 8673	0.326	13.7	17.4	1390	8.0	44	560	200	77	890	5.1	12.8	8.1	2.27	0.723	0.48	1.93	0.277	1.74	0.23	23.0	9.6	1.02	0.49	2085	65
s	0.026	0.9	1.5	110	1.5	48	700	40	26	1050	1.2	3.0	2.0	0.51	0.035	0.10	0.37	0.052	0.40	0.05	22	15	0.22	0.15		
95%	0.006	0.2	0.4	30	0.4	12	170	10	6	260	0.3	0.7	0.5	0.13	0.009	0.03	0.09	0.013	0.10	0.01	5	4	0.05	0.04		
NWA 8701	0.45	15.4	19	960	6.6	13.6	100	250	126	170	11	25	15	4.2	0.89	0.9	4.0	0.56	3.6	0.5	4.3	2.9	3.2	1.4	632	20
s	0.08	0.7	8	260	1.9	1.5	40	60	88	120	8	19	10	2.8	0.09	0.6	2.8	0.40	2.6	0.4	1.5	1.6	2.9	0.9		
95%	0.036	0.3	4	120	0.9	0.7	20	30	41	60	4	9	4	1.3	0.04	0.3	1.3	0.18	1.2	0.2	0.7	0.8	1.4	0.4		
NWA 10141	0.313	16.5	7.40	580	3.99	14.0	140	290	51	1840	2.73	6.8	4.5	1.23	0.733	0.250	0.91	0.132	0.89	0.119	5.6	2.3	0.44	0.20	635	19
s	0.006	0.8	0.26	60	0.24	1.5	30	90	7	1280	0.35	0.7	0.6	0.11	0.019	0.026	0.08	0.011	0.10	0.018	1.4	0.6	0.06	0.05		
95%	0.003	0.4	0.12	30	0.11	0.7	10	40	3	620	0.17	0.3	0.3	0.05	0.009	0.012	0.04	0.006	0.05	0.008	0.7	0.3	0.03	0.02		
NWA 10495	0.36	15.7	12	720	5.0	10.7	50	260	35	3420	1.69	3.7	3.1	0.83	0.84	0.18	0.71	0.106	0.50	0.062	1.7	1.3	0.17	0.11	692	21
s	0.06	1.7	4	280	1.4	3.2	30	70	13	2750	0.40	0.9	0.8	0.22	0.16	0.06	0.26	0.039	0.18	0.026	1.1	0.8	0.05	0.05		
95%	0.03	0.8	2	130	0.6	1.4	10	30	6	1250	0.18	0.4	0.4	0.10	0.07	0.03	0.12	0.018	0.08	0.012	0.5	0.3	0.02	0.02		
NWA 10509	0.333	14.2	13.3	910	5.9	17.7	120	220	41	4680	2.5	6.1	4.1	1.09	0.752	0.229	0.89	0.131	0.70	0.095	4.0	2.0	0.38	0.15	1274	41
s	0.018	1.3	2.4	170	0.8	5.5	120	40	11	4510	0.7	2.1	1.3	0.25	0.055	0.047	0.15	0.022	0.17	0.019	3.1	1.0	0.12	0.07		
95%	0.006	0.4	0.7	50	0.3	1.7	40	10	3	1420	0.2	0.7	0.4	0.08	0.017	0.015	0.05	0.007	0.05	0.006	1.0	0.3	0.04	0.02		
NWA 11243	0.446	14.4	12.9	920	5.77	18.1	150	240	122	1610	7.4	18	12.3	3.6	1.07	0.71	2.6	0.36	2.6	0.30	4.2	3.5	1.22	0.45	322	10
s	0.016	0.4	0.9	80	0.25	2.0	20	20	30	870	1.0	3	1.8	0.5	0.07	0.11	0.4	0.06	0.6	0.06	1.1	0.9	0.25	0.11		
95%	0.011	0.3	0.7	60	0.18	1.4	20	10	21	620	0.7	2	1.3	0.4	0.05	0.08	0.3	0.04	0.4	0.05	0.8	0.7	0.18	0.08		
Rabt Sbayta 007	0.361	15.4	9.6	800	4.9	16.6	150	200	63	230	3.7	9.0	5.8	1.72	0.84	0.36	1.31	0.187	1.25	0.151	5.9	3.3	0.60	0.28	356	9
s	0.024	0.5	0.7	70	0.3	1.1	10	20	13	160	0.4	1.1	0.6	0.18	0.03	0.03	0.12	0.016	0.16	0.014	0.9	2.0	0.07	0.10		
95%	0.019	0.4	0.6	50	0.2	0.8	10	20	10	124	0.3	0.9	0.5	0.14	0.02	0.03	0.09	0.012	0.12	0.011	0.7	1.5	0.05	0.07		

Notes and Abbreviations

FeO_T total Fe as FeO
s sample standard deviation
95% 95% confidence limit
N number of subsamples averaged

Table S3b is also provided as Table_S3b_INAA_clan_means.xls

Table S4. Results of EPMA of fused beads: Major-element data

plot	stone	data	SiO_2	TiO_2	Al_2O_3	Cr_2O_3	FeO_T[5]	MnO	MgO	CaO	Na_2O[6]	K_2O	P_2O_5	SO_3	Σ	*Mg'*	*N* [3]	analyst	note	ref.
2	DaG 262	INAA[2]	n.a.	n.a.	n.a.	0.094	4.38	n.a.	n.a.	16.7	0.349	n.a.	n.a.	n.a.	n.a.	n.a.				1
2	DaG 262	FB	43.79	0.20	28.38	0.08	4.47	0.06	5.50	17.10	0.350	0.052	0.060	n.a.	100.04	68.7	15	RAZ		
2	DaG 262	unc.	0.13	0.05	0.11	0.04	0.06	0.03	0.07	0.07	0.020	0.006	0.011	n.a.	0.16	0.2				
4	DaG 400	INAA[2]	n.a.	n.a.	n.a.	0.073	3.38	n.a.	n.a.	18.1	0.349	n.a.	n.a.	n.a.	n.a.	n.a.			8	
4	DaG 400	FB	43.48	0.18	28.83	0.08	3.62	0.07	4.62	18.44	0.341	0.090	0.220	n.a.	99.97	69.5	12	RAZ	8	1
4	DaG 400	unc.	0.19	0.04	0.11	0.04	0.09	0.04	0.03	0.07	0.024	0.005	0.037	n.a.	0.17	0.5				
2	DaG 996	INAA[2]	n.a.	n.a.	n.a.	0.090	4.25	n.a.	n.a.	16.0	0.357	n.a.	n.a.	n.a.	n.a.	n.a.				
2	DaG 996	FB	43.95	0.19	27.64	0.11	4.37	0.067	5.53	16.97	0.331	0.051	0.250	n.a.	99.46	69.3	29	RAZ		
2	DaG 996	unc.	0.17	0.03	0.09	0.02	0.05	0.013	0.03	0.06	0.016	0.006	0.017	n.a.	0.20	0.3				
¿	Galb Inal	INAA[2]	n.a.	n.a.	n.a.	0.212	9.86	n.a.	n.a.	15.1	0.450	n.a.	n.a.	n.a.	n.a.	n.a.				
¿	Galb Inal	FB	45.4	0.54	21.7	0.179	9.22	0.132	7.70	14.20	0.432	0.082	0.092	0.161	99.89	59.9	20	AW		
¿	Galb Inal	unc.	0.4	0.04	0.5	0.013	0.51	0.013	0.12	0.16	0.015	0.004	0.014	0.015	0.34	1.3				
8	Kalahari 008	INAA[2]	n.a.	n.a.	n.a.	0.104	4.67	n.a.	n.a.	15.4	0.561	n.a.	n.a.	n.a.	n.a.	n.a.				
8	Kalahari 008	FB	45.88	0.27	29.03	0.13	4.54	0.069	4.48	15.18	0.620	0.140	0.033	n.a.	100.47	63.7	44	RAZ	7	2
8	Kalahari 008	unc.[4]	0.11	0.03	0.28	0.03	0.10	0.012	0.09	0.08	0.019	0.007	0.008	n.a.	0.09	0.2				
9	Kalahari 009	INAA[2]	n.a.	n.a.	n.a.	0.421	16.43	n.a.	n.a.	11.6	0.485	n.a.	n.a.	n.a.	n.a.	n.a.				
9	Kalahari 009	FB	48.1	0.51	15.7	0.358	15.29	0.242	7.86	11.32	0.522	0.164	0.17	n.a.	100.24	47.9	57	RAZ	7	2
9	Kalahari 009	unc.[4]	0.2	0.05	0.8	0.014	0.50	0.012	0.20	0.13	0.017	0.004	0.05	n.a.	0.09	0.5				
1	NEA 001	INAA[2]	n.a.	n.a.	n.a.	0.121	5.29	n.a.	n.a.	17.0	0.337	n.a.	n.a.	n.a.	n.a.	n.a.				
1	NEA 001	FB	43.92	0.266	26.52	0.121	5.58	0.079	5.67	17.64	0.325	0.053	0.051	n.a.	100.23	64.4	117	RAZ		
1	NEA 001	unc.[4]	0.13	0.014	0.19	0.008	0.11	0.007	0.10	0.21	0.008	0.003	0.006	n.a.	0.07	0.6				
3	NEA 003 RB	INAA[2]	n.a.	n.a.	n.a.	0.508	24.92	n.a.	n.a.	11.4	0.201	n.a.	n.a.	n.a.	n.a.	n.a.				
3	NEA 003 RB	FB	44.74	1.82	4.6	0.560	24.86	0.328	13.01	9.95	0.164	0.039	0.069	n.a.	100.10	48.2	88	RAZ		
3	NEA 003 RB	unc.[4]	0.18	0.08	0.32	0.016	0.37	0.009	0.25	0.16	0.018	0.003	0.006	n.a.	0.06	0.2				
A	NWA 032	INAA[2]	n.a.	n.a.	n.a.	0.401	22.12	n.a.	n.a.	n.a.	0.347	n.a.	n.a.	n.a.	n.a.	n.a.				
A	NWA 032	FB	45.1	3.04	9.42	0.365	22.03	0.287	7.90	10.69	0.341	0.091	0.088	n.a.	99.35	38.7	48	RAZ		
A	NWA 032	unc.[4]	0.2	0.08	0.18	0.016	0.24	0.014	0.40	0.20	0.009	0.005	0.009	n.a.	0.09	0.94				
A	NWA 479	INAA[2]	n.a.	n.a.	n.a.	0.398	22.42	n.a.	n.a.	n.a.	0.336	n.a.	n.a.	n.a.	n.a.	n.a.				
A	NWA 479	FB	45.47	3.04	9.12	0.35	22.38	0.292	7.93	10.47	0.336	0.106	0.101	n.a.	99.58	38.6	31	RAZ		
A	NWA 479	unc.[4]	0.17	0.04	0.25	0.03	0.28	0.013	0.26	0.08	0.028	0.006	0.009	n.a.	0.12	0.5				
B	NWA 482	INAA[2]	n.a.	n.a.	n.a.	0.076	3.76	n.a.	n.a.	17.1	0.377	n.a.	n.a.	n.a.	n.a.	n.a.				1
B	NWA 482	FB	43.81	0.16	29.35	0.41	3.79	0.05	4.28	18.43	0.26	0.035	0.041	n.a.	100.32	66.8	14	RAZ		
B	NWA 482	unc.[4]	0.13	0.10	0.10	0.04	0.04	0.04	0.04	0.10	0.02	0.009	0.010	n.a.	0.18	0.3				
D	NWA 2200	INAA[2]	n.a.	n.a.	n.a.	0.074	3.95	n.a.	n.a.	16.8	0.330	n.a.	n.a.	n.a.	n.a.	n.a.				
D	NWA 2200	FB	44.52	0.17	30.12	0.072	3.66	0.046	3.49	17.37	0.282	0.039	0.030	n.a.	99.79	63.0	38	RAZ		
D	NWA 2200	unc.[4]	0.16	0.03	0.10	0.015	0.03	0.010	0.03	0.05	0.013	0.005	0.010	n.a.	0.15	0.2				
E	NWA 2995	INAA[2]	n.a.	n.a.	n.a.	0.227	9.80	n.a.	n.a.	13.9	0.467	n.a.	n.a.	n.a.	n.a.	n.a.				
E	NWA 2995	FB	46.21	0.61	20.65	0.229	9.69	0.140	8.11	13.52	0.470	0.177	0.140	n.a.	99.95	59.9	67	RAZ	7	2
E	NWA 2995	unc.[4]	0.10	0.03	0.32	0.012	0.19	0.009	0.07	0.06	0.013	0.020	0.011	n.a.	0.07	0.3				

Table S4, continued

plot	stone	data	SiO_2	TiO_2	Al_2O_3	Cr_2O_3	FeO_T[5]	MnO	MgO	CaO	Na_2O[6]	K_2O	P_2O_5	SO_3	Σ	*Mg*'	*N* [3]	analyst	note	ref.
E	NWA 2996	INAA[2]	n.a.	n.a.	n.a.	0.231	9.70	n.a.	n.a.	14.7	0.475	n.a.	n.a.	n.a.	n.a.	n.a.				
E	NWA 2996	FB	45.64	0.75	20.59	0.248	10.01	0.151	8.31	13.66	0.46	0.138	0.122	n.a.	100.08	59.8	63	RAZ	7	2
E	NWA 2996	unc.[4]	0.25	0.08	0.71	0.020	0.58	0.014	0.44	0.33	0.03	0.024	0.012	n.a.	0.10	0.2				
F	NWA 2998	INAA[2]	n.a.	n.a.	n.a.	0.052	2.67	n.a.	n.a.	17.4	0.344	n.a.	n.a.	n.a.	n.a.	n.a.				
F	NWA 2998	FB	44.14	0.110	31.75	0.049	2.68	0.043	2.48	18.37	0.347	0.030	0.028	n.a.	100.03	62.2	29	RAZ		
F	NWA 2998	unc.[4]	0.05	0.013	0.35	0.007	0.18	0.009	0.18	0.11	0.011	0.002	0.005	n.a.	0.10	0.2				
G	NWA 3136	INAA[2]	n.a.	n.a.	n.a.	0.419	15.36	n.a.	n.a.	n.a.	0.295	n.a.	n.a.	n.a.	n.a.	n.a.				
G	NWA 3136	FB	46.07	1.23	13.87	0.424	15.24	0.249	10.41	11.66	0.304	0.102	0.062	n.a.	99.63	54.9	48	RAZ	7	2
G	NWA 3136	unc.[4]	0.13	0.03	0.09	0.017	0.10	0.012	0.07	0.07	0.011	0.004	0.007	n.a.	0.11	0.3				
H	NWA 3163	INAA[2]	n.a.	n.a.	n.a.	0.150	5.84	n.a.	n.a.	15.8	0.288	n.a.	n.a.	n.a.	n.a.	n.a.				
H	NWA 3163	FB	45.4	0.21	25.3	0.16	7.08	0.112	6.13	15.32	0.268	0.022	0.019	n.a.	100.03	60.7	39	RAZ	13	
H	NWA 3163	unc.[4]	0.3	0.03	0.8	0.02	0.52	0.011	0.45	0.32	0.008	0.004	0.007	n.a.	0.14	0.2				
I	NWA 4472	INAA[2]	n.a.	n.a.	n.a.	0.225	9.25	n.a.	n.a.	n.a.	0.612	n.a.	n.a.	n.a.	n.a.	n.a.				
I	NWA 4472	FB	47.86	1.25	17.54	0.246	9.69	0.138	9.62	12.12	0.601	0.412	0.257	n.a.	99.74	63.9	69	RAZ	7	2
I	NWA 4472	unc.[4]	0.10	0.04	0.11	0.012	0.05	0.009	0.08	0.03	0.013	0.010	0.008	n.a.	0.08	0.2				
I	NWA 4485	INAA[2]	n.a.	n.a.	n.a.	0.233	9.51	n.a.	n.a.	n.a.	0.573	n.a.	n.a.	n.a.	n.a.	n.a.				
I	NWA 4485	FB	47.90	1.17	18.16	0.228	9.34	0.137	9.03	12.08	0.606	0.431	0.248	n.a.	99.34	63.3	76	RAZ	7	2
I	NWA 4485	unc.[4]	0.13	0.05	0.21	0.011	0.10	0.008	0.11	0.07	0.014	0.011	0.012	n.a.	0.05	0.4				
J	NWA 4734	INAA[2]	n.a.	n.a.	n.a.	0.327	21.78	n.a.	n.a.	n.a.	0.377	n.a.	n.a.	n.a.	n.a.	n.a.				
J	NWA 4734	FB	46.11	2.83	8.44	0.306	21.64	0.300	7.98	11.06	0.34	0.116	0.11	n.a.	99.25	39.5	25	RAZ		
J	NWA 4734	unc.[4]	0.45	0.35	0.80	0.019	0.72	0.015	0.54	0.27	0.03	0.014	0.02	n.a.	0.09	1.2				
N	NWA 4819	INAA[2]	n.a.	n.a.	n.a.	0.208	7.03	n.a.	n.a.	14.9	0.363	n.a.	n.a.	n.a.	n.a.	n.a.				
N	NWA 4819	FB	46.3	0.36	22.05	0.209	6.90	0.104	7.40	16.30	0.374	0.151	0.087	n.a.	100.24	65.7	54	RAZ	7	2
N	NWA 4819	unc.[4]	0.2	0.03	0.12	0.014	0.05	0.010	0.03	0.37	0.013	0.007	0.010	n.a.	0.11	0.1				
H	NWA 4881	INAA[2]	n.a.	n.a.	n.a.	0.194	6.00	n.a.	n.a.	15.9	0.283	n.a.	n.a.	n.a.	n.a.	n.a.				
H	NWA 4881	FB	45.6	0.213	25.8	0.165	6.02	0.103	5.91	15.74	0.277	0.030	0.045	n.a.	99.84	63.2	64	RAZ		
H	NWA 4881	unc.[4]	0.3	0.019	1.0	0.025	0.51	0.010	0.58	0.42	0.008	0.002	0.005	n.a.	0.14	0.3				
L	NWA 4884	INAA[2]	n.a.	n.a.	n.a.	0.300	13.72	n.a.	n.a.	n.a.	0.366	n.a.	n.a.	n.a.	n.a.	n.a.				
L	NWA 4884	FB	46.69	0.613	16.27	0.300	13.86	0.192	9.29	12.26	0.366	0.064	0.068	n.a.	99.98	54.4	42	RAZ	7	2
L	NWA 4884	unc.[4]	0.15	0.012	0.21	0.028	0.19	0.007	0.13	0.09	0.008	0.002	0.005	n.a.	0.09	0.3				
M	NWA 4898	INAA[2]	n.a.	n.a.	n.a.	0.442	17.17	n.a.	n.a.	n.a.	0.296	n.a.	n.a.	n.a.	n.a.	n.a.				
M	NWA 4898	FB	46.85	2.54	11.75	0.46	18.05	0.268	8.00	11.29	0.290	0.045	0.038	n.a.	99.58	44.1	21	RAZ	7	
M	NWA 4898	unc.[4]	0.14	0.14	0.40	0.04	0.31	0.013	0.17	0.08	0.010	0.004	0.006	n.a.	0.15	0.7				
K	NWA 4932	INAA[2]	n.a.	n.a.	n.a.	0.219	8.55	n.a.	n.a.	13.5	0.307	n.a.	n.a.	n.a.	n.a.	n.a.				2
K	NWA 4932	FB	45.10	0.33	21.34	0.21	8.82	0.129	9.56	12.87	0.316	0.112	0.056	n.a.	98.85	65.9	10	RAZ	7	
K	NWA 4932	unc.[4]	0.15	0.03	0.95	0.02	0.54	0.016	0.61	0.27	0.016	0.014	0.012	n.a.	0.24	0.3				
O	NWA 4936	INAA[2]	n.a.	n.a.	n.a.	0.114	5.94	n.a.	n.a.	14.4	0.512	n.a.	n.a.	n.a.	n.a.	n.a.				
O	NWA 4936	FB	44.74	0.685	25.96	0.104	5.49	0.073	7.17	14.80	0.517	0.128	0.134	n.a.	99.80	69.9	60	RAZ	7	2
O	NWA 4936	unc.[4]	0.05	0.014	0.15	0.005	0.07	0.005	0.15	0.09	0.007	0.003	0.008	n.a.	0.07	0.2				

Table S4, continued

plot	stone	data	SiO_2	TiO_2	Al_2O_3	Cr_2O_3	FeO_T[5]	MnO	MgO	CaO	Na_2O[6]	K_2O	P_2O_5	SO_3	Σ	*Mg'*	*N* [3]	analyst	note	ref.
P	NWA 5000 sd	INAA[2]	n.a.	n.a.	n.a.	0.114	5.75	n.a.	n.a.	15.0	0.441	n.a.	n.a.	n.a.	n.a.	n.a.				
P	NWA 5000 sd	FB	45.29	0.359	26.86	0.113	4.62	0.073	6.77	15.47	0.444	0.066	0.041	n.a.	100.10	72.4	37	RAZ	9	
P	NWA 5000 sd	unc.[4]	0.13	0.017	0.20	0.008	0.23	0.007	0.14	0.08	0.007	0.002	0.007	n.a.	0.19	1.0				
Q	NWA 5153	INAA[2]	n.a.	n.a.	n.a.	0.287	12.72	n.a.	n.a.	n.a.	0.476	n.a.	n.a.	n.a.	n.a.	n.a.				
Q	NWA 5153	FB	46.3	0.71	16.88	0.257	13.10	0.184	8.86	12.73	0.464	0.103	0.097	n.a.	99.67	54.7	45	RAZ	7	2
Q	NWA 5153	unc.[4]	0.3	0.10	0.55	0.010	0.37	0.009	0.23	0.12	0.011	0.006	0.010	n.a.	0.16	0.9				
R	NWA 5207	INAA[2]	n.a.	n.a.	n.a.	0.156	7.56	n.a.	n.a.	14.9	0.484	n.a.	n.a.	n.a.	n.a.	n.a.				
R	NWA 5207	FB	46.01	0.527	23.92	0.149	7.52	0.105	6.83	14.38	0.484	0.094	0.068	n.a.	100.10	61.9	31	RAZ	7	2
R	NWA 5207	unc.[4]	0.12	0.014	0.26	0.008	0.23	0.007	0.06	0.08	0.009	0.006	0.005	n.a.	0.11	0.6				
O	NWA 5406	INAA[2]	n.a.	n.a.	n.a.	0.112	5.82	n.a.	n.a.	14.4	0.546	n.a.	n.a.	n.a.	n.a.	n.a.				
O	NWA 5406	FB	44.91	0.716	25.45	0.111	5.80	0.070	7.72	14.50	0.524	0.120	0.133	n.a.	100.06	70.4	28	RAZ		
O	NWA 5406	unc.[4]	0.07	0.018	0.06	0.008	0.07	0.005	0.03	0.06	0.008	0.002	0.009	n.a.	0.10	0.2				
S	NWA 5744	INAA[2]	n.a.	n.a.	n.a.	0.158	5.97	n.a.	n.a.	13.9	0.244	n.a.	n.a.	n.a.	n.a.	n.a.				
S	NWA 5744	FB	43.93	0.158	22.83	0.158	5.72	0.084	12.69	14.05	0.213	0.038	0.023	n.a.	99.89	79.8	30	RAZ		
S	NWA 5744	unc.[4]	0.07	0.009	0.05	0.007	0.02	0.007	0.04	0.06	0.009	0.002	0.004	n.a.	0.09	0.1				
S	NWA 5744 pair	INAA[2]	n.a.	n.a.	n.a.	0.177	5.91	n.a.	n.a.	13.1	0.245	n.a.	n.a.	n.a.	n.a.	n.a.				
S	NWA 5744 pair	FB	45.14	0.169	22.93	0.157	6.10	0.091	12.37	12.85	0.242	0.023	0.034	0.091	100.20	78.3	20	AW		
S	NWA 5744 pair	unc.[4]	0.14	0.008	0.32	0.008	0.18	0.012	0.27	0.15	0.009	0.004	0.010	0.012	0.14	0.3				
E	NWA 6252	INAA[2]	n.a.	n.a.	n.a.	0.313	12.95	n.a.	n.a.	13.7	0.386	n.a.	n.a.	n.a.	n.a.	n.a.				
E	NWA 6252	FB	45.7	0.58	17.12	0.293	12.73	0.22	9.17	12.73	0.391	0.105	0.082	0.115	99.27	56.2	19	AW		
E	NWA 6252	unc.[4]	0.2	0.03	0.54	0.019	0.27	0.02	0.21	0.12	0.011	0.009	0.017	0.015	0.11	0.4				
H	NWA 6275	INAA[2]	n.a.	n.a.	n.a.	0.073	3.40	n.a.	n.a.	17.5	0.312	n.a.	n.a.	n.a.	n.a.	n.a.				
H	NWA 6275	FB	44.11	0.15	32.27	0.068	3.12	0.045	2.56	17.35	0.305	0.020	0.014	0.034	100.04	59.4	18	AW		
H	NWA 6275	unc.[4]	0.15	0.03	0.42	0.012	0.22	0.011	0.18	0.15	0.012	0.006	0.009	0.015	0.25	0.4				
T	NWA 6481	INAA[2]	n.a.	n.a.	n.a.	0.108	4.74	n.a.	n.a.	15.9	0.479	n.a.	n.a.	n.a.	n.a.	n.a.				
T	NWA 6481	FB	44.34	0.342	27.28	0.096	4.77	0.075	5.89	15.87	0.505	0.056	0.056	n.a.	99.29	68.7	20	AW		
T	NWA 6481	unc.[4]	0.13	0.018	0.16	0.009	0.12	0.015	0.08	0.13	0.011	0.008	0.013	n.a.	0.17	0.3				
E	NWA 6554	INAA[2]	n.a.	n.a.	n.a.	0.310	11.32	n.a.	n.a.	n.a.	0.442	n.a.	n.a.	n.a.	n.a.	n.a.				
E	NWA 6554	FB	45.18	0.545	19.79	0.26	10.94	0.156	9.54	12.73	0.461	0.089	0.091	0.132	99.90	60.9	20	AW		
E	NWA 6554	unc.[4]	0.21	0.02	0.48	0.02	0.43	0.016	0.13	0.20	0.011	0.007	0.015	0.015	0.29	0.7				
E	NWA 6555	INAA[2]	n.a.	n.a.	n.a.	0.257	12.32	n.a.	n.a.	n.a.	0.386	n.a.	n.a.	n.a.	n.a.	n.a.				
E	NWA 6555	FB	45.60	0.56	18.77	0.243	11.58	0.183	8.63	12.95	0.387	0.085	0.092	0.138	99.20	57.2	17	AW		
E	NWA 6555	unc.[4]	0.08	0.02	0.86	0.027	0.80	0.016	0.23	0.20	0.013	0.005	0.022	0.015	0.08	1.1				
U	NWA 6578	INAA[2]	n.a.	n.a.	n.a.	0.087	4.18	n.a.	n.a.	16.9	0.324	n.a.	n.a.	n.a.	n.a.	n.a.				
U	NWA 6578	FB	43.77	0.224	29.02	0.082	4.37	0.061	4.03	17.56	0.339	0.097	0.030	n.a.	99.59	62.2	20	AW		
U	NWA 6578	unc.[4]	0.07	0.010	0.10	0.006	0.06	0.010	0.05	0.09	0.011	0.006	0.011	n.a.	0.11	0.2				
v	NWA 6687r	INAA[2]	n.a.	n.a.	n.a.	0.223	16.30	n.a.	n.a.	n.a.	0.515	n.a.	n.a.	n.a.	n.a.	n.a.				
v	NWA 6687r	FB	40.8	3.59	11.27	0.224	17.09	0.223	7.54	16.28	0.522	0.379	0.38	0.38	98.67	44.1	20	AW		
v	NWA 6687r	unc.[4]	0.6	0.14	0.14	0.010	0.51	0.013	0.06	1.29	0.012	0.011	0.03	0.02	0.15	0.7				

Table S4, continued

plot	stone	data	SiO_2	TiO_2	Al_2O_3	Cr_2O_3	FeO_T[5]	MnO	MgO	CaO	Na_2O[6]	K_2O	P_2O_5	SO_3	Σ	*Mg*'	*N* [3]	analyst	note	ref.
V	NWA 6687c	INAA[2]	n.a.	n.a.	n.a.	0.242	17.72	n.a.	n.a.	n.a.	0.560	n.a.	n.a.	n.a.	n.a.	n.a.			10	
V	NWA 6687c	FB	43.92	3.86	11.99	0.242	18.39	0.240	8.10	9.94	0.563	0.409	0.41	0.41	98.67	44.1	20	AW	10	
V	NWA 6687c	unc.[4]	0.15	0.11	0.12	0.011	0.31	0.013	0.13	0.11	0.013	0.014	0.03	0.03	0.15	0.7				
W	NWA 6721	INAA[2]	n.a.	n.a.	n.a.	0.107	4.96	n.a.	n.a.	15.6	0.457	n.a.	n.a.	n.a.	n.a.	n.a.				
W	NWA 6721	FB	44.25	0.307	28.51	0.101	5.00	0.092	4.63	15.55	0.48	0.115	0.054	n.a.	99.09	62.3	20	AW		
W	NWA 6721	unc.[4]	0.07	0.013	0.09	0.007	0.07	0.014	0.03	0.09	0.02	0.007	0.012	n.a.	0.11	0.2				
X	NWA 6888	INAA[2]	n.a.	n.a.	n.a.	0.132	5.66	n.a.	n.a.	14.2	0.460	n.a.	n.a.	n.a.	n.a.	n.a.				
X	NWA 6888	FB	45.90	0.34	26.68	0.125	5.80	0.11	4.94	14.46	0.482	0.166	0.051	n.a.	99.05	60.3	16	AW		
X	NWA 6888	unc.[4]	0.06	0.03	0.41	0.009	0.34	0.02	0.28	0.17	0.014	0.008	0.015	n.a.	0.12	0.2				
Y	NWA 7022 m	INAA[2]	n.a.	n.a.	n.a.	0.099	5.31	n.a.	n.a.	15.2	0.603	n.a.	n.a.	n.a.	n.a.	n.a.				
Y	NWA 7022 m	FB	45.08	0.57	26.75	0.103	5.14	0.057	5.79	15.07	0.565	0.111	0.066	n.a.	99.29	66.8	15	AW	11	
Y	NWA 7022 m	unc.[4]	0.11	0.05	0.26	0.012	0.24	0.012	0.19	0.09	0.032	0.008	0.017	n.a.	0.10	0.33				
Y	NWA 7022 c	INAA[2]	n.a.	n.a.	n.a.	0.107	6.29	n.a.	n.a.	15.0	0.711	n.a.	n.a.	n.a.	n.a.	n.a.				
Y	NWA 7022 c	FB	45.89	0.87	25.35	0.100	6.38	0.083	4.95	14.74	0.61	0.118	0.16	n.a.	99.25	58.0	11	AW	11	
Y	NWA 7022 c	unc.[4]	0.18	0.05	0.18	0.011	0.11	0.019	0.06	0.09	0.06	0.015	0.03	n.a.	0.28	0.3				
f	NWA 7262	INAA	n.a.	n.a.	n.a.	0.059	3.13	n.a.	n.a.	17.0	0.347	n.a.	n.a.	n.a.	n.a.	n.a.				
f	NWA 7262	FB	43.81	0.14	31.94	0.060	2.98	0.055	2.78	17.72	0.343	0.044	0.021	0.060	99.95	62.4	20	AW		
f	NWA 7262	unc.[4]	0.15	0.02	0.26	0.015	0.13	0.010	0.12	0.08	0.007	0.006	0.010	0.007	0.12	0.4				
Z	NWA 7274	INAA[2]	n.a.	n.a.	n.a.	0.153	6.07	n.a.	n.a.	15.0	0.368	n.a.	n.a.	n.a.	n.a.	n.a.				
Z	NWA 7274	FB	44.3	0.391	24.81	0.149	6.08	0.098	8.09	15.11	0.360	0.142	0.112	0.133	99.74	70.4	35	AW		
Z	NWA 7274	unc.[4]	0.3	0.013	0.13	0.010	0.10	0.009	0.08	0.17	0.008	0.004	0.015	0.009	0.27	0.3				
[	NWA 7493	INAA[2]	n.a.	n.a.	n.a.	0.085	4.37	n.a.	n.a.	16.5	0.336	n.a.	n.a.	n.a.	n.a.	n.a.				
[	NWA 7493	FB	44.03	0.246	29.22	0.091	4.57	0.085	4.29	16.64	0.328	0.040	0.053	n.a.	99.60	62.5	37	AW		
[	NWA 7493	unc.[4]	0.10	0.018	0.22	0.008	0.09	0.010	0.14	0.08	0.014	0.005	0.011	n.a.	0.10	0.7				
L	NWA 7611	INAA[2]	n.a.	n.a.	n.a.	0.257	12.11	n.a.	n.a.	n.a.	0.398	n.a.	n.a.	n.a.	n.a.	n.a.				
L	NWA 7611	FB	46.6	0.57	17.87	0.280	12.42	0.180	8.75	12.67	0.389	0.070	0.080	n.a.	99.88	55.7	40	AW		
L	NWA 7611	unc.[4]	0.2	0.02	0.62	0.015	0.46	0.008	0.25	0.18	0.010	0.004	0.009	n.a.	0.15	0.4				
®	NWA 7834	INAA[2]	n.a.	n.a.	n.a.	0.234	9.86	n.a.	n.a.	14.1	0.399	n.a.	n.a.	n.a.	n.a.	n.a.				
®	NWA 7834	FB	45.5	0.53	20.25	0.225	10.45	0.152	8.62	13.50	0.400	0.097	0.14	0.129	100.01	60.1	38	AW		
®	NWA 7834	unc.[4]	0.3	0.03	1.38	0.027	0.96	0.011	0.47	0.34	0.015	0.004	0.03	0.014	0.19	1.1				
#	NWA 7931	INAA[2]	n.a.	n.a.	n.a.	0.173	7.54	n.a.	n.a.	14.8	0.336	n.a.	n.a.	n.a.	n.a.	n.a.				
#	NWA 7931	FB	44.39	0.400	24.99	0.176	7.34	0.108	6.24	15.25	0.329	0.062	0.054	0.194	99.54	60.3	20	AW		
#	NWA 7931	unc.[4]	0.11	0.011	0.07	0.014	0.06	0.009	0.04	0.08	0.008	0.003	0.015	0.018	0.10	0.3				
®	NWA 7948	INAA[2]	n.a.	n.a.	n.a.	0.234	9.56	n.a.	n.a.	13.2	0.400	n.a.	n.a.	n.a.	n.a.	n.a.				
®	NWA 7948	FB	44.87	0.48	21.15	0.232	9.34	0.127	9.06	13.58	0.393	0.072	0.086	0.148	99.54	63.6	30	AW		
®	NWA 7948	unc.[4]	0.08	0.02	0.94	0.024	0.72	0.013	0.48	0.37	0.008	0.006	0.013	0.010	0.10	0.7				
©	NWA 7959	INAA	n.a.	n.a.	n.a.	0.069	3.35	n.a.	n.a.	16.7	0.336	n.a.	n.a.	n.a.	n.a.	n.a.				
©	NWA 7959	FB	43.34	0.151	29.91	0.064	3.53	0.054	5.14	17.44	0.356	0.054	0.070	0.118	100.23	72.2	19	AW		
©	NWA 7959	unc.[4]	0.09	0.008	0.15	0.005	0.16	0.008	0.06	0.07	0.008	0.004	0.012	0.012	0.16	0.7				

Table S4, continued

plot	stone	data	SiO_2	TiO_2	Al_2O_3	Cr_2O_3	FeO_T[5]	MnO	MgO	CaO	Na_2O[6]	K_2O	P_2O_5	SO_3	Σ	*Mg*'	*N* [3]	analyst	note	ref.
@	NWA 8001	INAA[2]	n.a.	n.a.	n.a.	0.095	4.74	n.a.	n.a.	15.9	0.393	n.a.	n.a.	n.a.	n.a.	n.a.	10	AW	12	
@	NWA 8001	FB	44.28	0.376	28.19	0.097	4.85	0.07	4.92	16.15	0.412	0.144	0.08	0.172	99.72	64.4				
@	NWA 8001	unc.[4]	0.15	0.019	0.19	0.015	0.05	0.03	0.4	0.05	0.014	0.006	0.03	0.017	0.11	0.3				
/	NWA 8010	INAA[2]	n.a.	n.a.	n.a.	0.125	5.83	n.a.	n.a.	15.0	0.476	n.a.	n.a.	n.a.	n.a.	n.a.				
/	NWA 8010	FB	44.5	0.60	24.32	0.134	6.59	0.094	7.59	14.69	0.531	0.265	0.27	0.14	99.72	67.2	20	AW	12	
/	NWA 8010	unc.[4]	0.2	0.04	0.32	0.012	0.21	0.016	0.26	0.35	0.027	0.020	0.04	0.03	0.24	0.3				
$	NWA 8022	INAA[2]	n.a.	n.a.	n.a.	0.070	3.71	n.a.	n.a.	16.4	0.458	n.a.	n.a.	n.a.	n.a.	n.a.				
$	NWA 8022	FB	43.82	0.194	30.60	0.065	3.18	0.041	3.94	17.15	0.476	0.068	0.059	0.076	99.66	68.8	20	AW	12	
$	NWA 8022	unc.[4]	0.05	0.011	0.09	0.012	0.04	0.011	0.03	0.04	0.011	0.005	0.012	0.008	0.07	0.3				
%	NWA 8046	INAA[2]	n.a.	n.a.	n.a.	0.101	4.53	n.a.	n.a.	15.5	0.315	n.a.	n.a.	n.a.	n.a.	n.a.				
%	NWA 8046	FB	43.66	0.194	27.54	0.099	4.45	0.085	6.43	16.48	0.320	0.029	0.056	0.110	99.45	72.0	20	AW		
%	NWA 8046	unc.[4]	0.06	0.012	0.17	0.015	0.06	0.012	0.18	0.18	0.009	0.005	0.019	0.012	0.09	0.5				
&	NWA 8055	INAA[2]	n.a.	n.a.	n.a.	0.132	6.41	n.a.	n.a.	15.0	0.419	n.a.	n.a.	n.a.	n.a.	n.a.				
&	NWA 8055	FB	44.13	0.382	27.18	0.12	5.57	0.081	4.71	16.85	0.450	0.082	0.09	0.09	99.73	60.1	10	AW	12	
&	NWA 8055	unc.[4]	0.10	0.019	0.07	0.03	0.08	0.019	0.03	0.07	0.011	0.005	0.03	0.02	0.16	0.2				
½	NWA 8182	INAA[2]	n.a.	n.a.	n.a.	0.249	10.48	n.a.	n.a.	12.2	0.522	n.a.	n.a.	n.a.	n.a.	n.a.				
½	NWA 8182	FB	45.6	0.97	19.44	0.25	10.67	0.141	8.82	12.88	0.510	0.128	0.144	0.172	99.72	59.6	10	AW		
½	NWA 8182	unc.[4]	1.2	0.05	0.64	0.03	0.28	0.021	0.25	0.23	0.033	0.011	0.052	0.025	0.25	0.2				
L	NWA 8277	INAA[2]	n.a.	n.a.	n.a.	0.325	14.54	n.a.	n.a.	n.a.	0.352	n.a.	n.a.	n.a.	n.a.	n.a.				
L	NWA 8277	FB	46.7	0.59	15.86	0.302	14.06	0.198	9.40	12.09	0.367	0.073	0.071	0.130	99.81	54.4	42	AW		
L	NWA 8277	unc.[4]	0.2	0.02	0.52	0.013	0.35	0.011	0.24	0.14	0.012	0.004	0.008	0.015	0.15	0.3				
§	NWA 8632	INAA[2]	n.a.	n.a.	n.a.	0.491	22.78	n.a.	n.a.	n.a.	0.267	n.a.	n.a.	n.a.	n.a.	n.a.				
§	NWA 8632	FB	44.44	2.54	8.00	0.45	22.61	0.304	10.83	9.61	0.273	0.110	0.092	0.251	99.49	46.0	16	AW		
§	NWA 8632	unc.[4]	0.19	0.04	0.16	0.04	0.21	0.019	0.25	0.17	0.011	0.010	0.014	0.012	0.21	0.4				
5	OA 01	INAA[2]	n.a.	n.a.	n.a.	0.060	3.45	n.a.	n.a.	17.2	0.361	n.a.	n.a.	n.a.	n.a.	n.a.				
5	OA 01	FB	44.30	0.162	31.47	0.062	3.09	0.047	2.42	17.66	0.362	0.028	0.035	0.027	99.66	58.2	16	AW	12	
5	OA 01	unc.[4]	0.11	0.013	0.20	0.012	0.11	0.015	0.07	0.05	0.012	0.006	0.014	0.010	0.11	0.7				
t	rock 004	INAA[2]	n.a.	n.a.	n.a.	0.292	11.49	n.a.	n.a.	13.9	0.322	n.a.	n.a.	n.a.	n.a.	n.a.				
t	rock 004	FB	47.38	0.49	19.11	0.294	11.44	0.187	7.53	13.00	0.333	0.086	0.028	n.a.	99.92	54.0	20	RAZ		
t	rock 004	unc.[4]	0.08	0.04	0.14	0.019	0.07	0.014	0.05	0.04	0.024	0.002	0.007	n.a.	0.12	0.1				

Footnotes

All values in mass percent
1) analysts: Ryan A. Zeigler and Axel Wittmann
2) INAA = values from Table S3; n.a. = not analyzed
3) *N* = number of EPMA spots analyzed
4) uncertainties ("unc.") are 95% confidence limits: *st*/SQRT(*N*) where *s* = standard deviation and *t* = Excel® function TINV(0.05,SQRT(*N-1*))
5) mean ± standard deviation: (FeO_T FB)/(FeO_T INAA) = 0.997 ± 0.061. FeO_T = Total Fe as FeO.
6) mean ± standard deviation: (Na_2O FB)/(Na_2O INAA) = 0.993 ± 0.067
7) recalculated as simple mean of raw data of Korotev et al. (2009)
8) excludes 4 clast-rich subsamples with <3.0% FeO
9) based on sawdust (sd) samples, which contains less FeNi metal than INAA chip samples; see text.
10) corrected for calcite contamination (Fig. S38)
11) matrix (m) and clast (c). Note high Na_2O in clast (INAA), Na loss in FB?
12) large (>10%) FeO difference from INAA

References (first published)

1) Korotev et al. (2003a)
2) Korotev et al. (2009)

Table S4 is also provided as Table_S4_major_elements.xls

Table S5. Mean composition of typical feldspathic lunar meteorites

	unit	P, 1991	K, 2003	analysis	**mean**	*s*	95% CL	*N*	min	max
SiO_2	%	(46.3)	44.7	FB	**44.24**	0.44	0.19	24	43.37	45.30
TiO_2	%	0.26	0.22	FB	**0.184**	0.041	0.017	24	0.074	0.265
Al_2O_3	%	26.1	28.2	FB	**29.55**	1.4	0.6	24	25.8	31.9
Cr_2O_3	%	0.123	0.10	FB	**0.080**	0.015	0.006	24	0.055	0.130
Cr_2O_3	%			INAA	**0.080**	0.015	0.005	35	0.054	0.133
FeO_T	%	5.24	4.40	FB	**3.90**	0.54	0.23	24	2.90	5.44
FeO_T	%			INAA	**3.82**	0.54	0.18	35	2.79	5.44
MnO	%	0.074	0.06	FB	**0.061**	0.012	0.005	24	0.044	0.089
MgO	%	6.1	5.40	FB	**4.33**	1.35	0.57	24	2.53	8.07
CaO	%	15.4	16.3	FB	**16.8**	0.7	0.3	24	15.0	18.0
CaO	%			INAA	**16.6**	0.7	0.2	35	14.9	18.4
Na_2O	%	0.335	0.35	FB	**0.336**	0.023	0.010	24	0.297	0.379
Na_2O	%			INAA	**0.343**	0.022	0.007	35	0.312	0.388
K_2O[1]	%	0.024	0.026	FB	**0.027**	0.006	0.008	5	0.021	0.038
K_2O[2]	%			FB	**0.028**	0.007	0.004	13	0.016	0.039
P_2O_5[1]	%	0.024	0.027	FB	**0.029**	0.012	0.015	5	0.018	0.049
P_2O_5[2]	%			FB	**0.029**	0.010	0.006	13	0.017	0.049
Σ	%	(100.0)	99.8	FB	**99.8**	0.3	0.1	24	99.3	100.4
Mg´	%	68.4	69.5	FB	**65.5**	5.0	2.1	24	56.7	77.3
norm. plag.	wt%	72.2	78.1		**81.9**					
norm. plag.	vol%	76.4	81.7		**85.1**					
K[1]	µg/g	203.	216.	INAA	**228**	53	66	5	178	315
K[2]	µg/g			INAA	**235**	54	33	13	133	323
Sc	µg/g	11.	8.0	INAA	**7.0**	1.1	0.4	35	4.8	8.7
V	µg/g	30.	n.a.	n.a.	**n.a.**					
Cr	µg/g	843.	660.	INAA	**546**	104	36	35	356	907
Co	µg/g	18.	17.0	INAA	**13.9**	4.1	1.4	35	8.1	22.4
Ni	µg/g	152.	185.	INAA	**139**	74	25	35	27	299
Zn	µg/g	20.	n.a.	n.a.	**n.a.**					
Ga	µg/g	3.0	n.a.	n.a.	**n.a.**					
Br	µg/g	0.07	n.a.	n.a.	**n.a.**					
Rb	µg/g	0.69	0.7	INAA	**0.9**	0.7	0.2	35	<0.5	2.1
Sr	µg/g	138.	150.	INAA	**153**	8	9	5	142	160
Y	*µg/g*	*8.5*	*9.*	INAA	***7.8***	*2.3*	*0.9*	*26*	*3.4*	*11.6*
Zr	µg/g	29.	35.	INAA	**31**	12	4	34	5	55
Nb	µg/g	2.1	n.a.	n.a.	**n.a.**					
Cs	µg/g	0.02	n.a.	INAA	**0.034**	0.017	0.006	35	0.010	0.075
Ba	µg/g	28.	33.	INAA	**28**	4	5	5	24	34
La	µg/g	1.98	2.3	INAA	**2.0**	0.6	0.3	26	0.8	3.2
Ce	µg/g	5.48	6.0	INAA	**5.2**	1.6	0.7	26	2.0	8.0
Pr	*µg/g*	*n.a.*	*0.8*	INAA	***0.68***	*0.21*	*0.09*	*26*	*0.27*	*1.06*
Nd	µg/g	3.08	3.6	INAA	**3.3**	1.0	0.4	26	1.3	5.5
Sm	µg/g	0.99	1.1	INAA	**0.95**	0.29	0.12	26	0.38	1.46
Eu	µg/g	0.75	0.78	INAA	**0.772**	0.044	0.018	26	0.680	0.848
Gd	*µg/g*	*0.72*	*1.3*	INAA	***1.10***	*0.33*	*0.13*	*26*	*0.47*	*1.66*
Tb	µg/g	0.22	0.23	INAA	**0.20**	0.06	0.02	26	0.09	0.30
Dy	*µg/g*	*1.46*	*1.5*	INAA	***1.284***	*0.384*	*0.155*	*26*	*0.556*	*1.912*
Ho	*µg/g*	*0.33*	*0.33*	INAA	***0.28***	*0.08*	*0.03*	*26*	*0.12*	*0.42*
Er	*µg/g*	*n.a.*	*0.90*	INAA	***0.79***	*0.23*	*0.09*	*26*	*0.35*	*1.16*
Tm	*µg/g*	*n.a.*	*0.14*	INAA	***0.116***	*0.033*	*0.013*	*26*	*0.052*	*0.170*
Yb	µg/g	0.92	0.89	INAA	**0.75**	0.21	0.09	26	0.34	1.10
Lu	µg/g	0.13	0.13	INAA	**0.107**	0.030	0.012	26	0.048	0.155
Hf	µg/g	0.73	0.80	INAA	**0.70**	0.22	0.08	35	0.22	1.07
Ta	µg/g	0.11	0.11	INAA	**0.090**	0.027	0.009	35	0.036	0.141
Ir	ng/g	6.	7.5	INAA	**5.7**	3.4	1.2	35	0.4	14.5
Au	ng/g	2.	2.8	INAA	**2.2**	1.3	0.6	22	<2	4.6
Pb	µg/g	0.62	n.a.	n.a.	**n.a.**					
Th	µg/g	0.24	0.37	INAA	**0.33**	0.13	0.04	35	0.12	0.65
U	µg/g	0.077	0.16	INAA	**0.13**	0.06	0.03	25	0.03	0.27

Footnotes

P, 1999	Values of Palme et al. (1999) based on 5 feldspathic lunar meteorites, all from Antarctica.
K, 2003	Values of Korotev et al. (2003a) based on 8 feldspathic lunar meteorites, 4 from hot deserts.
mean	Values of this work based on the number of lunar meteorites in column *N*
s	sample standard deviation
CL	confidence limits
FeO_T	Total Fe as FeO
Mg'	mole % MgO/(MgO+FeO_T)
norm. plag.	normative plagioclase, from Excel® spreadsheet of Hollocher (2019).
n.a.	not analyzed
italics	Values for Y, Pr, Gd, Dy, Ho, Er, and Tm are estimated from concentrations of analyzed REE.
[1]	Based on Antarctic meteorites only.
[2]	Based on Antarctic meteorites and those hot-desert meteorites having K/Sm or P/Sm values less than those of the Antarctic meteorite with the highest ratio.

Procedure

Trace-element data (INAA) are based on mass-weighted mean concentrations of all subsamples of 35 meteorites and clans presumably representing about 35 lunar launch craters in Feldspathic Highlands Terrane: **ALHA 81005**, **Graves Nunataks 06157**, **Larkman Nunatak 6638**, **MacAlpine Hills 88105 clan** (*N*=2 stones), **Miller Range 090034 clan** (*N*=2, MIL 090075 excluded), **Abar al' Uj 012**, **DaG 262 clan** (*N*=4), **DaG 400 clan** (*N*=2), **Dhofar 026 clan** (*N*=3), **Dhofar 081 clan** (*N*=3), **Dhofar 302**, **Dhofar 490 clan** (*N*=2 stones), **Dhofar 1428**, **NWA 482**, **NWA 2200**, **NWA 2998** (*N*=2), **NWA 6275**, **NWA 6578**, **NWA 7493**, **NWA 7959**, **NWA 8046 clan** (*N*=25), NWA 8222 clan (*N*=8), NWA 8586, NWA 8753, NWA 10073 clan (*N*=2), NWA 10141 clan (*N*=3), NWA 10665, NWA 11006, NWA 11061, NWA 11077, NWA 11352, **Oued Awlitis 001**, **Shişr 160**, **Shişr 166,** and Sueilila 005. The "mean" values of the table are simple numeric averages. Data from Table S3, Korotev and Zeigler (2014), and Korotev (2017).

For Sr and Ba, means are calculated only from data for Antarctic meteorites. For the REE, any meteorite for which CI-normalized La/Sm exceeds 1.38 is excluded from the mean (Fig. S7). For U, all meteorites for which the CI-normalized U/Th exceeds 1.93 (the highest Antarctic value) are excluded from the mean. For Au, all meteorites having CM-chondrite-normalized Au/Ir >2.0 are excluded from the mean (Fig. S56).

For major elements, we use our own "fused bead" data (Table S4) and, for meteorite names in **bold** in the list above, all available literature data. For DaG 262 (CaO/Al_2O_3 = 0.610), DaG 400 (0.656), NWA 482 (0.600), NWA 6578 (0.603), and NWA 8046 (0.597) CaO/Al_2O_3 ratios are high compared to the others (range 0.541–0.588, mean: 0.569), suggesting significant contamination with terrestrial calcite. For these 5 meteorites we discarded the measured values and substituted $0.569 \cdot Al_2O_3$**.** For the normative mineralogy of Table 3, we use the INAA data for FeO, Cr_2O_3, and Na_2O.

Data from Table S4, Bischoff et al. (1988), Cohen et al. (2004), Demidova et al. (2007), Hidaka et al. (2014), Joy et al. (2010), Kallemeyn and Warren (1983), Korotev (2012, 2017), Korotev and Zeigler (2014), Palme et al. (1983, 1991), Taylor et al. (2001), Warren et al. (2005), Warren and Kallemeyn (1991a), Wittmann et al. (2019), and Zipfel et al. (1998).

Table S6. Results of regression analysis of Ni, Ir, and Au against Co for some metal-rich meteorites

	N	Co		Ni		Ir		Au			Ni/Co		Ir/Co		Au/Co	
NWA 4472/4485																
slope				9.51	g/g	0.974	µg/g	0.142	µg/g							
intercept				-88.3	µg/g	-19.0	ng/g	-2.0	ng/g							
concentration	23	=5000	µg/g	47400	µg/g	4850	ng/g	710	ng/g	ratio	9.49	g/g	0.971	µg/g	0.142	µg/g
± 95%				1000	µg/g	80	ng/g	90	ng/g	± 95%	0.21	g/g	0.016	µg/g	0.018	µg/g
R^2				0.998		0.999		0.928								
NWA 4932																
slope				15.03	g/g	0.792	µg/g	0.266	µg/g							
intercept				-64.7	µg/g	-7.7	ng/g	-3.8	ng/g							
concentration	8	=5000	µg/g	75100	µg/g	3950	ng/g	1330	ng/g	ratio	15.02	g/g	0.790	µg/g	0.266	µg/g
± 95%				6400	µg/g	480	ng/g	50	ng/g	± 95%	1.29	g/g	0.096	µg/g	0.011	µg/g
R^2				0.993		0.985		0.998								
NWA 4936 clan																
slope				15.08	g/g	0.590	µg/g	0.281	µg/g							
intercept				-26.7	µg/g	-7.1	ng/g	1.1	ng/g							
concentration	54	=5000	µg/g	75400	µg/g	2950	ng/g	1410	ng/g	ratio	15.07	g/g	0.589	µg/g	0.281	µg/g
± 95%				1200	µg/g	110	ng/g	50	ng/g	± 95%	0.25	g/g	0.021	µg/g	0.011	µg/g
R^2				0.996		0.983		0.981								
NWA 5000																
slope				15.49	g/g	0.787	µg/g	0.268	µg/g							
intercept				-49.2	µg/g	-5.6	ng/g	-0.6	ng/g							
concentration	20	=5000	µg/g	77400	µg/g	3930	ng/g	1340	ng/g	ratio	15.48	g/g	0.786	µg/g	0.267	µg/g
± 95%				1200	µg/g	90	ng/g	60	ng/g	± 95%	0.24	g/g	0.018	µg/g	0.012	µg/g
R^2				0.999		0.998		0.992								
NWA 6555																
slope				17.50	g/g	1.194	µg/g	0.365	µg/g							
intercept				-542.8	µg/g	-51.2	ng/g	-11.4	ng/g							
concentration	7	=5000	µg/g	87000	µg/g	5920	ng/g	1810	ng/g	ratio	17.4	g/g	1.2	µg/g	0.36	µg/g
± 95%				19100	µg/g	3360	ng/g	420	ng/g	± 95%	3.8	g/g	0.7	µg/g	0.08	µg/g
R^2				0.964		0.803		0.960								
NWA 8010																
slope				13.17	g/g	0.237	µg/g	0.197	µg/g							
intercept				-99.4	µg/g	-1.2	ng/g	-0.8	ng/g							
concentration	7	=5000	µg/g	65800	µg/g	1180	ng/g	980	ng/g	ratio	13.2	g/g	0.24	µg/g	0.20	µg/g
± 95%				19200	µg/g	540	ng/g	970	ng/g	± 95%	3.8	g/g	0.11	µg/g	0.19	µg/g
R^2				0.939		0.861		0.574								
NWA 8455 clan																
slope				19.77	g/g	0.696	µg/g	0.430	µg/g							
intercept				-183.4	µg/g	-10.9	ng/g	-3.1	ng/g							
concentration	76	=5000	µg/g	98700	µg/g	3470	ng/g	2150	ng/g	ratio	19.73	g/g	0.69	µg/g	0.43	µg/g
± 95%				8900	µg/g	340	ng/g	300	ng/g	± 95%	1.79	g/g	0.07	µg/g	0.06	µg/g
R^2				0.866		0.849		0.747								
NWA 8673 clan																
slope				14.68	g/g	0.445	µg/g	0.302	µg/g							
intercept				-87.2	µg/g	3.4	ng/g	-3.7	ng/g							
concentration	65	=5000	µg/g	73300	µg/g	2230	ng/g	1510	ng/g	ratio	14.67	g/g	0.45	µg/g	0.301	µg/g
± 95%				1500	µg/g	160	ng/g	80	ng/g	± 95%	0.30	g/g	0.03	µg/g	0.015	µg/g
R^2				0.994		0.923		0.961								
rock 65																
slope				21.68	g/g	1.245	µg/g	0.184	µg/g							
intercept				-158.1	µg/g	-11.9	ng/g	0.6	ng/g							
concentration	5	=5000	µg/g	108300	µg/g	6210	ng/g	920	ng/g	ratio	21.65	g/g	1.24	µg/g	0.184	µg/g
± 95%				1700	µg/g	130	ng/g	100	ng/g	± 95%	0.34	g/g	0.03	µg/g	0.019	µg/g
R^2				1.000		1.000		0.997								

The values of this table were determined from the regression procedure described in Fig. S54.

Table S7. Estimated number of lunar meteorites and launch craters

	1	2	3	4	5	6	7	8	9	10	11	12	13	14	15	16	17
					evidence for or against pairing		*N* of discrete meteorites			*N* of meteorites		launch pairs		launch crater			
	as of 2019-12-31	mass (g)	where	*N* of stones	compo-sition	including other	(first of pair group)	terrestrially paired with	issue, note, or caveat	min	max	group no.	pair	min	max	refer-ence	figure or table
1	Asuka 881757	442	Antarctica	1	1		1	0		1	1		1	0	0	KZ, WK	
2	ALHA 81005	31.4	Antarctica	1	1		1	0		1	1			1	1		
3	DEW 12007	94.2	Antarctica	1	1		1	0		1	1		2	0	0	C3	S42
4	DOM 18262	6.777	Antarctica	1		FL P	1	4 DOM 18xxx	no BC data; new launch pair or possible YQEND (col. 15) launch pair	1	1		2?	0	1	MB	
5	DOM 18509	16.52	Antarctica	1		FL P	0	DOM 18262	no BC data	0	0			0	0	MB	
6	DOM 18543	13.59	Antarctica	1		FL P	0	DOM 18262	no BC data	0	0			0	0	MB	
7	DOM 18666	45.87	Antarctica	1		FL P	0	DOM 18262	no BC data	0	0			0	0	MB	
8	DOM 18678	11.64	Antarctica	1		FL P	0	DOM 18262	no BC data	0	0			0	0	MB	
9	EET 87521	30.7	Antarctica	1	1		1	EET 96008		1	1		2	0	0	K2	
10	EET 96008	52.97	Antarctica	1	1		0	EET 87521		0	0			0	0	K5	
11	GRA 06157	0.788	Antarctica	1	1		1	0		1	1			1	1		
12	LAP 02205	1226.30	Antarctica	1	1		1	5 LAP		1	1		3	0	0	KZ	S51, S52
13	LAP 02224	252.5	Antarctica	1	1		0	LAP 02205		0	0			0	0	MB, Z	
14	LAP 02226	244.1	Antarctica	1	1		0	LAP 02205		0	0			0	0	MB, Z	
15	LAP 02436	58.97	Antarctica	1	1		0	LAP 02205		0	0			0	0	MB, Z	
16	LAP 03632	92.566	Antarctica	1	1		0	LAP 02205		0	0			0	0	MB, Z	
17	LAP 04841	55.992	Antarctica	1	1		0	LAP 02205		0	0			0	0	MB, K4	
18	LAR 06638	5.293	Antarctica	1	1		1	0		1	1			1	1	KZ	
19	MAC 88104	61.2	Antarctica	1	1		1	MAC 88105		1	1			1	1	KZ	
20	MAC 88105	662.5	Antarctica	1	1		0	MAC 88104		0	0			0	0	MB	
21	MET 01210	22.83	Antarctica	1	1		1	0		1	1		1	0	0	KZ	
22	MIL 05035	142.216	Antarctica	1	1		1	0		1	1		1	0	0	KZ	
23	MIL 07006	1.368	Antarctica	1	1		1	0	BC very similar to Y-791197 but not identical (Na, Eu); preliminary CRE data not a match; not a good BC match to NWA 10508	1	1		7	0	1	KZ, N, NC	S71, S81
24	MIL 090034	195.565	Antarctica	1	1		1	MIL 090070 & 090075		1	1			1	1	KZ	
25	MIL 090036	244.83	Antarctica	1	1		1	0		1	1	**6**		1	1	KZ	S38
26	MIL 090070	137.461	Antarctica	1	1		0	MIL 090034		0	0			0	0	KZ	
27	MIL 090075	143.523	Antarctica	1	1		0	MIL 090034		0	0			0	0	KZ	
28	MIL 13317	32.25	Antarctica	1	1		1	0		1	1			1	1		S39
29	PCA 02007	22.372	Antarctica	1	1		1	0		1	1			1	1	KZ	
30	QUE 93069	21.4	Antarctica	1	1		1	QUE 94269		1	1			1	1	KZ	
31	QUE 94269	3.2	Antarctica	1	1		0	QUE 93069		0	0			0	0	KZ	
32	QUE 94281	23.4	Antarctica	1	1		1	0		1	1		2	0	0	AW	S42
33	Y-791197	52.4	Antarctica	1	1		1	0		1	1	**7**		1	1	KZ	S81
34	Y-793169	6.1	Antarctica	1	1		1	0		1	1	**1**		1	1	WK	

Table S7. Estimated number of lunar meteorites and launch craters

	1	2	3	4	5	6	7	8	9	10	11	12	13	14	15	16	17
				N of stones	evidence for or against pairing		*N* of discrete meteorites			*N* of meteorites		launch pairs		launch crater			
	as of 2019-12-31	mass (g)	where		compo-sition	including other	(first of pair group)	terrestrially paired with	issue, note, or caveat	min	max	group no.	pair	min	max	refer-ence	figure or table
35	Y-793274	8.7	Antarctica	1	1		1	Y-981031		1	1	2		1	1	AW	S42
36	Y-82192	36.67	Antarctica	1	1		1	2 Yamato		1	1			1	1	KZ	
37	Y-82193	27.04	Antarctica	1	1		0	Y-82192		0	0			0	0		
38	Y-86032	648.43	Antarctica	1	1		0	Y-82192		0	0			0	0		
39	Y-981031	185.8	Antarctica	1	1		0	Y-793274		0	0			0	0	K5	
40	Y-983885	289.71	Antarctica	1	1		1	0		1	1			1	1	KZ	
41	Calc. Creek	19	Australia	1	1		1	0		1	1			1	1		S39, S66
42	Lynch 002	36.54	Australia	1	1		1	0		1	1			1	1		S39, S66
43	Dhofar 025	751	Oman	1	1		1	3 Dho		1	1			1	1	D, K1	
44	Dhofar 026	148	Oman	1	1		1	13 Dho		1	1			1	1	W	
45	Dhofar 081	174	Oman	1	1		1	3 Dho		1	1			1	1	K1	
46	Dhofar 280	251.2	Oman	1	1		0	Dho 081		0	0			0	0	D, K1	
47	Dhofar 287	154	Oman	1	1		1	0		1	1			1	1	K1	
48	Dhofar 301	9	Oman	1	1		0	Dho 025		0	0			0	0	D, K1	
49	Dhofar 302	3.83	Oman	1	1		1	Dho 303?	Same find location as 303 clan but distinctly different composition, but then, so does 081 clan fpund at same location	0	1			0	1	K1	
50	Dhofar 303	4.15	Oman	1	1		1	14 Dho		1	1			1	1	D, K1	
51	Dhofar 304	10	Oman	1	1		0	Dho 025		0	0			0	0	D, K1	
52	Dhofar 305	34.11	Oman	1	1		0	Dho 303		0	0			0	0	D, K1	
53	Dhofar 306	12.86	Oman	1	1		0	Dho 303		0	0			0	0	D, K1	
54	Dhofar 307	50	Oman	1	1		0	Dho 303		0	0			0	0	D	
55	Dhofar 308	2	Oman	1	1		0	Dho 025		0	0			0	0	D	
56	Dhofar 309	81.3	Oman	1	1		0	Dho 303		0	0			0	0	D, K1	
57	Dhofar 310	10.8	Oman	1	1		0	Dho 303		0	0			0	0	D, K1	
58	Dhofar 311	4	Oman	1	1		0	Dho 303		0	0			0	0	D	
59	Dhofar 457	99.5	Oman	1	1		0	Dho 026	found 12 km WNW of Dho 026	0	0			0	0	W	
60	Dhofar 458	36.7	Oman	1	1		0	Dho 026 & 457	found 12 km WNW of Dho 026	0	0			0	0	W	
61	Dhofar 459	31.5	Oman	1	1		0	Dho 026 & 457	found 12 km WNW of Dho 026	0	0			0	0	W	
62	Dhofar 460	73.1	Oman	1		FL	0	Dho 026 & 457	found 12 km WNW of Dho 026	0	0			0	0	MB	
63	Dhofar 461	33.7	Oman	1	1		0	Dho 026 & 457	found 12 km WNW of Dho 026	0	0			0	0	W	
64	Dhofar 462	44.7	Oman	1	1		0	Dho 026 & 457	found 12 km WNW of Dho 026	0	0			0	0	W	
65	Dhofar 463	24.3	Oman	1	1		0	Dho 026 & 457	found 12 km WNW of Dho 026	0	0			0	0	W	

Table S7. Estimated number of lunar meteorites and launch craters

	1	2	3	4	5	6	7	8	9	10	11	12	13	14	15	16	17
				N of stones	evidence for or against pairing		*N* of discrete meteorites			*N* of meteorites		launch pairs		launch crater			
	as of 2019-12-31	mass (g)	where		compo-sition	including other	(first of pair group)	terrestrially paired with	issue, note, or caveat	min	max	group no.	pair	min	max	refer-ence	figure or table
66	Dhofar 464	22.3	Oman	1	1		0	Dho 026 & 457	found 12 km WNW of Dho 026	0	0			0	0	W	
67	Dhofar 465	70.7	Oman	1	1		0	Dho 026 & 457	found 12 km WNW of Dho 026	0	0			0	0	W	
68	Dhofar 466	69.2	Oman	1	1		0	Dho 026 & 457	found 12 km WNW of Dho 026	0	0			0	0	W	
69	Dhofar 467	36.2	Oman	1	1		0	Dho 026 & 457	found 12 km WNW of Dho 026	0	0			0	0	W	
70	Dhofar 468	18.9	Oman	1	1		0	Dho 026 & 457	found 12 km WNW of Dho 026	0	0			0	0	W	
71	Dhofar 489	34.4	Oman	1	1		0	Dho 303	found 23 km NW of Dho 303 et al. but same petrography	0	0			0	0	K1	
72	Dhofar 490	34.05	Oman	1	1		1	Dho 1084		1	1			1	1	K1	
73	Dhofar 730	108	Oman	1	1		0	Dho 303		0	0			0	0	D	
74	Dhofar 731	36	Oman	1	1		0	Dho 303		0	0			0	0	D	
75	Dhofar 733	98	Oman	1	1		1	Dho 1766		1	1			1	1	K1, K4	
76	Dhofar 908	245	Oman	1	1		0	Dho 303		0	0			0	0	K1	
77	Dhofar 909	3.9	Oman	1		FL P	0	Dho 303		0	0			0	0	MB	
78	Dhofar 910	142	Oman	1	1		0	Dho 081		0	0			0	0	K1	
79	Dhofar 911	194	Oman	1	1		0	Dho 303		0	0			0	0	K1	
80	Dhofar 925	49	Oman	1	1		1	960, 961		1	1	4		1	1	K1, K4	S53
81	Dhofar 950	21.7	Oman	1	1		0	Dho 303		0	0			0	0	D	
82	Dhofar 960	35.4	Oman	1	1		0	Dho 925		0	0			0	0	K4	
83	Dhofar 961	21.6	Oman	1	1		0	Dho 925		0	0			0	0	K3	
84	Dhofar 1084	90	Oman	1	1		0	Dho 490		0	0			0	0	K1	
85	Dhofar 1085	197	Oman	1	1		0	Dho 303		0	0			0	0	K1	
86	Dhofar 1180	115.2	Oman	1	1		1	0		1	1			1	1	K1, K3	
87	Dhofar 1224	4.57	Oman	1		FL	0	Dho 081		0	0			0	0	MB	
88	Dhofar 1428	213	Oman	1	1		1	0		1	1			1	1	K1	
89	Dhofar 1436	24.2	Oman	1	1		1	Dho 1443		1	1			1	1	K1	
90	Dhofar 1442	106.5	Oman	1	1		1	0		1	1			1	1	K1, K3	
91	Dhofar 1443	36.7	Oman	1	1		0	Dho 1436		0	0			0	0	K1	
92	Dhofar 1527	42.6	Oman	1	1		1	0		1	1			1	1	K1	
93	Dhofar 1528	213.2	Oman	1	1		1	0		1	1			1	1	K1	
94	Dhofar 1627	86.1	Oman	1	1		1	1980		1	1		5	0	0	K4	S39
95	Dhofar 1629	2.51	Oman	1	1		1	0		1	1			1	1	K4	
96	Dhofar 1669	3.3	Oman	1	1		0	Dho 026	but 22.5 km NNE of 026 and 26 km NE of 457-468	0	1			0	1	K4	
97	Dhofar 1673	15.1	Oman	1	1		1	1983, 1984		1	1			1	1	H	
98	Dhofar 1766	292	Oman	1	1		0	Dho 733		0	0			0	0	K4	

Table S7. Estimated number of lunar meteorites and launch craters

	1	2	3	4	5	6	7	8	9	10	11	12	13	14	15	16	17
					evidence for or against pairing		*N* of discrete meteorites			*N* of meteorites		launch pairs		launch crater			
	as of 2019-12-31	mass (g)	where	*N* of stones	compo-sition	including other	(first of pair group)	terrestrially paired with	issue, note, or caveat	min	max	group no.	pair	min	max	refer-ence	figure or table
99	Dhofar 1769	125.4	Oman	1	1		1	0		1	1			1	1	K4	
100	Dhofar 1980	23.5	Oman	1	1		0	Dho 1627		0	0			0	0	K4	
101	Dhofar 1983	56.3	Oman	1	1		0	Dho 1673		0	0			0	0	H	
102	Dhofar 1984	32.1	Oman	1	1		0	Dho 1673		0	0			0	0	H	
103	Dhofar 2047	4.95	Oman	1	1		0	Dho 303		0	0			0	0	K4	
104	Dhofar 2101	13	Oman	1			?	?	10 km from 1627/1980 but different petrography	?	?			?	?		
105	JaH 348	18.4	Oman	1	1		1	0		1	1			1	1	K1, K4	
106	JaH 838	34.36	Oman	1	1		1	0		1	1			1	1	K1, K4	
107	Sau 169	206.454	Oman	1	1		1	0		1	1			1	1	K3	
108	Sau 300	152.6	Oman	1	1		1	0		1	1			1	1	K1	
109	Sau 449	16.5	Oman	1	1		1	0		1	1		4	0	0	K1, KZ	
110	Shişr 160	100.86	Oman	1	1		1	0		1	1			1	1	K1	
111	Shişr 161	57.2	Oman	1	1		1	0		1	1			1	1	K1	
112	Shişr 162	5525.0	Oman	1	1		1	0		1	1			1	1	K1	
113	Shişr 166	128.8	Oman	1	1		1	0		1	1			1	1	K1	
114	AaU 012	122.78	Saudi Arabia	1	1		1	0		1	1			1	1	M	
115	AP 007	1337	Saudi Arabia	1		P	1	0	numerous basalt clasts, which are rare in AaU 012	1	1			1	1	MB	
116	Kalahari 008	585	Botswana	1	1		1	Kal 009		1	1			1	1		S64
117	Kalahari 009	13,500	Botswana	1	1		0	Kal 008		0	0			0	0		S64
118	Anoual	5.92	No. Africa	1	1		0	NWA 773		0	0			0	0		
119	Aridal 017	590	No. Africa	1	1		1	NWA 10608?		1	1			1	1		S4
120	DaG 262	513	No. Africa	1	1		1	3 DaG		1	1			1	1		S22, S60
121	DaG 400	1425	No. Africa	1	1		1	DaG 1058		1	1			1	1		S6, S22
122	DaG 996	12.31	No. Africa	1	1		0	DaG 262		0	0			0	0		
123	DaG 1042	801	No. Africa	1	1		0	DaG 262		0	0			0	0		
124	DaG 1048	0.801	No. Africa	1		FL	0	DaG 262		0	0			0	0		
125	DaG 1058	1815	No. Africa	1	1		0	DaG 400		0	0			0	0		
126	Errachidia	156	No. Africa	1			?	?		?	?			?	?		
127	Galb Inal	4050	No. Africa	1	1		0	NWA 7834	but find year (2011) earlier than other 7834-clan stones (2013-2016)	0	1			0	1		
128	La'gad	337.74	No. Africa	1	1		0	NWA 8455		0	0			0	0		
129	La'gad 003	27,249	No. Africa	1	1		0	NWA 10509		0	0			0	0		S70
130	Lahmada 020	12,168	No. Africa	1			?	Lahmada 046? & 047?	but no BC data; may be new	0	1			0	1		
131	Lahmada 046	71.24	No. Africa	1			0	Lahmada 020?	no BC data	0	0			0	0		
132	Lahmada 047	182	No. Africa	1			0	Lahmada 020?	no BC data	0	0			0	0		

Table S7. Estimated number of lunar meteorites and launch craters

	1	2	3	4	5	6	7	8	9	10	11	12	13	14	15	16	17
					evidence for or against pairing		*N* of discrete meteorites			*N* of meteorites		launch pairs		launch crater			
	as of 2019-12-31	mass (g)	where	*N* of stones	compo-sition	including other	(first of pair group)	terrestrially paired with	issue, note, or caveat	min	max	group no.	pair	min	max	refer-ence	figure or table
133	NEA 001	262	No. Africa	1	1		1	0		1	1			1	1		S70, S71, S72
134	NEA 003	124	No. Africa	1	1		1	0		1	1			1	1		13, S4, S5, S40, S51, S52
135	NWA 032	300	No. Africa	1	1		1	NWA 479	different BC and $^{147}Sm/^{144}Nd$ than NWA 4734 & LAP clans	1	1	**3**		1	1	E	13, S17, S51, S52
136	NWA 479	156	No. Africa	1	1		0	NWA 032		0	0			0	0		
137	NWA 482	1015	No. Africa	1	1		1	0		1	1			1	1		S6, S7, S72
138	NWA 773	633	No. Africa	1	1		1	~14 NWA & Anoual	Some of the "pairs" may be launch pairs.	1	1			1	1		S51, S52, S53
139	NWA 2200	552	No. Africa	1	1		1	0		1	1			1	1		S17-22
140	NWA 2402	500	No. Africa	1	1		0	NWA 7611?	likely launch paired with Y-793274	0	0			0	0	MB	
141	NWA 2420	395	No. Africa	1			?	?		?	?			?	?		
142	NWA 2425	810	No. Africa	1	1		?	NWA 8046?	similar: Al_2O_3, Mg#, Th	0	0			0	0	MB	
143	NWA 2700	31.7	No. Africa	1	1		0	NWA 773		0	0			0	0		
144	NWA 2727	191.2	No. Africa	1	1		0	NWA 773		0	0			0	0		
145	NWA 2977	233	No. Africa	1	1		0	NWA 773		0	0			0	0		
146	NWA 2995	538	No. Africa	1	1		1	9 NWA		1	1			1	1	K3	S46, S47, S48
147	NWA 2996	968	No. Africa	1	1		0	NWA 2995		0	0			0	0		
148	NWA 2998	163	No. Africa	1	1		1	NWA 7262		1	1			1	1		S68
149	NWA 3136	95.1	No. Africa	1	1		1	0		1	1			1	1		S3, S4, S6, S13, S41, S44
150	NWA 3160	34	No. Africa	1	1		0	NWA 773		0	0			0	0		S52
151	NWA 3163	1634	No. Africa	1	1		1	3 NWA		1	1			1	1		S15, S45, S71
152	NWA 3170	60	No. Africa	1	1		0	NWA 773		0	0			0	0		
153	NWA 3190	40.7	No. Africa	1	1		0	NWA 2995		0	0			0	0		
154	NWA 3333	33	No. Africa	1	1		0	NWA 773		0	0			0	0		
155	NWA 4472	64.3	No. Africa	1	1		1	NWA 4485		1	1			1	1		6, S5, S32, S33, S39
156	NWA 4483	208	No. Africa	1	1		0	NWA 3163		0	0			0	0		
157	NWA 4485	188	No. Africa	1	1		0	NWA 4472		0	0			0	0		
158	NWA 4503	70	No. Africa	1	1		0	NWA 2995		0	0			0	0		

Table S7. Estimated number of lunar meteorites and launch craters

	1	2	3	4	5	6	7	8	9	10	11	12	13	14	15	16	17
					evidence for or against pairing					N of meteorites		launch pairs		launch crater			
	as of 2019-12-31	mass (g)	where	N of stones	compo-sition	including other	N of discrete meteorites (first of pair group)	terrestrially paired with	issue, note, or caveat	min	max	group no.	pair	min	max	refer-ence	figure or table
159	NWA 4734	1372	No. Africa	1	1		1	10597		1	1		3	0	0		13, S17, S51, S52
160	NWA 4819	234	No. Africa	1	1		1	0		1	1			1	1		S4, S46, S71
161	NWA 4881	606	No. Africa	1	1		0	NWA 3163		0	0			0	0		
162	NWA 4884	42	No. Africa	1	1		1	7611 clan?		1	1		2	0	0		S20 , S41, S42
163	NWA 4898	137	No. Africa	1	1		1	0		1	1			1	1		13, S44, S51, S52
164	NWA 4932	93.3	No. Africa	1	1		1	0		1	1			1	1		S7, S71, S79
165	NWA 4936	179	No. Africa	1	1		1	8 NWA		1	1			1	1		S35, S44, S69
166	NWA 5000	11,528	No. Africa	1	1		1	0	connection to NWA 8641 clan tenuous	1	1		8	0	1		S25, S29, S30. S33
167	NWA 5151	289	No. Africa	1	1		0	NWA 2995		0	0			0	0		
168	NWA 5152	38	No. Africa	1	1		0	NWA 2995		0	0			0	0		
169	NWA 5153	50.4	No. Africa	1	1		1	NWA 2995?	Fe-rich end of NWA 2995 clan, Fe, Ni, & Sr (only) significantly different at 99% confidence.	0	1			0	1	K3	S46
170	NWA 5207	101	No. Africa	1	1		1	NWA 2995?	Fe-poor end of NWA 2995 clan? T Bunch says "not paired" Na, Sc, Fe, Co, Ba, & Cr/Sc significantly different at 99% confidence.	0	1			0	1	K3	S46
171	NWA 5406	281	No. Africa	1	1		0	NWA 4936		0	0			0	0		
172	NWA 5744	170	No. Africa	1	1		1	8 NWA		1	1			1	1		5, S3, S7, S16, S30
173	NWA 6221	109.4	No. Africa	1	1		0	NWA 4936		0	0			0	0		
174	NWA 6252	113	No. Africa	1	1		0	NWA 2995		0	0			0	0		
175	NWA 6275	1.3	No. Africa	1	1		0	NWA 3163		0	0			0	0		
176	NWA 6355	760	No. Africa	1	1		0	NWA 4936		0	0			0	0		
177	NWA 6470	96	No. Africa	1	1		0	NWA 4936		0	0			0	0		
178	NWA 6481	13.7	No. Africa	1	1		1	0		1	1			1	1		S25
179	NWA 6554	138	No. Africa	1	1		0	NWA 2995		0	0			0	0		
180	NWA 6555	29.72	No. Africa	1	1		0	NWA 2995		0	0			0	0		
181	NWA 6570	415	No. Africa	1	1		0	NWA 4936		0	0			0	0		
182	NWA 6578	1638	No. Africa	1	1		1	0		1	1			1	1		S17, S19, S72, S75, S80

Table S7. Estimated number of lunar meteorites and launch craters

	1	2	3	4	5	6	7	8	9	10	11	12	13	14	15	16	17
					evidence for or against pairing					*N* of meteorites		launch pairs		launch crater			
	as of 2019-12-31	mass (g)	where	*N* of stones	compo-sition	including other	(first of pair group)	terrestrially paired with	issue, note, or caveat	min	max	group no.	pair	min	max	refer-ence	figure or table
183	NWA 6687	42.4	No. Africa	1	1		1	0		1	1			1	1		S3 S4, S5, S6, S38
184	NWA 6721	181	No. Africa	1	1		1	0		1	1			1	1		S25
185	NWA 6831	20	No. Africa	1			?	?		?	?			?	?		
186	NWA 6888	208	No. Africa	1	1		1	0		1	1			1	1		S6, S46, S71
187	NWA 6950	1649	No. Africa	1	1		0	NWA 773		0	0			0	0		
188	NWA 7007	91	No. Africa	1	1		0	NWA 773		0	0			0	0		
189	NWA 7022	444	No. Africa	1	1		1	0	identical in composition to MIL 90036 but CRE data inconsistent with launch pairing	1	1		6	0	1		S7, S34, S35, S38
190	NWA 7190	5.28	No. Africa	1	1		0	NWA 4936		0	0			0	0		
191	NWA 7262	413	No. Africa	1	1		0	NWA 2998	but buyer/owner of the 2 stones is doubtful of pairing considering purchase location	0	1			0	1		
192	NWA 7274	372.6	No. Africa	1	1		1	0		1	1			1	1		S3, S35, S46
193	NWA 7493	503	No. Africa	1	1		1	0		1	1			1	1		S24, S72, S76
194	NWA 7611	916	No. Africa	1	1		1	NWA 4884?	7611 clan is substantially more contaminated with terrestrial Ba than 4884 suggesting different find location; does not "look like" 4884.	1	1		2	0	0		S20, S41, S42, S47
195	NWA 7834	905	No. Africa	1	1		1	23 NWA		1	1			1	1		S36, S46, S48, S49
196	NWA 7931	5.92	No. Africa	1	1		1	0		1	1			1	1		S71
197	NWA 7948	59.8	No. Africa	1	1		0	NWA 7834		0	0			0	0		
198	NWA 7959	156	No. Africa	1	1		1	0		1	1			1	1		S17
199	NWA 7986	12.2	No. Africa	1	1		0	NWA 4936		0	0			0	0		
200	NWA 8001	23.4	No. Africa	1	1		1	0		1	1			1	1		S25
201	NWA 8010	58	No. Africa	1	1		1	0		1	1			1	1		S35, S69
202	NWA 8022	1226	No. Africa	1	1		1	10082		1	1			1	1		S5, S17, S23, S25, S72
203	NWA 8046	47.3	No. Africa	1	1		1	19 NWA+		1	1			1	1		S17, S24
204	NWA 8055	98	No. Africa	1	1		1	0		1	1			1	1		S71, S72
205	NWA 8127	529	No. Africa	1	1		0	NWA 773		0	0			0	0		
206	NWA 8181	18.2	No. Africa	1	1		0	NWA 4936		0	0			0	0		

Table S7. Estimated number of lunar meteorites and launch craters

	1	2	3	4	5	6	7	8	9	10	11	12	13	14	15	16	17
				N of stones	evidence for or against pairing		*N* of discrete meteorites			*N* of meteorites		launch pairs		launch crater			
	as of 2019-12-31	mass (g)	where		compo-sition	including other	(first of pair group)	terrestrially paired with	issue, note, or caveat	min	max	group no.	pair	min	max	refer-ence	figure or table
207	NWA 8182	15.6	No. Africa	1	1		1	0		1	1			1	1		S6, S44, S46, S66
208	NWA 8222	208.6	No. Africa	1	1		1	3 NWA & 2 (4?) Rabt Sbayta		1	1			1	1		S4, S17, S25, S72
209	NWA 8277	773	No. Africa	1	1		0	NWA 7611		0	0			0	0		
210	NWA 8306	1389	No. Africa	1	1		0	NWA 7834		0	0			0	0		
211	NWA 8455	2814	No. Africa	1	1		1	10 NWA & La'gad		1	1	**5**		1	1		S5, S35, S36, S39, S69
212	NWA 8586	704.5	No. Africa	1	1		1	0		1	1			1	1		S8, S15, S25
213	NWA 8599	36.5	No. Africa	1	1		0	NWA 5744		0	0			0	0		
214	NWA 8607	261	No. Africa	1	1		0	NWA 8455?	similar DFB shock melt	0	0			0	0	MB	
215	NWA 8609	45	No. Africa	1	1		0	NWA 8455		0	0			0	0		
216	NWA 8632	23.8	No. Africa	1	1		1	0		1	1			1	1		13, S51, S52
217	NWA 8641	5895	No. Africa	1	1		1	5 NWA		1	1	**8**		1	1		S25, S26, S29, S33, S46
218	NWA 8651	598	No. Africa	1	1		0	NWA 8455		0	0			0	0		
219	NWA 8668	166.3	No. Africa	1	1		0	NWA 8455		0	0			0	0		
220	NWA 8673	263	No. Africa	1	1		1	12 NWA		1	1		4	0	0		2
221	NWA 8682	82	No. Africa	1	1		0	NWA 8641		0	0			0	0		
222	NWA 8687	562.5	No. Africa	1	1		0	NWA 5744		0	0			0	0		
223	NWA 8701	72	No. Africa	1	1		1	0		1	1			1	1		S4, S6, S15, S44, S46, S62
224	NWA 8727	2436.3	No. Africa	1	1		0	NWA 8455		0	0			0	0		
225	NWA 8733	51	No. Africa	1	1		0	NWA 8673		0	0			0	0		
226	NWA 8746	69.9	No. Africa	1	1		0	NWA 8673		0	0			0	0		
227	NWA 8753	1345	No. Africa	1	1		1	0		1	1			1	1		S17
228	NWA 8783	27.5	No. Africa	1	1		0	NWA 8455		0	0			0	0		
229	NWA 10048	352.3	No. Africa	1	1		0	NWA 8673		0	0			0	0		
230	NWA 10049	56	No. Africa	1	1		0	NWA 8641		0	0			0	0		
231	NWA 10065	282.8	No. Africa	1	1		0	NWA 8673		0	0			0	0		
232	NWA 10073	64	No. Africa	1	1		1	0		1	1			1	1		S17, S25, S75
233	NWA 10077	5.27	No. Africa	1	1		0	NWA 8641		0	0			0	0		
234	NWA 10082	5.2	No. Africa	1	1		0	NWA 8022		0	0			0	0		

Table S7. Estimated number of lunar meteorites and launch craters

	1	2	3	4	5	6	7	8	9	10	11	12	13	14	15	16	17
				N of stones	evidence for or against pairing		*N* of discrete meteorites			*N* of meteorites		launch pairs		launch crater			
	as of 2019-12-31	mass (g)	where		compo-sition	including other	(first of pair group)	terrestrially paired with	issue, note, or caveat	min	max	group no.	pair	min	max	refer-ence	figure or table
235	NWA 10123	149.5	No. Africa	1	1		0	NWA 8673	but compositionally anomalous	0	1			0	1		
236	NWA 10130	191	No. Africa	1	1		0	NWA 8455		0	0			0	0		
237	NWA 10133	54.2	No. Africa	1	1		0	NWA 8641		0	0			0	0		
238	NWA 10140	68	No. Africa	1	1		0	NWA 5744		0	0			0	0		
239	NWA 10141	39	No. Africa	1	1		1	3 NWA		1	1	**9**		1	1		S17, S34, S74, S75, S80
240	NWA 10142	102	No. Africa	1	1		?	NWA 10141?	BC is DFB EPMA	0	0			0	0	MB	
241	NWA 10149	1815	No. Africa	1	1		0	NWA 7834		0	0			0	0		
242	NWA 10172	788	No. Africa	1	1		0	NWA 7834		0	0			0	0		
243	NWA 10178	1279.3	No. Africa	1	1		0	NWA 5744		0	0			0	0		
244	NWA 10203	3300	No. Africa	1	1		0	NWA 7834		0	0			0	0		
245	NWA 10228	19.4	No. Africa	1	1		0	NWA 8455		0	0			0	0		
246	NWA 10253	6674.1	No. Africa	1	1		0	NWA 7834		0	0			0	0		
247	NWA 10258	58	No. Africa	1	1		0	NWA 7834		0	0			0	0		
248	NWA 10263	1015	No. Africa	1	1		0	NWA 7834		0	0			0	0		
249	NWA 10272	74.25	No. Africa	1	1		0	NWA 7834		0	0			0	0		
250	NWA 10291	10.01	No. Africa	1	1		0	NWA 7834		0	0			0	0		
251	NWA 10309	16,518	No. Africa	1	1		0	NWA 8046		0	0			0	0		
252	NWA 10317	11.0	No. Africa	1	1		0	NWA 7834		0	0			0	0		
253	NWA 10318	31.0	No. Africa	1	1		0	NWA 5744	but noritic, not troctolitic	0	1			0	1	MB	
254	NWA 10376	20	No. Africa	1	1		0	NWA 7834		0	0			0	0		
255	NWA 10401	354	No. Africa	1	1		0	NWA 5744		0	0			0	0		
256	NWA 10404	229	No. Africa	1	1		1	0		1	1			1	1		S25
257	NWA 10415	164	No. Africa	1	1		0	NWA 10141		0	0			0	0		
258	NWA 10447	21.73	No. Africa	1	1		1	7611?	BC anomalous	0	1			0	1		S4, S7, S41
259	NWA 10461	285.75	No. Africa	1	1		0	NWA 8046		0	0			0	0		
260	NWA 10480	33	No. Africa	1	1		0	NWA 7611		0	0			0	0		
261	NWA 10495	15600	No. Africa	1	1		1	Sueilila 005		1	1			1	1		S4, S71, S72
262	NWA 10509	660	No. Africa	1	1		1	2 NWA & La'gad 003		1	1	**10**		1	1		S71, S71, S72, S73
263	NWA 10546	43.35	No. Africa	1	1		0	NWA 7834		0	0			0	0		
264	NWA 10566	130	No. Africa	1	1		0	NWA 7611		0	0			0	0		
265	NWA 10597	350	No. Africa	1	1		0	NWA 4734		0	0			0	0		S17, S52
266	NWA 10599	77.8	No. Africa	1	1		0	NWA 7834		0	0			0	0		
267	NWA 10608	2014	No. Africa	1		FL	0	Aridal?	no BC data; found near Aridal	0	0			0	0	MB	
268	NWA 10609	43.02	No. Africa	1	1		0	NWA 8046		0	0			0	0		
269	NWA 10621	22	No. Africa	1	1		0	NWA 8455		0	0			0	0		

Table S7. Estimated number of lunar meteorites and launch craters

	1	2	3	4	5	6	7	8	9	10	11	12	13	14	15	16	17
				N of stones	evidence for or against pairing		*N* of discrete meteorites			*N* of meteorites		launch pairs		launch crater			
	as of 2019-12-31	mass (g)	where		compo-sition	including other	(first of pair group)	terrestrially paired with	issue, note, or caveat	min	max	group no.	pair	min	max	refer-ence	figure or table
270	NWA 10626	1849	No. Africa	1	1		1	0	similar but not identical BC match to NWA 10509	1	1		10	0	1		S70, S71, S72, S81
271	NWA 10643	43.56	No. Africa	1	1		0	NWA 8046		0	0			0	0		
272	NWA 10644	166	No. Africa	1	1		0	NWA 7834		0	0			0	0		
273	NWA 10649	41.3	No. Africa	1	1		0	NWA 8046		0	0			0	0		
274	NWA 10656	262.5	No. Africa	1	1		0	NWA 773		0	0			0	0		
275	NWA 10665	24.73	No. Africa	1	1		1	0		1	1			1	1		S17, S59
276	NWA 10678	49.15	No. Africa	1	1		1	0		1	1			1	1		S25
277	NWA 10713	60.2	No. Africa	1			?	?		?	?			?	?		
278	NWA 10756	125.0	No. Africa	1	1		0	NWA 8046		0	0			0	0		
279	NWA 10782	39.0	No. Africa	1	1		0	NWA 7834		0	0			0	0		
280	NWA 10783	22.0	No. Africa	1	1		1	0	similar but not identical BC match to NWA 8641	1	1		8	0	1		S25, S26, S29, S46
281	NWA 10798	318.6	No. Africa	1	1		0	NWA 10509		0	0			0	0		S70
282	NWA 10810	402.4	No. Africa	1	1		0	NWA 7834		0	0			0	0		
283	NWA 10822	56	No. Africa	1	1		0	NWA 8046		0	0			0	0		
284	NWA 10823	202.0	No. Africa	1	1		0	NWA 8222		0	0			0	0		
285	NWA 10901	68.04	No. Africa	1	1		0	NWA 8046		0	0			0	0		
286	NWA 10902	36.28	No. Africa	1	1		0	NWA 8673		0	0			0	0		
287	NWA 10953	55.0	No. Africa	1	1		0	NWA 8455		0	0			0	0		
288	NWA 10964	26	No. Africa	1	1		0	NWA 8673		0	0			0	0		
289	NWA 10973	25	No. Africa	1	1		1	0		1	1			1	1		S35, S69
290	NWA 10985	250	No. Africa	1	1		0	NWA 773		0	0			0	0		
291	NWA 10986	108.2	No. Africa	1	1		0	NWA 10509		0	0			0	0	R	
292	NWA 10989	14.4	No. Africa	1	1		0	NWA 7834		0	0			0	0		
293	NWA 11006	2245	No. Africa	1	1		1	0		1	1			1	1		S7, S17, S25
294	NWA 11029	75	No. Africa	1	1		0	NWA 8046		0	0			0	0		
295	NWA 11061	1040	No. Africa	1	1		1	0		1	1			1	1		S17, S25
296	NWA 11077	1139.7	No. Africa	1	1		1	0	similar but not identical BC match to NWA 10509	1	1		9	0	1		S45, S74, S75, S80
297	NWA 11109	77	No. Africa	1	1		0	NWA 7834		0	0			0	0		
298	NWA 11110	62	No. Africa	1	1		0	NWA 8673		0	0			0	0		
299	NWA 11111	111	No. Africa	1	1		0	NWA 10141		0	0			0	0		
300	NWA 11127	474.6	No. Africa	1	1		1	0		1	1			1	1		S15, S71
301	NWA 11159	10.7	No. Africa	1			?	?		?	?			?	?		
302	NWA 11182	60	No. Africa	1	1		1	0		1	1			1	1		S15, S17, S44, S72
303	NWA 11185	94.02	No. Africa	1	1		0	NWA 7834		0	0			0	0		

Table S7. Estimated number of lunar meteorites and launch craters

	1	2	3	4	5	6	7	8	9	10	11	12	13	14	15	16	17
					evidence for or against pairing					N of meteorites		launch pairs		launch crater			
	as of 2019-12-31	mass (g)	where	N of stones	compo-sition	including other	N of discrete meteorites (first of pair group)	terrestrially paired with	issue, note, or caveat	min	max	group no.	pair	min	max	refer-ence	figure or table
304	NWA 11193	155	No. Africa	1	1		0	NWA 7834		0	0			0	0		
305	NWA 11212	197.5	No. Africa	1	1		0	NWA 8222		0	0			0	0		
306	NWA 11216	222	No. Africa	1	1		0	NWA 8222		0	0			0	0		
307	NWA 11223	28	No. Africa	1	1		1	NWA 11809		1	1			1	1		S6, S15, S25
308	NWA 11228	140	No. Africa	1	1		0	NWA 8673		0	0			0	0		
309	NWA 11237	583	No. Africa	1	1		0	NWA 8222		0	0			0	0		
310	NWA 11243	80	No. Africa	1	1		1	0		1	1			1	1		S26, S46, S71, S78
311	NWA 11249	73.6	No. Africa	1	1		0	NWA 7834		0	0			0	0		
312	NWA 11252	22.9	No. Africa	1	1		0	NWA 5744		0	0			0	0		
313	NWA 11266	1017.0	No. Africa	1	1		0	NWA 8046		0	0			0	0		
314	NWA 11269	220	No. Africa	1	1		0	NWA 8046		0	0			0	0		
315	NWA 11273	2808	No. Africa	1	1		0	NWA 8046		0	0			0	0		
316	NWA 11303	6000	No. Africa	1	1		0	NWA 8046		0	0			0	0		
317	NWA 11331	318	No. Africa	1			?	NWA 8046?		?	?			?	?		
318	NWA 11352	74.5	No. Africa	1	1		1	0		1	1			1	1		S17, S25, S71, S72, S75, S80
319	NWA 11367	305.0	No. Africa	1			?	?		?	?			?	?		
320	NWA 11379	150.87	No. Africa	1	1		0	NWA 8046		0	0			0	0		
321	NWA 11407	700	No. Africa	1			?	NWA 8046?		?	?			?	?		
322	NWA 11421	912	No. Africa	1			?	NWA 8046?		?	?			?	?		
323	NWA 11428	783	No. Africa	1	1		0	NWA 8046		0	0			0	0		
324	NWA 11444	1323	No. Africa	1			?	NWA 8046?		?	?			?	?		
325	NWA 11457	273	No. Africa	1			?	?		?	?			?	?		
326	NWA 11460	286	No. Africa	1	1		0	NWA 8046		0	0			0	0		
327	NWA 11472	840	No. Africa	1			?	NWA 8046?		?	?			?	?		
328	NWA 11474	586	No. Africa	1			?	?		?	?			?	?		
329	NWA 11479	504	No. Africa	1	1		0	NWA 8046		0	0			0	0		
330	NWA 11515	330	No. Africa	1	1		0	NWA 8046		0	0			0	0		
331	NWA 11517	88	No. Africa	1			?	NWA 8046?		?	?			?	?		
332	NWA 11523	3362	No. Africa	1			?	?		?	?			?	?		
333	NWA 11524	820	No. Africa	1	1		1	?	No other NWA basaltic breccia has 3% TiO_2 & 11% Al_2O_3; need real BC	0	1			0	1	MB: DFB shock melt	
334	NWA 11532	70	No. Africa	1			?	NWA 8046?		?	?			?	?		
335	NWA 11563	54.5	No. Africa	1	1		0	NWA 7834		0	0			0	0		
336	NWA 11616	2550.8	No. Africa	1	1		0	NWA 773		0	0			0	0		
337	NWA 11695	350	No. Africa	1			?	NWA 8046?		?	?			?	?		

Table S7. Estimated number of lunar meteorites and launch craters

	1	2	3	4	5	6	7	8	9	10	11	12	13	14	15	16	17
					evidence for or against pairing		*N* of discrete meteorites			*N* of meteorites		launch pairs		launch crater			
	as of 2019-12-31	mass (g)	where	*N* of stones	compo-sition	including other	(first of pair group)	terrestrially paired with	issue, note, or caveat	min	max	group no.	pair	min	max	refer-ence	figure or table
338	NWA 11703	5309.1	No. Africa	1	1		0	NWA 773		0	0			0	0		
339	NWA 11767	15	No. Africa	1		P	0	NWA 773?	need BC	0	0			0	0		
340	NWA 11783	65	No. Africa	1			?	?		?	?			?	?		
341	NWA 11787	23500	No. Africa	1			?	NWA 8046?		?	?			?	?		
342	NWA 11788	10441	No. Africa	1			?	NWA 8673?		?	?			?	?		
343	NWA 11789	5492	No. Africa	1			?	NWA 8046?		?	?			?	?		
344	NWA 11801	67.05	No. Africa	1			?	?		?	?			?	?		
345	NWA 11809	67	No. Africa	1	1		0	NWA 11223		0	0			0	0		
346	NWA 11828	5340	No. Africa	1			?	?		?	?			?	?		
347	NWA 11851	227	No. Africa	1	1		1	0		1	1			1	1		S4, S15
348	NWA 11871	21.9	No. Africa	1			?	?		?	?			?	?		
349	NWA 11886	36	No. Africa	1	1		1	0		1	1			1	1		6, S6, S15
350	NWA 11898	768	No. Africa	1			?	NWA 8046?		?	?			?	?		
351	NWA 11962	85.8	No. Africa	1			?	?	basaltic breccia?	?	?			?	?		
352	NWA 11966	157.13	No. Africa	1			?	NWA 8046?		?	?			?	?		
353	NWA 11968	427.8	No. Africa	1			?	NWA 8046?		?	?			?	?		
354	NWA 12008	577	No. Africa	1	1		1	0	BC is all but indistinguishable from NWA 032/479 but texture is different	1	1		3	0	1	C2	13, S17
355	NWA 12216	34.4	No. Africa	1			?	?		?	?			?	?		
356	NWA 12248	37.3	No. Africa	1			?	?		?	?			?	?		
357	NWA 12270	1300	No. Africa	1			?	?		?	?			?	?		
358	NWA 12279	1830	No. Africa	1			?	NWA 8046?		?	?			?	?		
359	NWA 12368	1868	No. Africa	1			?	?		?	?			?	?		
360	NWA 12384	244	No. Africa	1	1		1	NEA 003?	Composition is unlike any other NWA basaltic breccia (high MgO)	0	1			0	1	C1	13
361	NWA 12393	1267.1	No. Africa	1		P	1	NWA 773?	olivine gabbronorite more magnesian (Fo_{73}) than NWA 773 clan olivine gabbro ($Fo_{\sim 68}$); need BC	0	1			0	1	MB, V	
362	NWA 12422	43	No. Africa	1			?	?		?	?			?	?		
363	NWA 12427	3469	No. Africa	1			?	?		?	?			?	?		
364	NWA 12428	2070	No. Africa	1			?	?		?	?			?	?		
365	NWA 12592	1420	No. Africa	1			?	?		?	?			?	?		
366	NWA 12593	332.8	No. Africa	1			?	?		?	?			?	?		
367	NWA 12603	47	No. Africa	1			?	?		?	?			?	?		
368	NWA 12604	631	No. Africa	1	1		1	0		1	1			1	1		S46
369	NWA 12630	233	No. Africa	1			?	NWA 8046?		?	?			?	?		
370	NWA 12643	2602	No. Africa	1			?	?		?	?			?	?		
371	NWA 12691	103770	No. Africa	1	1		0	NWA 8046		0	0			0	0		
372	NWA 12695	224	No. Africa	1			?	NWA 8046?		?	?			?	?		

Table S7. Estimated number of lunar meteorites and launch craters

	1	2	3	4	5	6	7	8	9	10	11	12	13	14	15	16	17
				N of stones	evidence for or against pairing		*N* of discrete meteorites			*N* of meteorites		launch pairs		launch crater			
	as of 2019-12-31	mass (g)	where		compo-sition	including other	(first of pair group)	terrestrially paired with	issue, note, or caveat	min	max	group no.	pair	min	max	refer-ence	figure or table
373	NWA 12697	140	No. Africa	1			?	?		?	?			?	?		
374	NWA 12760	58090	No. Africa	1		FL	0	NWA 8046		0	0			0	0		
375	NWA 12765	15949	No. Africa	1			?	NWA 8046?		?	?			?	?		
376	NWA 12826	25	No. Africa	1			?	?		?	?			?	?		
377	NWA 12830	232	No. Africa	1			?	?		?	?			?	?		
378	NWA 12831	151	No. Africa	1			?	?	first from Niger	?	?			?	?		
379	NWA 12839	68.75	No. Africa	1		BC, P	1	?	As with NWA 12008, BC is very similar to NWA 032/479, but NWA 12839 is a diabase	1	1		3	0	1	B	
380	NWA 12870	30	No. Africa	1			?	NWA 8046?		?	?			?	?		
381	NWA 12909	2742	No. Africa	1			?	?		?	?			?	?		
382	NWA 12952	808	No. Africa	1			?	?		?	?			?	?		
383	NWA 12966	1.39	No. Africa	1			?	NWA 8046?		?	?			?	?		
384	NWA 12971	280	No. Africa	1		P	1	NWA 5744?	troctolitic melt rock distinct from NWA 5744 clan	0	1			0	1	MB	
385	NWA 12980	1300	No. Africa	1			?	?		?	?			?	?		
386	NWA 12985	33	No. Africa	1			?	?		?	?			?	?		
387	NWA 12997	60	No. Africa	1		P	0	NWA 5744	troctolite but, no BC data or photo	0	0			0	0		
388	Oued Awlitis 001	432.5	No. Africa	1	1		1	0		1	1			1	1		S72
389	Rabt Sbayta 002	6371.9	No. Africa	1	1		0	NWA 8222		0	0			0	0		
390	Rabt Sbayta 004	15464	No. Africa	1	1		0	NWA 8222		0	0			0	0		
391	Rabt Sbayta 005	20.78	No. Africa	1		FL	0	NWA 8222?	no BC data; found near RaSb 002 & 004	0	0			0	0		
392	Rabt Sbayta 006	4810	No. Africa	1		FL	0	NWA 8222?	no BC data; found near RaSb 002 & 004	0	0			0	0		
393	Rabt Sbayta 007	4432	No. Africa	1	1		1	0		1	1			1	1		S25
394	Rabt Sbayta 008	229	No. Africa	1	1		1	0		1	1			1	1		S71
395	Sueilila 005	282	No. Africa	1	1		0	NWA 10495	but more feldspathic and lower Sm/Th than NWA 10495	0	1			0	1		S72
396	Swayyah 001	4602	No. Africa	1		P	1	?	coarse-grained gabbro distinct from 773 clan	0	1			0	1	MB	
397	Talhat Lihoudi	61.5	No. Africa	1	1		1	0		1	1			1	1		S25, S46

Table S7. Estimated number of lunar meteorites and launch craters

	1	2	3	4	5	6	7	8	9	10	11	12	13	14	15	16	17
				N of stones	evidence for or against pairing		*N* of discrete meteorites			*N* of meteorites		launch pairs		launch crater			
	as of 2019-12-31	mass (g)	where		compo-sition	including other	(first of pair group)	terrestrially paired with	issue, note, or caveat	min	max	group no.	pair	min	max	refer-ence	figure or table
398	Tichiya	9354	No. Africa	1	1		1	0		1	1			1	1		S16, S25, S46, S66, S78
406	**count**					**20**						**10**	**22**				
407	**sum**	**524,268**		**398**	**321**	**341**	**140**			**131**	**147**			**109**	**134**		
408	**%**				81%	86%	41%										
	40	Antarctica		40	35	5	23			23	23						
	2	Australia		2	2	0	2			2	2						
	71	Oman		71	67	3	28			27	29						
	2	Saudi Arabia		2	1	1	2			2	2						
	2	Botswana		2	2	0	1			1	1						
	281	northern Africa		281	214	11	84			76	90						
	398	**total**		**398**	**321**	**6**	**140**			**131**	**147**						

Column	
1	Meteorite name or abbreviation
2	Mass of named stone (grams)
3	Find country or continent
4	Row 407 (column sum) = total number of named stones (MetBull)
5	Compositional evidence exists for or against pairing: 1 = yes, blank = no data
5	Row 407 (column sum) = number of compositionally characterized stones
5	Row 408 = sum column 5 / sum column 4 = fraction (%) of all stones for which there is compositional evidence for or against pairing
6	Other evidence for or against pairing: P = petrography, FL = reported find location. Row 406 (column count) = total number of other "characterized" stones
7	1 = only, first, or most conspicuous stone of a presumed pair group; 0 = paired with stone of column 8; "?" = insufficient data
7	Row 407 (column sum) = **preferred estimated number of discrete meteorites**
7	Row 408 = column 7 sum / column 6 sum = fraction (%) of characterized stones that are discrete meteorites
8	Name of presumed terrestrial pair(s): 1 = name(s), 0 = none known, ? = unknown (insufficient data)
9	Issue, note, or caveat that may affect meteorite count or launch-crater count
10-15	"?" = not "characterized: no data; do not include in counts
10&11	(0 & 0), (1 &1), or (? &?) = no reason to suspect value of column 8

Table S7. Estimated number of lunar meteorites and launch craters

1	2	3	4	5	6	7	8	9	10	11	12	13	14	15	16	17
				evidence for or against pairing		*N* of discrete meteorites			*N* of meteorites		launch pairs		launch crater			
as of 2019-12-31	mass (g)	where	*N* of stones	compo-sition	including other	(first of pair group)	terrestrially paired with	issue, note, or caveat	min	max	group no.	pair	min	max	refer-ence	figure or table

10&11	(0 & 1) and value of column 8 = 0: preferably, the stone is terrestrially paired, but issue of col. 10 (unpairing) might **increase** number of meteorites from preferred value.
10&11	(0 & 1) and value of column 8 = 1: preferably, the stone is not terrestrially paired, but issue of col. 10 (pairing) might **decrease** number of meteorites from preferred value.
10	Row 407 (column sum) = **estimated minimum number of discrete meteorites (and meteoroids) represented among characterized meteorites**
11	Row 408 (column sum) = **estimated maximum number of discrete meteorites (and meteoroids) represented among characterized meteorites**
12	First or most prominent meteorite, with group number, of likely (1-5) or possible (6-10) launch-pair group. (These count as launch craters.)
13	Group number for likely or possible launch pairs. (These do not count as launch craters.)
14	= value of column 10: If it counts as a meteorite (column 7 = 1), then count it as a launch crater, but if it is a terrestrial *pair* of a meteorite (0), then do not count it as a launch crater. UNLESS = 0 if value of column 10 = 1 and value in column 13 is nonzero: Do not count "likely" (0, 1, 2, 3, 4,& 5) or "possible" (6, 7, 8, 9, & 10) launch pairs as launch craters.
14	Row 407 (column sum) = **estimated minimum number of launch craters represented among characterized meteorites**
15	= value of column 11: If it counts as a meteorite (column 7 = 1), then count it as a launch crater, but if it is a terrestrial pair of a meteorite (0), then do not count it as a launch crater. UNLESS = 0 if value of column 11 = 1 and value in column 13 = 1, 2, 3, 4, or 5: Include "possible" launch pairs (6, 7, 8, 9, & 10) as possible new launch craters because of issue of column 9.
15	Row 407 (column sum) = **estimated maximum number of launch craters represented among characterized meteorites**
16	references
17	figure or table number

Abbreviations

BC	bulk composition
DFB	defocused beam EPMA
EPMA	electron probe microanalysis
FL	field location
MB	Meteoritical Bulletin
P	petrography

References

AW	Arai T. and Warren P. H. 1999 Lunar meteorite Queen Alexandra Range 94281: Glass compositions and other evidence for launch pairing with Yamato 793274. *Meteoritics & Planetary Science* 34:209-234.
B	Burney D., Neal C. R., Irving A. J., Carpenter P. K., Tepper J. H., and Hoefnagels B. 2020. Petrology and chemical composition of lunar mare diabase Northwest Africa 12839: Comparisons with Apollo basalts. 51st Lunar and Planetary Science Conference, abstract no. 2613.
C1	Carpenter P. K., Jolliff B. L., Korotev R. L., Tepper J. H., Irving A. J., and Labenne L. 2019. Petrology and bulk composition of lunar mare basalt breccia Northwest Africa 12384. 50th Lunar and Planetary Science Conference, abstract no. 2125.
C2	Cohen M. E., Kuehner S. M., Tepper J. H., Burney D. C., Neal C. R., Irving A. J., Korotev R. L., and B. Hoefnagels. 2019. Mineralogy and bulk composition of lunar mare basalt Northwest Africa 12008. 50th Lunar and Planetary Science Conference, abstract no. 2508.
C3	Collareta A., D'Orazio M., Gemelli M., Pack A., Folco L. 2016. High crustal diversity preserved in the lunar meteorite Mount DeWitt 12007 (Victoria Land, Antarctica). *Meteoritics & Planetary Science* 51:351-371.
D	Demidova S. I., Nazarov M. A., Lorenz C. A., Kurat G., Brandstätter F., and Ntaflos Th. 2007. Chemical composition of lunar meteorites and the lunar crust. *Petrology* 15:386-407.

Table S7. Estimated number of lunar meteorites and launch craters

	1	2	3	4	5	6	7	8	9	10	11	12	13	14	15	16	17
				N of stones	evidence for or against pairing		*N* of discrete meteorites			*N* of meteorites		launch pairs		launch crater			
	as of 2019-12-31	mass (g)	where		compo-sition	including other	(first of pair group)	terrestrially paired with	issue, note, or caveat	min	max	group no.	pair	min	max	refer-ence	figure or table
	E	Elardo S. M., Shearer C. K. Jr., Fagan A. L., Borg L. E., Gaffney A. M., Burger P. V., Neal C. R., Fernandes V. A., and McCubbin F. M. 2013. The origin of young mare basalts inferred from lunar meteorites Northwest Africa 4734, 032, and LaPaz Icefield 02205. *Meteoritics & Planetary Science* 49:261–291.															
	H	Hill P. J. A., Osinski G. R., Banerjee N. R., Korotev R. L., Nasir S. J., Herd C. D. K. 2018. Petrography and geochemistry of lunar meteorites Dhofar 1673, 1983, and 1984. *Meteoritics & Planetary Science* 54:300-320.															
	K1	Korotev R. L. Lunar meteorites from Oman. 2012. *Meteoritics & Planetary Science* 47:1365–1402.															
	K2	Korotev R. L., Jolliff B. L., Zeigler R. A., and Haskin L. A.2003. Compositional constraints on the launch pairing of three brecciated lunar meteorites of basaltic composition. *Antarctic Meteorite Research* 16:152-175, National Institute of Polar Research, Tokyo.															
	K3	Korotev R. L., Zeigler R. A., Jolliff B. L., Irving A. J., and Bunch T. E. 2009. Compositional and lithological diversity among brecciated lunar meteorites of intermediate iron concentration. *Meteoritics & Planetary Science* 44:1287–1322.															
	K4	Korotev R. L. 2017. Update (2012–2017) on lunar meteorites from Oman. *Meteoritics & Planetary Science* 52:1251-1256.															
	K5	Korotev R. L., Jolliff B. L., Zeigler R. A., and Haskin L. A. (2003) Compositional constraints on the launch pairing of three brecciated lunar meteorites of basaltic composition. *Antarctic Meteorite Research* 16:152-175.															
	KZ	Korotev R. L. and Zeigler R. A. 2014 Chapter 6. ANSMET Meteorites from the Moon, *Thirty-five Seasons of U.S. Antarctic Meteorites (1976–2010): A Pictorial Guide to the Collection* (editors K. Righter, R. P. Harvey, C. M. Corrigan, and T. J. McCoy), 101–130, Special Publications 68, American Geophysical Union, Washington, D. C., 296 pages, ISBN: 978-1-118-79832-4.															
	M	Mészáros M., Hofmann B. A., Lanari P., Korotev R. L., Gnos E., Greber N. D., Leya I., Greenwood R. C., Jull A. J. T., Al-Wagdani K., Mahjoub A., Al-Solami A. A., and Habibullah S. N. 2016. Petrology and geochemistry of feldspathic impact-melt breccia Abar al' Uj 012, the first lunar meteorite from Saudi Arabia. *Meteoritics & Planetary Science* 51:1830-1848.															
	MB	Meteoritical Bulletin: https://www.lpi.usra.edu/meteor/metbull.php															
	N	Nishiizumi K., Arnold J. R., Klein J., Fink D., Middleton R., Kubik P. W., Sharma P., Elmore D., and Reedy R. C. (1991) Exposure histories of lunar meteorites: ALHA81005, MAC81004, MAC81005, and Y791197. *Geochimica et Cosmochimica Acta* :55, 3149-3155.															
	NC	Nishiizumi K. and Caffee M. W. (2013) Relationships among six lunar meteorites from Miller Range, Antarctica based on cosmogenic radionuclides. 44th Lunar and Planetary Science Conference, abstract no. 2715.															
	R	Roberts S. E., McCanta M. C., Jean M. M., and Taylor L. A. 2019. New lunar meteorite NWA 10986: A mingled impact melt breccia from the highlands—A complete cross section of the lunar crust. *Meteoritics & Planetary Science* 54:3018–3035.															
	V	Valencia S. N., Jolliff B. L., Korotev R. L. 2019). Petrography, relationships, and petrogenesis of the gabbroic lithologies in Northwest Africa 773 clan members Northwest Africa 773, 2727, 3160, 3170, 7007, and 10656. *Meteoritics & Planetary Science* 54:2083-2115.															
	W	Warren P. H., Ulff-Møller F., and Kallemeyn G. W. 2005 "New" lunar meteorites: Impact melt and regolith breccias and large-scale heterogeneities of the upper lunar crust. *Meteoritics & Planetary Science* 40:989-1014.															
	WK	Warren P. H. and Kallemeyn G. W. 1993. Geochemical investigations of two lunar mare meteorites: Yamato-793169 and Asuka-881757. *Proceedings of the NIPR Symposium on Antarctic Meteorites* 6:35-57.															
	Z	Zeigler R. A., Korotev R. L., Jolliff B. L., and Haskin L. A. 2005. Petrology and geochemistry of the LaPaz icefield basaltic lunar meteorite and source-crater pairing with Northwest Africa 032. *Meteoritics & Planetary Science* 40, 1073-1102.															

Figures Cited in Main Text

Fig. S1. Twelve breccia samples, as received, with millimeter ticks for scale. (a–h) Sawn slices, typically 1-mm thick. (a) NWA 2998 is the most feldspathic meteorite studied here. (b) NWA 4932 is a crystalline impact-melt breccia; the light spots are grains of FeNi metal. (c) For NWA 6481 (fragmental breccia), the facing side has been polished. We have seen no self-evident contamination effects in such samples. (d) NWA 6687 is basaltic and KREEPy. (e) NWA 7493 is feldspathic and analyzed subsamples are highly variable in composition (Fig. S76). (f) NWA 8687 is greenish because it is rich in olivine (troctolitic anorthosite), but note the large, pink chromite grain on the lower left edge. (g) NWA 10480 is a mafic breccia (NWA 7611 clan). (h) Two sides of our sample of NWA 11182. The speckly clast on the left is mafic (10% FeO) while the gray glassy matrix on the right is feldspathic (5% FeO). Cr/Sc suggest that the clast is troctolitic but only ferroan gabbros are reported by Boyle et al. (2018). (i–l) Fragment samples. (i) For NWA 2996, the fusion crust (e.g., fragment on right) is weathered. (j) For NWA 6275, the image is that of one "piece" of the 5 pieces (MetBull) of this tiny (1.3 g) meteorite; the polish is due to wind abrasion. (j) NWA 10073 is a feldspathic fragmental breccia. (l) Weathering effects are evident as discoloration in NWA 10291 (NWA 7834 clan).

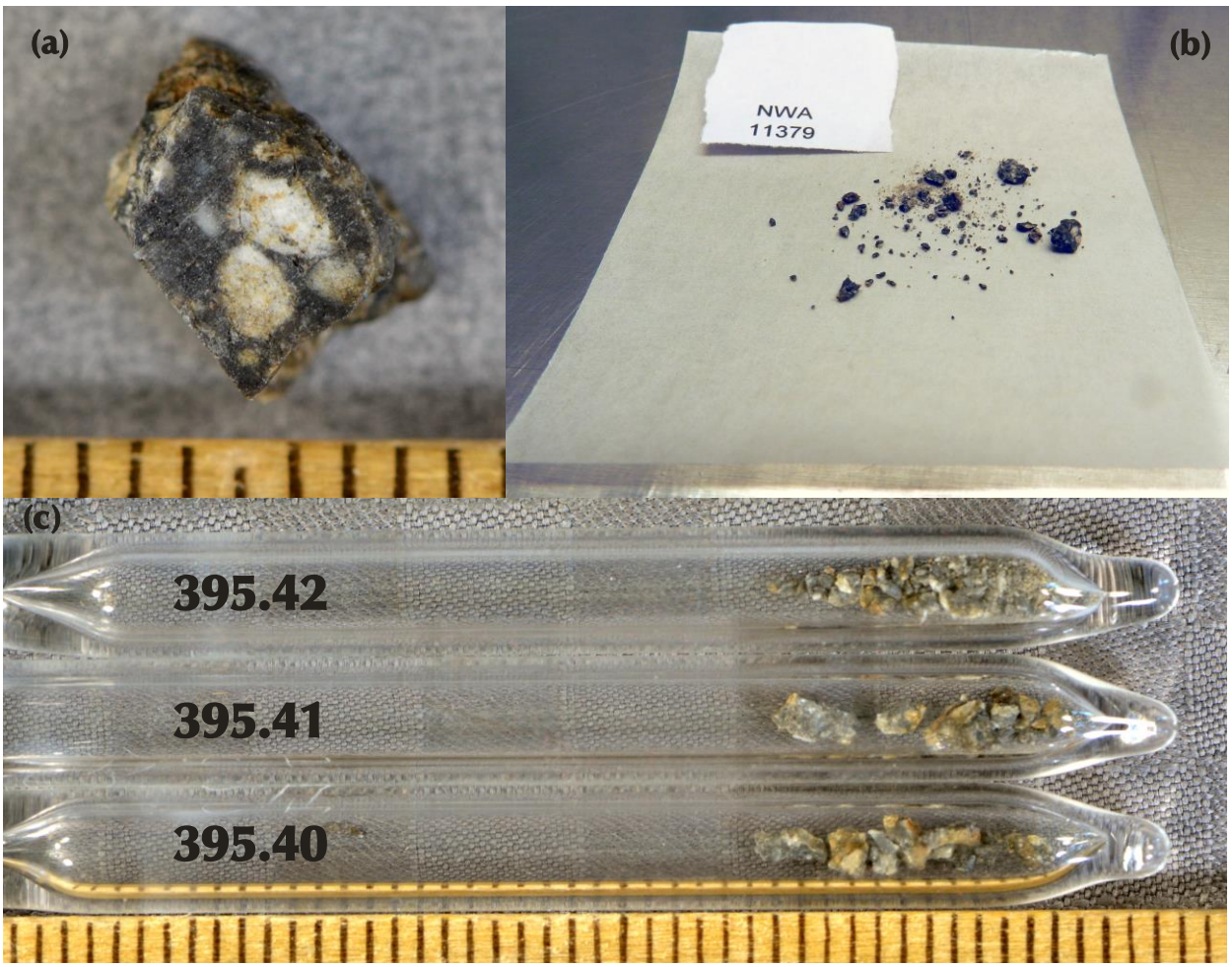

Fig. S2. INAA subsampling. The 206-mg sample of NWA 11379 (NWA 8046 clan), which is cut flat on the bottom and top faces (millimeter ticks for scale). (b) The sample after being wrapped in weighing paper and struck with a hammer. The sheet of weighing paper is 3 inches wide. (c) INAA samples sealed into ultrapure fused silica tubing: 31.98 mg (395.40), 33.35 mg (395.41), and 33.02 (395.42). The tubes are 5 mm in outside diameter. The numbers represent the consecutive irradiation number (395) and the tube sequence number within the sample pack (tubes 40, 41, and 42 out of 61). These identification numbers are presented in Table S2 for each analysis.

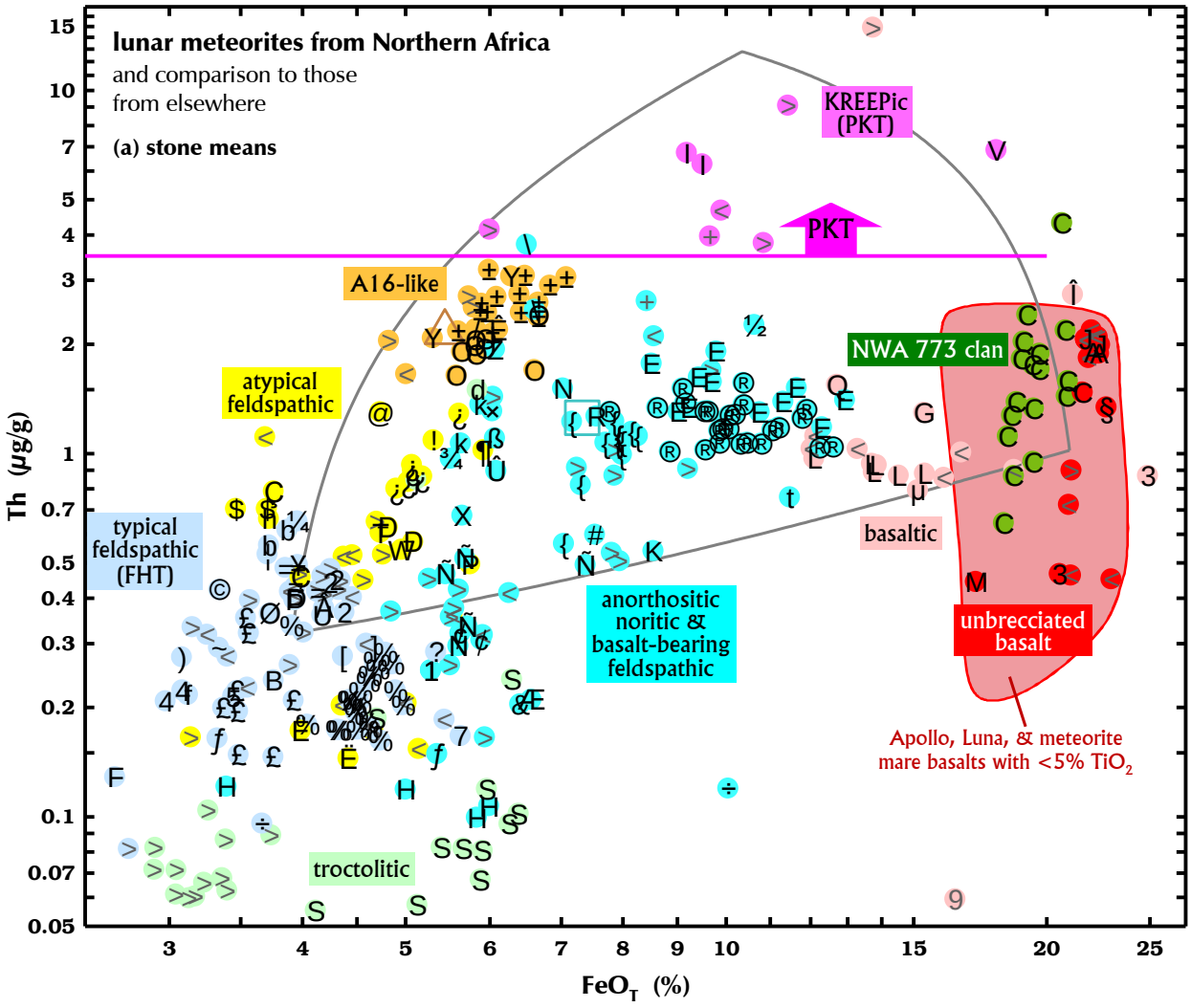

Fig. S3a. Like Fig. 6 but for FeO and Th. The "triangle" is the mixing triangle of Fig. 2 distorted by the logarithmic scales. The horizontal line at 3.5 µg/g Th represents the boundary of the Procellarum KREEP Terrane (Jolliff et al., 2000). See Table S1 for symbol key.

< Antarctica

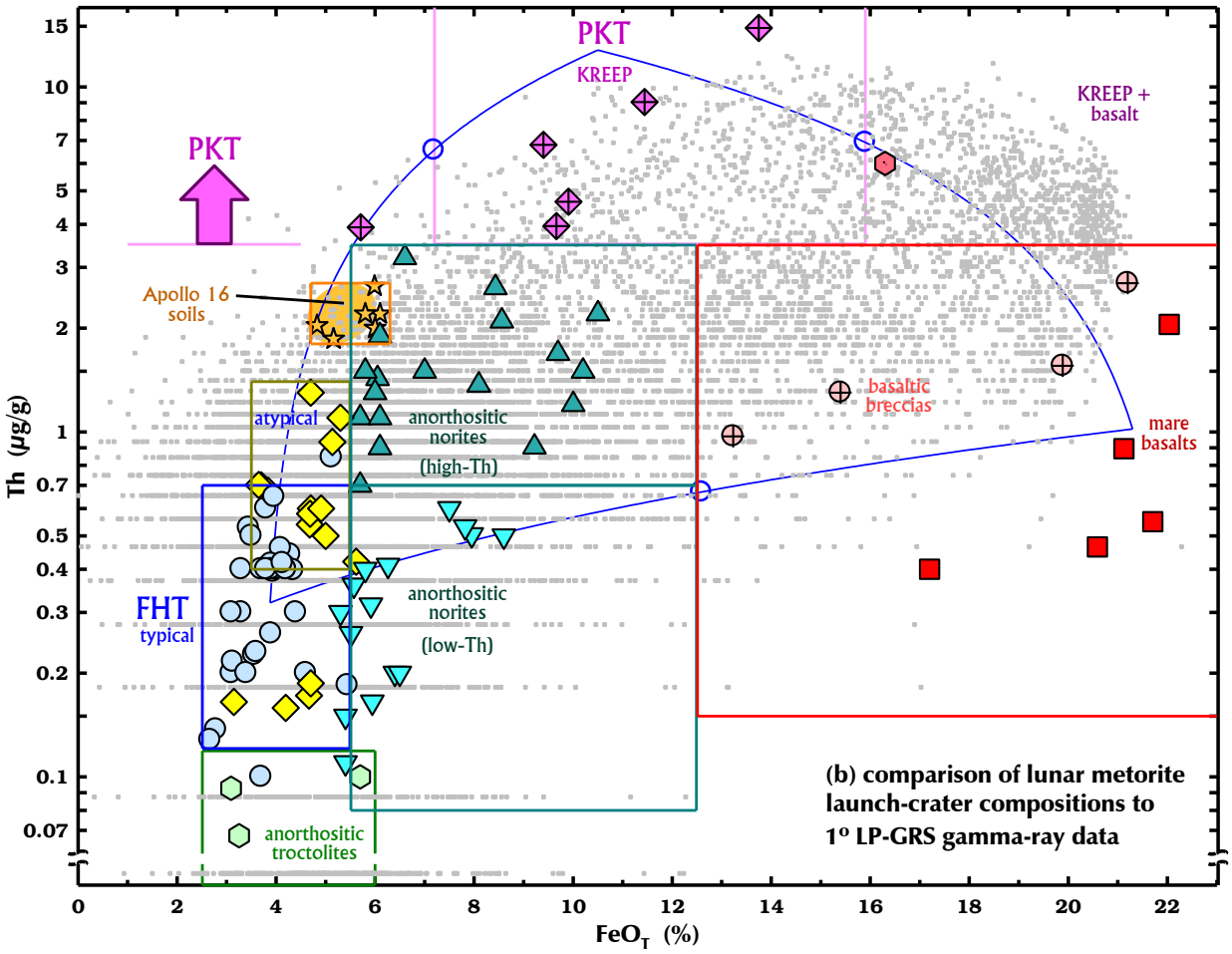

Fig. S3b. Small gray points represent the 1° (30-km) derived data from the Lunar Prospector Gamma-Ray Spectrometer (LP-5GRS, Lawrence et al., 2000, and Prettyman et al., 2006, with calibration of Gillis et al., 2004). Large colored points each represent a presumed meteorite launch crater ("minimum" estimate of Table 4). The blue "triangle" is the mixing triangle of Fig. 3a and the blue circles represent 50:50 binary mixtures of 3 the end members. LP-GRS data points plotting below the Th break are those for which the derived concentrations are ≤0 (*N*=296, or 2.8% of the data set). The six orange stars represent the "Apollo-16-like" launch craters of Fig. S35. The triangle in the field represents NWA 7274, which is dissimilar to Apollo 16 for some other elements; Fig. S35. Points plotting above 3.5 μg/g Th likely represent meteorites that derive from the PKT (Jolliff et al., 2000). The rectangles depict the ranges used to bin the LP-GRS data for the analysis of Table 5. Note that the FeO boundary between the anorthositic norites corresponds to approximately 50:50 mixtures on the FHT and mare endmembers. Similarly, the FeO boundaries of the KREEP bin are set at the 50:50 FHT:KREEP and 50:50 KREEP:mare basalt points.

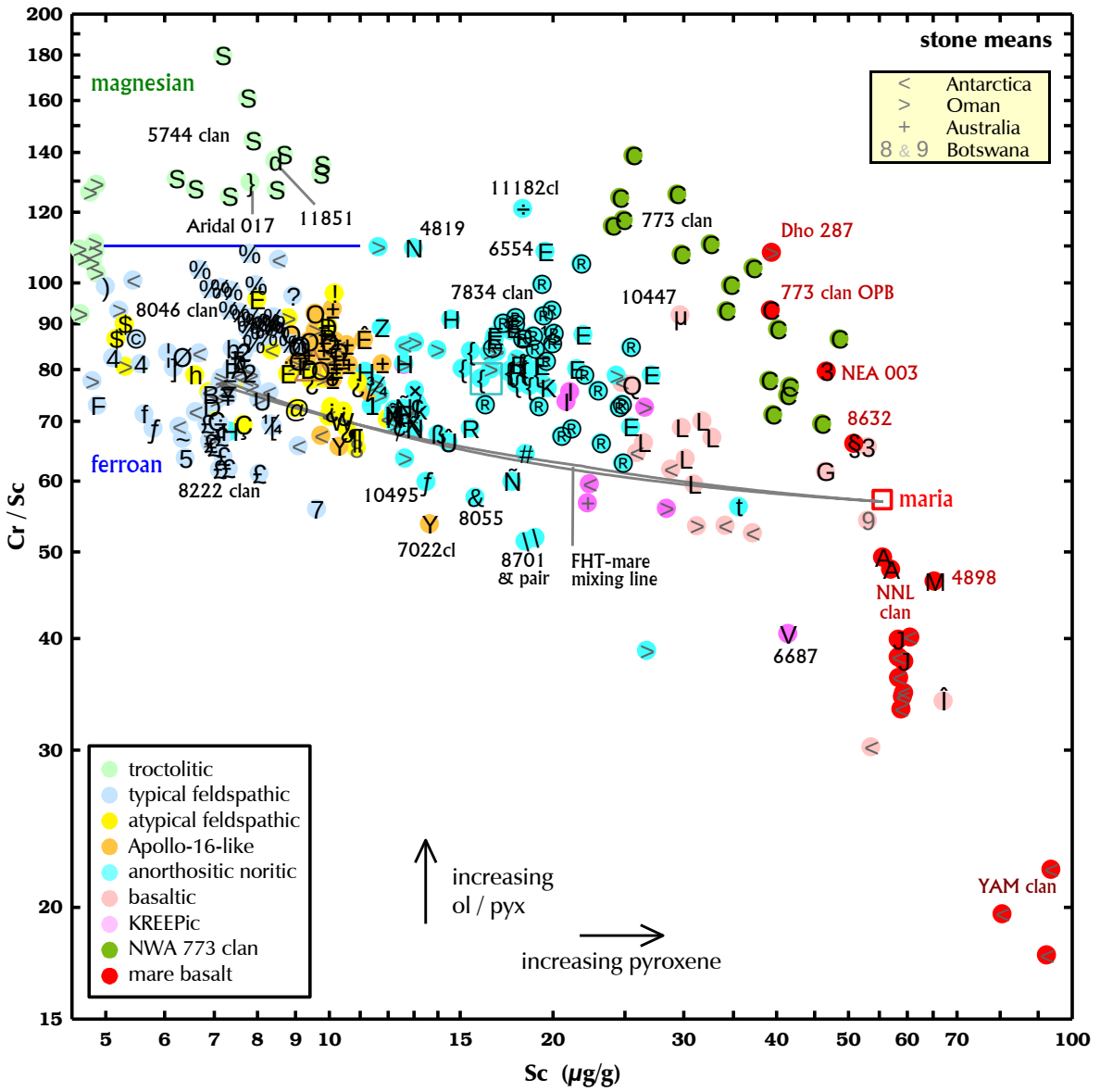

Fig. S4. Cr/Sc in lunar meteorites. Each point represents a stone, except that the red C symbol does not represent a meteorite stone but the mean of subsamples, mainly from NWA 3160 and NWA 3333, of the olivine-phyric basalt (OPB) lithology of the NWA 773 clan (Valencia et al., 2019). On the Moon, Cr/Sc is a proxy for Mg/Fe and olivine/pyroxene (Fig. 4). The curved lines are the mixing "triangles" of Figs. 2 and 6, highly flatted because the Cr/Sc of the KREEP component at 22 μg/g Sc (upper curve) is virtually identical to that of a mixture of the FHT component and the mare component having 22 μg/g Sc (lower curve). There is a large range in Cr/Sc among feldspathic meteorites, which represent the FHT; some are substantially more magnesian than ferroan anorthosite (Fig. 10). Similarly, most meteorites of noritic anorthosite composition have greater Cr/Sc than the FHT-mare mixing line. Mare basalts also have a large range in Cr/Sc. In this plot and others, the mare apex of the triangle (red square at 56 μg/g Sc) is the mean of the 7 basaltic points or clans having red labels: (1) Dhofar 287, (2) the NWA 773 OPB, (3) the NEA 003 basalt, (4) NWA 8632, (5) NWA 4898, (6) the mean of the NNL-clan meteorites (NWA 032/479, NWA 4734/10597, and the LaPaz Icefield stones of Antarctica, and (7) the mean of the YAMM-clan stones (Yamato 793169, Asuka 881757, and MET 01210, MIL 05045). Each of the 7 meteorites or clans represent a different launch crater. Regolith from the Luna 20 site (large square at 16 μg/g Sc) has high Cr/Sc because it contains mafic, nonmare lithologies like troctolite and spinel troctolites; the presence of such lithologies is also the likely cause of the high Cr/Sc (and high *Mg´*; Fig. 10) of the anorthositic-noritic meteorites. See Table S1 for symbol key.

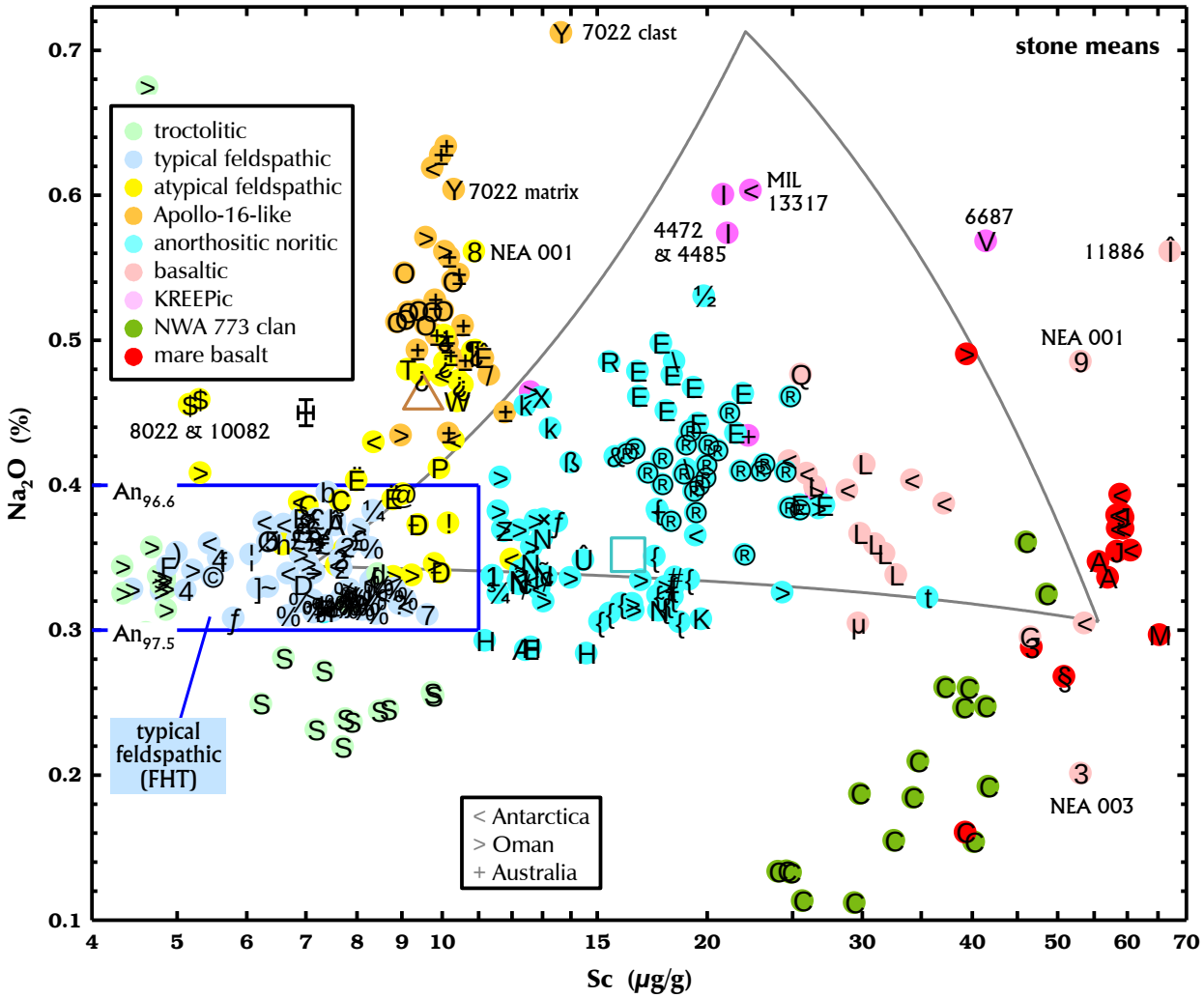

Fig. S5. Stone means in Sc-Na_2O space. Low-Na_2O meteorites of the NWA 5744 clan (symbol S) and the NWA 733 clan (symbol C) are rich in olivine. On the basis of this figure, we define a "typical feldspathic lunar meteorite" as one for which the mass-weighted mean of the pair group (or the only stone for unpaired stones) has 0.30–0.40% Na_2O, equivalent to $An_{97.5–96.6}$ in pure plagioclase. Some of the high-Na_2O meteorites have plagioclase compositions more albitic. For example, plagioclase in NWA 8022 is $An_{95.9}$ and mean plagioclase compositions among the stones of the NWA 8455 clan (orange ± symbols) range from $An_{91.1}$ to $An_{95.1}$. For reference, the triangle in the "A16-like" field represents the mean composition of typical Apollo 16 soils and the square in the middle of the diagram represents the Luna 20 soil. The error bars represent ±2σ analytical uncertainties. The large, distorted "triangle" is the mixing triangle of Figs. 2 and 6. The Apollo-16-like meteorites and some atypical feldspathic meteorites contain more Na_2O than mixtures of typical feldspathic meteorites and the KREEP component of the model, Apollo 14 soil. See Table S1 for symbol key. See also Fig. S16 (Eu vs. Sc).

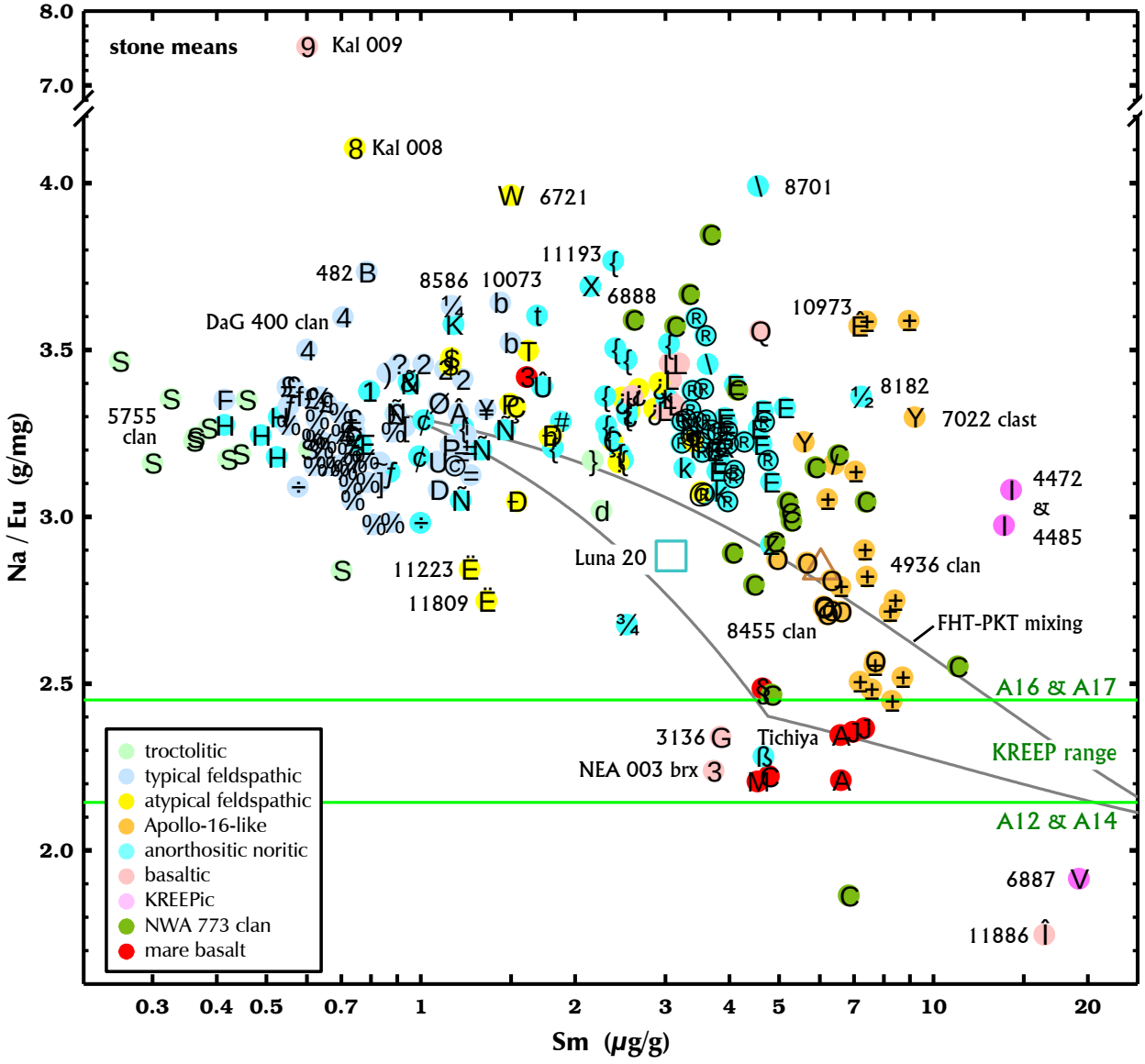

Fig. S6. Note Sm, not Sc, abscissa. Na/Eu is rather constant (<factor of 2) among feldspathic lunar meteorites because both elements are carried mainly by plagioclase, but some meteorites are distinct in deviating from the norm. Basaltic Kalahari 009 and feldspathic Kalahari 008 have the highest Na/Eu among lunar meteorites and this circumstance provides additional geochemical evidence (Sokol et al., 2008) that the stones are paired. The KREEP ranges are defined by KREEP-rich mafic impact-melt breccias from the Apollo sites (Korotev, 2000). The Apollo-16-like meteorites, as well as the Apollo 16 regolith (large triangle), have low and KREEP-like Na/Eu because, unlike the typical feldspathic lunar meteorites, a significant portion of the Eu is carried in phosphate minerals. Tichiya (ß) and paired stones NWA 11223 and NWA 11809 (Ë) have low Na/Eu because Eu is anomalously high (Fig. S16). They each also have negative Ce anomalies (Fig. S63), so Eu is likely enriched through some chemical alteration process. KREEP-rich basaltic breccia NWA 6887 and NWA 11886 have lower Na/Eu than that of KREEP impact-melt breccias (horizontal green lines) from the Apollo missions. Note that the Luna 20 regolith (large square) does not plot with the basaltic and anorthositic-noritic breccias on this plot (compare with Figs. 6, S4, S5, S16, and S44). The large, distorted "triangle" is the mixing triangle of Figs. 2 and 6. Nearly all of the basaltic and noritic-anorthositic breccias plot outside triangle in having high Na/Eu, unlike KREEP. See Table S1 for symbol key.

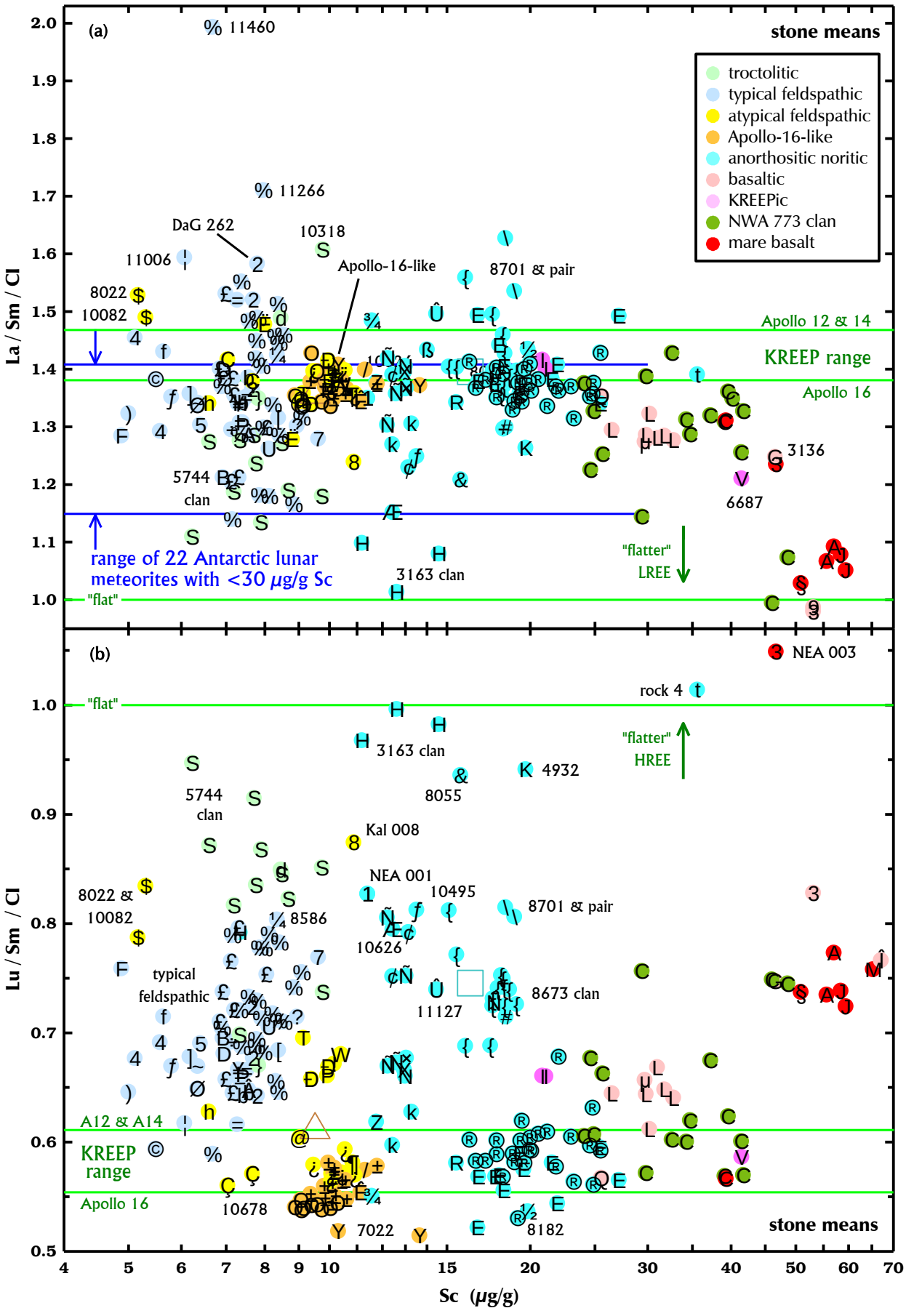
(a)
stone means
troctolitic
typical feldspathic
atypical feldspathic
Apollo-16-like
anorthositic noritic
basaltic
KREEPic
NWA 773 clan
mare basalt
% 11460
% 11266
DaG 262
10318
11006
Apollo-16-like
8701 & pair
8022
10082
Apollo 12 & 14
KREEP range
Apollo 16
3136
6687
5744 clan
range of 22 Antarctic lunar meteorites with <30 μg/g Sc
"flat"
"flatter" LREE
3163 clan
La / Sm / CI
(b)
NEA 003
rock 4
"flatter" HREE
4932
8055
Kal 008
NEA 001
10495
8701 & pair
8022 & 10082
8586
10626
typical feldspathic
8673 clan
11127
A12 & A14
KREEP range
Apollo 16
10678
7022
8182
Lu / Sm / CI
Sc (μg/g)

Fig. S7. CI-chondrite-normalized ratios of light REE, La (a), and heavy REE, Lu (b), to middle rare earth, Sm, in lunar meteorites from northern Africa. Several non-mare breccias from northern Africa have greater La/Sm than do otherwise similar meteorites from Antarctica. Some of these differences may be due to mineralogy and crystallization history of the igneous precursors but most are probably due to terrestrial alteration processes leading to "light-REE enrichment." The Antarctic range is not shown in (b) but ranges from, 0.54 to 0.99, essentially the same as the African meteorites. The KREEP ranges are defined by KREEP-rich mafic impact-melt breccias from the Apollo sites (Korotev, 2000). The Apollo-16-like meteorites (orange) have REE ratios like those of the Apollo 16 impact-melt breccias. A few moderately-high-Sm meteorites have ratios dissimilar to KREEP, most notably NWA 8673 clan (symbol {) and NWA 8701 clan (\). Some of these have low La/Sm because they contain a substantial component of mare basalt: NWA 3136 (G), 4884 and pairs (L), NWA 6687 (V), and NWA 10447 (μ). In (a), aluminous mare basalt NWA 4898 (M) lies off scale at 0.65 and NWA 11886 (Î) lies off scale at 0.78. The large triangle represents Apollo 16 regolith and the large square represents Luna 20 regolith. See Table S1 for symbol key.

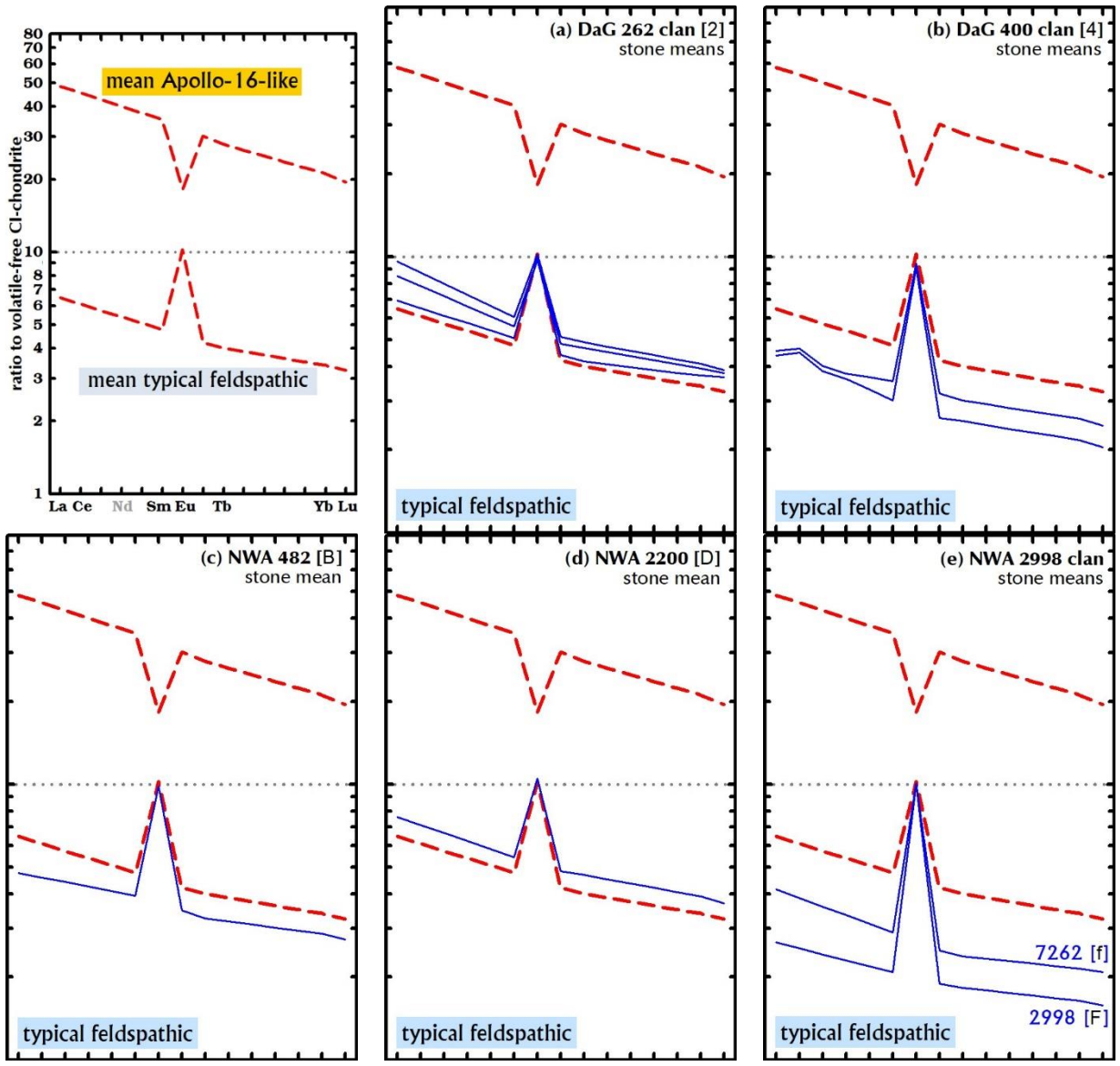

Fig. S8. REE concentrations normalized to those in volatile-free CI chondrites (Korotev et al., 2003a) in typical feldspathic lunar meteorites. Analyzed REE are shown in the upper left panel. The ordinate scale ranges from 1 to 80 with the dotted line at 10. For reference, dashed lines represent the mean REE concentrations in typical feldspathic lunar meteorites (bottom) the Apollo-16-like meteorites (top). The patterns are somewhat stylized in that the light REE segment is defined by Sm at the right end and the mean of La and Ce at the left except (except for those patterns with negative Ce anomalies) because Nd, and to a lesser extent Ce, are determined less precisely than La and Sm. Gd (between Eu and Tb) concentrations are estimated. Typical feldspathic lunar meteorites have positive Eu anomalies with CI-normalized Eu concentrations of ~10 because (1) Eu concentrations are nearly constant, ranging from 0.69 µg/g for DaG 1058 (DaG 400 clan, panel b) to 0.85 µg/g for Rabt Sbayta 004 (NWA 8222 clan, panel j) and (2) concentrations of trivalent REE are low.

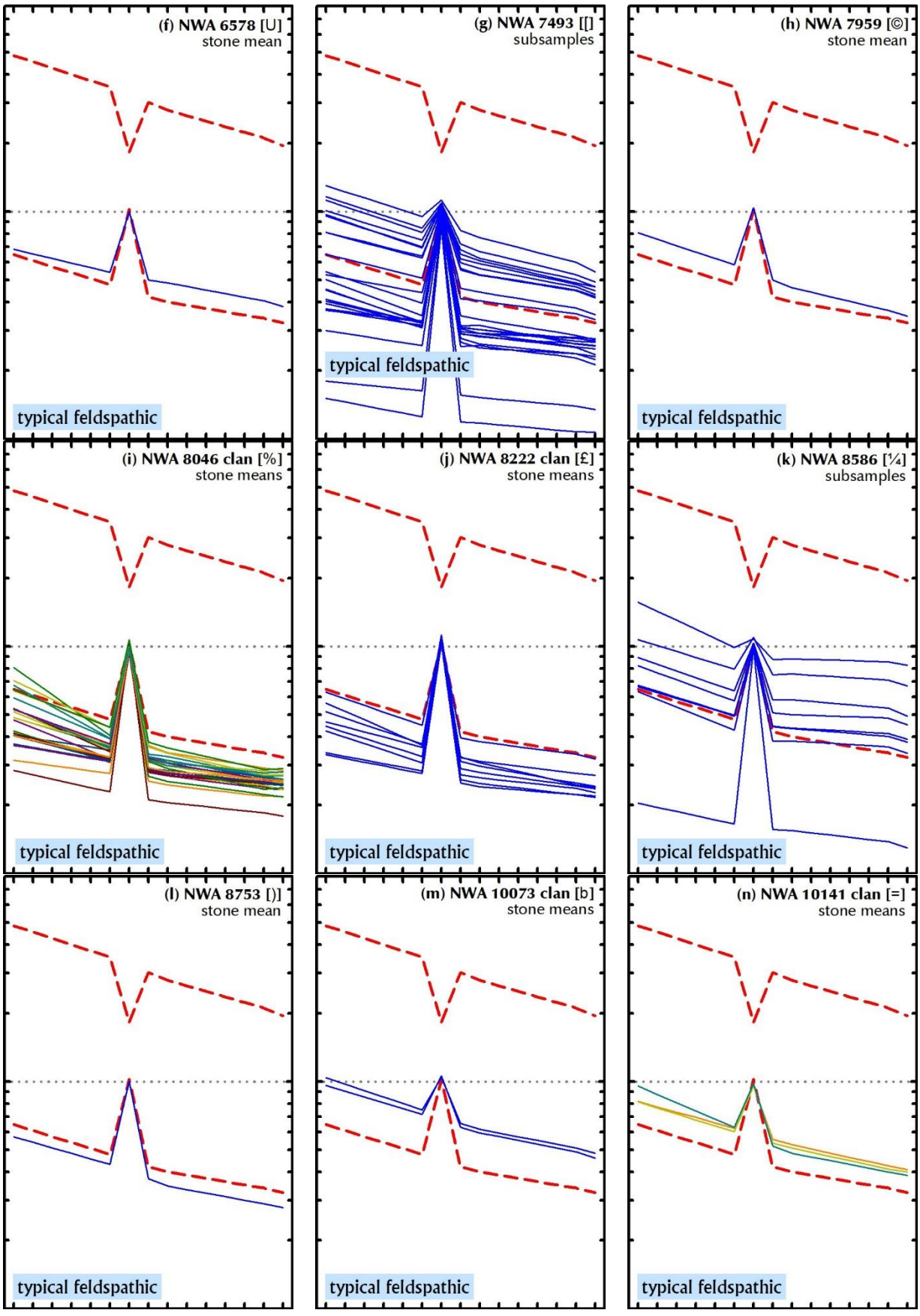

Fig. S8, continued. For NWA 8046 (panel i) the light REE enrichment in some subsamples is a terrestrial weathering effect. Heavy REE are unusually high in NWA 8586 (panel k).

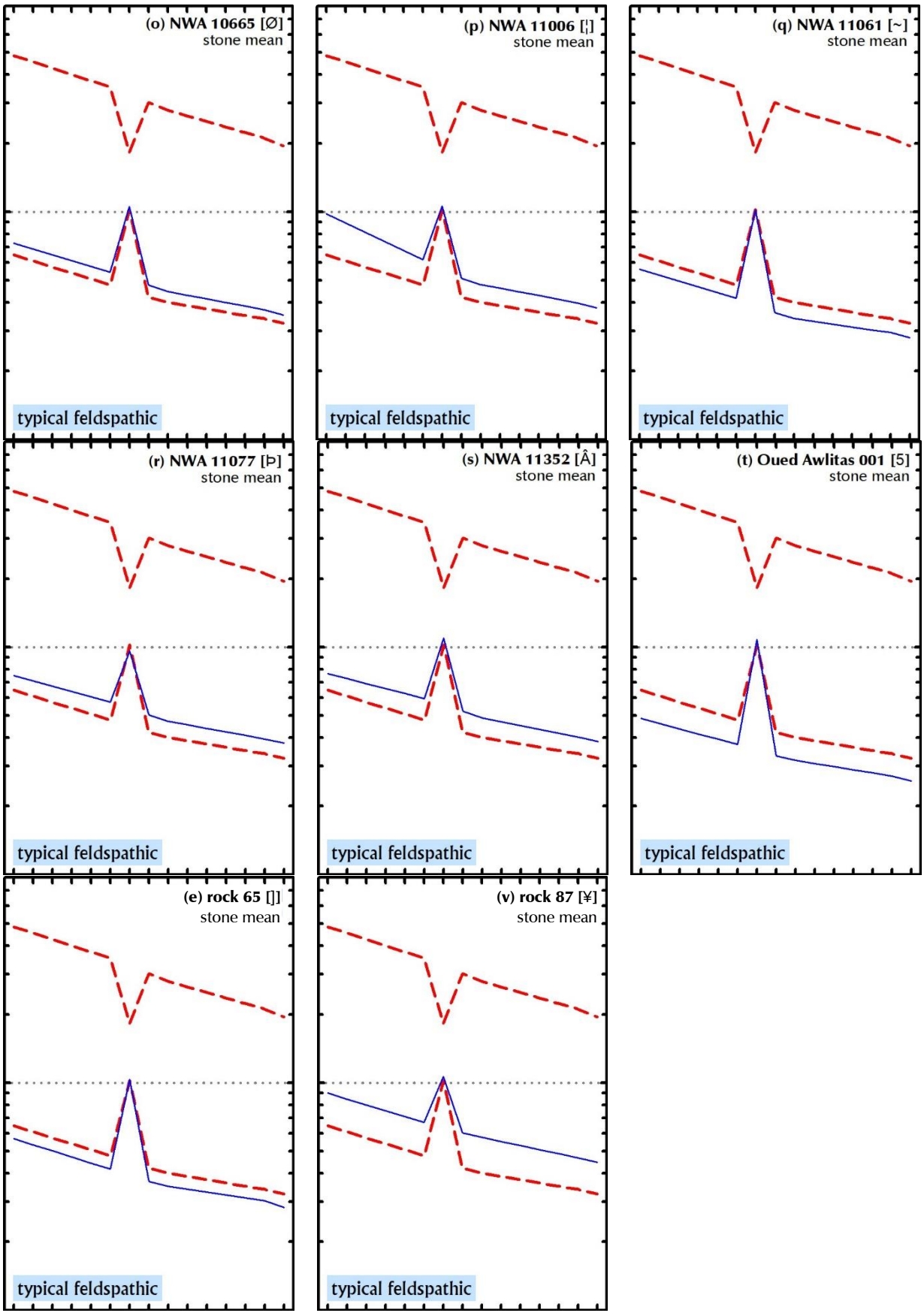

Fig. S8, continued.

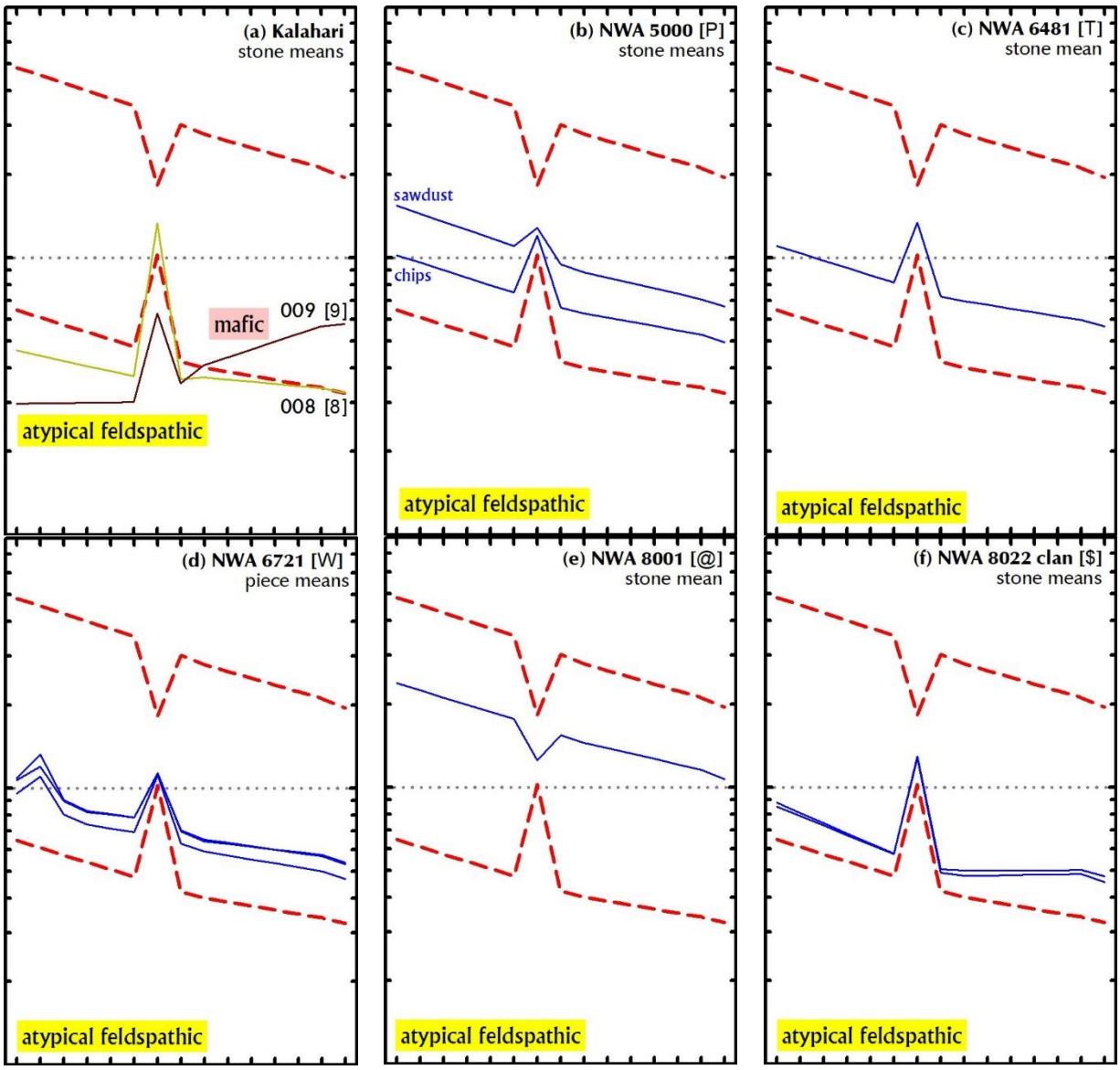

Fig. S9. Like Fig. S8 but for atypical feldspathic meteorites. Because Eu concentrations are nearly constant, samples with more than ~2.4 µg/g Sm have negative Eu anomalies (e.g., panel h). Heavy REE are unusually high in NWA 8022 (f). (d) NWA 6721 occurs as multiple stones and we received 3 pieces. For two, we analyzed 4 subsamples and for the other we analyzed 3. All 3 have positive Ce anomalies (mean Ce/Ce* = 1.24).

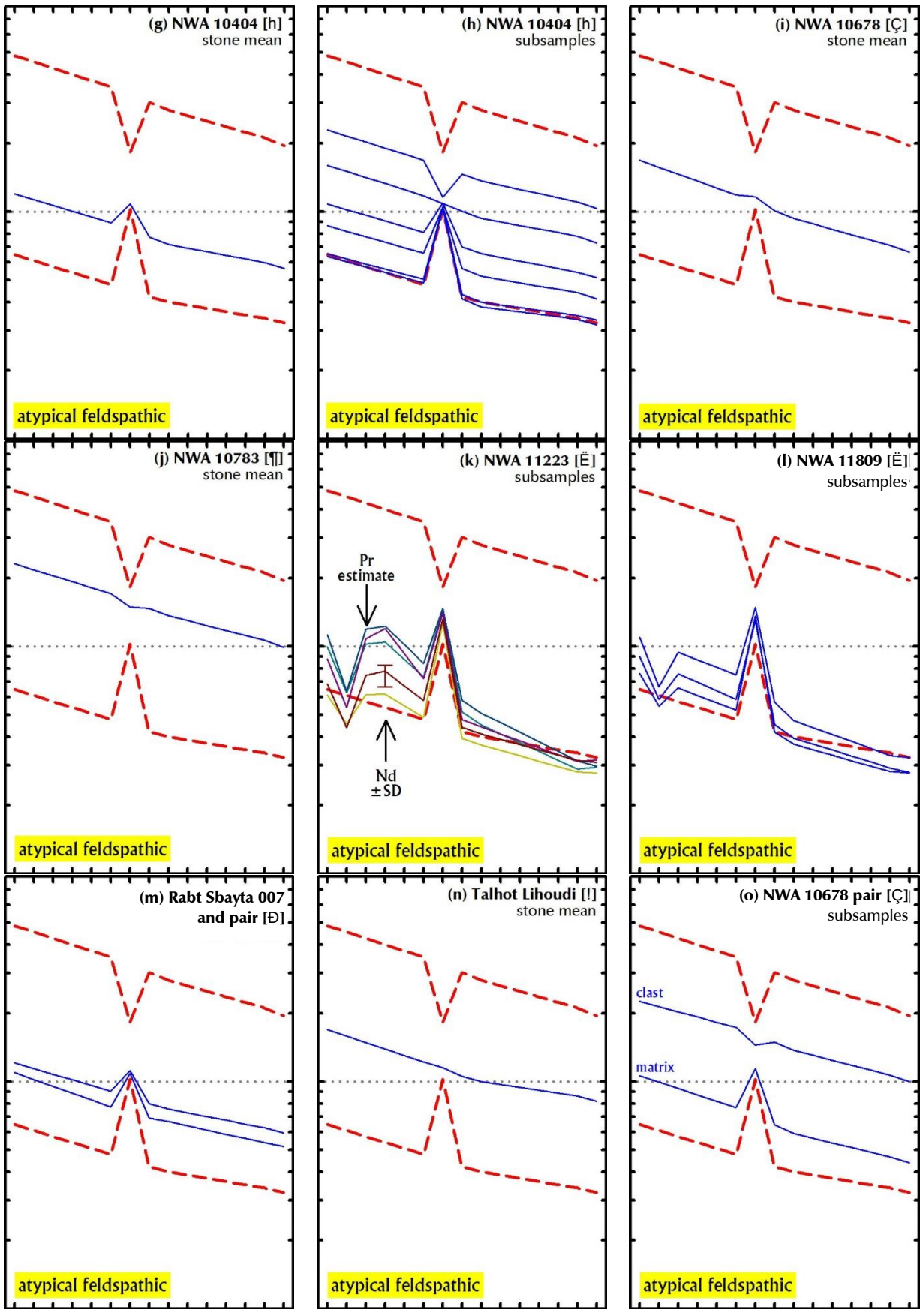

Fig. S9, continued. NWA 11223 and its pair NWA 11809 have deep negative Ce anomalies; Nd is determined imprecisely at low concentrations.

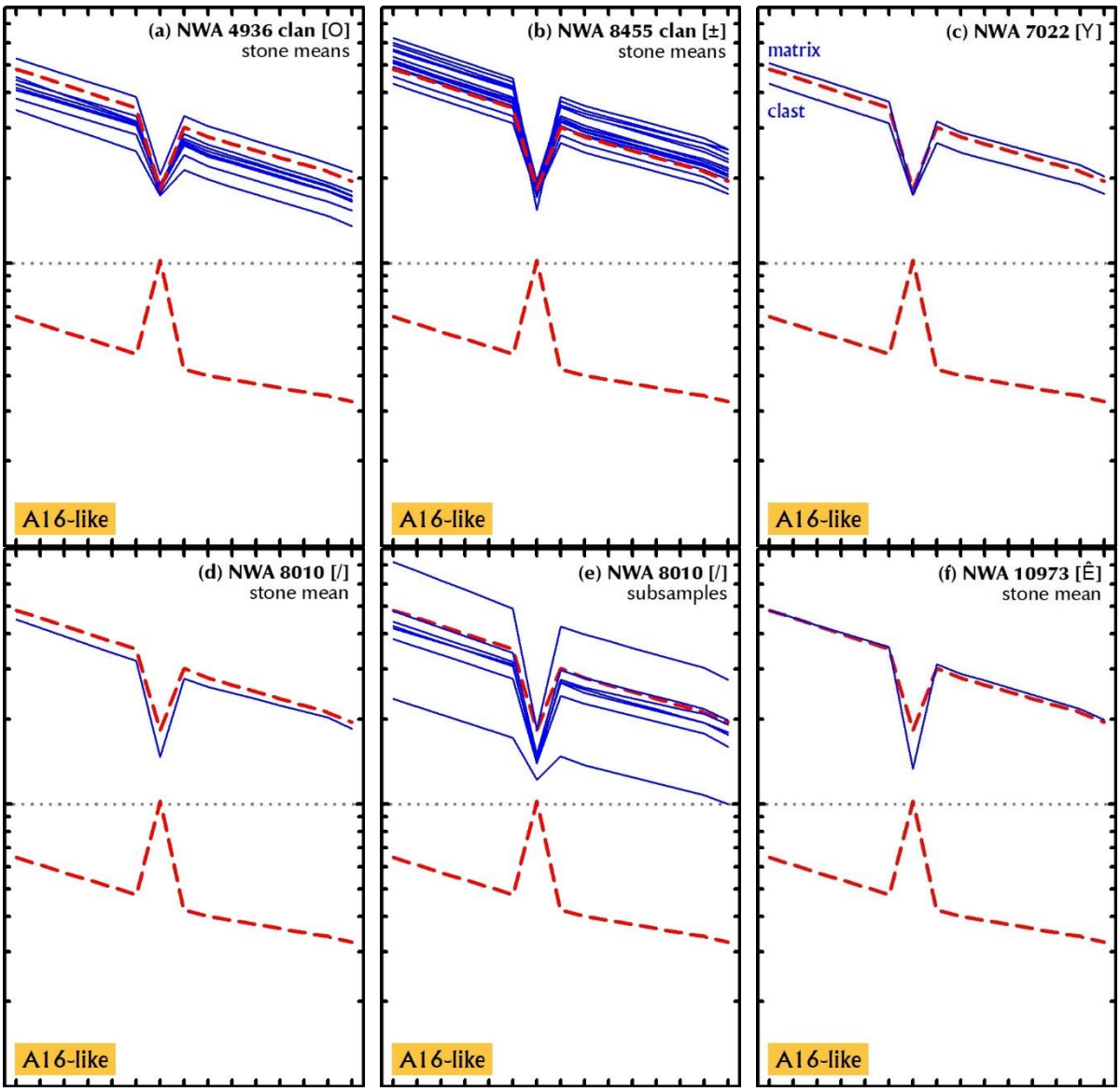

Fig. S10. Like Fig. S8 but for Apollo-16-like feldspathic meteorites. All these meteorites have KREEP-like REE patterns. NWA 8010 (panels d and e) and NWA 10973 (f) have lower concentrations of Eu than the others (also, Fig. S16).

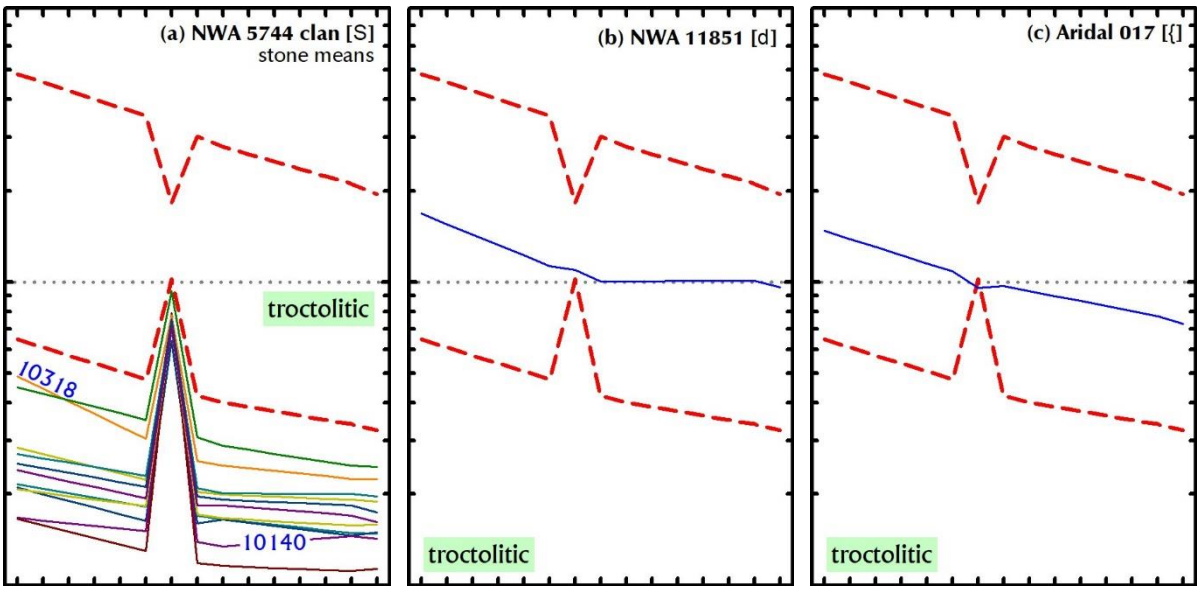

Fig. S11. REE concentrations in meteorites of troctolitic composition. (a) Absolute concentrations vary considerably but are uniformly low among the NWA 5744 stones, most of which derive from anorthositic troctolites. Mineralogically, NWA 10318 is an olivine-bearing anorthositic norite (see text) but it is not clear why that should lead to higher relative concentrations of light REE. NWA 10140 has 15% modal olivine and 10% low-Ca pyroxene (C. Agee in MetBull); the latter may account for higher relative concentrations of heavy REE. (b,c) We assume NWA 11851 and Aridal 017 to be troctolitic from their high Cr/Sc (Figs. 4 and S4).

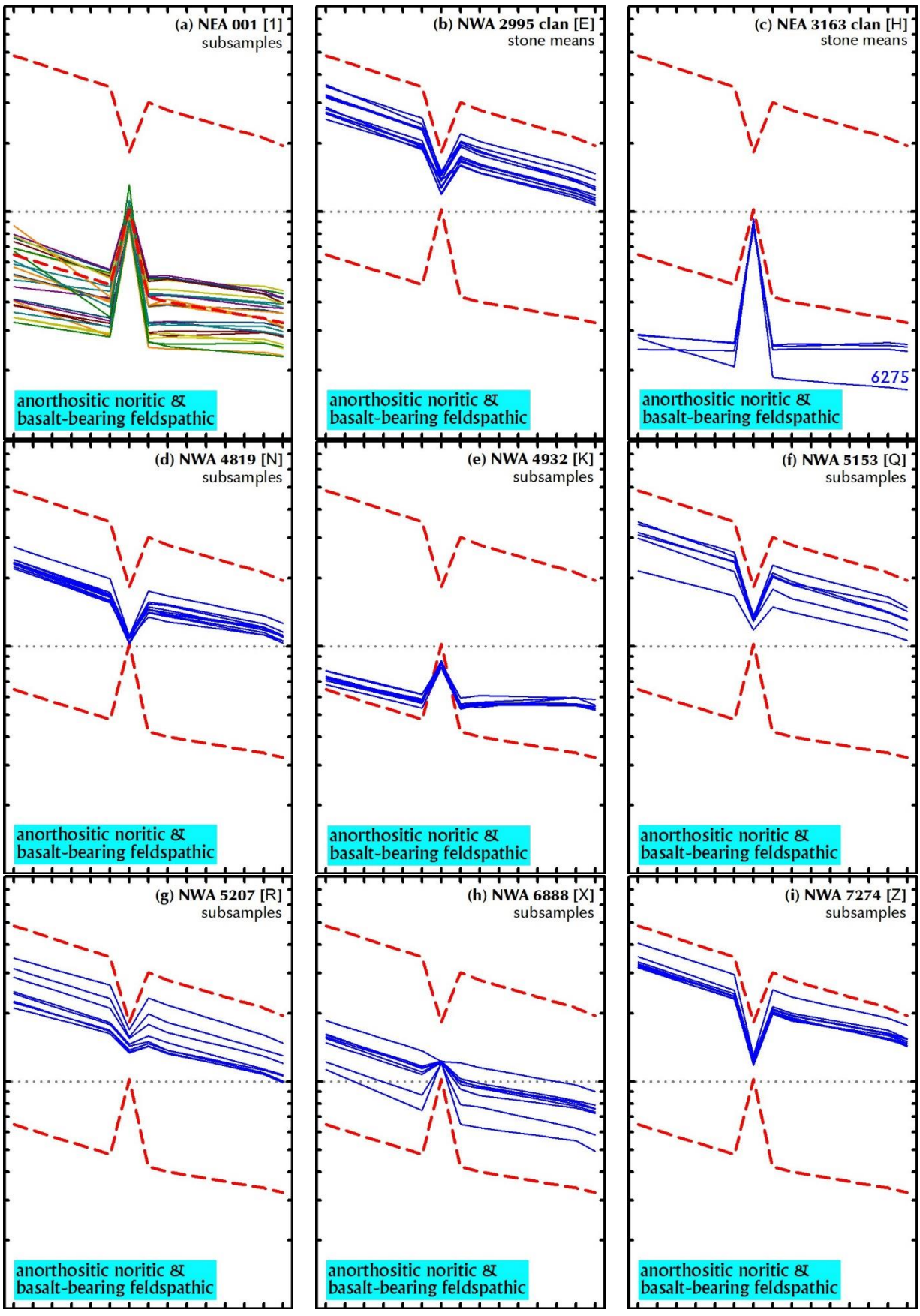

Fig. S12. Like Fig. S8 but for anorthositic-noritic and basalt-bearing breccias.

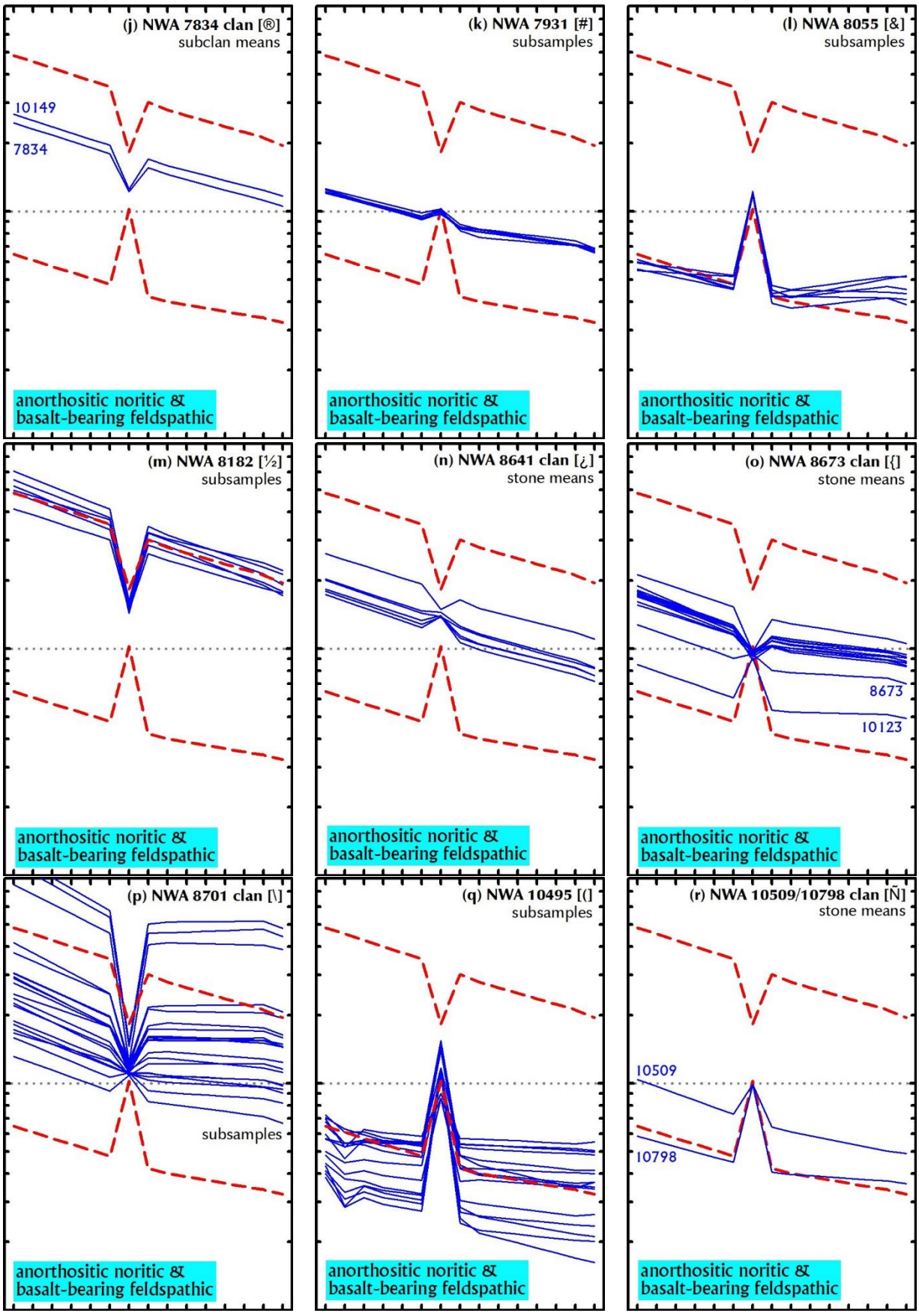

Fig. S12, continued.

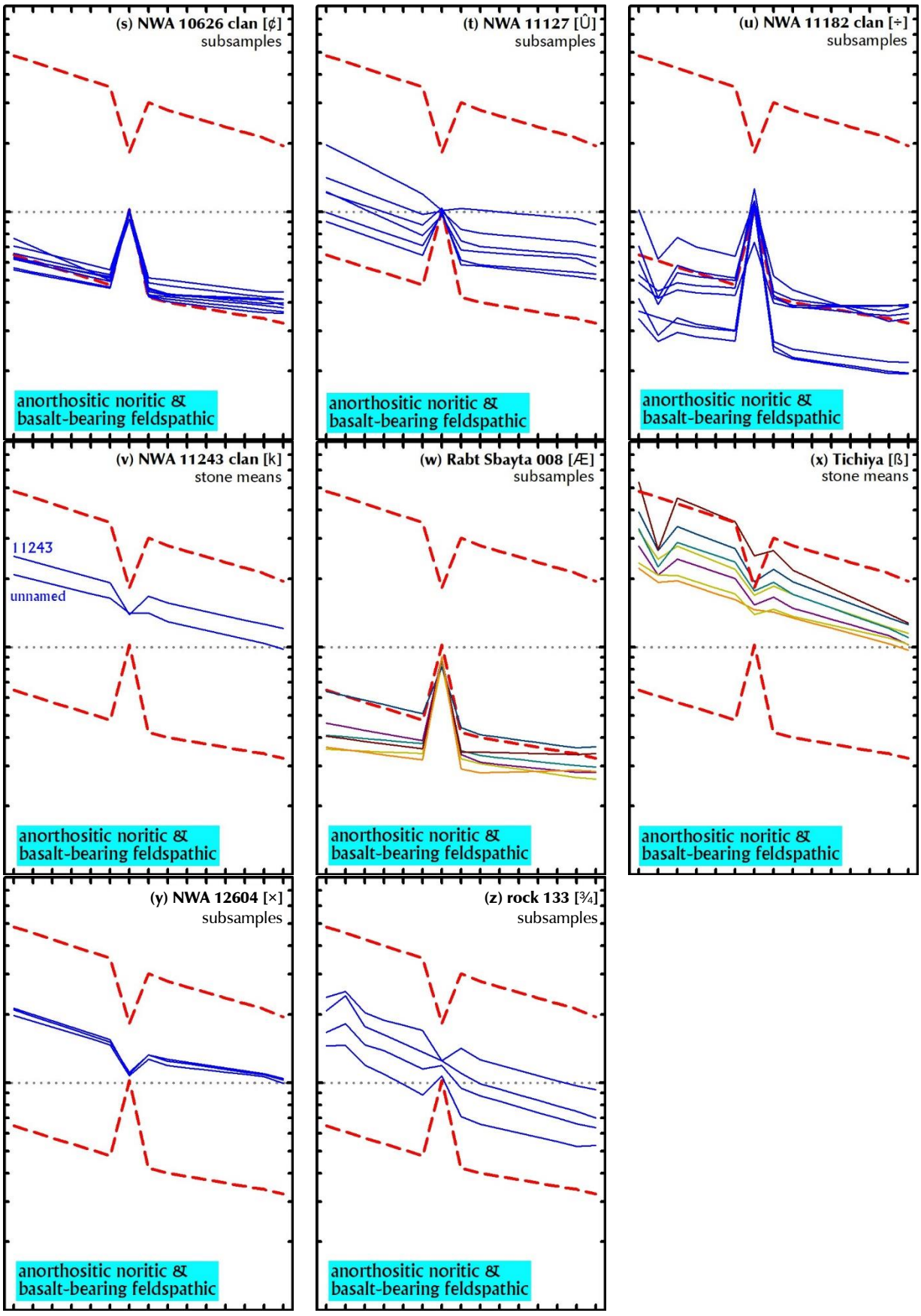

Fig. S12, continued.

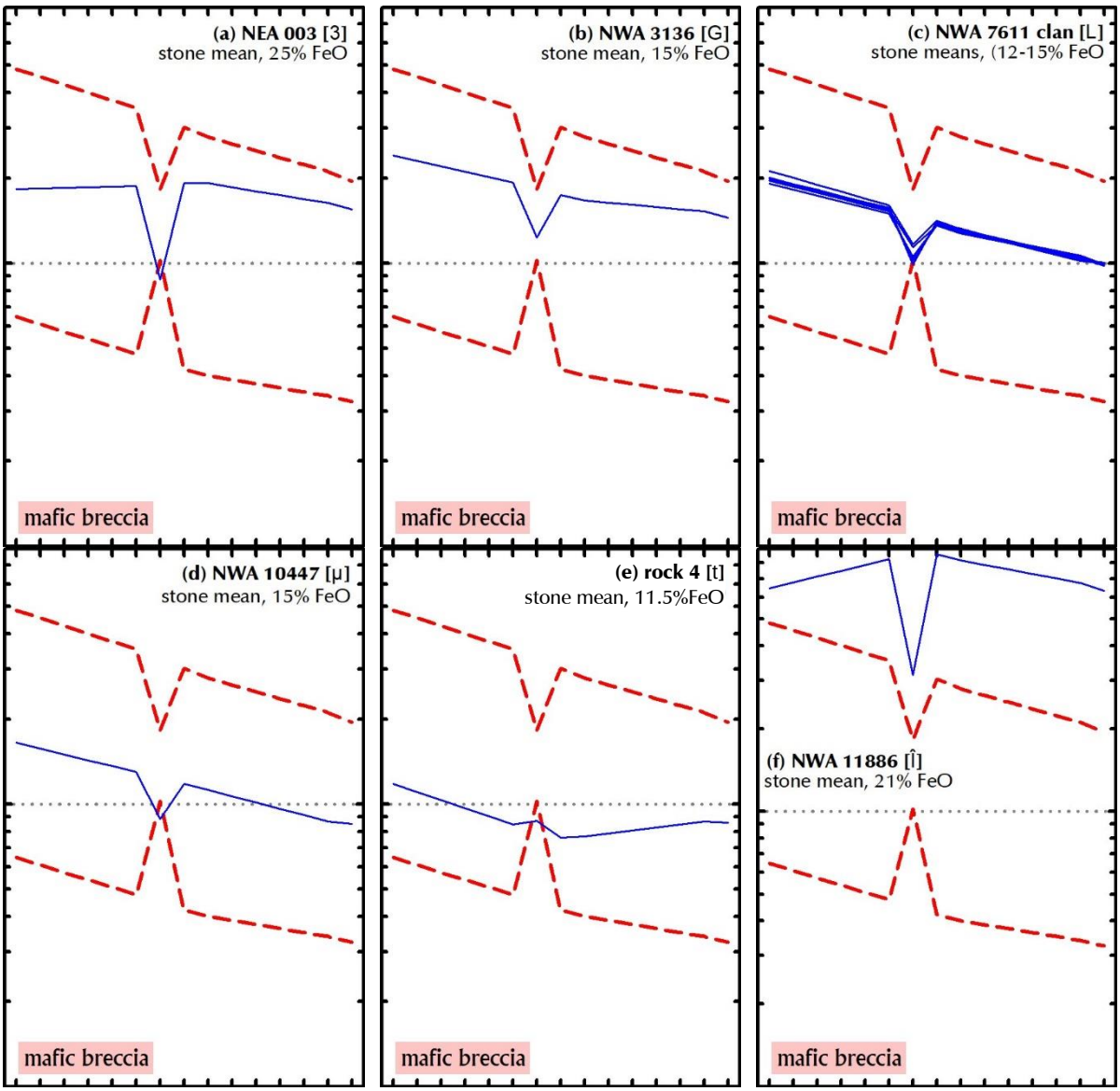

Fig. S13. All of the meteorites of this figure are breccias dominated by mare basalt. (a) With 25% FeO, the NEA 003 breccia must contain very little nonmare material; none is reported in the description of Haloda et al. (2006). (b,d) REE concentrations in NWA 3136 and NWA 10447 are consistent with mixtures of mare and nonmare material. (c) REE concentrations are consistent among the NWA 7611 clan. (f) Like NEA 003 (a), NWA 11886 has too much FeO to contain much feldspathic material (4–6% FeO) or KREEP material (10–12% FeO). The high REE concentrations and non-KREEP-like pattern must be inherent to the basalt component.

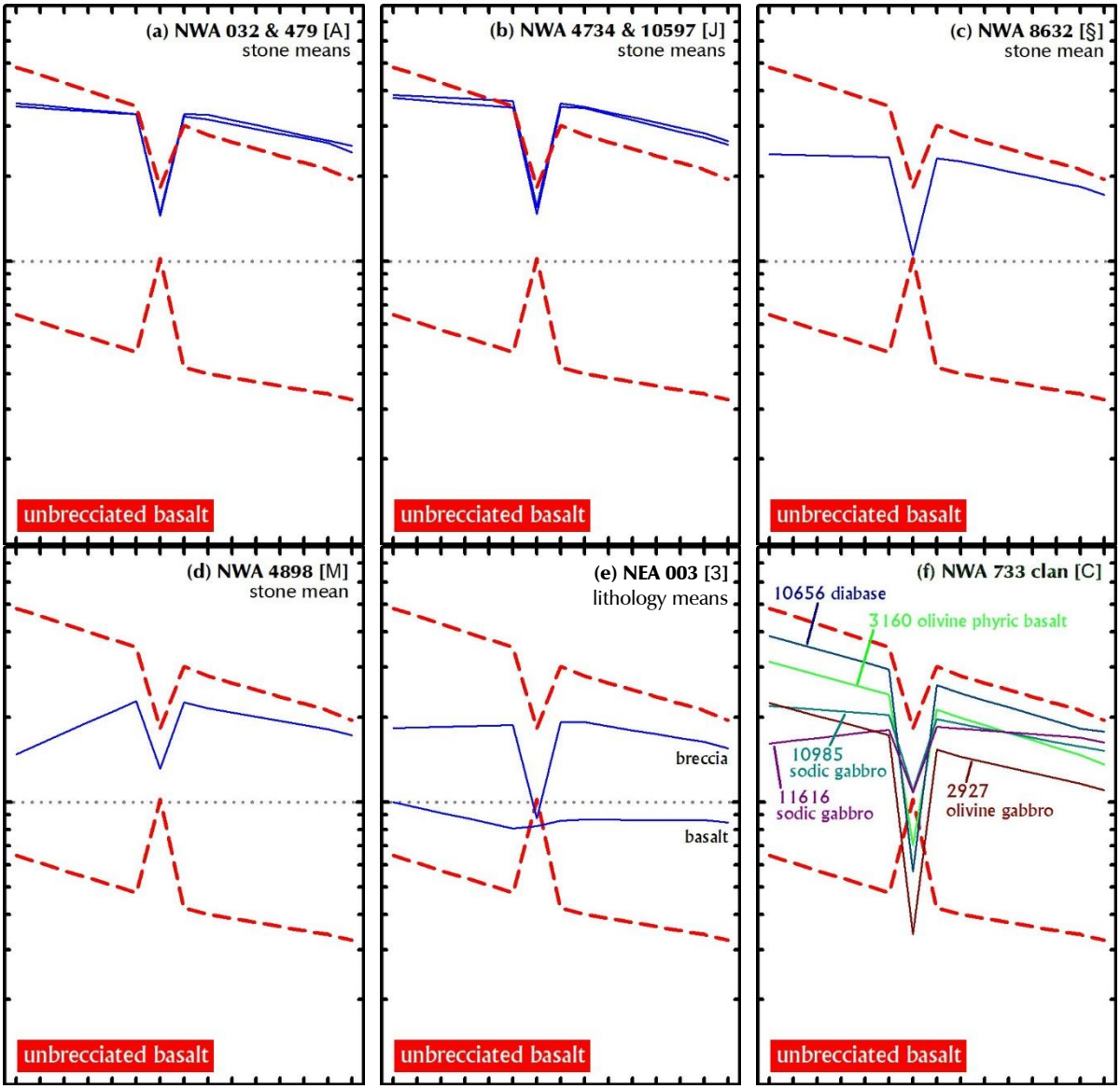

Fig. S14. Rare earth element in basalts from northern Africa. (a,b) NWA 032/479 (3.0% TiO_2) and NWA 4734/10597 (3.2% TiO_2) have similar absolute and relative concentrations of REEs. (c) NWA 8632 (2.5% TiO_2) has lower concentrations of both trivalent REE and Eu. (d) NWA 4898 (2.3% TiO_2, 12% Al_2O_3) is the most "light-REE depleted" of the NWA basalts. (e) The NEA 003 breccia lithology (1.8% TiO_2) is distinct from, and consequently must not include a large component of, the basalt lithology (1.3% TiO_2). (f) Although the sodic gabbro lithologies of NWA 10985 and NWA 11616 do not have identical relative concentrations of REE, both have higher concentrations of Na, Ca, and Eu than the NWA 3160 olivine-phyric basalt and NWA 10656 diabase lithologies presumably because of a greater abundance of plagioclase. See also Fig. S53.

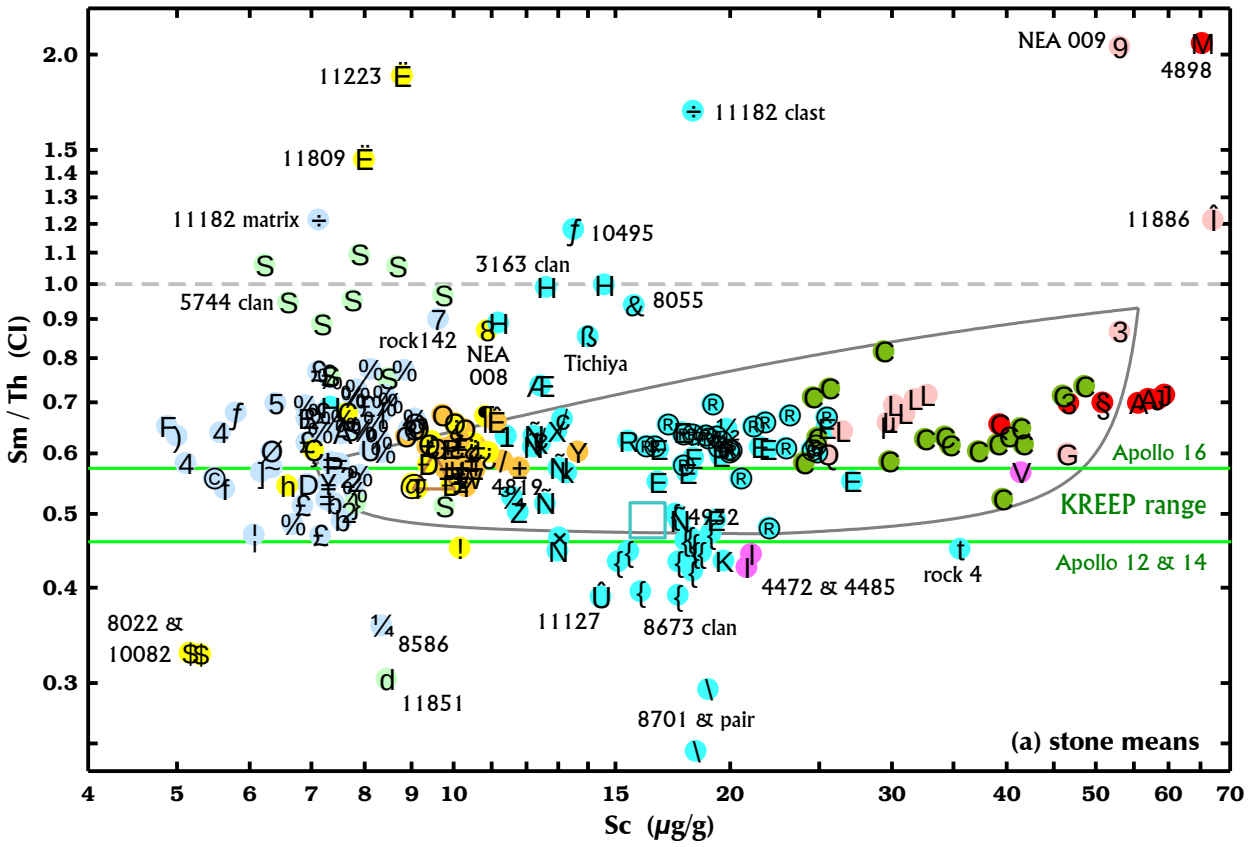
NEA 009
4898
11223
11182 clast
11809
11182 matrix
11886
10495
3163 clan
5744 clan
8055
rock142
NEA 008
Tichiya
Apollo 16
KREEP range
Apollo 12 & 14
4932
4472 & 4485
rock 4
8022 & 10082
8586
11127
8673 clan
11851
8701 & pair
(a) stone means
Sm / Th (CI)
Sc (μg/g)

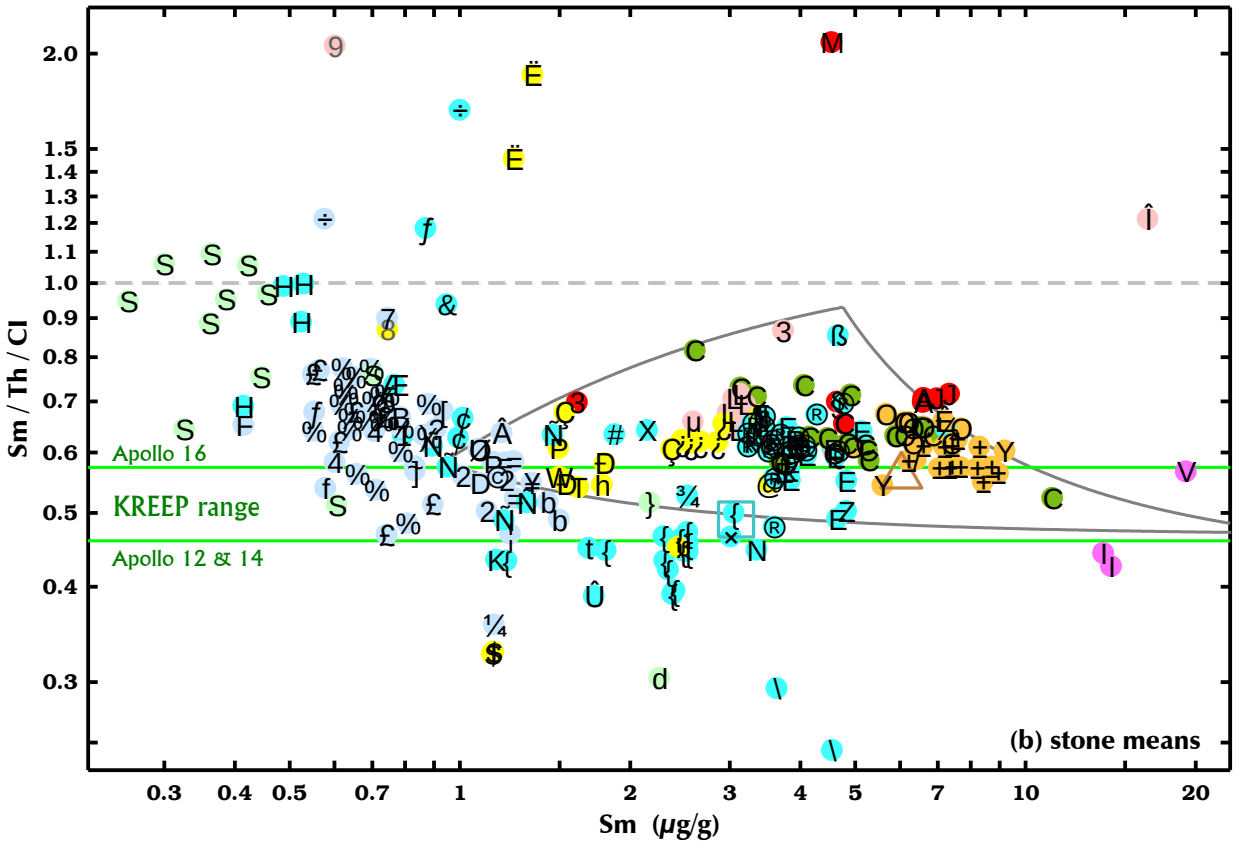
Apollo 16
KREEP range
Apollo 12 & 14
(b) stone means
Sm / Th / CI
Sm (μg/g)

Fig. S15. Most lunar meteorites have subchondritic Sm/Th. In the NWA 5744 clan (symbol S, anorthositic troctolites) and NWA 3163 clan (symbol H, anorthositic norites), which are all but devoid of KREEP (i.e., <0.6 µg/g Sm), heavy REE (Fig. S7) and Th are carried mainly by pyroxenes. For other breccias (all but red points) with low KREEP component (0.6–1.5 µg/g Sm), Sm/Th varies considerably, probably reflecting local differences in crystallization history or pyroxene/olivine of the feldspathic plutonic rocks from which they derive. Four of feldspathic meteorites with the highest Sm/Th each have negative Ce anomalies: paired stones, NWA 11223 and 11809 (Ë), NWA 11182 (÷), NWA 10495 (ƒ), and Tichiya (ß) as a result of enrichment of light REE, apparently including Sm, from terrestrial weathering processes (Fig. 17). (b) The large, distorted “triangle” is the mixing triangle of Figs. 2 and 6. The large orange triangle represents Apollo 16 regolith and the large cyan square represents Luna 20 regolith. See Table S1 and Fig. S4 for symbol key and color coding.

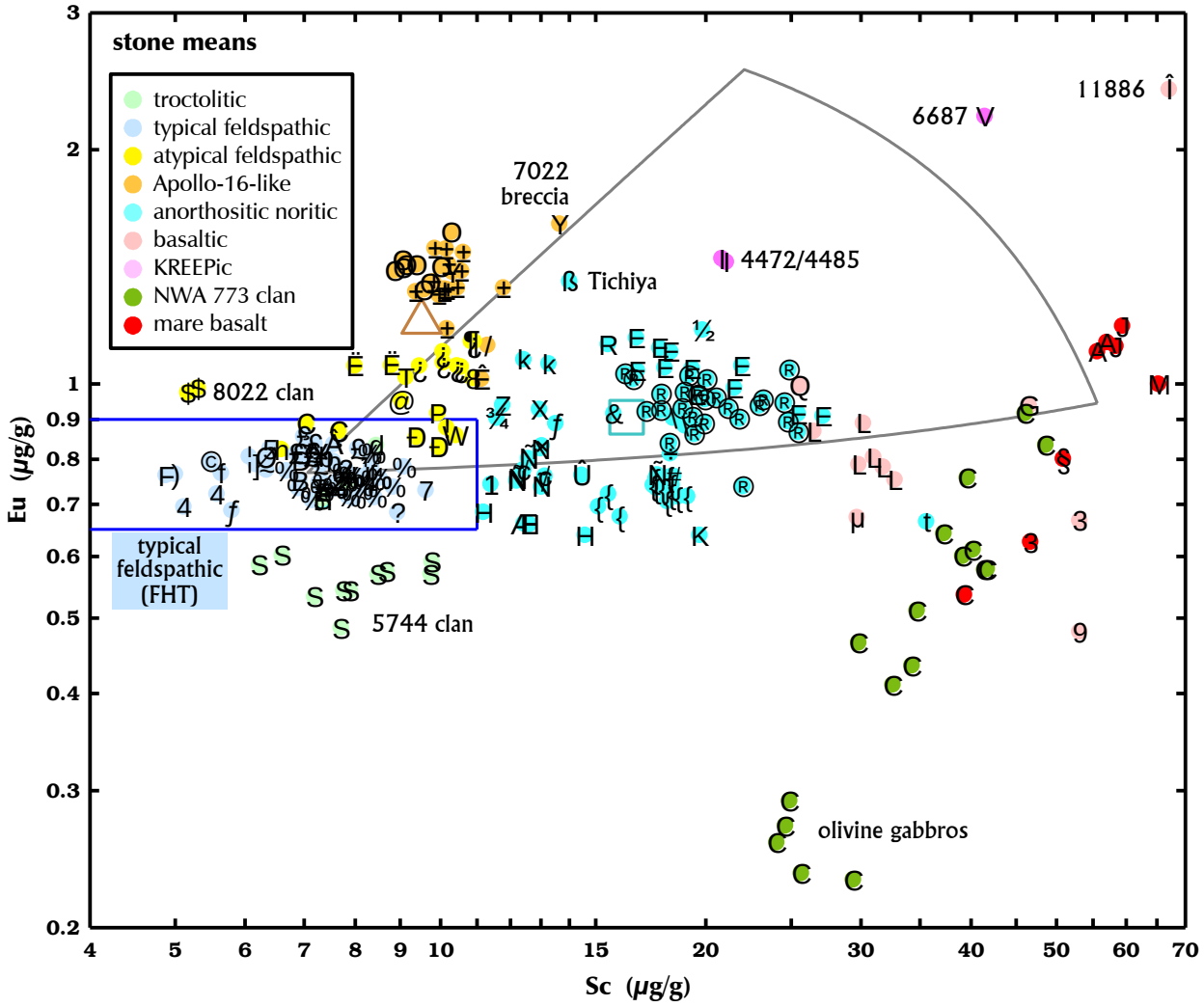

Fig. S16. Stone means in Sc-Eu space. As in Fig. S5 (Sc,Na), low-Eu meteorites of the NWA 5744 clan (symbol S) and the NWA 733 clan (symbol C) are rich in olivine. On the basis of this figure, we define a "typical feldspathic lunar meteorite" as one for which the mass-weighted mean of the pair group (or the only stone for unpaired stones) has 0.65–0.90 µg/g Eu (blue rectangle). The large triangle represents Apollo 16 regolith and the large square represents Luna 20 regolith. As for Na (Fig. S5), Eu is high in most of the Apollo-16-like stones because the plagioclase is slightly more albitic than that of typical feldspathic lunar meteorites. See Table S1 for symbol key.

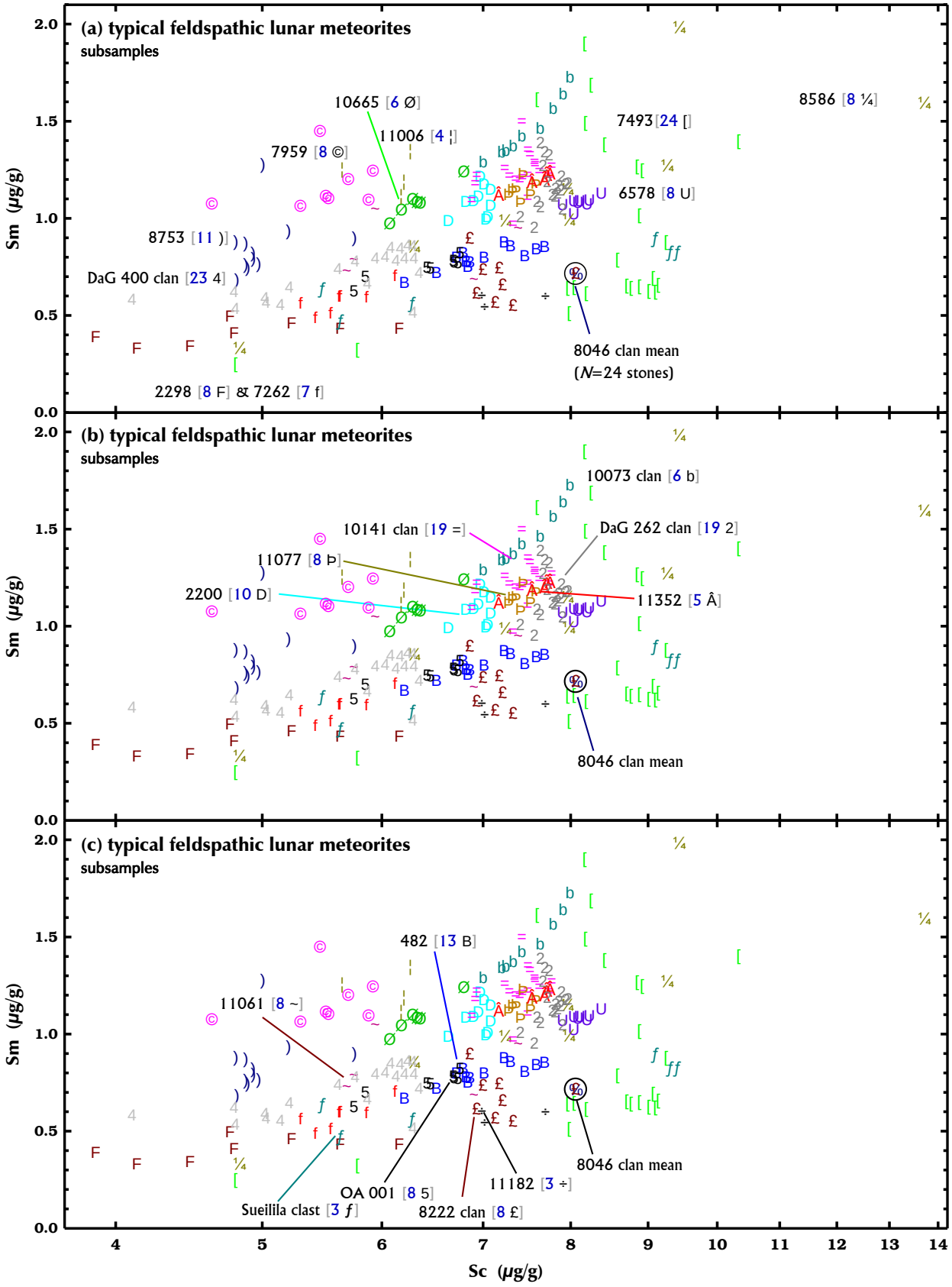
(a) typical feldspathic lunar meteorites
subsamples
10665 [6 Ø]
11006 [4 ¦]
7959 [8 ©]
8586 [8 ¼]
7493 [24 []
6578 [8 U]
8753 [11)]
DaG 400 clan [23 4]
8046 clan mean
(N=24 stones)
2298 [8 F] & 7262 [7 f]
(b) typical feldspathic lunar meteorites
subsamples
10073 clan [6 b]
10141 clan [19 =]
DaG 262 clan [19 2]
11077 [8 Þ]
2200 [10 D]
11352 [5 Â]
8046 clan mean
(c) typical feldspathic lunar meteorites
subsamples
482 [13 B]
11061 [8 ~]
8046 clan mean
11182 [3 ÷]
OA 001 [8 5]
8222 clan [8 £]
Sueilila clast [3 f]
Sm (µg/g)
Sc (µg/g)
0.0
0.5
1.0
1.5
2.0
4
5
6
7
8
9
10
11
12
13
14

Fig. S17. Sc and Sm subsample data for 19 typical NWA feldspathic lunar meteorites (Fig. 6) plus, for simplicity (and also for Figs. S18-S21), only the mass-weighted mean of all 86 subsamples of the 24 analyzed stones of the heterogeneous NWA 8046 clan (Fig. S24) and the mass-weighted mean of each of the 8 stones (37 subsamples) of the large NWA 8222 clan (Fig. S23). The same data are plotted on all three panels and the symbol key is the same as that of Table S1. For the labeled meteorites, the number following the left bracket ([) is the number of points (each representing a subsample or stones for NWA 8222) of its kind.

(a) The 9 named meteorites are 'self evidentially' unique in that, for example, although the points for NWA 8586 (symbol ¼) scatter across the diagram, all the points represent subsamples of one sample of the heterogeneous meteorite. Although points for several other meteorites lie mostly or entirely within the range of NWA 8586, the point distributions for those meteorites are much more compact and distinct. Also, most of these NWA-8586-like meteorites plot outside the range of NWA 8586 on at least one of the plots of Figs. S18–S20. For example, NWA 8753 (symbol ")") has substantially greater Cr/Sc (Fig. S18a) than NWA 8586. Similarly, NWA 7959 (©), NWA 10665 (Ø), and NWA 11006 (¦) nearly overlap here but differ in Figs. S18, S19, and S20.

Although NWA 2298 (F) and 7262 (f) just overlap in Sc concentration, with NWA 7262 being more mafic, we assume they are paired or launch paired. On this plot, as well as Figs. S18a and S19, subsamples plot along a common mixing line. (See also Fig. S68). Both stones are low in siderophile elements (Fig. S20a,b).

(b) The 5 meteorites of this panel are the most typical of the typical feldspathic lunar meteorites but:

(1) DaG 262 (2) is distinct from most of the others in Figs. S19b, S20a,b, and S21a,

(2) NWA 2200 (D) is distinct in Fig. S19c,

(3) The NWA 10073 clan (b) is distinct in Fig. S18a and, to a lesser extent, the trend of the data in this panel (see also Fig. S74).

(4) NWA 10141 clan (=) is distinct in Figs. S18b,c, S19b,c, and S21 (see also Fig. S74),

(5) NWA 11077 (Þ) is distinct from most of the others in Figs. S18a, S19a, and S21c (see also Fig. S74),

(6) NWA 11352 (Â) is very similar in composition to DaG 262 but is distinct from it in Fig. S19. Also, in this figure and several others, the trends of the data are different.

(c) NWA 11182 (symbol ÷) falls in the range of the 8 stones of the NWA 8222 clan (£, Fig. S23) but differs from the NWA 8222 clan in Figs. S19c and S20. NWA 482, NWA 11061, and OA (Oued Awlitis) 001 overlap but NWA 482 differs from OA 001 in Figs. S18a,b and all three have different Na/Eu (Fig. S19c). One of our two samples of Sueilila 005 (*ƒ*, 5–6 µg/g Sc) is apparently dominated by a feldspathic clast compared to the other (9 µg/g Sc). Most samples of its presumed pair, NWA 10495, are even more mafic (Fig. S72).

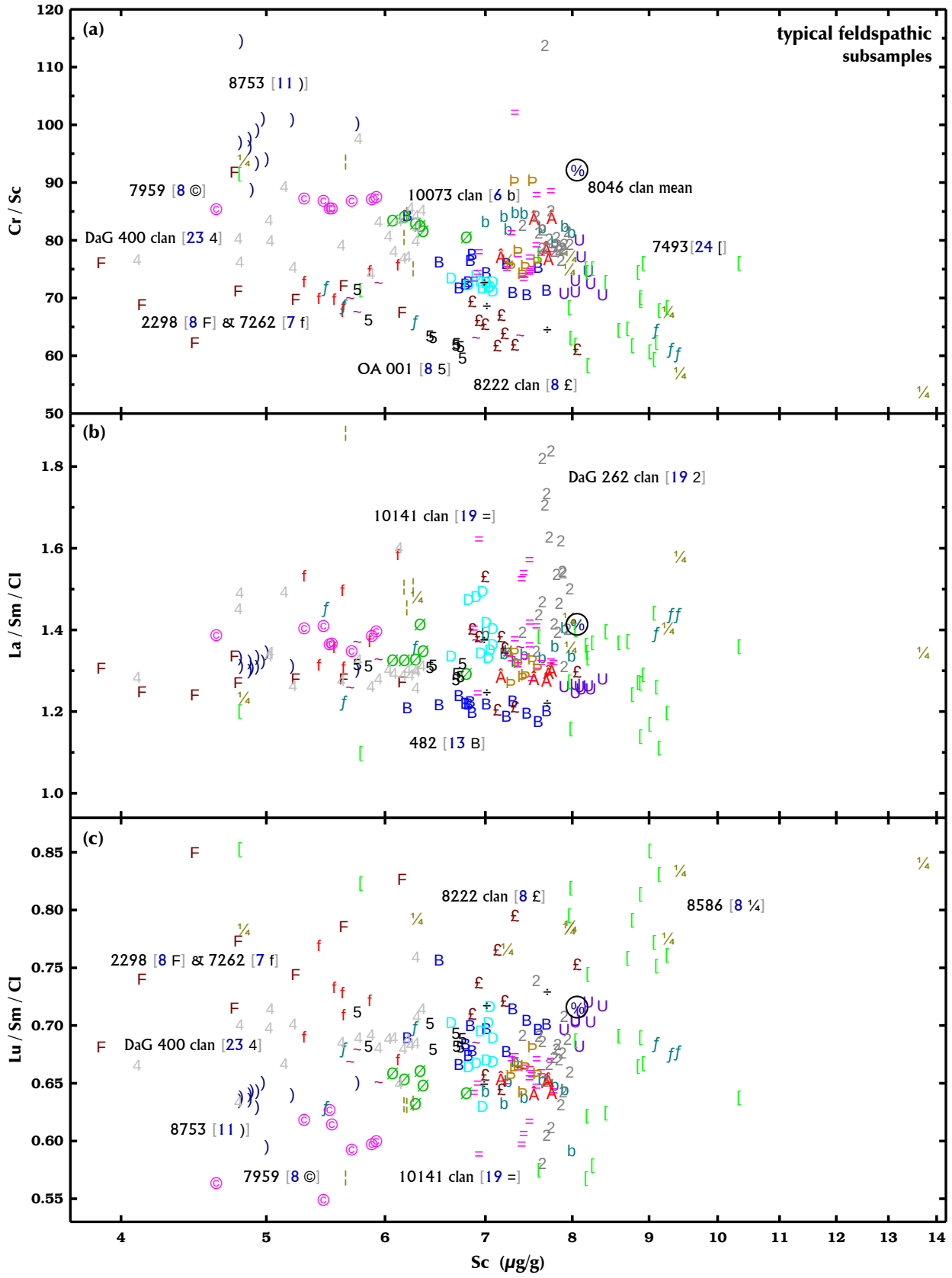

Fig. S18. Like Fig. S17 but for Cr/Sc, La/Sm, and Lu/Sm. Labeled points represent distinct meteorites.

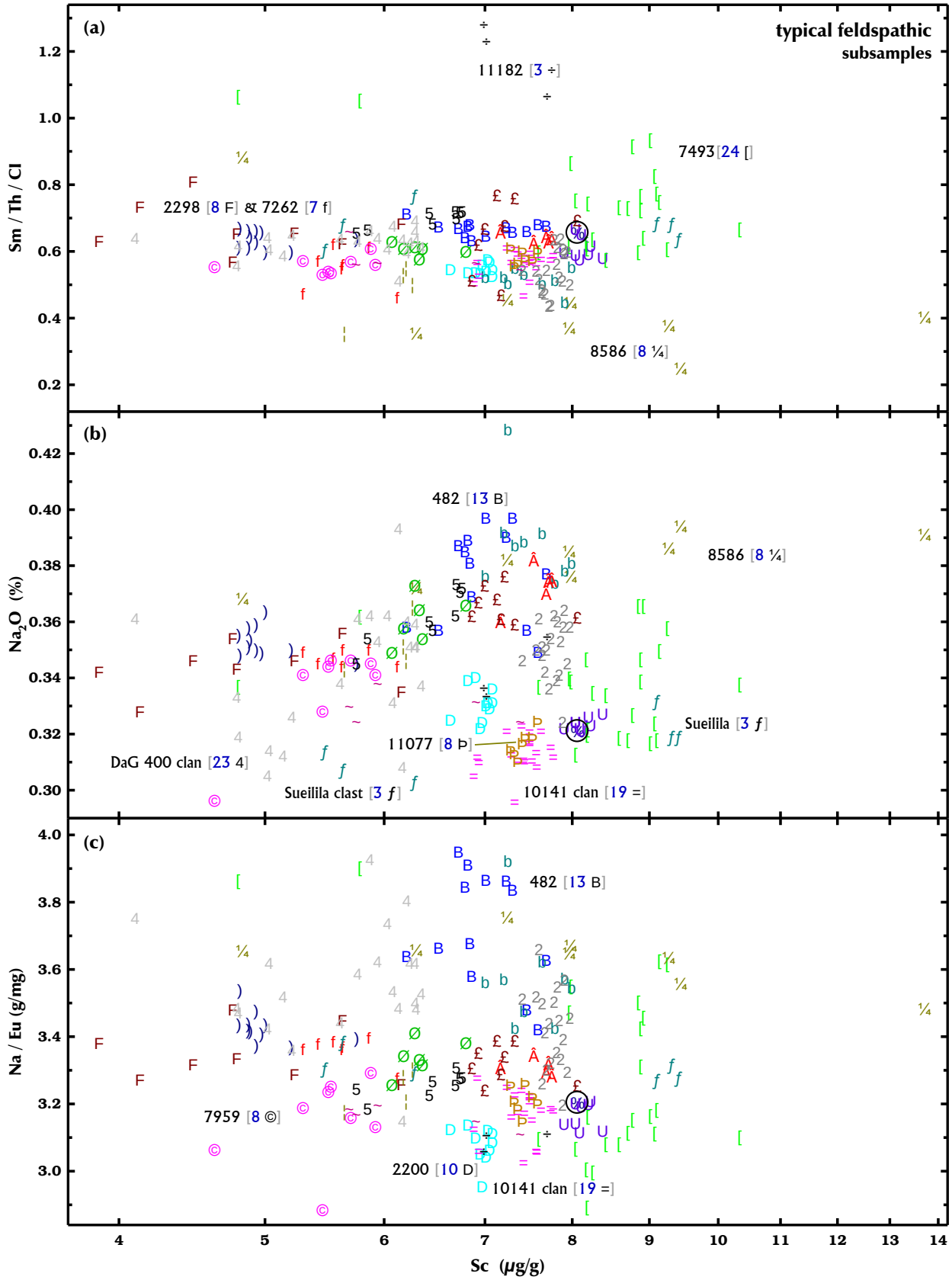

Fig. S19. Like Fig. S17 but for Sm/Th, Na_2O, and Na/Eu. Labeled points represent distinct meteorites.

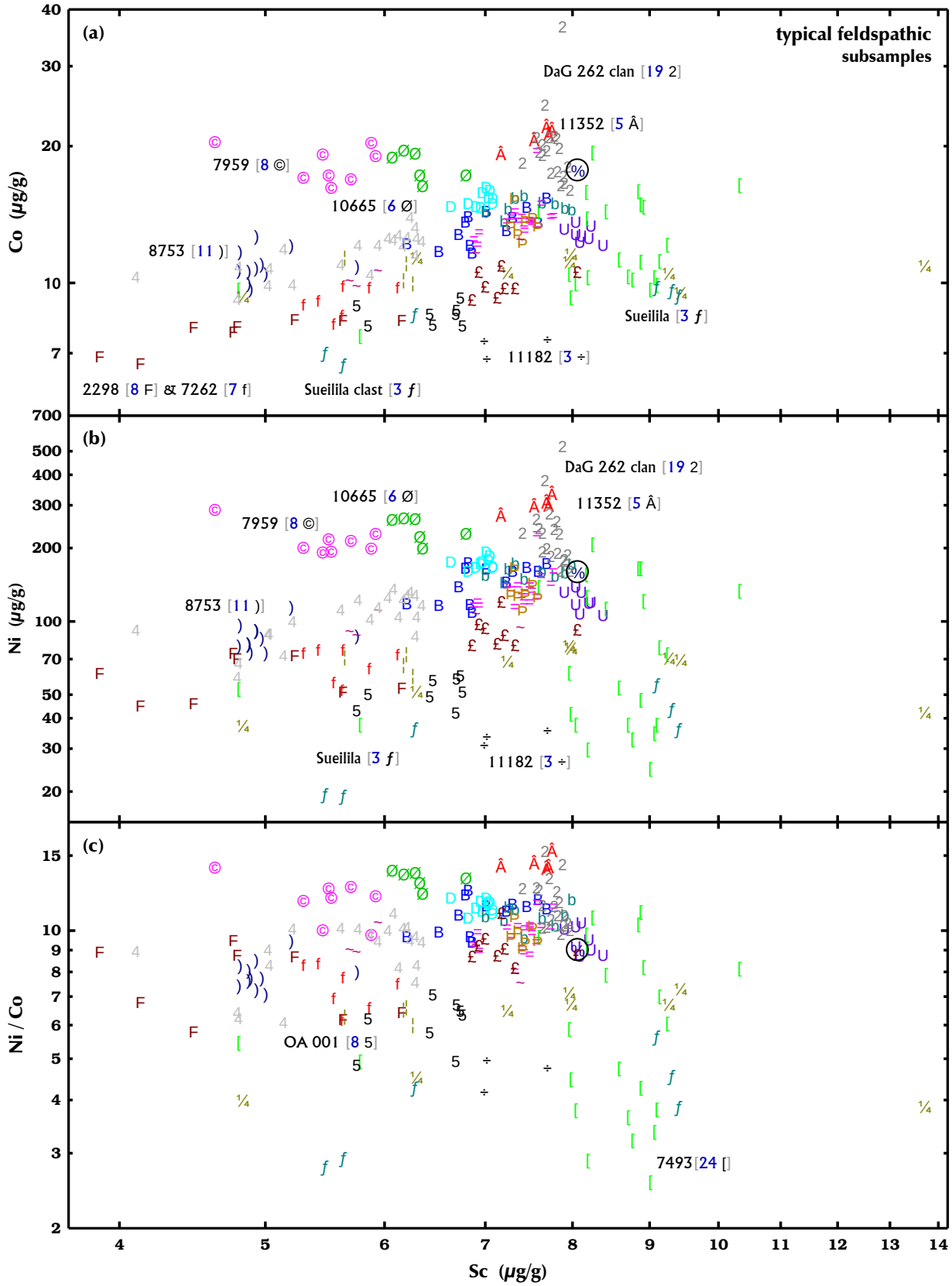

Fig. S20. Like Fig. S17 but for Co, Ni, and Ni/Co. Labeled points represent distinct meteorites.

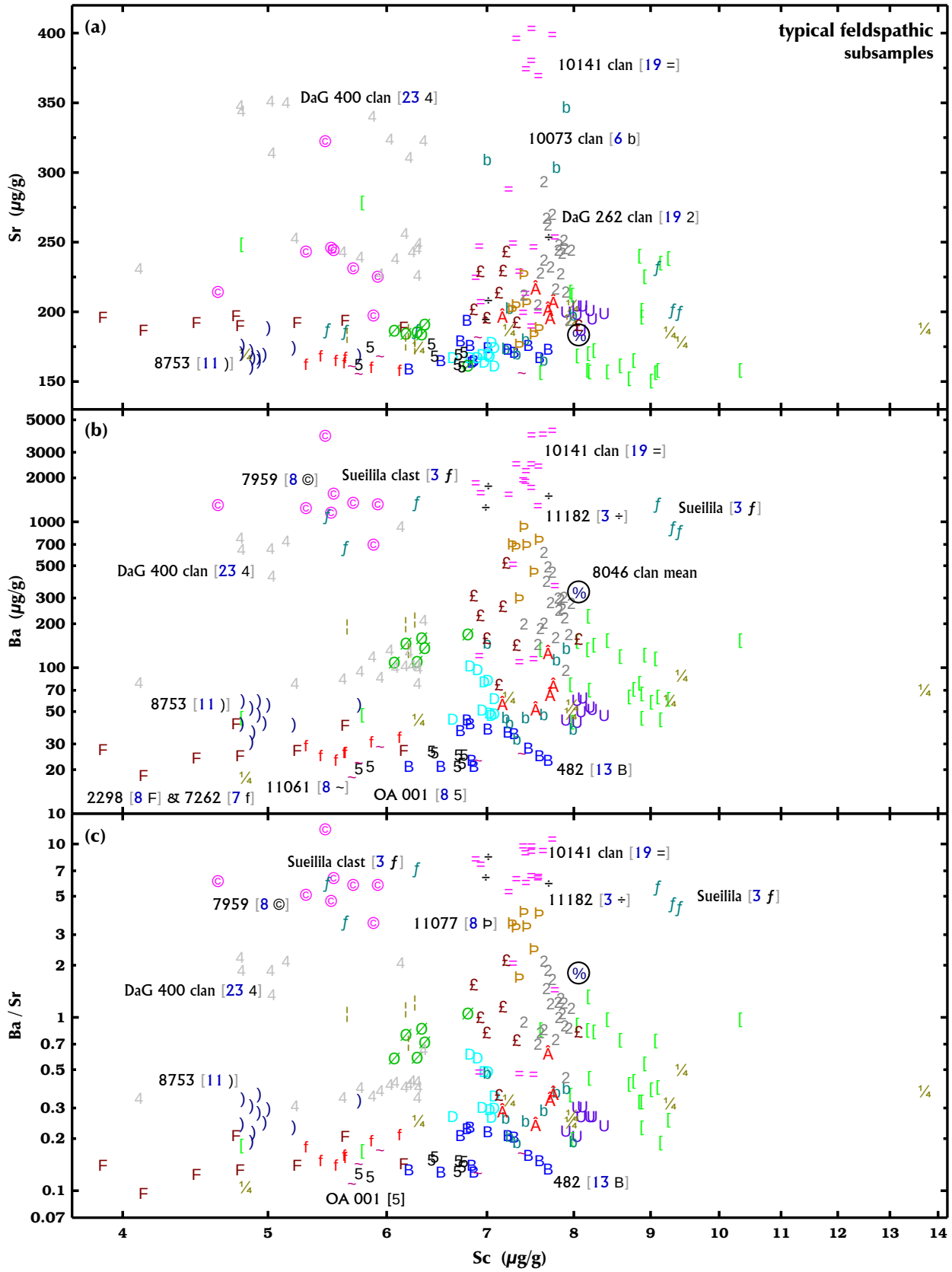

Fig. S21. Like Fig. S17 but for Ba, Sr, and Ba/Sr.

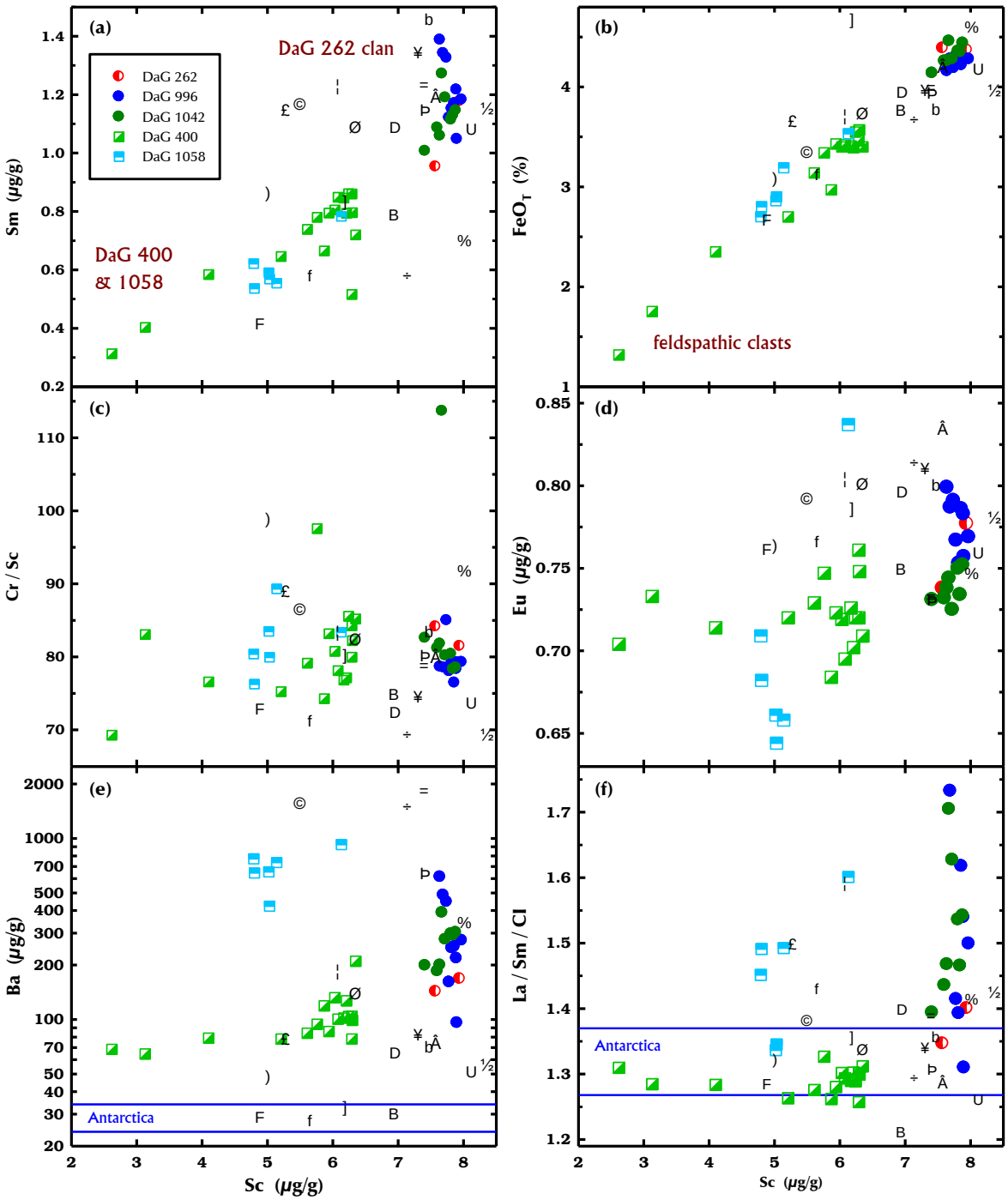

Fig. S22. Comparison of subsample data for stones of the DaG (Dar al Gani, Libya) 262 (clan mass: 1.3 kg) and DaG 400 (3.2 kg) clans to clan means of other feldspathic lunar meteorites, all NWAs, of similar composition. Panels (a) through (d) together support the hypotheses that (1) DaG 400 is paired with DaG 1058, (2) DaG 262, DaG 996, and DaG 1058 are paired with each other, (3) DaG 262 is not paired with DaG 400, and (4) it is not likely that any of the NWA meteorites are launch paired with either of the DaG meteorites. Panels (e) and (f) reflect terrestrial weathering effects (Fig. S60). Our sample of DaG 1058 (which visibly appears more weathered) is richer In Ba and has greater La/Sm than our samples of DaG 400. The DaG-262-clan is seriously contaminated with Ba and has undergone some effect that enriches La over Sm (Fig. S60). Note that our two analyses of DaG 400 reported in Korotev et al. (2003a) were made on a sample (not plotted here but at 6.0 µg/g Sc) of sawdust provided by a collector. Compared to the data on chips and fines presented here, the 2003 sample was contaminated with As, Br, Zr, REE, Hf, Ta, W, Au, and Th (Table S2). See Table S1 for symbol key.

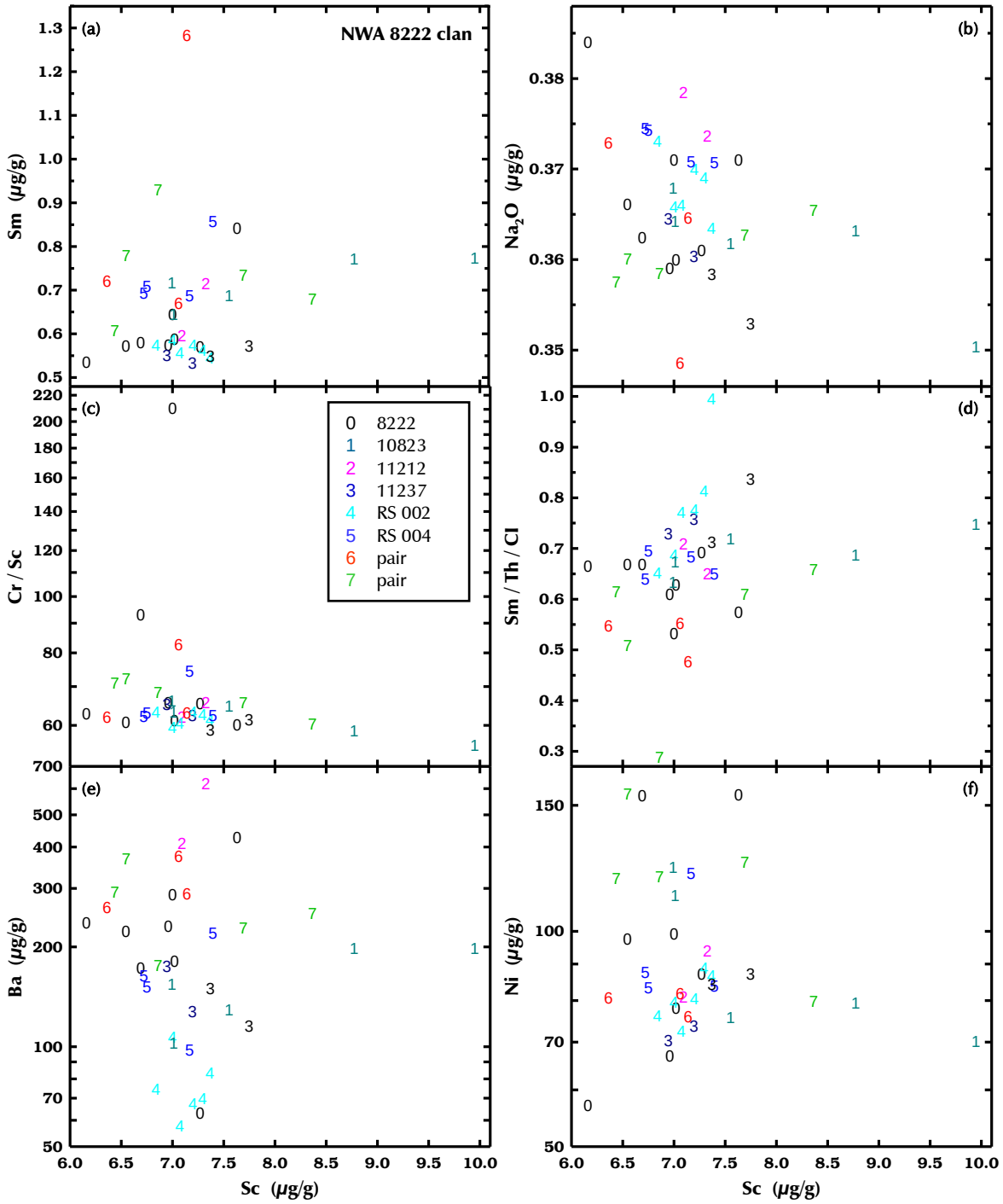

Fig. S23. Subsample data for the NWA 8222 clan. For no other lunar meteorite do the stone means plot within the range of the subsample clusters in all of the top four panels of this figure. We have not studied Rabt Sbayta 005 and Rabt Sbayta 006 but assume that they are paired with Rabt Sbayta 002 (symbol 2) and Rabt Sbayta 004 (4) ("RS" in the legend) on the basis of the MetBull descriptions. This assumption might be erroneous. Rabt Sbayta 007 ((Sc,Sm) = (9.4,1.8), Fig. S25) and Rabt Sbayta 008 ((12.5,0.8), Fig. S45) are not paired with each other nor with the meteorites of this figure.

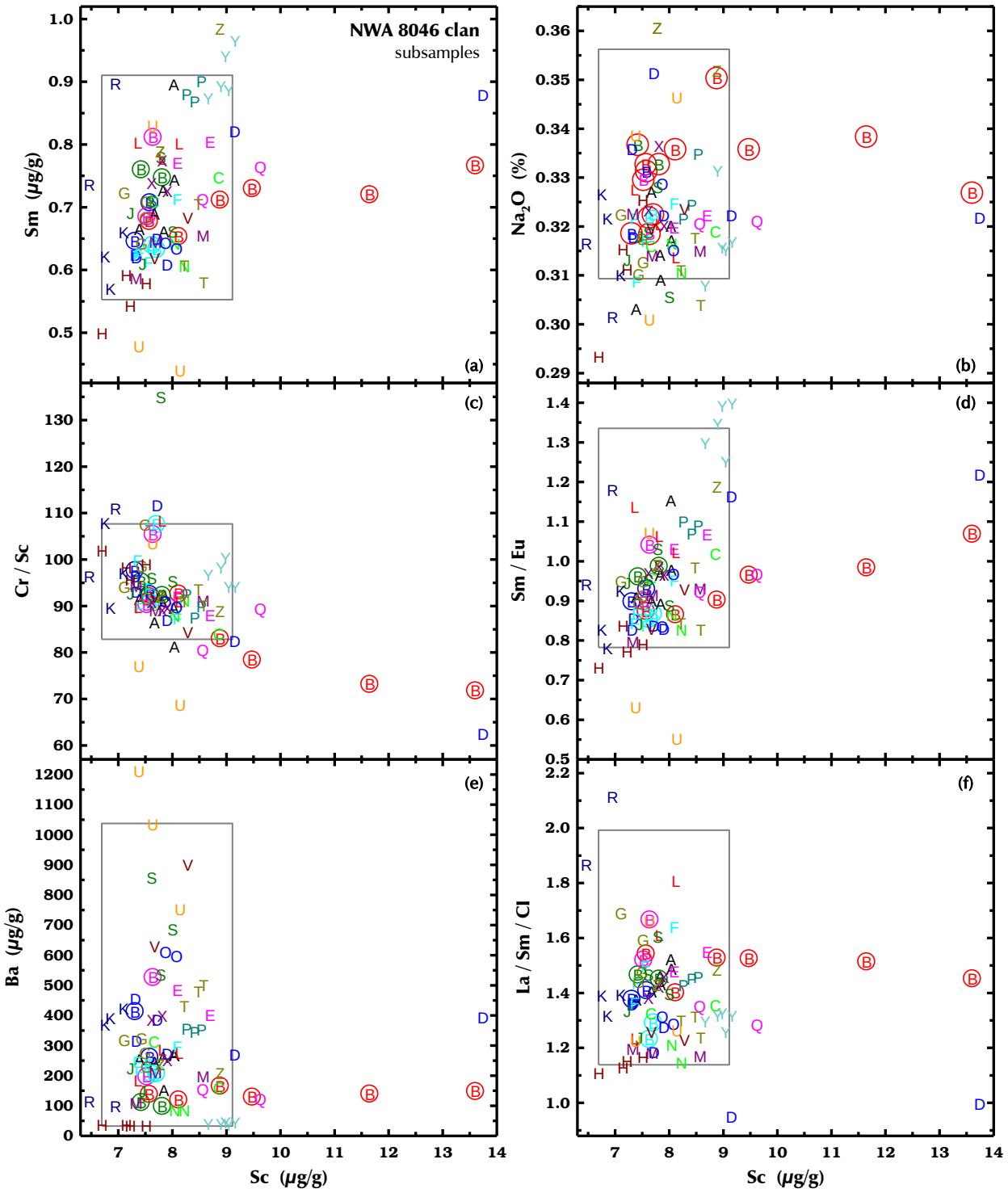

Fig. S24. Subsample data for 24 stones of the large NWA 8046-clan. The large rectangles define the range of the mass-weighted mean concentrations of the 24 stones. Mass-weighted means for no other lunar meteorites plot within the rectangles of all 6 panels of this figure. Data for NWA 10309 (B, *N*=14) derive from 5 different pieces (Fig. S77). With >8.5 μg/g Sc, 4 of the 6 subsamples of one of the pieces (encircled points in red) contain mare basalt but the other 2 subsamples are 'normal' as are the other 4 pieces (Fig. S77). Two of the 6 subsamples of NWA 10609 (D) are also rich in mare basalt. (a) The stone data largely overlap but NWA 11029 (symbol K) and NWA 11460 (R) are at the low-Sc end of the range and NWA 11379 (P) is at the high-Sm end of the range whereas data for NWA 12691 (T) nearly covers the whole range of Sm concentrations. (f) There is a wide range

in La/Sm among the stones due to varying degrees of terrestrial enrichment in light REE (Fig. S8i). NWA 11266 (L, Ce/Ce*=0.86) and 11460 (R, Ce/Ce*=0.82) have negative Ce anomalies. Petrologically, The NWA 8046 clan is characterized by olivine typically in the $Fo_{66\pm5}$ range (Fig. 5).

A	8046	J	10901	R	11460
B	10309	K	11029	S	11479
C	10461	L	11266	T	11515
D	10609	M	11269	U	12691
E	10643	N	11273	V	12760
F	10649	O	11303	X	pair
G	10756	P	11379	Y	pair
H	10822	Q	11428	Z	pair

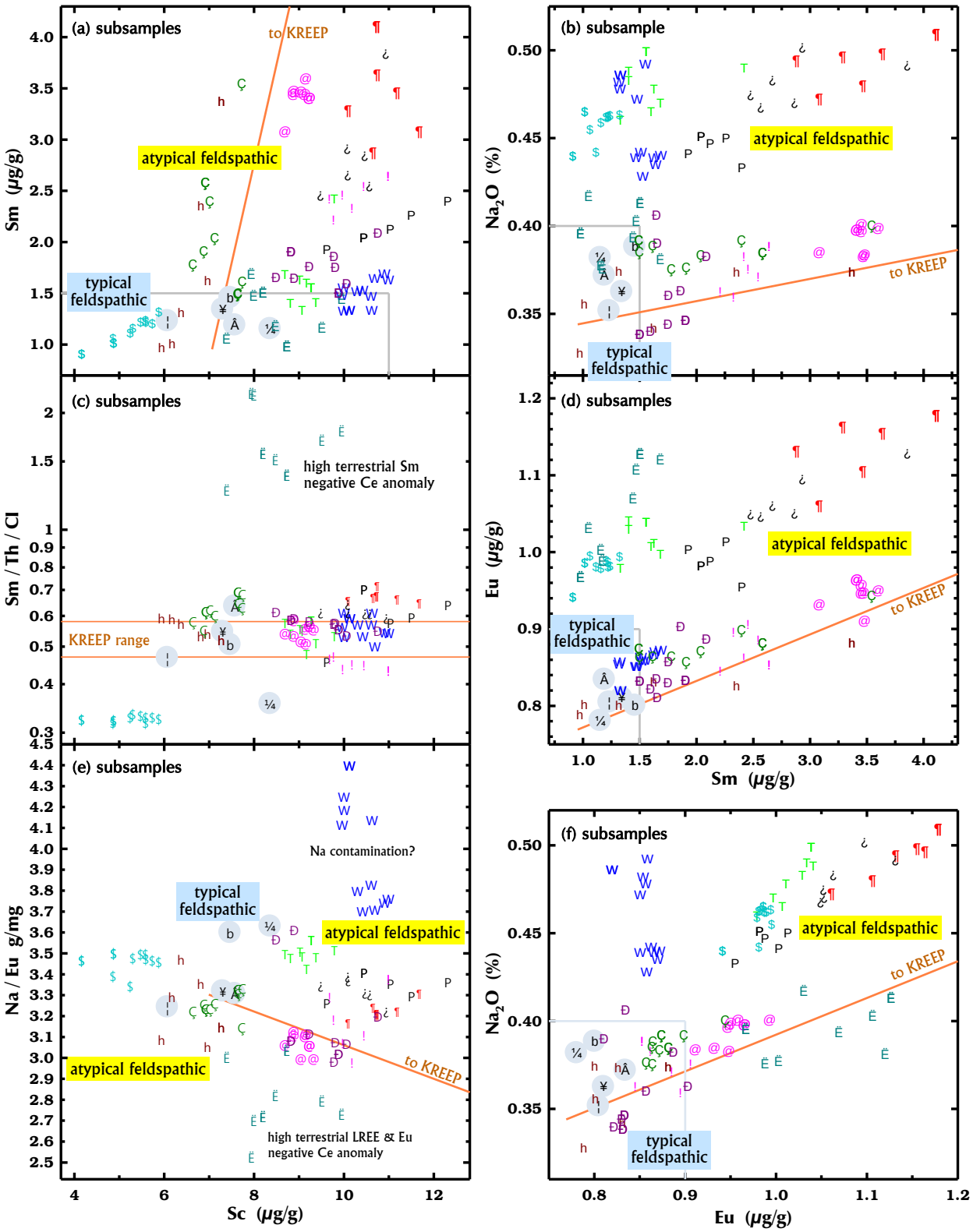
(a) subsamples
to KREEP
atypical feldspathic
typical feldspathic
Sm (μg/g)
(b) subsample
atypical feldspathic
to KREEP
typical feldspathic
Na2O (%)
(c) subsamples
high terrestrial Sm
negative Ce anomaly
KREEP range
Sm / Th / Cl
(d) subsamples
atypical feldspathic
to KREEP
typical feldspathic
Eu (μg/g)
Sm (μg/g)
(e) subsamples
Na contamination?
typical feldspathic
atypical feldspathic
to KREEP
high terrestrial LREE & Eu
negative Ce anomaly
Na / Eu g/mg
Sc (μg/g)
(f) subsamples
atypical feldspathic
to KREEP
typical feldspathic
Na2O (%)
Eu (μg/g)

atypical feldspathic subsamples		**typical feldspathic** stone means	
P	NWA 5000 (2.0–3.9)	¼	NWA 8586 (2.6–3.1)
T	NWA 6481 (3.5–4.9)	b	NWA 10073 (1.5–4.5)
W	NWA 6721 (2.1–4.1)	¦	NWA 11006 (2.4–5.8)
@	NWA 8001 (2.7–3.2)	Â	NWA 11352 (2.1–4.3)
$	NWA 8022 clan (4.1)	¥	rock 87
¿	NWA 8641 clan (3.4–6.0)		
h	NWA 10404 (3.0–3.9)		
Ç	NWA 10678 clan (1.8–5.0)		
¶	NWA 10783 (4.9–6.1)		
Ë	NWA 11223 & 11809 (1.4–8.1)		
Ð	Rabt Sbayta 007 clan (4.3–7.0)		
!	Talhat Lihoudi (3.5)		

Fig. S25. Subsample data for atypical feldspathic lunar meteorites and comparison to stone means for those typical feldspathic meteorites (pale blue filled circles; Fig. S17) that are on or near the somewhat arbitrary boundary between this distinction, i.e., (a) 1.5 μg/g Sm and (b) 0.4% Na_2O (see also Figs. S5 and S16). The diagonal lines are the FHT end of the FHT-PKT side of the mixing triangle of Figs. 6 and S5. For NWA 5000 (symbol P), only the matrix subsamples are plotted here (Fig. S29). For the NWA 8641 clan (¿) the points do not represent subsamples but stone means for the six stones of the clan (Fig. S26). NWA 10783 (¶) is largely indistinguishable from the NWA 8641 clan (¿) except that Fe (1.15×), Ba (0.3×) and, Cr/Sc (0.89×), and Sm/Th (1.1×, panel c) are significantly different (99% confidence level). Ni (1.9×) and Ir (2.1×) are greater in NWA 10783, so we assume that the two meteorites are not terrestrially paired but possibly launch paired. In the legend, the reported range of Ab (albite content of the plagioclase) is given. Simply averaging the range values for those meteorites with >0.4% Na_2O yields $Ab_{4.9}$. This value compares with a range of $Ab_{2.4–3.4}$ (normative) in the typical feldspathic lunar meteorites (panel f and Fig. 11). For NWA 8001 (@), NWA 10404 (h), NWA 10678 (Ç), Rabt Sbayta 007 (Ð), and Talhat Lihoudi (!) the atypically high Na_2O, Sm, and Eu concentrations are consistent with a minor component of KREEP. (f) Except for NWA 6721 (W), there is a tendency for Na and Eu to correlate with each other as both are carried by plagioclase. The high Na_2O in NWA 6721 (W) may be a terrestrial weathering effect. (b,e,f) NWA 5000 (P), NWA 6481 (T), the NWA 8022 clan ($), the NWA 8641 clan (¿), and NWA 10783 (¶) appear to contain a component with greater Na_2O/Sm, Eu/Sm, and Na_2O/Eu than KREEP apparently as a result on greater albite component in the plagioclase.

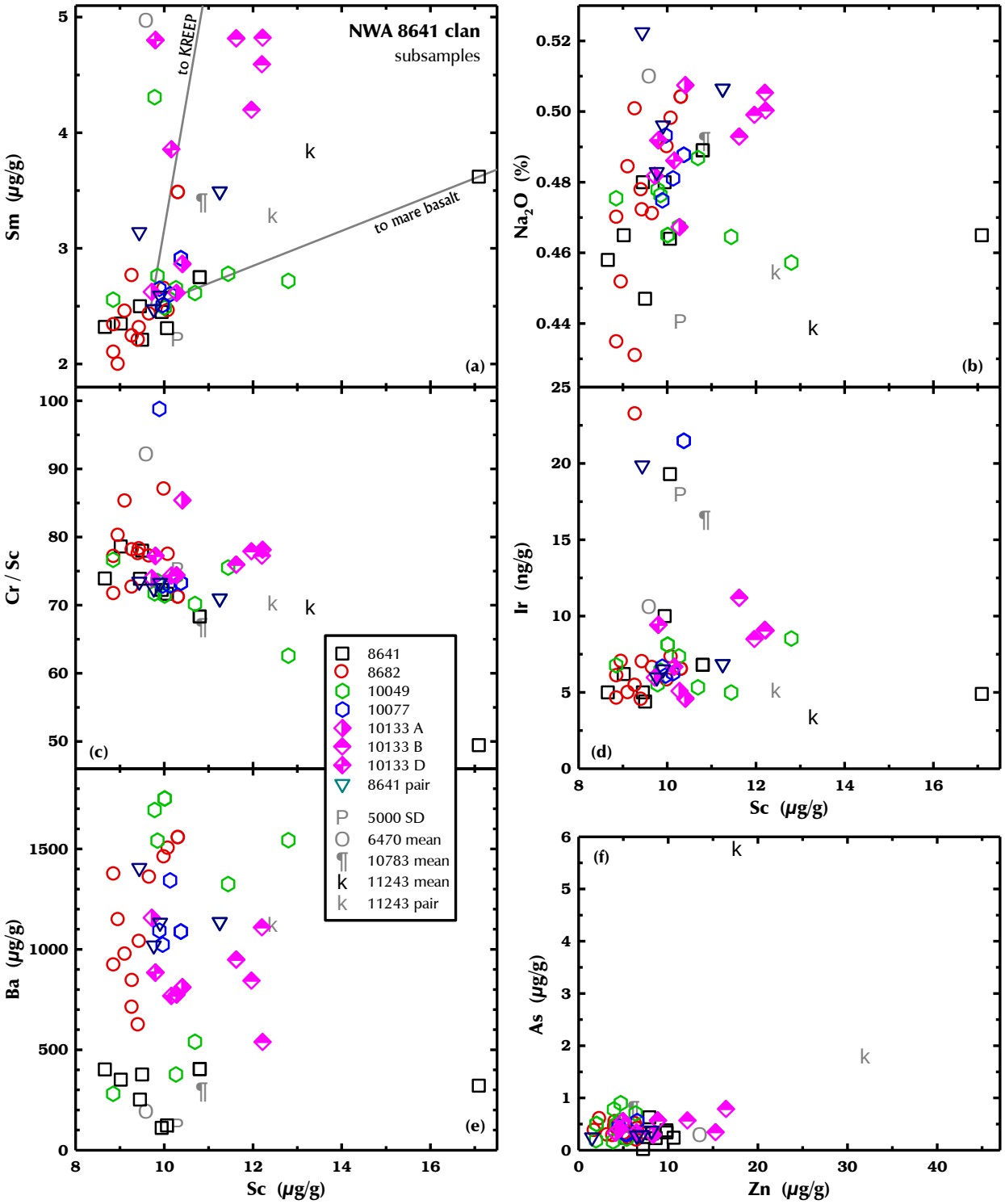
NWA 8641 clan
subsamples
to KREEP
to mare basalt
Sm (μg/g)
Na2O (%)
Cr / Sc
Ir (ng/g)
Ba (μg/g)
As (μg/g)
Sc (μg/g)
Zn (μg/g)
(a)
(b)
(c)
(d)
(e)
(f)
8641
8682
10049
10077
10133 A
10133 B
10133 D
8641 pair
5000 SD
6470 mean
10783 mean
11243 mean
11243 pair

Fig.S26(a-e) Data for subsamples of the NWA 8641 clan (regolith breccia; 6.1 kg: geometric symbols) and comparison TO other meteorites for which the mean compositions plot in the range of all 5 panels of the figure (but with <13 μg/g Sc). (a) The upper diagonal line is defined by the mean Sc and Sm concentrations of the low-Sc, low-Sm subsamples and the PKT component of Fig. 6. Some of the subsamples are enriched in a KREEP component. The lower diagonal line is defined by the mean Sc and Sm concentrations of the low-Sc, low-Sm subsamples and the high-Sc NWA-8641 subsample at 17 μg/g Sc. The high-Sc subsample likely contains a clast of some form of mare basalt. The MetBull description of NWA 8641 includes "symplectitic intergrowths of fayalite + hedenbergite + silica polymorph," an assemblage commonly seen in lunar mare material. Extrapolation of the "to mare basalt" line to 40–60 μg/g Sc leads to 7–10 μg/g Sm, a range typical of mare basalt (Fig. 6). (c) The high-Sc subsample has low-Cr/Sc, another characteristic of mare basalt (Fig. S4). (e) Our sample of NWA 8641 has less Ba than our samples of the other 5 stones but it was from the interior of the 5.9-kg NWA 8641 stone whereas the other stones are much smaller (82 g, 56 g, 5 g, 54 g for the named pairs). NWA 10133 consists of several pieces and we analyzed subsamples of three of them (A, B, and D). Piece B is richer in Sc and Sm than the other two (a).

(a) NWA 6470 (symbol O) is the stone of the NWA 4936 clan with the lowest Sm concentration and is not likely related to the NWA 8641 clan (Fig. S35).

NWA 5000 (P), represented here by the mean composition of the sawdust, appears to contain a Sm-rich component compositionally like the NWA 8641 clan (Fig. S29), which in part accounts for the similarity here.

NWA 10783 (¶) is similar to the NWA 8641 clan for most well-behaved elements but has significantly greater FeO (1.15×), Sm/Th (1.08×), Sm/Eu (1.12×), and Ni/Co (1.20×) but lower Cr/Sc (c, 0.89×), Na/Sm (0.84×), and Ba (0.32×) than the NWA 8641 clan. We have seen photographs of slices NWA 10783 (22 g) that are ~95% granulitic breccia with ~5% attached regolith breccia and our sample is entirely granulitic breccia, so it is possible that NWA 10783 is simply a clastic component of the NWA 8641 clan meteorite, allowing for terrestrial or launch pairing.

NWA 11243 (k) and its presumed pair (k) is compositionally similar to the NWA 8641 clan (a–c) but has much greater concentrations of Zn and As (e) as well as having a lower Na/Sc ratio (b). In (e), NWA 11243 plots off scale at 2040 μg/g Ba.

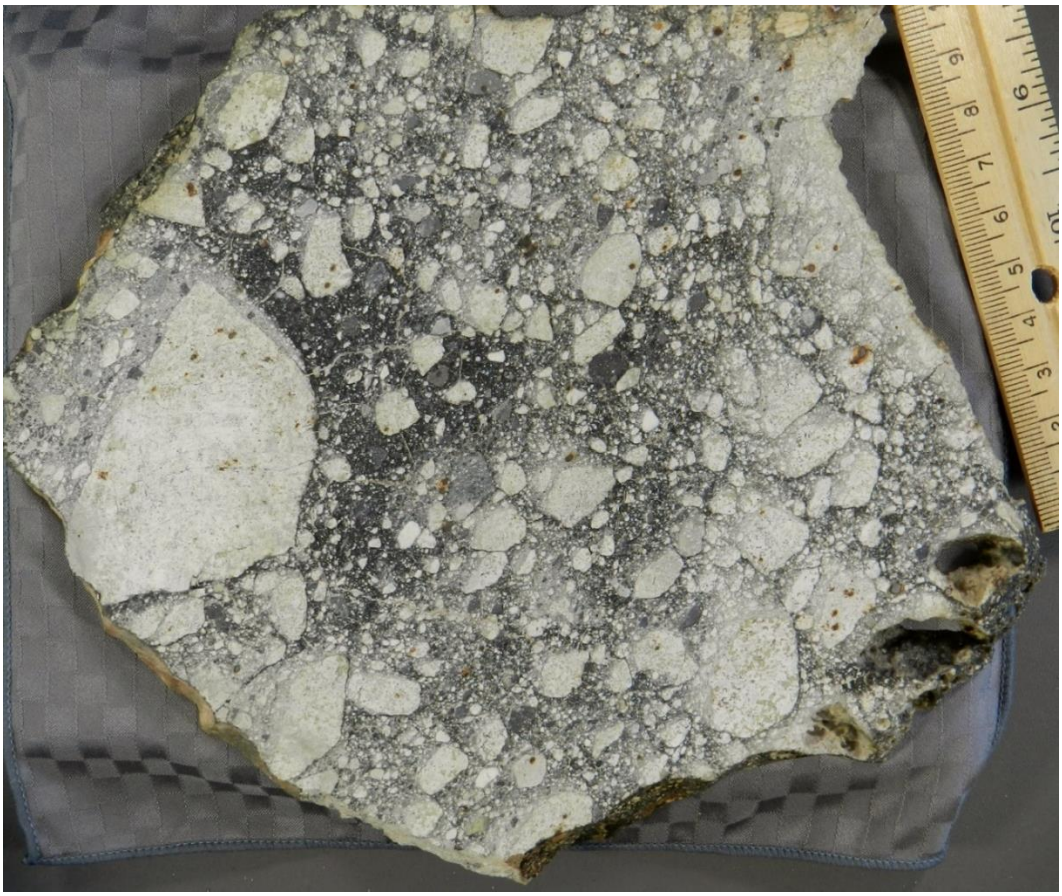

Fig.S27.A large sawn slab of NWA 5000. Millimeter ticks on ruler to right. NWA 5000 is unique among lunar meteorites in being a nearly monomict regolith or fragmental breccia with large clasts of impact-melt breccia of leucogabbronorite mineralogy (Irving et al., 2008; Nagurney et al., 2016). Clast sizes range at least to 8 cm in longest dimension. All the rust-colored spots are grains of FeNi metal. The dark matrix is different in composition from the clasts (Fig. S29).

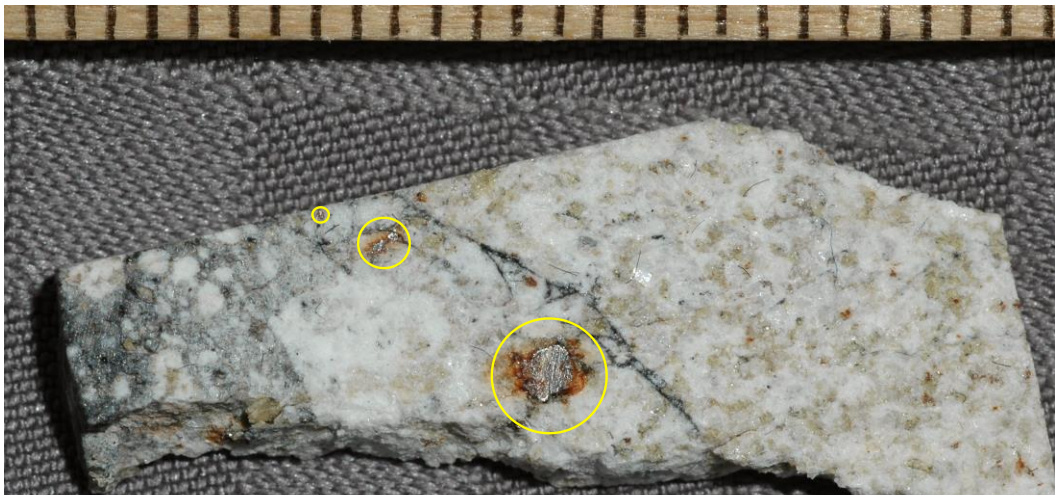

Fig. S28. Both the clasts and matrix contain large, rusty grains of FeNi metal (Irving et al., 2008; Humayun and Irving, 2008; Nagurney et al., 2016), which lead to anomalously high concentrations of siderophile elements in some subsamples (e.g., Fig. S29d). Millimeter ticks for scale.

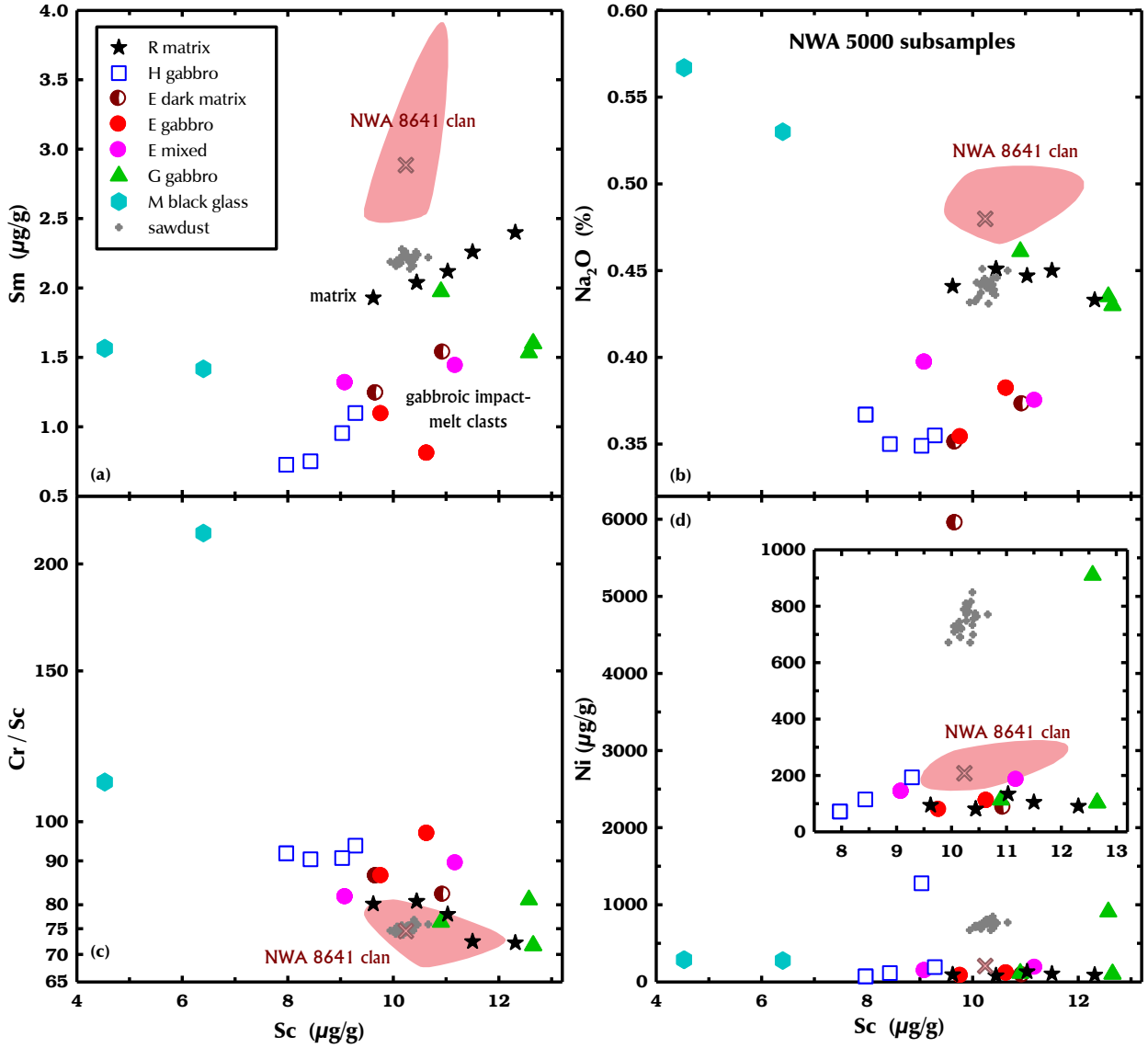

Fig. S29. We analyzed 20 "chip" subsamples of NWA 5000 (11.5kg): (1) 5 matrix subsamples from the interior of the rock (R subsamples), (2) 4 subsamples of a gabbronorite clast from the interior (H), (3) 6 subsamples of a dilithologic sample consisting of clast and dark matrix from the exterior of the rock (E), (4) 3 subsamples of a light-colored gabbro clast from the exterior of the rock (G), and (5) 2 subsamples of black glass on the exterior of the rock (M). We have also analyzed 27 samples of sawdust from cutting of the rock (Table S8). (a) The matrix samples plot along a mixing line (R^2=0.981, N=5) that extrapolates to the origin (plagioclase). The sawdust is similar in composition to the breccia matrix. The inferred mafic component of the breccia matrix is richer in incompatible elements and Sc (also Fe and Cr) than the gabbronoritic melt-breccia clasts. The clasts range in Sc concentration, which reflects variation in pyroxene/olivine. The black glass appears to be unrelated to the other lithologies and may simply be splash from a small impact into surface regolith. Assuming that matrix samples contain small clasts of the gabbronorite, the remaining material must be richer in incompatible elements. To a good first approximation, the lithophile element composition of the NWA 5000 matrix samples (★) can be duplicated by a 1:1 mixture of the gabbronoritic clasts (○ & ▲) and material (regolith?) with a composition like the NWA 8641 clan (Fig. S26), suggesting possible launch pairing. (c) The higher Cr/Sc of the impact-melt clasts compared to the matrix suggests higher olivine/pyroxene (Fig. 4). (d) The sawdust is contaminated with Ni (also Zn, Ag, Sb, and Au; Table S2). On the basis of the 18.0 ng/g of Ir we observe in the NWA 5000 sawdust (Table S5) and the 3930 ng/g Ir we infer in the metal (Table S6), the meteorite contains 0.46% FeNi metal, and 9% of the Fe in the meteorite is in metallic form.

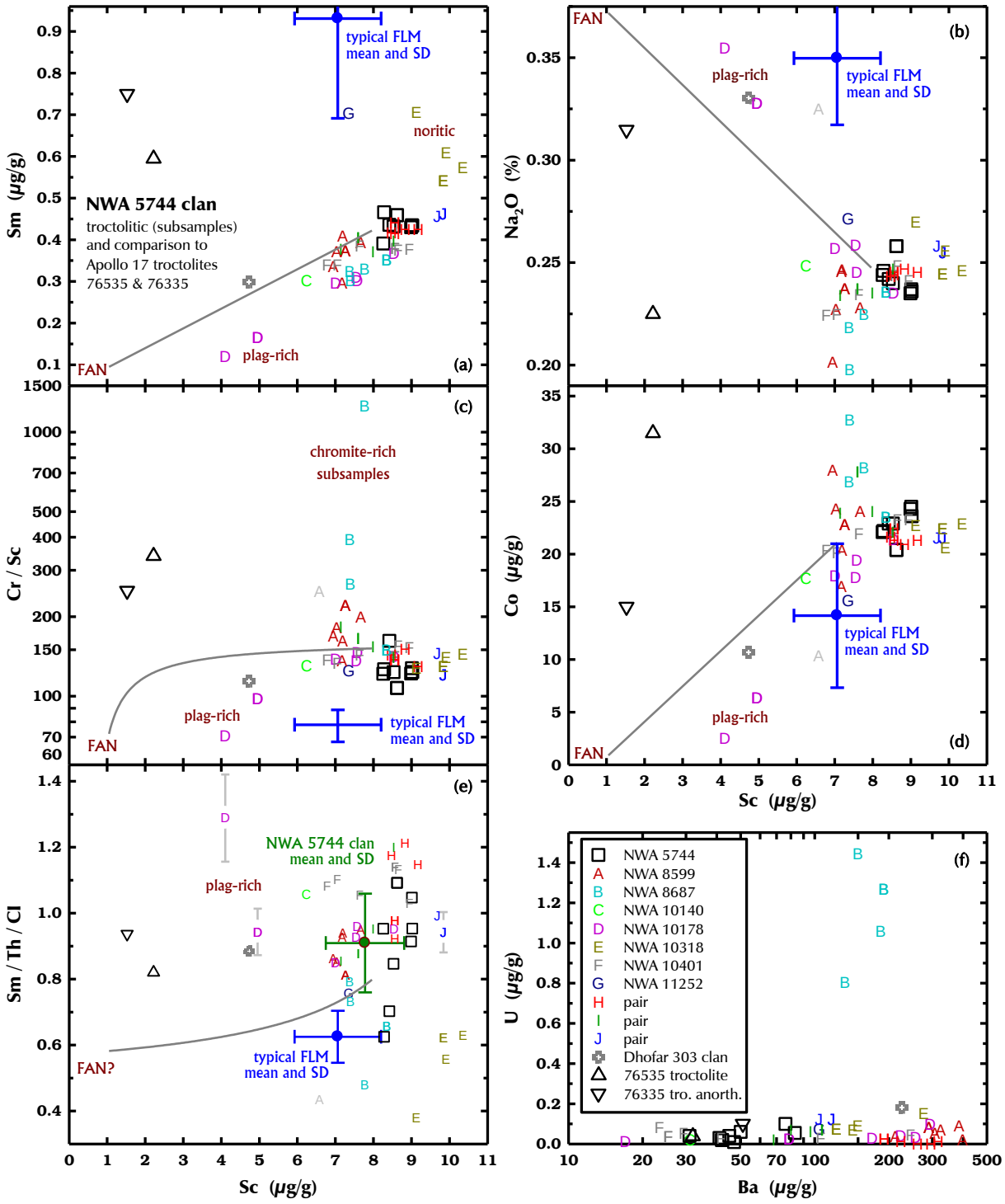
(a)
Sm (μg/g)
typical FLM
mean and SD
noritic
NWA 5744 clan
troctolitic (subsamples)
and comparison to
Apollo 17 troctolites
76535 & 76335
plag-rich
FAN
(b)
Na2O (%)
typical FLM
mean and SD
plag-rich
FAN
(c)
Cr / Sc
chromite-rich
subsamples
plag-rich
typical FLM
mean and SD
FAN
(d)
Co (μg/g)
Sc (μg/g)
typical FLM
mean and SD
plag-rich
FAN
(e)
Sm / Th / Cl
NWA 5744 clan
mean and SD
plag-rich
typical FLM
mean and SD
FAN?
Sc (μg/g)
(f)
U (μg/g)
Ba (μg/g)
NWA 5744
NWA 8599
NWA 8687
NWA 10140
NWA 10178
NWA 10318
NWA 10401
NWA 11252
pair
pair
pair
Dhofar 303 clan
76535 troctolite
76335 tro. anorth.

Fig. S30. Subsample data for the NWA 5744 clan (at least 2.5 kg), a brecciated anorthositic troctolite, and comparison to the Dhofar (Oman) 303 clan (mass-weighted mean of 10 stones; Korotev,2012), a brecciated troctolitic anorthosite, and Apollo 17 unbrecciated troctolites 76335 and 76535 (Haskin et al., 1974; Warren and Wasson, 1977; M. Lindstrom, pers. comm.). The stones of the NWA 5744 clan have granulitic textures (compare with ferroan granulites of the NWA 3163 clan, Fig. S45). Data for the numerous stones of the NWA 5744 clan do not mutually overlap because of variable proportions of olivine, pyroxene, and plagioclase among the small subsamples. Sc concentrations in the NWA 5744 clan are greater than those of otherwise similar Apollo 17 rocks because they contain 5–13% normative pyroxene (~5–11 vol.%) whereas the Apollo 17 samples contain no pyroxene (Gooley et al.,1974; Dymek et al., 1975; Warren and Wasson, 1977). For comparison, the "typical FLM" (feldspathic lunar meteorite) mean and SD (standard deviation) are from Table S5. In (a–e), the mixing lines are defined by the simple mean of the 10 stones of the NWA 5744 clan (e) and the mass-weighted mean of 68 lithic fragments (1.75 g) from the Apollo 16 regolith with <2% FeO, <5 μg/g Sc, and <0.2 μg/g Sm representing ferroan anorthosite (from the FAN field of Fig. 9).

(a) At one extreme, compositionally anomalous NWA 10318 (symbol E) is described as a "granulitic breccia of olivine-bearing anorthositic norite precursor" (A. Bischoff and S. Ebertin in MetBull), which accounts for the high Sc concentrations. One of the pairs (J) is similar. At the other extreme, 2 NWA 10178 subsamples (D) are dominated by clasts of plagioclase or anorthosite. These 2 subsamples are similar in composition to the Dhofar 303 clan in all panels. The single sample of anomalous NWA 11252 (G) is cutting dust, not chips. Incompatible elements are more than 2× greater in the typical feldspathic lunar meteorites than in the NWA 5744 clan. The Apollo 17 troctolites, which likely formed in the PKT, are also richer in incompatible elements than the NWA 5744 clan.

(b) Except for the two plagioclase-rich subsamples of NWA 10178, all of these stones are low in Na_2O (and Eu, Fig. S16) compared to typical feldspathic lunar meteorites because of their high olivine content (Figs.5a and S5).

(c,d) Cr/Sc and Co are high compared to typical feldspathic lunar meteorites as a result of the high olivine abundances (Figs. 5 and 14). The NWA 8687 sample (B) contained a large chromite grain (photo: Fig. S1d) leading to anomalously high Cr/Sc and Co in three subsamples. Panels (a–d) allow that the plagioclase-rich samples are ferroan anorthosite, but one with 4–5 μg/g Sc.

(e) Th concentrations in the FAN samples have very high relative uncertainties so for this panel the FAN point is plotted at the same Sm/Th as the typical FLMs. The troctolites, and even the plagioclase-rich subsamples from NWA 10178 (D), have higher Th/Sm than the typical FLM's. This panel does not support the hypothesis that the anorthositic troctolites of the NWA 5744 clan are mixtures that contain a substantial component of ferroan anorthosite. Error bars (gray) representing ±1σ analytical uncertainties for Sm/Th are shown for 3 of the points. Uncertainties for Sc concentrations are 1% of the concentration value.

(f) These stones may not all be terrestrially paired. Low-Ba NWA 5744 (□) was reportedly found in Mali, while high-Ba NWA 10318 (E) was reportedly found in Morocco. The other NWA stones were all purchased in Morocco. NWA 8687 (B) has anomalously high U concentrations as a result of terrestrial alteration suggesting a different find location.

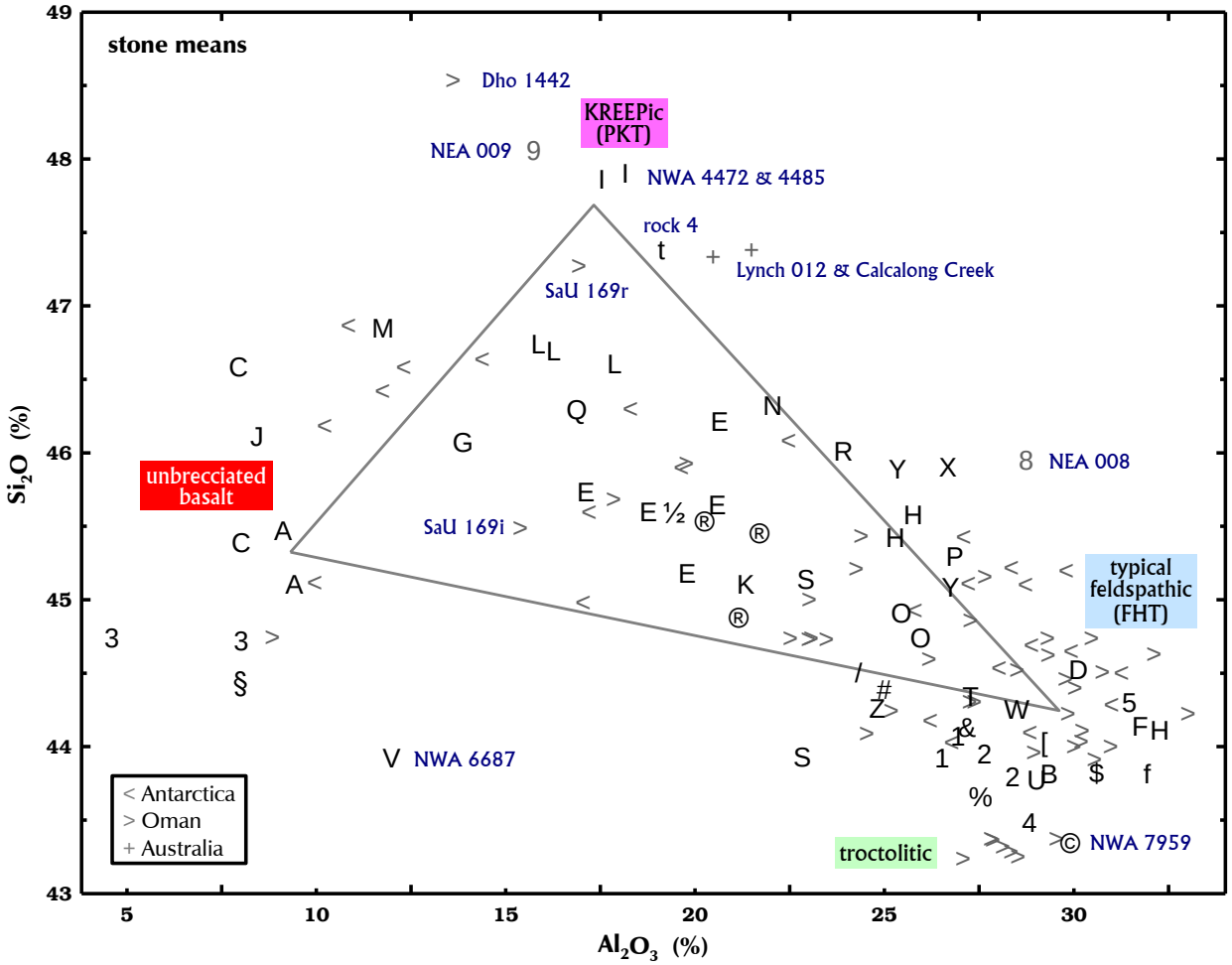

Fig. S31. Lunar meteorites in Al_2O_3-SiO_2 space. Calcalong Creek, Dhofar 1442, Lynch 012, NEA 4472/4485, and SaU 169r (regolith breccia) are all rich in incompatible elements and likely contain silica minerals. NWA 6687 (Fig. S38) is also rich in incompatible elements (19 µg/g Sm, Fig. 6) but is basaltic. Typical feldspathic lunar meteorites are low in SiO_2. Both Kalahari 008 and Kalahari 009 are rich in SiO_2. The triangle is the mixing triangle of Figs. 2 and 6. See Table S1 for symbol key.

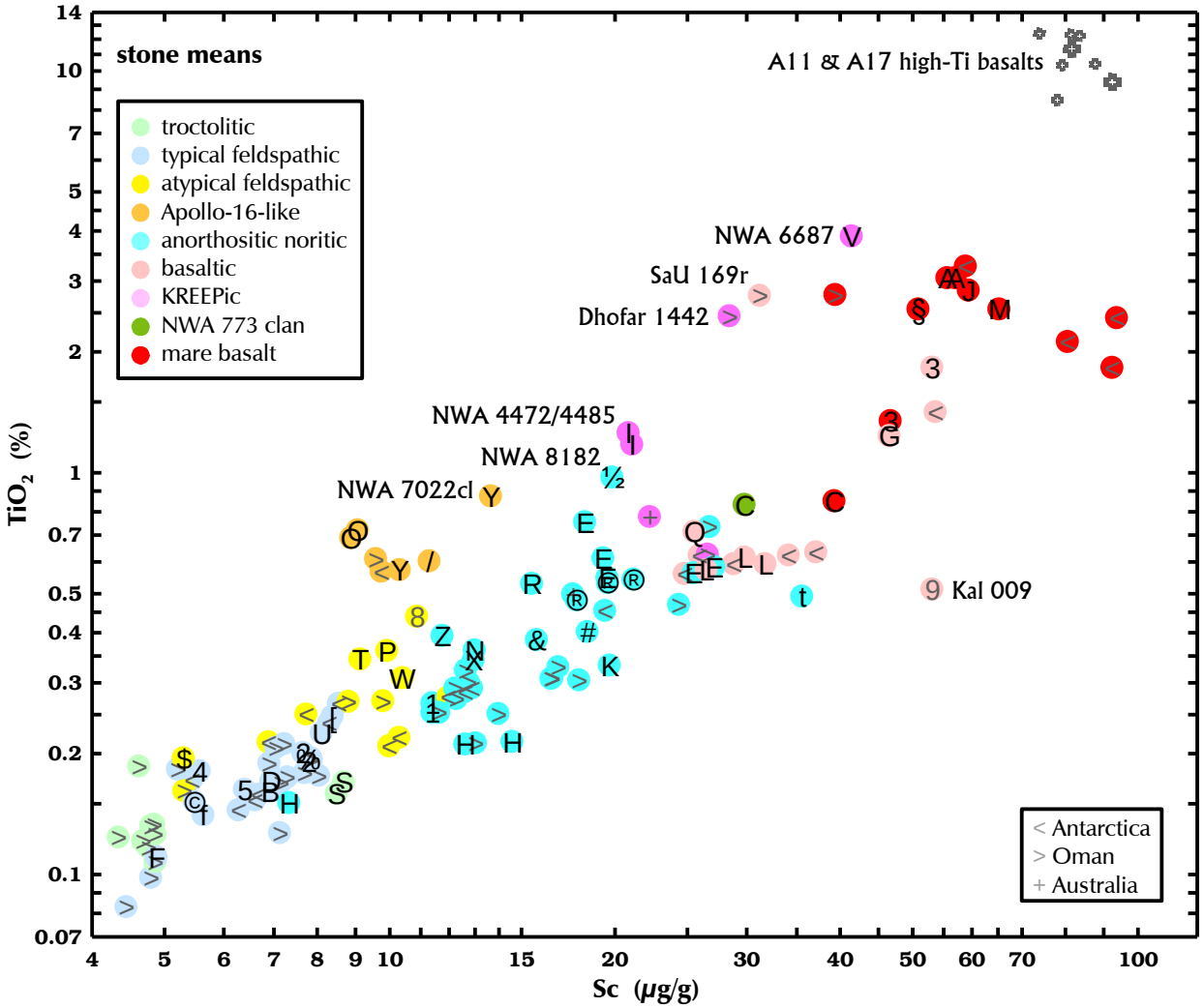

Fig. S32. TiO_2 tends to increase with increasing Sc in lunar rocks. NWA 6687, NWA 4472/4485, NWA 8182, SaU169r (regolith breccia), and the Apollo-16-like meteorites likely contain a component of high-Ti mare basalt. The NWA 3163 clan (symbol H), NWA 5744 clan (S), and Kalahari 009 (9) have low TiO_2/Sc ratios. See Table S1 for symbol key. Kalahari 009 does not plot with the mare basalts.

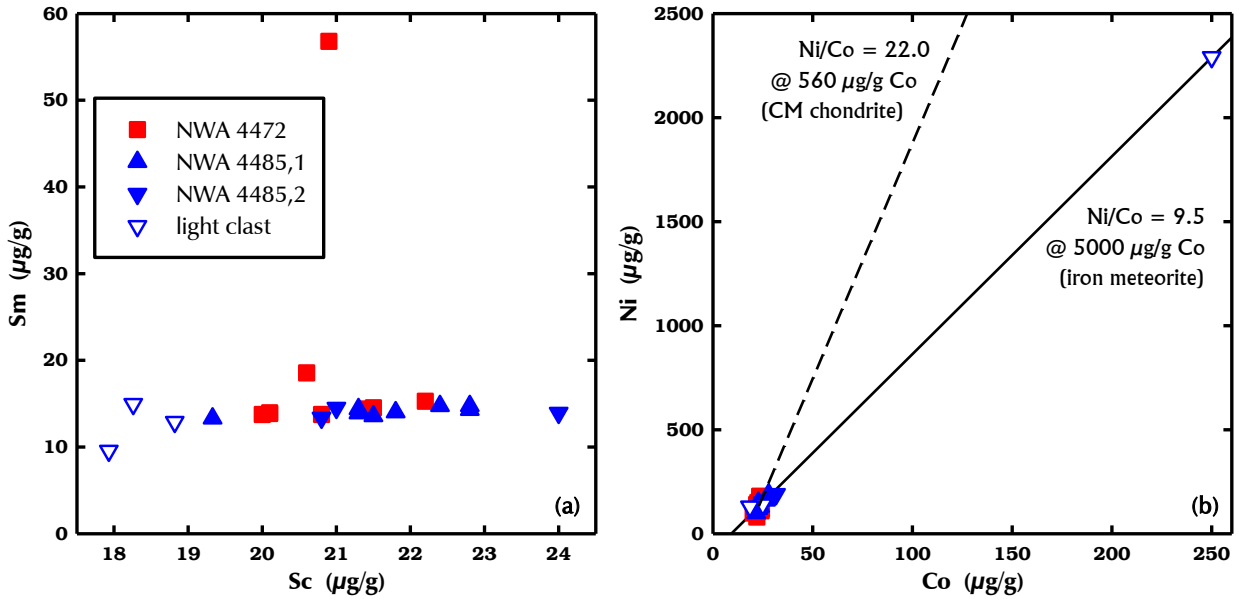

Fig. S33. (a) Subsamples of paired stones NWA 4472 and NWA 4485 (regolith breccias; total mass: 252 g) are variable in Sc concentration, a characteristic of breccias with a lithic component of mare basalt. Clasts of mare basalt have been observed in the NWA 4472 (Joy et al., 2011), and this plot shows that the relative abundance of basalt among the 24–38-mg subsamples is not uniform. We obtained two different samples of NWA 4485. The three unfilled NWA 4485 points represent a light-colored clast that is more feldspathic than the breccia matrix. One NWA 4772 subsample is considerably richer in trivalent REE (from 3.9× for La to 2.2× for Lu) and Th (1.65×) but not Zr (1.0×), Hf (1.0×), or U (1.0×). This pattern implicates a 'large' grain of RE-merrillite as the cause of the anomaly, not a large clast of KREEP basalt, which is a prominent lithic component of the meteorite (Arai et al., 2009; Joy et al., 2011). Assuming 3500 μg/g Sm in the RE-merrillite (Jolliff et al., 2006), the merrillite grain is 0.2 mg in mass. In other plots in this paper of mass-weighted mean concentrations, the points for NWA 4472 represent a mean from which two most Sm-rich subsamples were excluded. (b) One of the NWA 4472 subsamples contains a large nugget of FeNi metal, 8.6 mg in mass, assuming 5000 μg/g Co, a typical value for large metal grains in lunar samples (e.g., Hewins and Goldstein, 1975). The solid line is defined by the mean of low-Co points and the one high-Co point. The dashed line is defined by the mean of the low-Co points and CM chondrites (Lodders and Fegley, 1998). Ni/Co in the metal grain is half the chondritic ratio but typical of metal in, e.g., IIAB iron meteorites (Fig. S54 and Wasson et al., 2007).

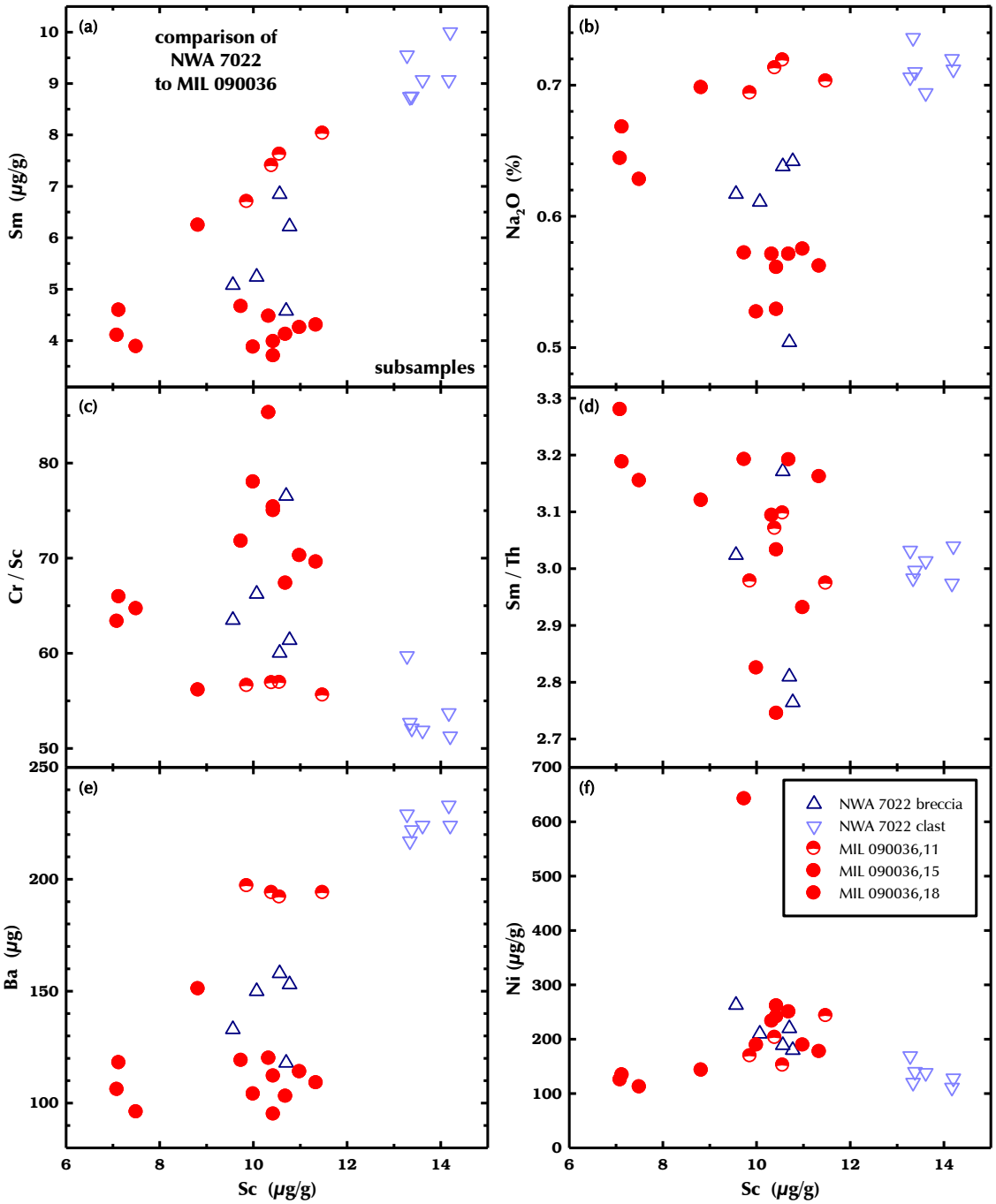

Fig.S34. NWA 7022 (444 g) is a fragmental breccia dominated by one large lithic clast, an impact-melt breccia, that accounts for about a third of the stone (Kuehner et al., 2012b). The breccia matrix is similar in composition to the Apollo-16-like NWA 4936 clan (Fig. S35) in being feldspathic but richer in Sm (6×) and Na_2O (1.8×) than typical feldspathic lunar meteorites. These characteristics are even more extreme in the clast. The clast differs in composition from any of the impact-melt breccias of Apollo 16 (Korotev, 1994), however, especially in having a very high Na concentration, the highest of any meteorite of this study (Fig. S5). The fragmental breccia lithology overlaps in composition with another heterogeneous lunar meteorite with large clasts, MIL 090036 (245 g) from Antarctica, for which we have analyzed several subsamples of 3 different samples (11, 15 ,and 18; Korotev and Zeigler et al., 2014). (b) High Na (Fig. S5) is a characteristic of both meteorites. There is no significant compositional difference (Welch's *t*-test) between the NWA 7022 breccia matrix and MIL 090036 for any precisely determined INAA element, allowing that the two meteorites are launch paired. Preliminary cosmic-ray exposure data are not consistent with the launch-pairing hypothesis (Kuehner et al., 2012b), however (Nishiizumi and Caffee, 2013). (e) There is little hint of terrestrial Ba in NWA 7022.

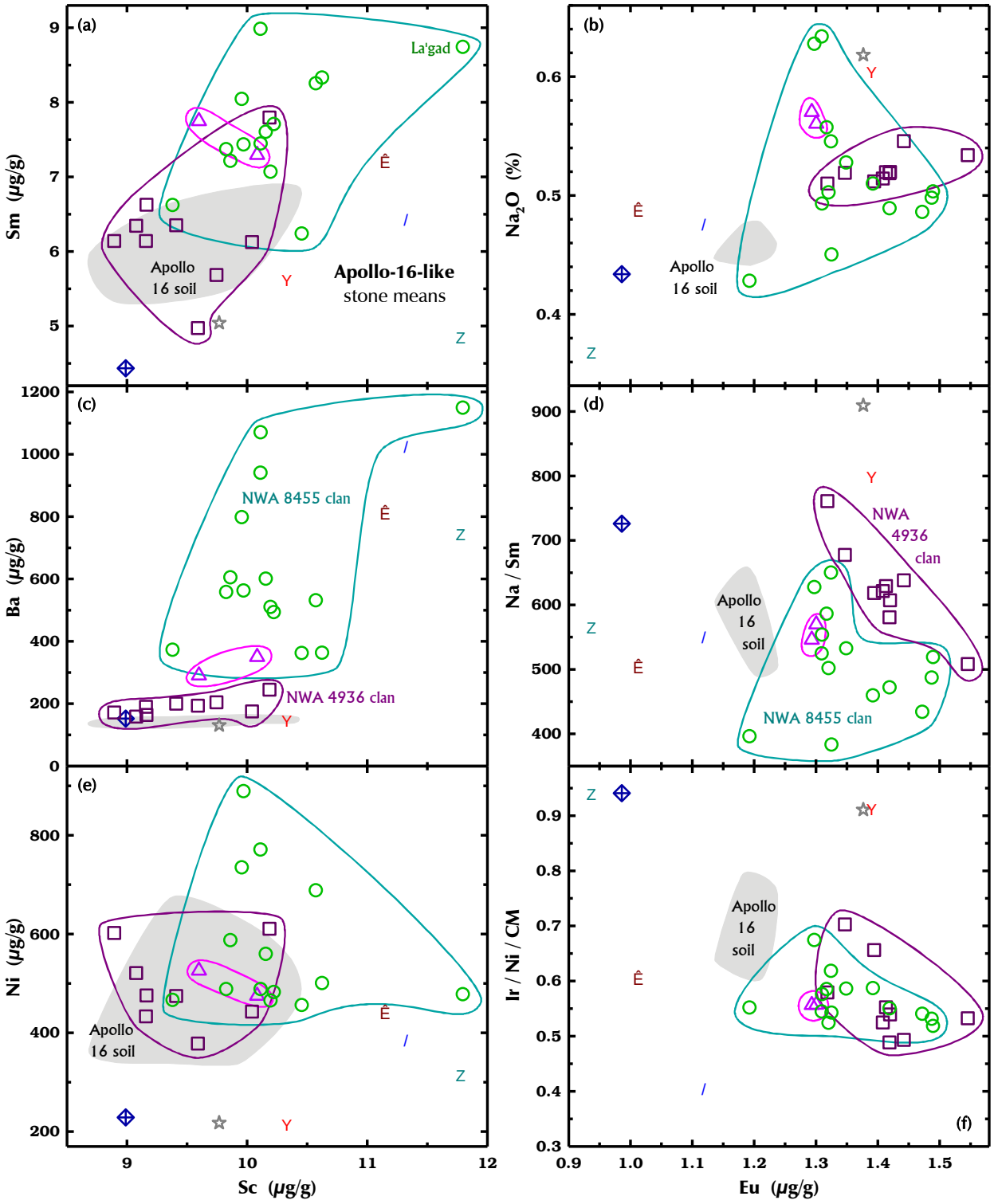
(a)
Sm (μg/g)
La'gad
Apollo
16 soil
Apollo-16-like
stone means
(b)
Na2O (%)
(c)
Ba (μg/g)
NWA 8455 clan
NWA 4936 clan
(d)
Na / Sm
NWA
4936
clan
(e)
Ni (μg/g)
(f)
Ir / Ni / CM
Sc (μg/g)
Eu (μg/g)

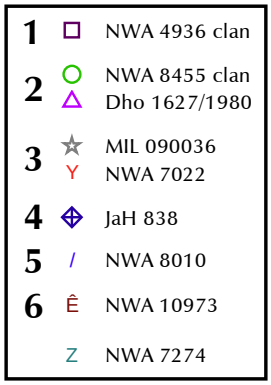

Fig. S35. (a) In Sc-Sm space, 8 lunar meteorite stones have compositions similar to those of mature and submature soils from Apollo16 (Korotev, 1997). (For reference, we also plot NWA 7274 (Z) here, but do not include it among the "Apollo-16-like" meteorites.) (a–f) Paired Dhofar stones 1627 and 1980 from Oman (Korotev, 2017) are indistinguishable in composition from the NWA 8455 clan and are candidate launch pairs. NWA 7022 and MIL 090036 (Antarctica; Korotev and Zeigler, 2014) are also possible launch pairs (Fig. S34). Both are breccias containing large clasts (Fig. S34; only the matrix of NWA7022 is plotted here). NWA 8010 and NWA 10973 plot near each other in some of these plots but subsample data do not overlap for many element and ratios (e.g., Fig. S69). (a,c,e) As does the Apollo 16 soil (Zeigler et al., 2006), most of these meteorite breccias contain some (<10%) mare basalt, a fragment of which likely accounts for the high Sc concentrations (also, Fe and Cr) in La'gad. (b) Several of these meteorites have significantly greater concentrations of Na (and Eu) than Apollo 16 soils. (c,d) Sm/Eu and Ba distinguish the NWA 4936 clan from the NWA 8455 clan (see also Fig. S69). NWA 8651 is described as a granulitic troctolitic breccia (Y. Wu in MetBull) and NWA 8727 is described as olivine leuco-gabbro (C. Agee in MetBull) while others of the NWA 8455 clan are described as feldspathic polymict or melt-matrix breccias. Photographs of NWA 8455-clan clearly show clasts up to several centimeters in size, so we suspect that examined thin sections of NWA 8651 and NWA 8727 may have been dominated by large clasts of granulitic or melt breccias and the large clast size accounts for the scatter in the NWA 8455 data. (f) Ir/Ni is nearly chondritic in NWA 7022, JaH 838 (Jiddat al Harasis, Oman), and MIL 090036, which distinguishes them both from the other meteorites plotted here and from the Apollo 16 regolith. In total, we conclude (Table S7) that the "Apollo-16-like" meteorites of this figure likely originate from six impacts on the Moon, those launching: (1) NWA 4936 clan, (2) NWA 8455 clan and Dhofar 1627/1980, (3) NWA 7022 and MIL 090036, (4) JaH 838, (5) NWA 8010, and (6) NWA 10973.

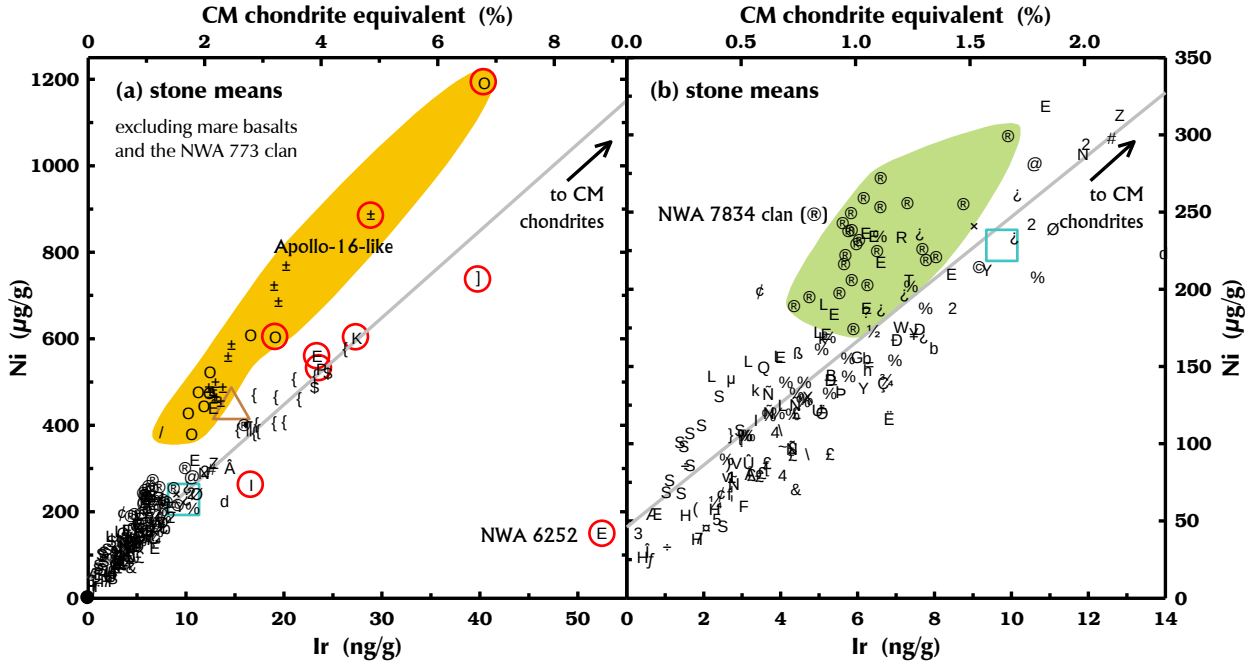

Fig. S36. Ni and Ir concentrations in brecciated lunar meteorites. For most of those with low concentrations of siderophile elements, Ir and Ni derive from micrometeorites, mainly CM chondrites (Wasson et al., 1975). (a) Encircled points represent stones for which subsamples vary by more than a factor of 3 in Ir concentration, which usually indicates the presence nuggets of FeNi metal that are usually not chondritic with respect to Ni/Ir (Figs. 12 and S54). These stones are NWA 6252 (symbol E) and NWA 6555 (E) of the NWA 2995 clan, NWA 4485 (I), NWA 4932 (K), NWA 5000 (P; Fig. S28), NWA 4936 (O) and 6221 (O) of the NWA 4936 clan, and NWA 10130 (±) of the NWA 8455 clan. One of the 3 subsample of NWA 6252 has 157 ng/g of Ir yet only 150 µg/g of Ni (see also Fig. S56). This anomaly is likely due to the presence of an OsIrRuMoPt-alloy nugget from a calcium-aluminum inclusion (e.g., Chou et al., 1976; Wark, 1987). Apollo 16 soils (large triangle) contain Ni and Ir subequally from chondrites and metal-rich impact-melt breccias with a non-chondritic Ni/Ir (Fig. S37). A number of NWA meteorites are similar: NWA 4936 clan (O), NWA 8455 clan (±), NWA 8010 (/), and NWA 10973 (Ê); all four of these are "Apollo-16-like meteorites" with respect to lithophile elements (Fig. S35). (b) Enlargement of the low-Ir meteorites of (a). The NWA 7834 clan (®) has high Ni/Ir. This characteristic is not due to a high-Ni/Ir meteoritic component but to a high-Co, high-Ni indigenous mafic component, presumably olivine (Fig. S49e). Analytical uncertainties (2σ) for low- Ir samples are typically in the 10–30 µg/g range for Ni and 0.5–1.5 ng/g range for Ir. See Table S1 for symbol key.

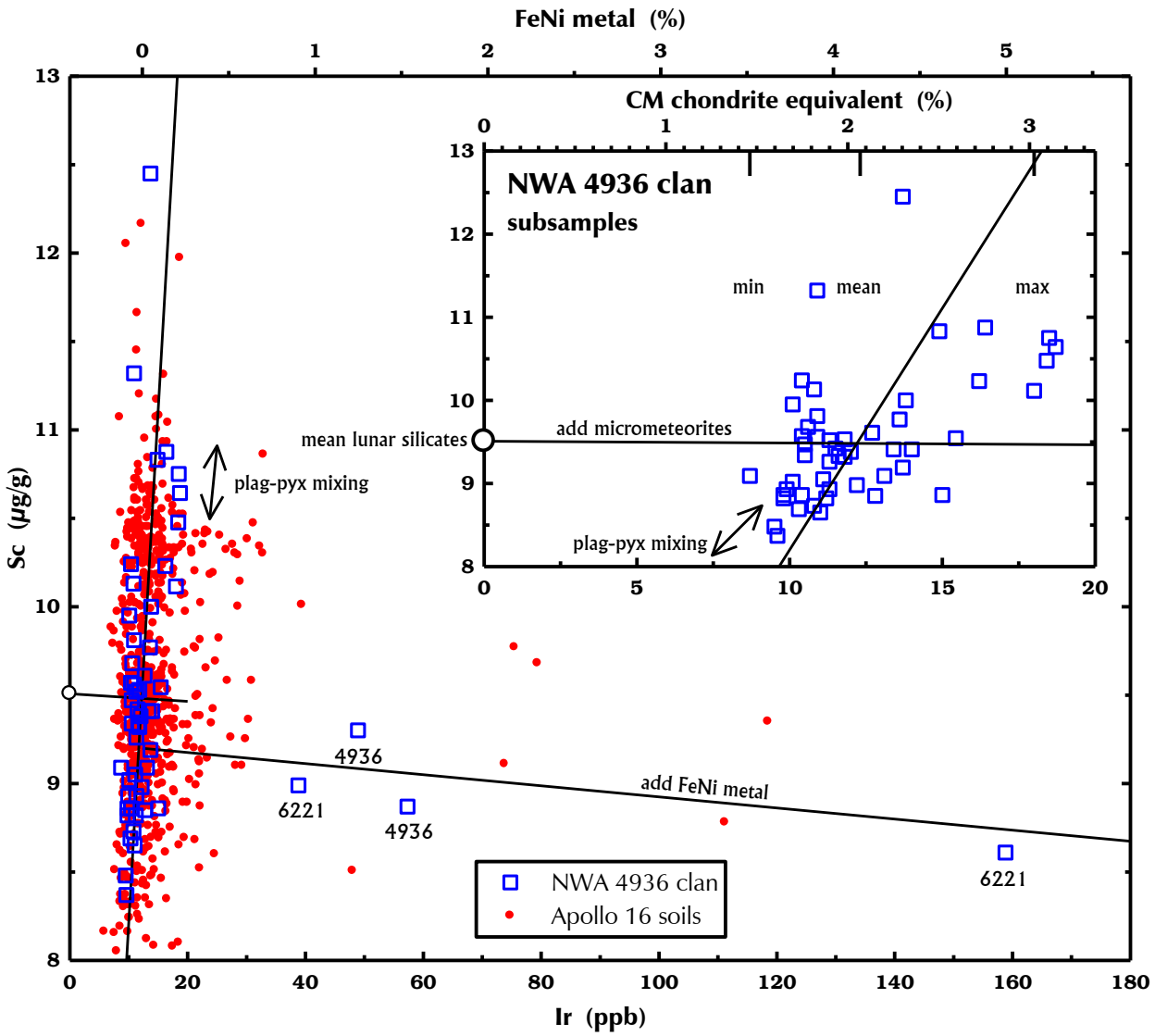

Fig. S37. Sc and Ir data for 54 subsamples of the nine stones of the Apollo-16-like NWA 4936 clan (1.99 kg) and comparison to Apollo 16 soils. Variation in Sc concentrations mainly reflects differing proportions of plagioclase-rich, Sc-poor material of the FHT and pyroxene-rich, Sc-rich material of the PKT. At least two meteorite components are required to account for the NWA 4936 Ir data. For 50 of the samples, Ir is carried mainly by a micrometeorite component ranging from 1.46% to 3.03% in abundance (inset), a range typical for regolith (Wasson et al., 1975; Korotev et al., 1997; Fig. 15). Four of the samples contain nuggets of FeNi metal of nonchondritic composition (Fig. S55) ranging in abundance from 1% to 5% by of the mass of the subsample. For comparison, each red circle represents a sample of Apollo 16 regolith, as represented by samples from four regolith cores (Korotev, 1991; Korotev and Morris, 1993; Korotev et al., 1997), which show the same trends.

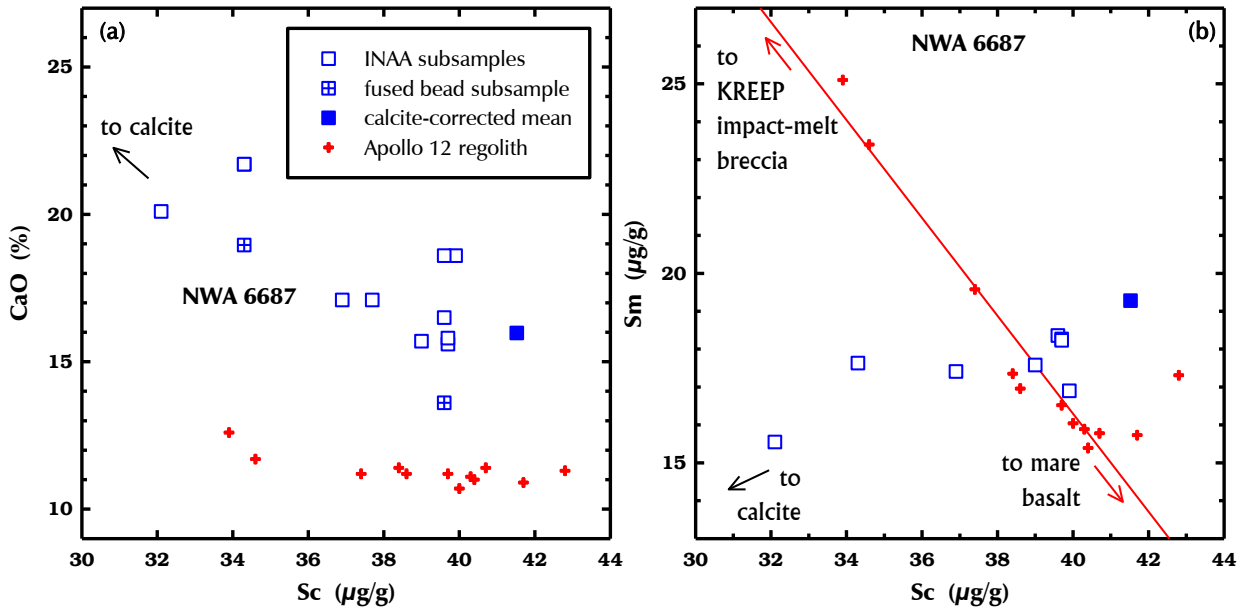

Fig. S38. NWA 6687 (42 g, glassy or regolith breccia) is unique among lunar meteorites in that for most elements the composition is similar to that of regolith from the Apollo 12 site, which itself is primarily a 2:1 mixture of mare basalt and KREEP impact-melt breccia (Korotev et al., 2011). Our sample of NWA 6687 is severely contaminated with Ca, presumably from calcite and perhaps some gypsum (0.44% SO_3; Table S4). (a) We prepared "fused beads" from two of the INAA samples to determine major-element concentrations. (INAA CaO data may be systematical high as a result of a gamma-ray spectral interference.) The "corrected mean" is based on the CaO concentrations calculated from mean Al_2O_3 concentration assuming $CaO/Al_2O_3 = 0.92$, which is the ratio for Apollo 12 soils of similar FeO concentration. Then, all mean major-element concentration values were multiplied by 1.064, the factor required to bring the mean sum of oxides (92.7%) back to the originally measured value (98.7%). In effect, ~6% of the original mass of the sample was CaO from calcite and gypsum. (There is no mention, however, of weathering products in Moggi-Cecchi et al., 2012.) (b) Most of the compositional scatter among the NWA 6687 subsamples results from variable calcite abundance, not variation in KREEP to mare basalt. The calcite-corrected composition of NWA 6687 is similar to typical Apollo 12 soil but differs mainly in having 1.3× Na_2O, 0.6× Cr, and 0.7× Co. The latter 2 differences imply that the mare component of NWA 6687 has a lower olivine abundance than the basalts of the Apollo 12 regolith. From mass balance, the implied mare component of NWA 8667 is not a good match to any mare basalt for which there are samples, although NEA 003 is an imperfect match. See also Fig. S39. Note that despite being classified as a "feldspathic breccia," the MetBull description of NWA 6687 includes augite as the only pyroxene and plagioclase of $An_{83.4}Or_{0.8}$ composition, i.e., a mineralogy more consistent with mare and KREEP rocks than rocks of the FHT.

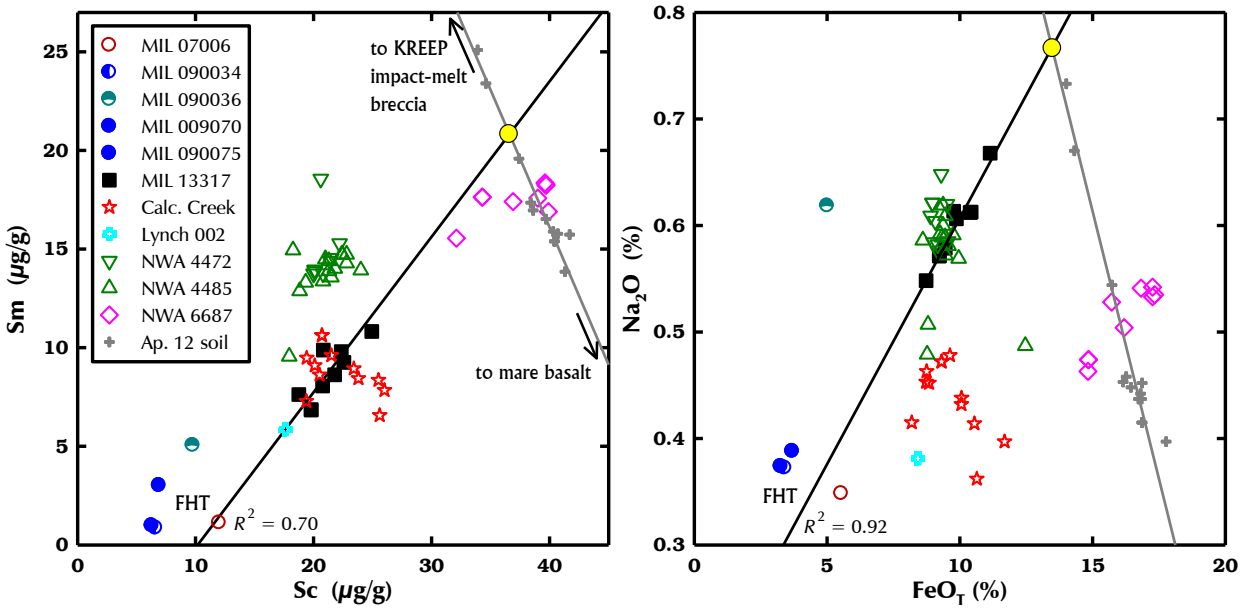

Fig. S39. Comparison of (1) subsample data for lunar meteorites that are moderately mafic and rich in incompatible elements, (2) stone-mean data for the 5 MIL (Miller Range, Antarctica) feldspathic lunar meteorite stones (FHT), and (3) Apollo 12 soils. The soils are primarily mixtures of varying proportions of mare basalt and KREEP impact-melt breccia (gray line), with a minor component of FHT material (Korotev et al., 2011). NWA 6687 (Fig. S38) is very similar in composition to Apollo 12 soils. Unlike for Calcalong Creek (Australia) and NWA 4472/4485 (Fig. S33), the MIL 13317 subsamples increase in Sm and Na concentrations with increasing Sc and Fe (diagonal black regression lines). The trends suggest that MIL 13317 is a mixture of (1) a mafic regolith, represented hypothetically by the yellow circle, which itself is a mare-KREEP mixture like Apollo 12 soils, and (2) feldspathic material with compositions like the feldspathic MIL stones. The mafic component of MIL 13317 cannot simply be mare basalt because extrapolation of the FeO_T-Na_2O trend (b) to 20% FeO_T, a typical value for mare basalt, leads to an absurdly high Na_2O concentration, 1.1%. Lynch 002 (Australia) is represented by one subsample, the “normal” subsample of Fig. S66.

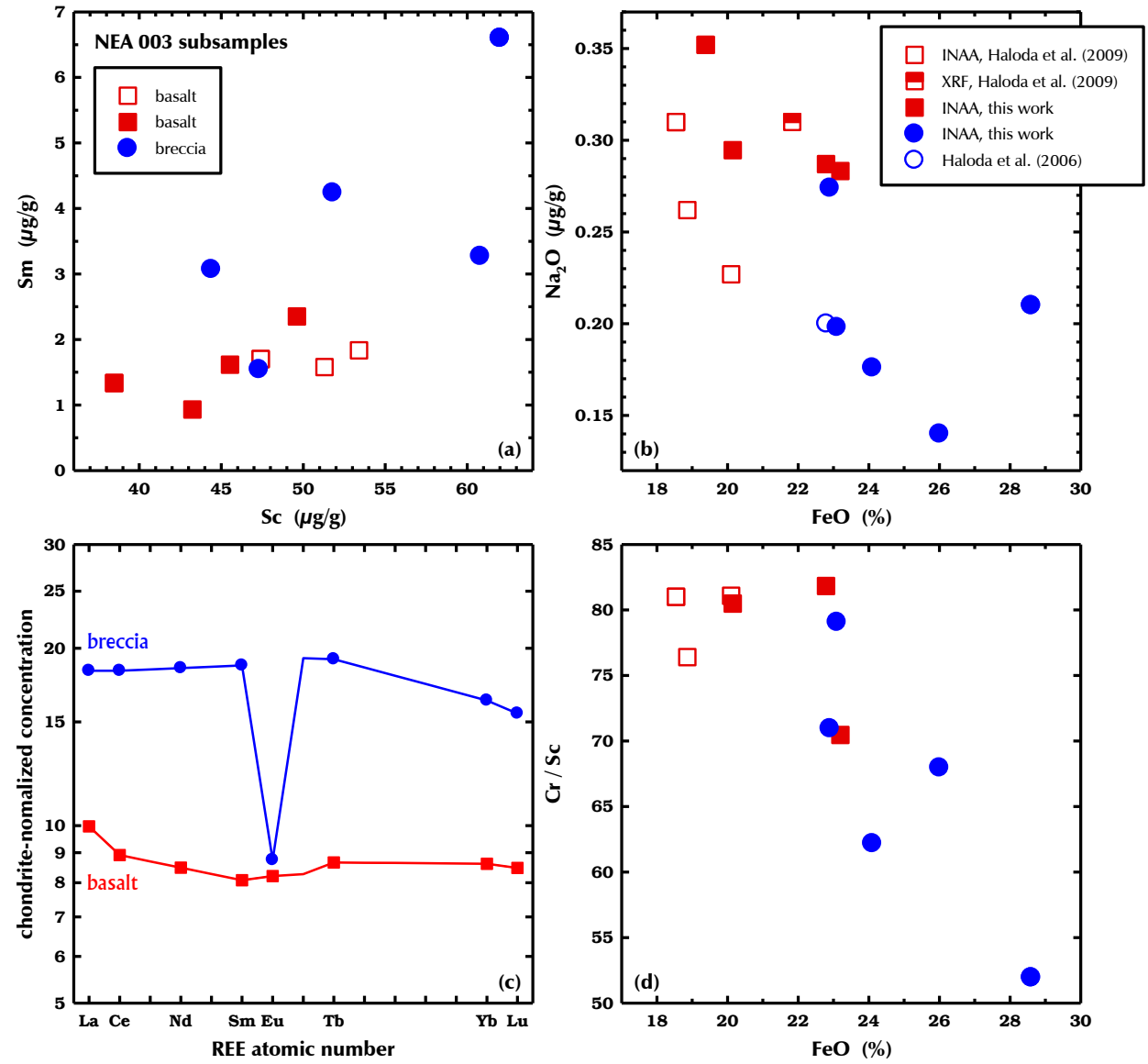

Fig. S40. Subsample and REE data for NEA 003 (123 g). (a, c, d) INAA data only. The open squares represent the three basalt subsamples of Haloda et al. (2009; from the "64-mg sample"). The filled squares represent a different 106-mg basalt sample that is richer in FeO and poorer in Sc, presumably as a result of greater olivine/pyroxene. (b) Our INAA data for the glassy breccia described in Haloda et al (2006) is richer in FeO (24.9±3.0%, 95% confidence limit) than the basalt (20.6±2.4%) and, in fact, any known type of mare basalt. The data of Haloda et al. (2006) is calculated from modal recombination. There is little evidence here that the Na-poor, REE-rich breccia lithology contains a significant fraction of the basalt lithology.

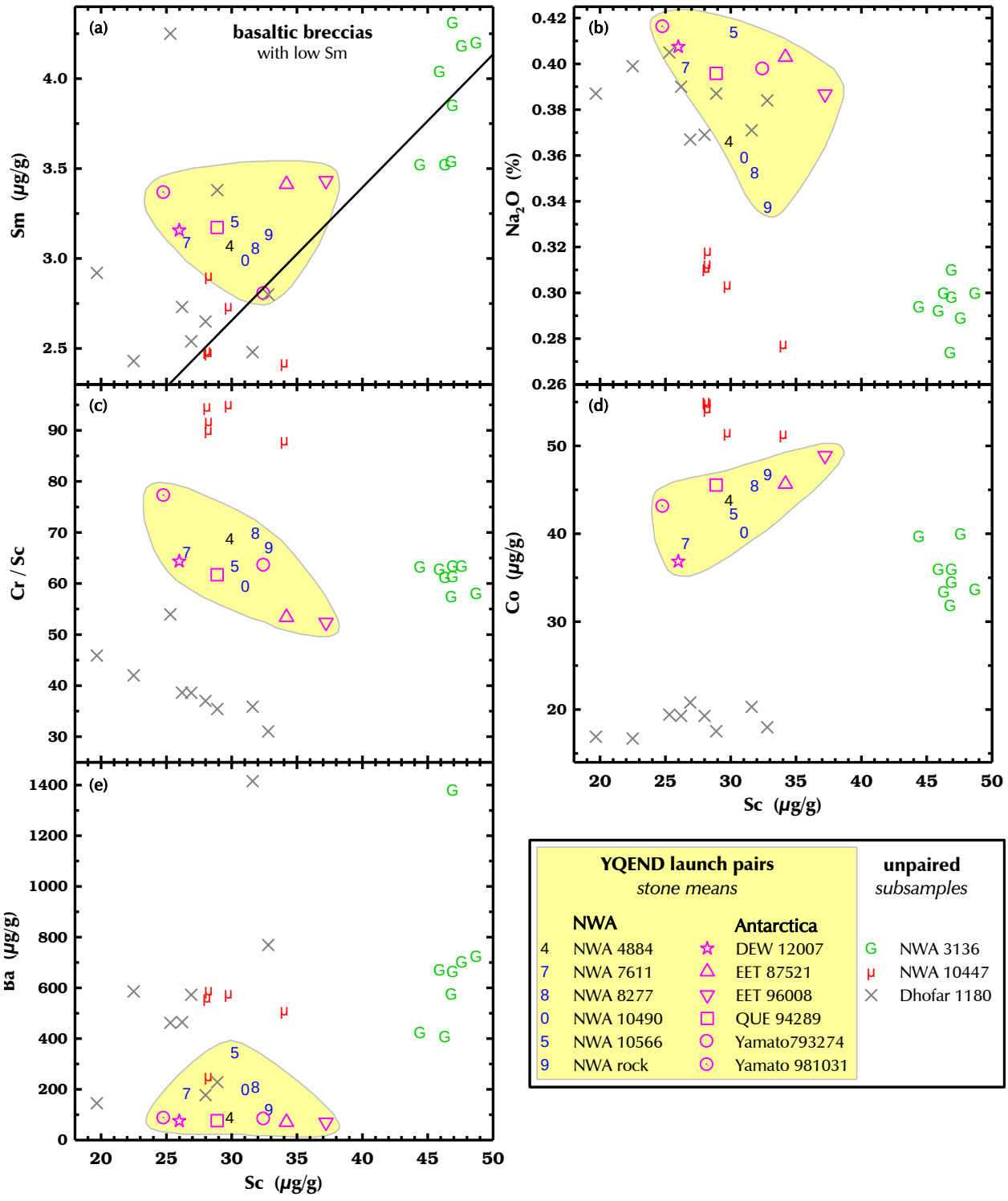

Fig. S41. Low-Sm meteorites plotting at or near the basaltic end of the FHT-maria join (diagonal line in a) of the mixing triangles of Figs. 2 and 6. The figure compares stone means for the YQEND launch pairs to subsample data for three other meteorites of similar composition but which are probably not paired with the YQEND launch pairs or to each other. The YQEND launch pairs may also include Meteorite Hills (Antarctica; Korotev et al., 2003b), which plots off scale at (54,3.6) in (a). NWA 10447 is most similar to the YQEND launch pairs but is likely richer in olivine (c); we assume, perhaps incorrectly, that it is a distinct meteorite.

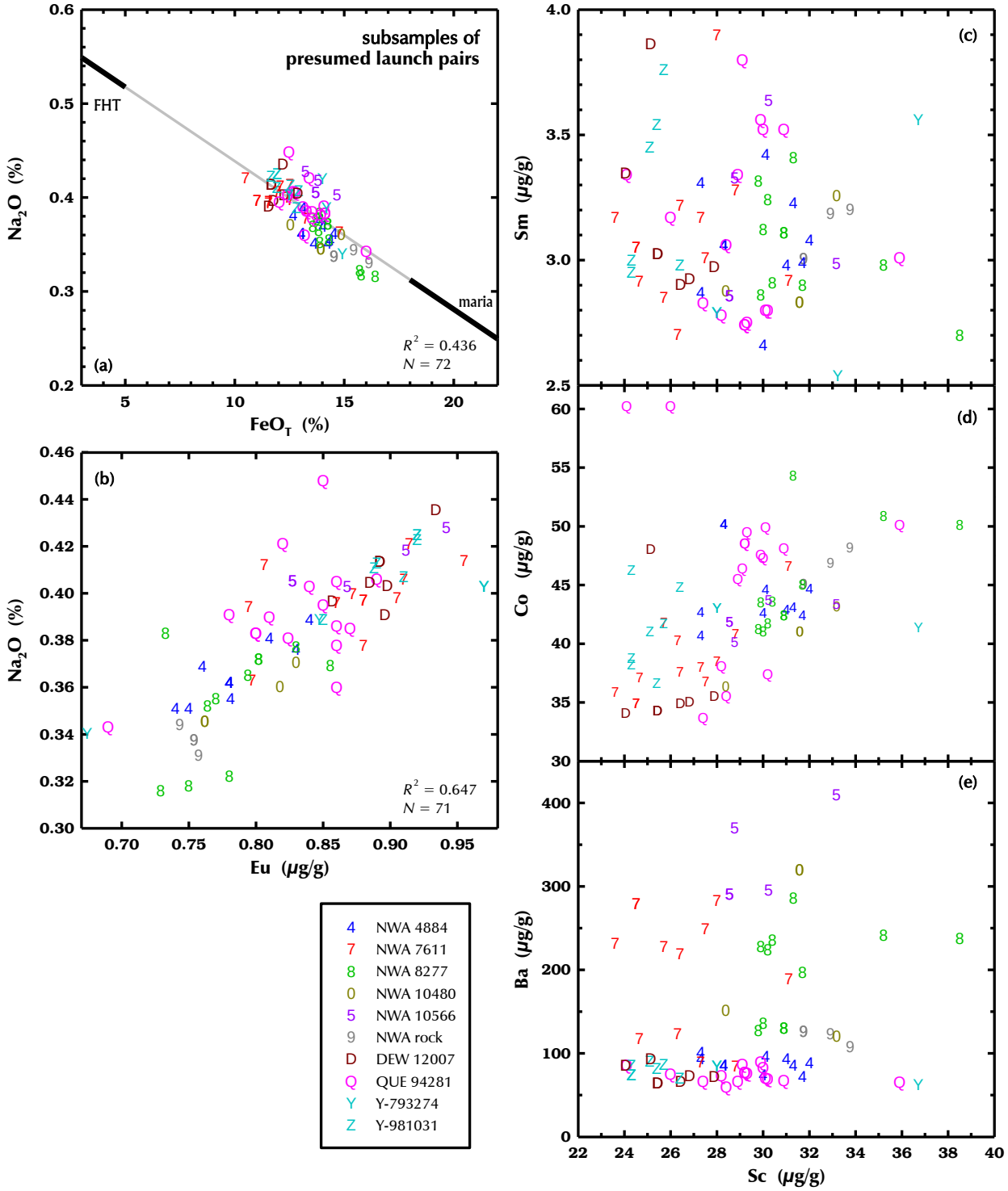

Fig. S42. Subsample data for five presumed launch pairs, at least two from Africa (NWA 4884, 42 g, and presumably-terrestrially-paired NWA 7611, NWA 8277, NWA 10480, and NWA 10566 (clan mass: 1.85 kg) and three from Antarctica (DEW 12007, QUE 94281, and terrestrially paired Yamato 793274 and Yamato 981031; to minimize clutter, data the 4th Antarctic launch pair, EET87521/96008 are not plotted but see Fig. S41 and Korotev et al., 2003b. (a) QUE 94281 and Y-981031 are breccias composed of subequal proportions of material from the feldspathic highlands (FHT) and very-low-Ti mare basalt (Jolliff et al., 1998, Arai and Warren, 1999, Korotev et al., 2003b). (a) The diagonal line is a simple linear regression to all the data. The implied highlands

component is richer in Na_2O (~0.55%) than are most feldspathic lunar meteorites (Fig. S5). (a–c) For most elements, subsamples of the ten stones overlap in composition, although samples of some are more mafic (basaltic) than others, on average. (d) Ignoring the 2 high-Co QUE 94281 points, which represent samples containing >600 µg/g Ni, Co weakly correlates with Sc (R^2=0.322), suggesting that most of the Co is carried by olivine in the basaltic component. (e) The meteorites from Antarctica contain <100 µg/g Ba, as does NWA 4884, whereas the others from Africa are contaminated with terrestrial Ba. Similarly, NWA 4884 has 0.08 ± 0.06 µg/g Br whereas the other five NWAs average 0.40 ± 0.09 µg/g. Both these observations suggest that NWA 4884 is a different fall (different find location) from the NWA 7611 pair group but that they are launch paired. Subsample data from this work, Jolliff et al. (1998), and Korotev et al. (2003b). Y-793274 data from Fukuoka (1990), Lindstrom et al. (1991), Koeberl et al. (1991), and Warren and Kallemeyn (1991b).

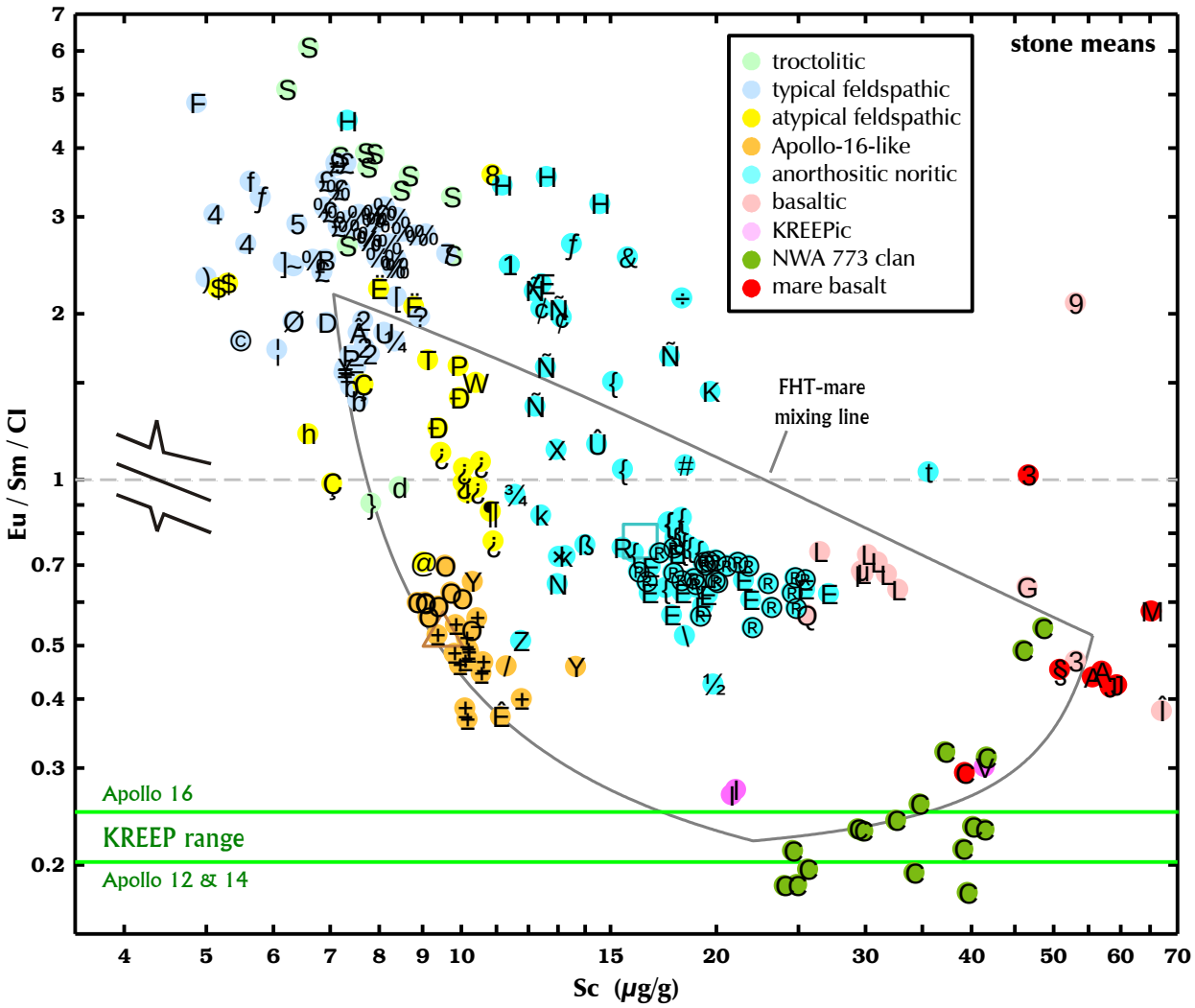

Fig. S43. Eu/Sm ratios. The distorted "triangle" is the mixing triangle of Figs. 2 and 6. Most of the "anorthositic noritic" breccias with 15–27 μg/g are not consistent with simple mixtures of material from the FHT and mare basalt. The large triangle (obscured in "Apollo-16-like" field) represents Apollo 16 regolith and the large square represents Luna 20 regolith. See Table S1 for symbol key.

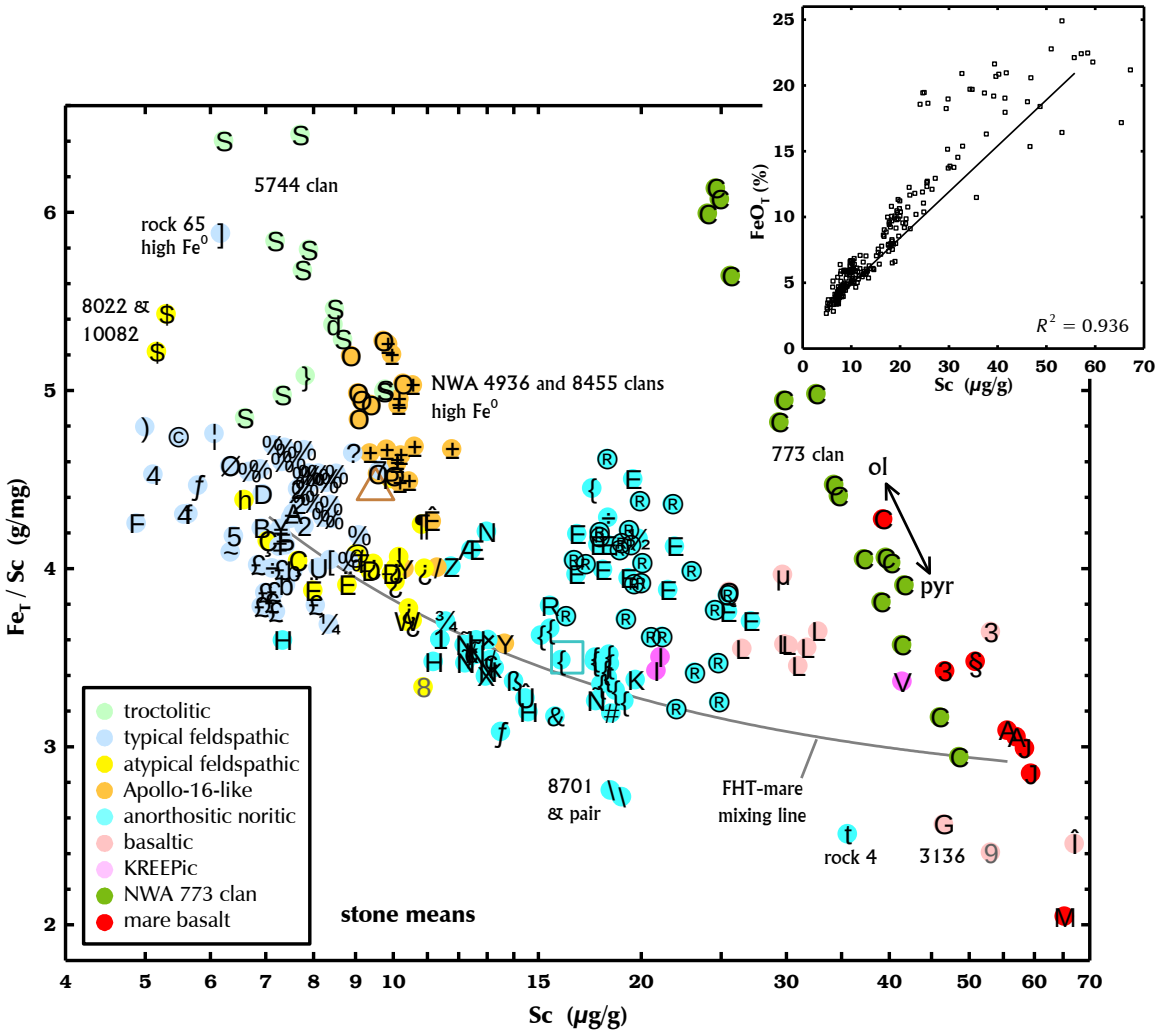

Fig. S44. Like Fig. S4 but for Fe/Sc. As in Fig. 14, the NWA 2995 clan (symbol E), NWA 05153 (Q), the NWA 7834 clan (®), NWA 8182 (½), and NWA 11182 (÷) plot above the FHT-mare mixing line because the meteorites are richer in olivine than most such mixtures. The anomalously high NWA 8673 clan point ({, NWA 11216) is rich in siderophile elements and FeNi metal (Fig. 12). The large triangle represents Apollo 16 regolith and the large square represents Luna 20 regolith. See Table S1 for symbol key. The inset shows the same data on linear axes.

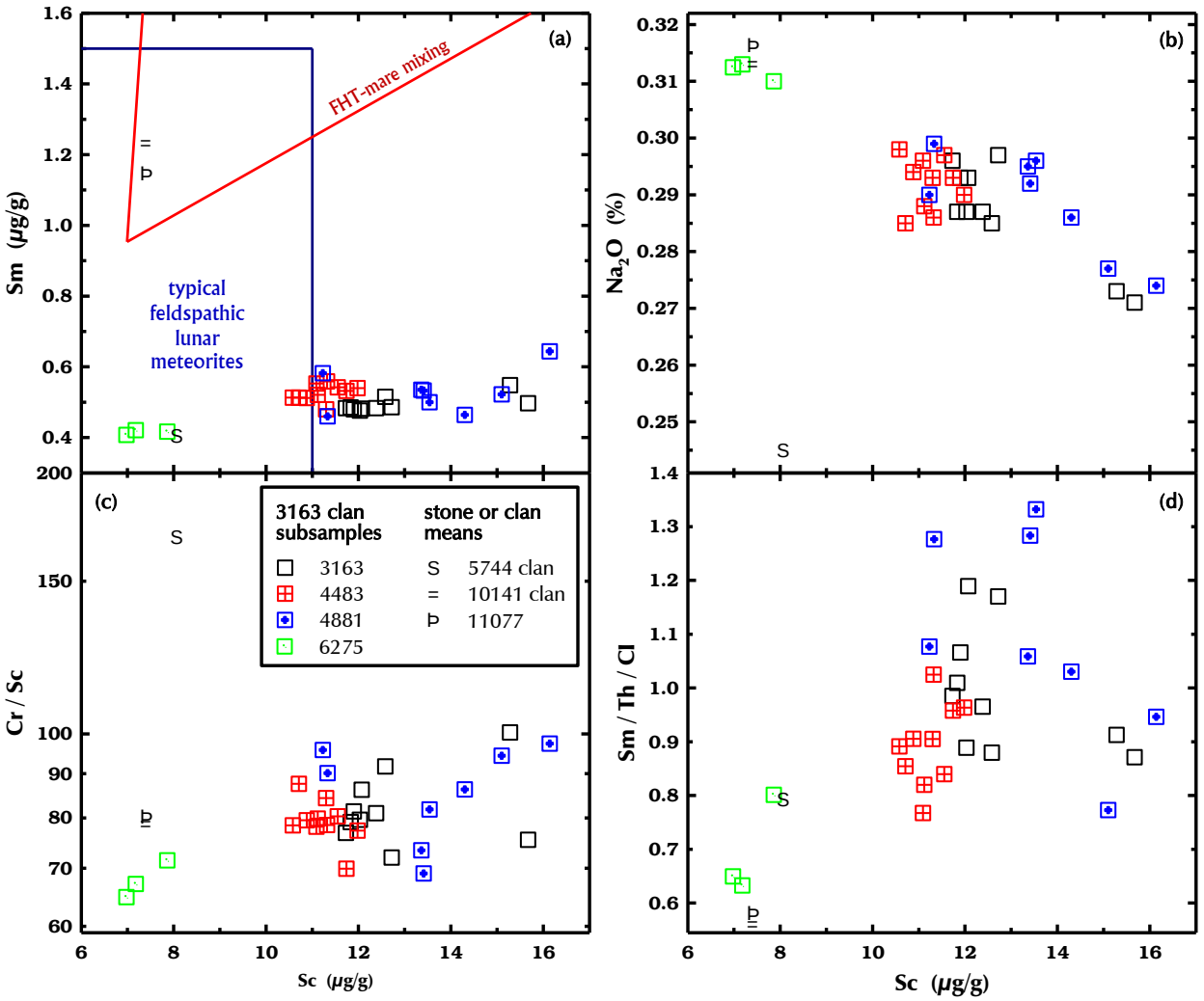

Fig. S45. Subsample data for the NWA 3163 clan (ferroan granulitic breccias; 2.45 kg) and stone-mean data for meteorites of similar composition but for which there is no evidence here for pairing. (a) The rectangle shows a corner of the range of typical feldspathic lunar meteorites (Fig. 6) and the diagonal lines are the FHT apex of the mixing triangle of Fig. 6. The four breccias of the NWA 3163 clan have low to very low concentrations of incompatible elements and Na (a,b), Cr/Sc that increases with increasing Sc (c), and chondritic Sm/Th (d). No basalt is reported in the MetBull descriptions, so the large range in Sc concentrations simply reflects nonmare plagioclase/pyroxene variation among the stones and subsamples.

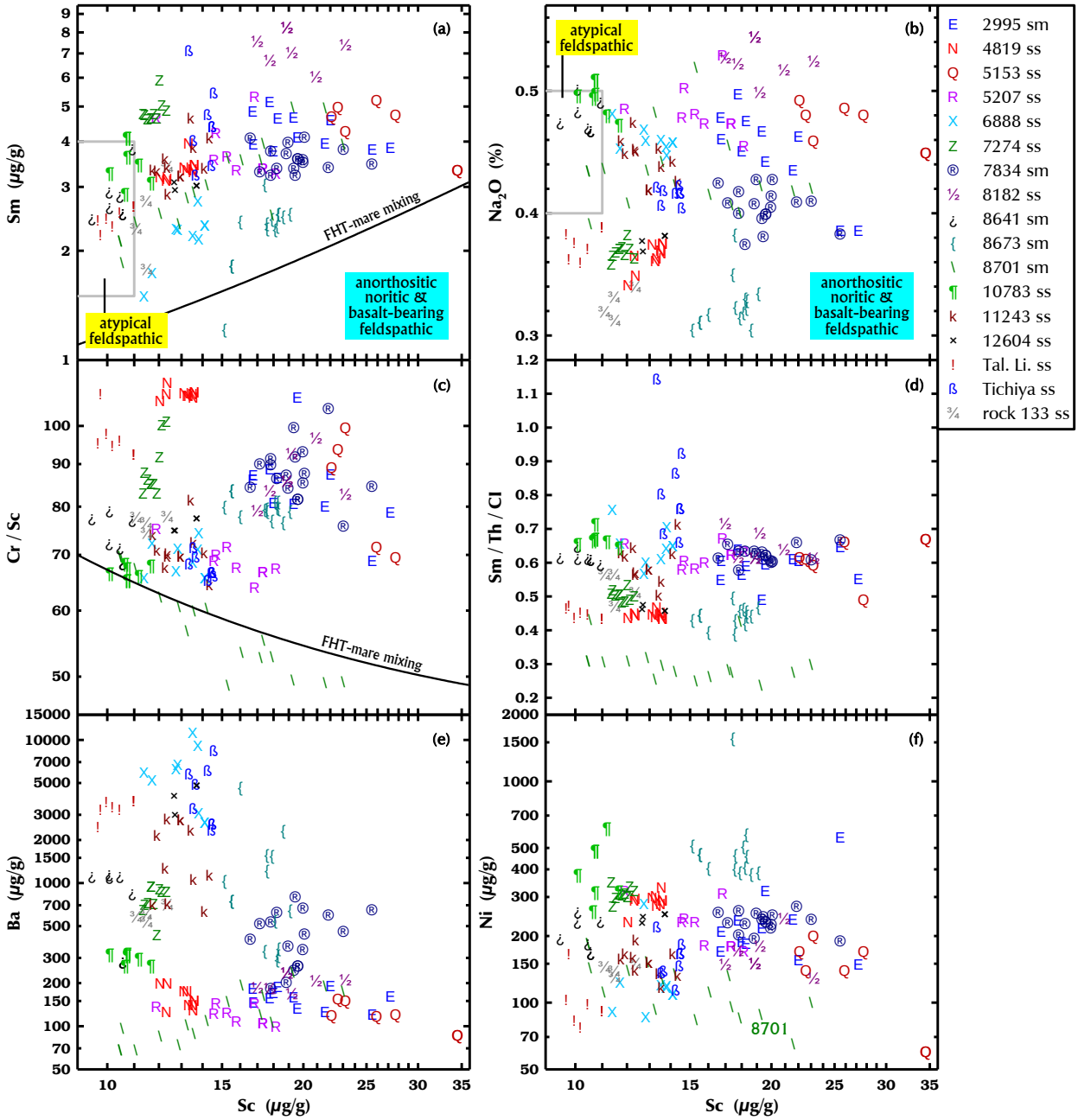

Fig. S46. Data for 13 "anorthositic-noritic and basalt-bearing feldspathic" meteorites at the high end of the Sm concentration range (Fig. 6) plus three "atypical feldspathic" meteorites (Fig. S25) that marginally overlap at low Sc concentrations (NWA 8641 clan, NWA 10783, and Talhat Lihoudi). For most of the meteorites, subsample data ("ss" in legend) are plotted. For five clans for which there are many stones, the stone means ("sm") are plotted. NWA 5153 and NWA 5207 largely lie in the fields of the NWA 2995 clan and may, in fact, be anomalous members of the clan but for reasons detailed in Korotev et al. (2009) we suspect that they are unique meteorites. For reasons presented in the table below, we suspect that the 16 meteorites or clans in the legend of this figure are unpaired. NWA 10783 (poikilitic melt breccia) largely overlaps with the NWA 8641 clan (regolith breccia) but the textures are very different. See also Figs. S48, S49, and S50. The diagonal lines in (a) and (c) are the mixing lines of Figs. 6 and S4.

NWA	plot	In Sc-Sm space, meteorites or clans (cl) in column NWA overlap or *nearly overlap* with meteorites of this column (but differ or *mostly differ* in these elements or ratios)	Lithic Clasts	
			MB	NM
2995cl	E	5153(Na) 5207(Cr/Sc Ba) 7834(Na *Sm* Ba; Fig. S48) 8701(Cr/Sc Sm/Th Ni △) *8182*(Na)	Y	Y
4819	N	*8701*(Na Cr/Sc Sm/Th △) 11243(Na Cr/Sc △) Tich(Na Cr/Sc Sm/Th Ba) 12604(Cr/Sc Ba) high *Mg´* (65.4)	N	Y
5153	Q	2995(*Na Ni*) *7834*(Na Ba) *8701*(Cr/Sc Th/Sm Ni △)	Y	Y
5207	R	2995(Cr/Sc Ba) 7274(Na Cr/Sc *Sm/Th* Ba) 7834(Na Cr/Sc Ba) *8673*(Na Cr/Sc Sm/Th Ba Ni) 8701(Cr/Sc Sm/Th Ni △) Tich(Na Sm/Th Ba △) *11243*(Na *Sm/Th* Ba Ni)	Y	Y
6888	X	8701(*Cr/Sc* Sm/Th Ba △) 12604(Na *Cr/Sc Sm/Th* Ba)	Y	Y
7274	Z	*5207*(Na Cr/Sc *Sm/Th* Ba) high *Mg´* (70.4)	0	0
7834cl	®	2995(Na *Sm* Ba; Fig. S48) *5153*(Na Ba) 5207(Na Cr/Sc Ba) 8701(Cr/Sc Sm/Th *Ba* Ni △) *8673*(Sm/Th Ni △)	Y	Y
8182	½	*2995*(Na)	0	0
8641cl	¿	*8701*(Na Cr Sm/Th Ba △) *10783*(Cr/Sc Ba *Ni*) TaLi(Na Cr Sm/Th Ba) *12604*(Na *Ba Ni*)	y	0
8673cl	{	*5207*(Na Cr/Sc Sm/Th Ba Ni) *7834*(Sm/Th Ni △) *8701*(Na Cr/Sc Sm/Th Ba Ni △)	y	0
8701	\	2995(Cr/ScSm/Th Ni △) *4819*(Na Cr/Sc Sm/Th △)*5153*(Cr/Sc Sm/Th Ni △) 5207(Cr/Sc Sm/Th Ni △) 6888(*Cr/Sc* Sm/Th Ba △) 7834(Cr/Sc Sm/Th *Ba* Ni △) *8641*(Na Cr Sm/Th Ba △) *8673*(Na Cr/Sc Sm/Th Ba Ni △) (Cr/Sc Ba △) *Tich*(Sm/Th Ba △) *12604*(Na Cr/Sc Sm/Th Ba △) high As (Fig. S62)	0	0
10783	¶	*8641*(Cr/Sc Ba *Ni*) *11243*(*Na* Ba Ni) *TaLi*(Na Cr/Sc Sm/Th Ba Ni) *12604*(Na Cr/Sc Ba Ni)	0	0
11243	k	4819(Na Cr/Sc △) *5207*(Na *Sm/Th* Ba Ni) Tich(Na *Ba* △)	0	y
12604	×	4819(Cr/Sc Ba) 6888(Na *Cr/Sc Sm/Th* Ba) *8641*(Na *Ba Ni* △) *8701*(Na Cr/Sc Sm/Th Ba △) *10783*(Na Cr/Sc Ba Ni) *11243*(Na Ba) *TaLi*(Na Cr/Sc *Sm/Th* Ba Ni)		
TalLi	!	8641(Na Cr Sm/Th Ba) 8701(Cr/Sc Ba △) *10783*(Na Cr/Sc Sm/Th Ba Ni) *12604*(Na Cr/Sc *Sm/Th* Ba Ni)	0	0
Tich	ß	4819(Na Cr/Sc Sm/Th Ba) 5207(Na Sm/Th Ba △) *8701*(Sm/Th Ba △) 11243(Na Sm/Th *Ba* △)	y	0

△ = Trend or distribution of data differs

TalLi = Talhat Lihoudi; Tich = Tichiya

Lithic Clasts: MB = mare basalt, NM = nonmare. Y = present, y = "rare" or "sparse," N = not present, 0 = no lithic clasts described. Based mainly on MetBull descriptions, also Boyle et al. (2018), Demidova el al. (2012), Korotev et al. (2009), Mercer et al. (2013), Sipiera et al. (2014), Stephant et al. (2019), and Zeng et al. (2018).

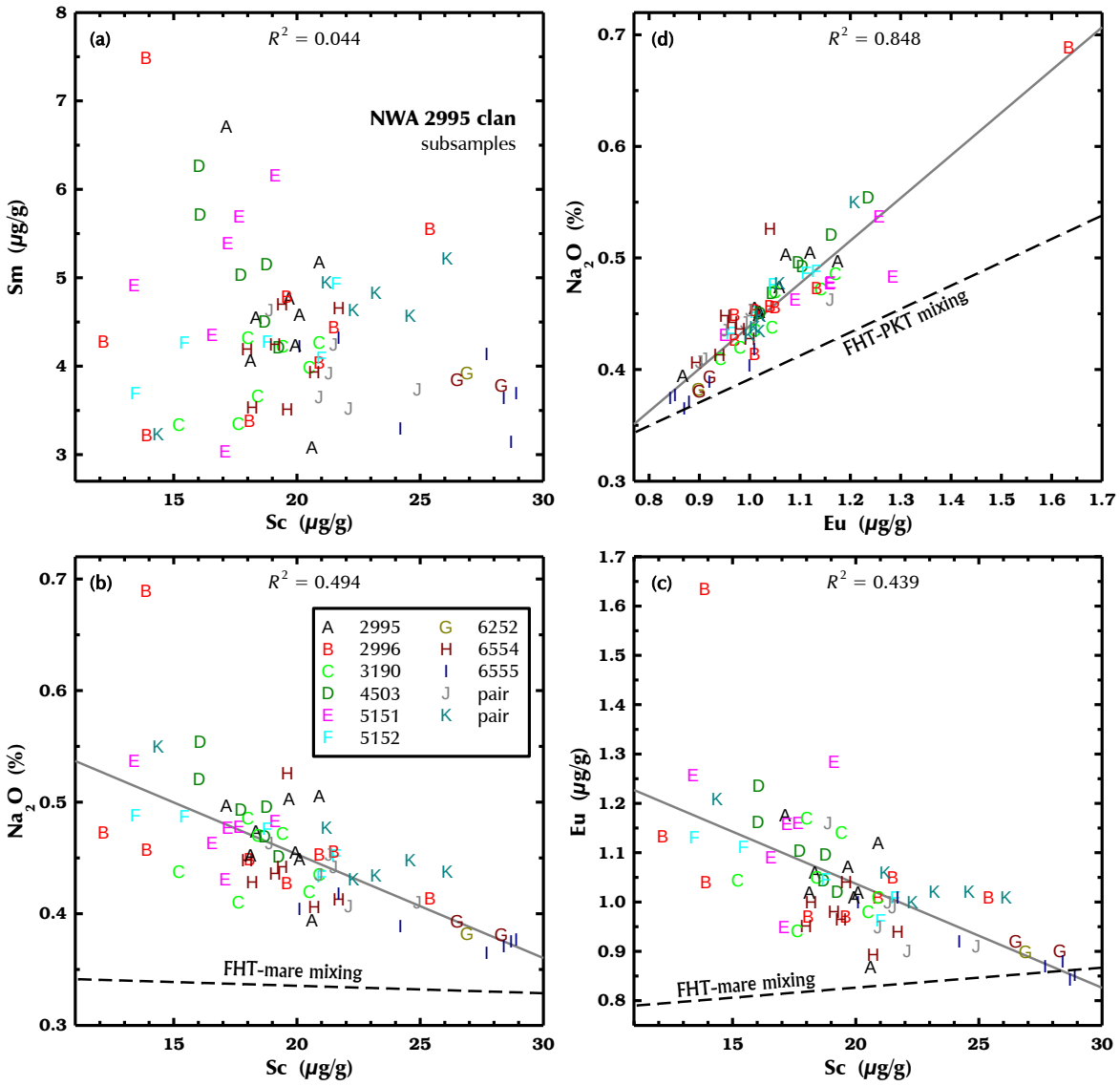

Fig. S47. Subsample (*N*=69) data for the 11 stones of the NWA 2995 clan (2.2 kg). The dashed diagonal lines are joins of the mixing triangles of Figs. 2 and 6. The solid diagonal lines are simple linear regressions. (a) Subsamples of some individual stones vary over most of the compositional range, e.g., NWA 2996 (symbol B). NWA 6252 (G) and NWA 6555 (I) are the richest in mare basalt (high Sc). (b,c) The implied feldspathic (low-Sc) component of the breccia is 1.7× richer in Na (0.57% Na_2O at 7 μg/g Sc) and 1.7× richer in Eu (1.3 μg/g) than most feldspathic lunar meteorites (Fig. S5). The high Na concentrations in the NWA 2995 clan is one of the features that distinguish the clan from the otherwise similar NWA 7834 clan (Fig. S48). Plotting off scale: an 8-mg clast of ferroan anorthosite (0.36 μg/g Sc, 0.20 % FeO, 0.56 %Na_2O, and 0.11 μg/g Sm) from NWA 3190 and a 16-mg feldspathic clast (3.6 μg/g Sc, 3.6 % FeO, 0.40% Na_2O, and 0.82 μg/g Sm) from NWA 5152 (Table S2). (d) In the high-Na subsamples, Na/Eu differs from that of KREEP.

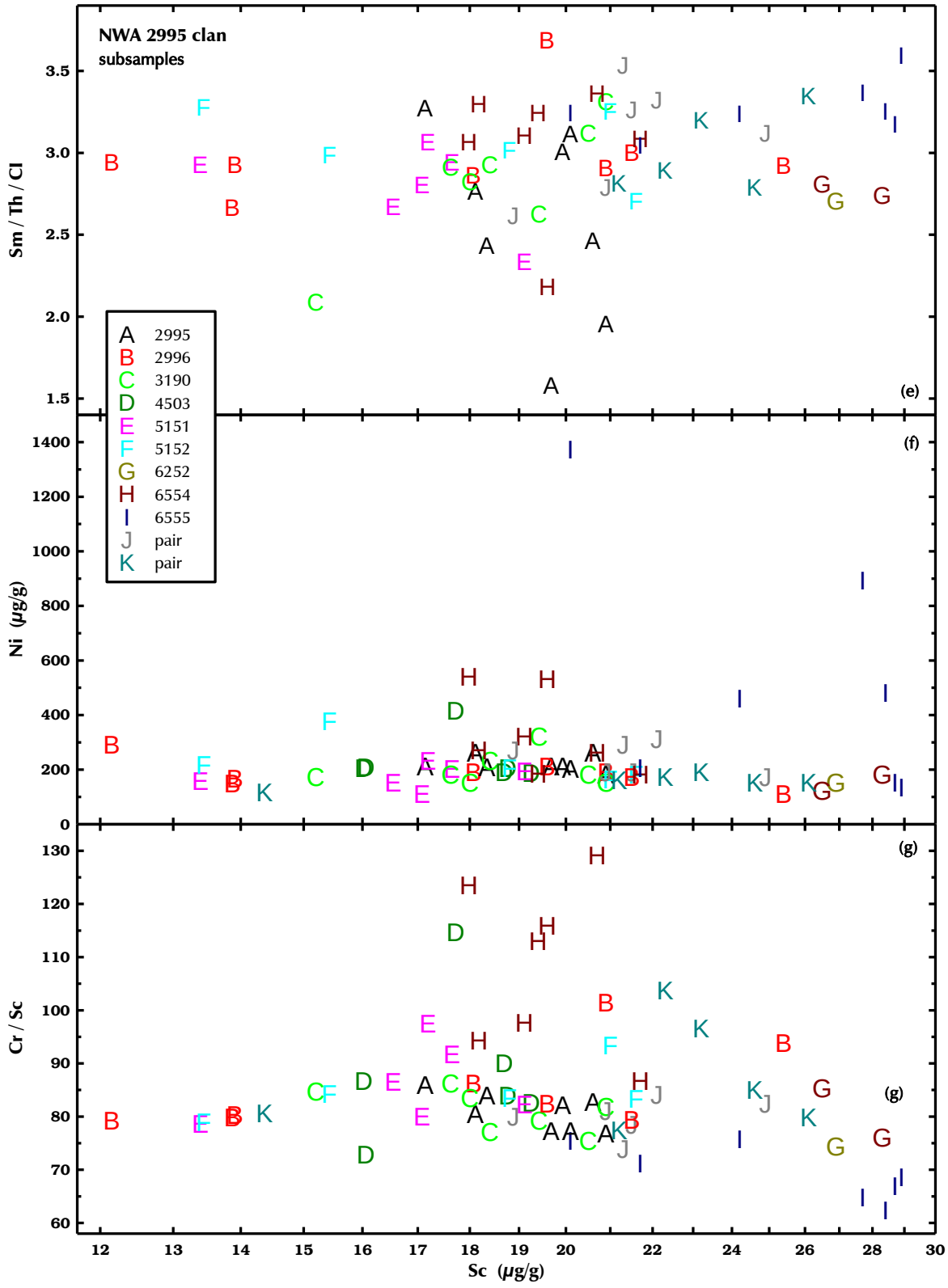

Fig. S47, continued. (e) On average, NWA 5151 (symbol E) and NWA 5152 (F) are the least mafic while NWA 6252 (G) and NWA 6555 (I) are the most mafic of the NWA 2995 clan and there is no overlap in Sc concentrations. Sm/Th scatters considerably among the clan members. (f) Some subsamples of NWA 6555 contain nuggets of FeNi metal (I) (Table S6). (g) Four of the seven subsamples of NWA 6554 (H) have anomalously high Cr/Sc, perhaps from chromite.

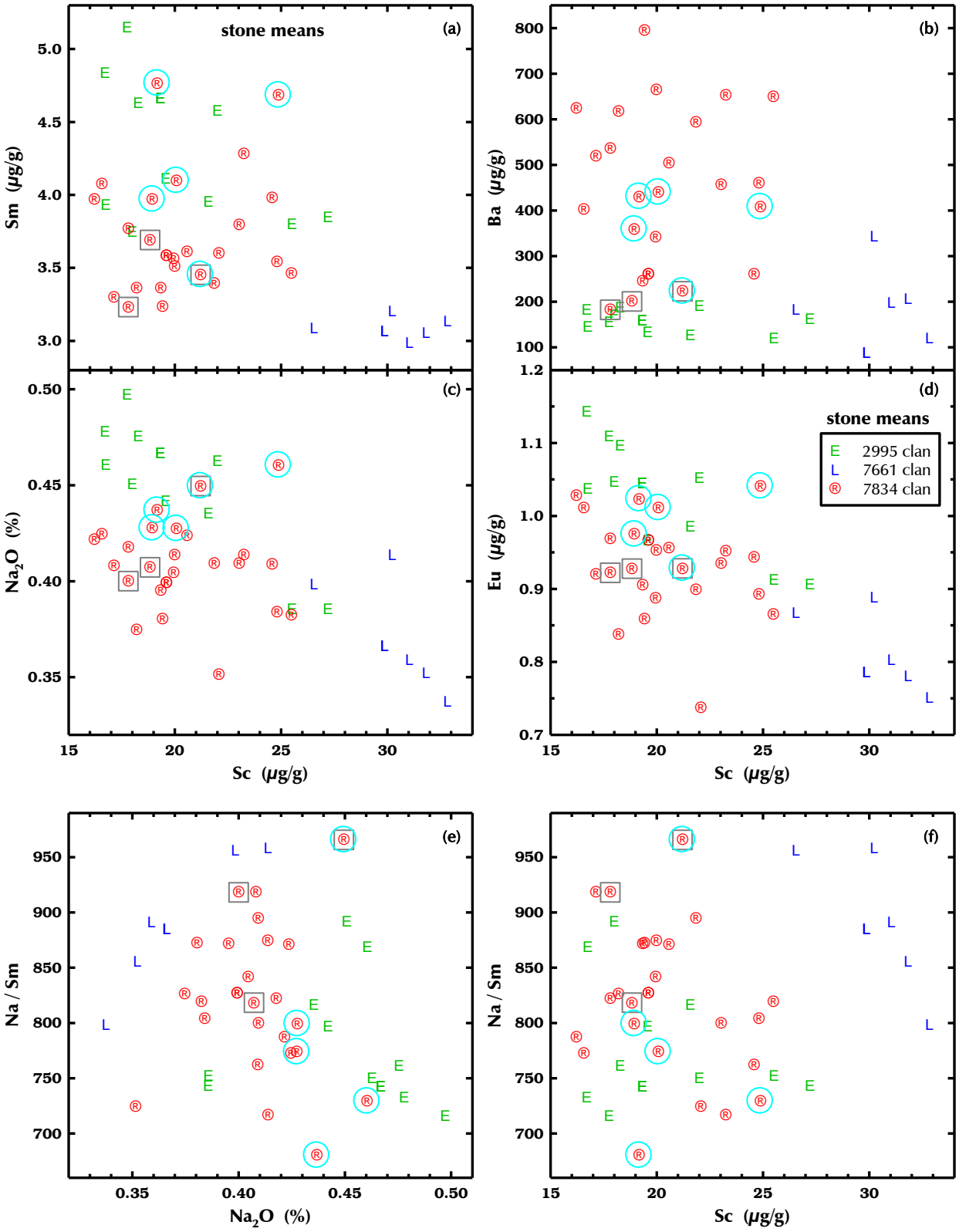
stone means
(a)
Sm (μg/g)
(b)
Ba (μg/g)
(c)
Na2O (%)
Sc (μg/g)
(d)
Eu (μg/g)
stone means
E 2995 clan
L 7661 clan
® 7834 clan
(e)
Na / Sm
Na2O (%)
(f)
Na / Sm
Sc (μg/g)

Fig. S48. Comparison of stone means for the NWA 2995 (Fig. S47), NWA 7611 (includes NWA 4884; Fig. S42), and the NWA 7834 clans (Fig. S49). Panels (a) and (f) distinguish the NWA 7611 clan from the other two. The NWA 2995 and NWA 7834 clans overlap for all elements measured. (b) On average, the NWA 7834 clan is significantly (2.8×) richer in Ba than the NWA 2995 clan but 3 low-Ba 7834-clan stones (large squares) plot with the 2995-clan stones. In other plots, however, there is no overlap for these 3 stones (d,e). (c,d) On average, the 2995 clan is 1.1× richer in Na and Eu but, again, ~5 NWA 7834 clan stones (circled points) are similarly rich in Na or Eu. For 4 of the 5 stones, there is no overlap in Ba (b), however. This is one case where we make the distinction between the 2 clans largely on the basis of timing and geography. The 9 NWA 2995-clan stones were all purchased from 2005 through 2010 (3 reported to have been purchased in Rissani, Morocco) whereas for the NWA 7834 clan, 24 of the 25 stones were purchased from 2013 through 2016 (7 reported to have come from near the Algeria-Mauritania-Mali triple junction, ~690 km south of Rissani).

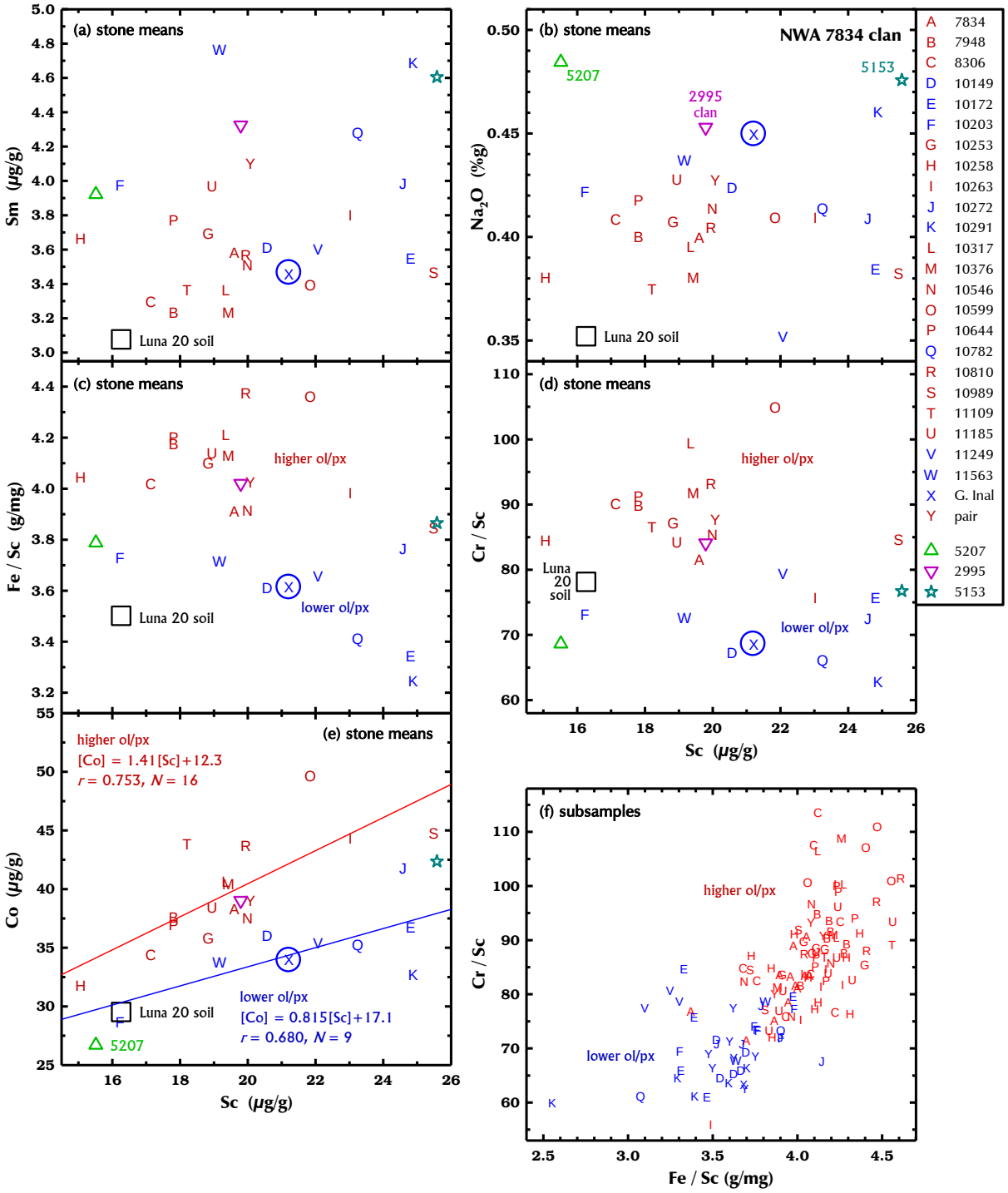

Fig. S49. Among the 25 stones of the NWA 7834 clan (21 kg), 16 have greater Fe/Sc, Cr/Sc, and Co/Sc than the other 9 (c–f). Each of these ratios reflect greater olivine/pyroxene in the high-Fe/Sc stones. There is no correlation between Ir and Co (not shown but R^2=0.098), which indicates that a negligible proportion of the Co is extralunar; nearly all is in lunar olivine. All these stones were purchased from 2013 through 2016, except for Galb Inal (circled X), which was reportedly found in Mauritania in 2011. Among lunar meteorites, the NWA 7834 clan and NWA 5207 are similar in composition to the Luna 20 soil, although the NWA 8673 clan is more similar (Fig. S50). Important differences, however, are that (1) *Mg´* in the NWA 7834 clan is ~62 (Table S4, data for NWA 7834 and NWA 7948 only) whereas *Mg´* for Luna 20 soil is 70 and (2) Na_2O is considerably lower (0.87×) in the Luna 20 soil (b). NWA 5153, NWA 5207 and the NWA 2995 clan (Fig. S47, mass-weighted means of all subsamples) are the only other meteorites that plot in the ranges of panels (a–e).

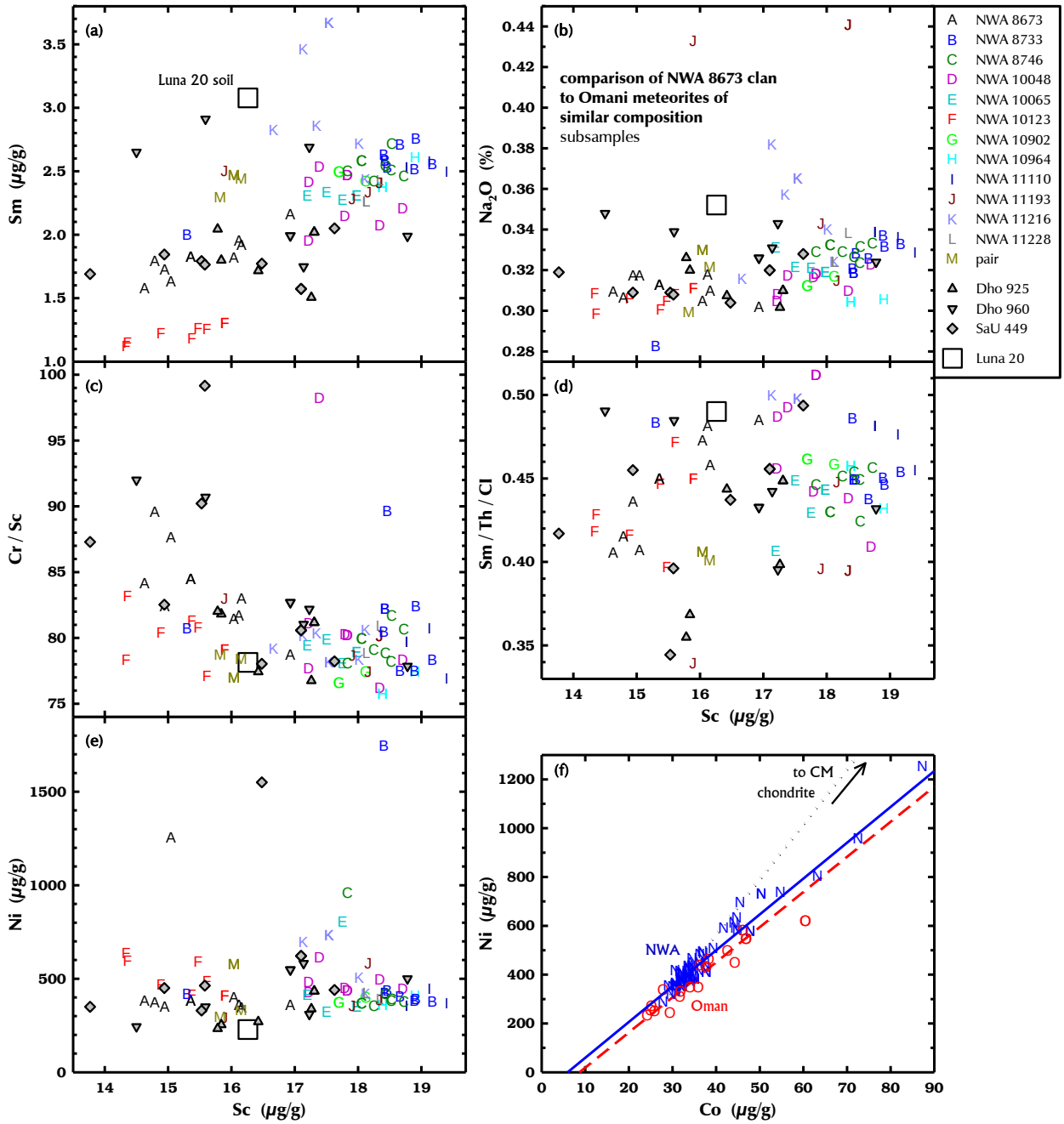

Fig. S50. The NWA 8673 clan (13 stones, symbols A through M; 12.3 kg) largely overlap in composition with each other except that NWA 8673 [symbol A], NWA 10123 [F], and NWA 11216 [K] plot outside the range of the others in (a) and (b). Together, the NWA 8673 clan is compositionally indistinguishable from launch pairs Dhofar 925/960 and Sayh al Uhaymir (SaU) 449 from Oman (Korotev, 2015, 2017), suggesting that the NWA 8673 clan is another meteorite of the launch-pair group. Among lunar meteorites those of this figure are most similar in composition to the soil from the Luna 20 site near Mare Crisium (Fig. S49). (f) All of the meteorites are rich in FeNi metal and siderophile elements. The meteoritic component of NWA 8673 clan and similar Omani stones have similar Ni/Co ratios, 14.6±0.3 and 13.7±0.9, both of which are subchondritic (22.0 in CM chondrites, Fig. S54) but are consistent with iron meteorites (Fig. S55).

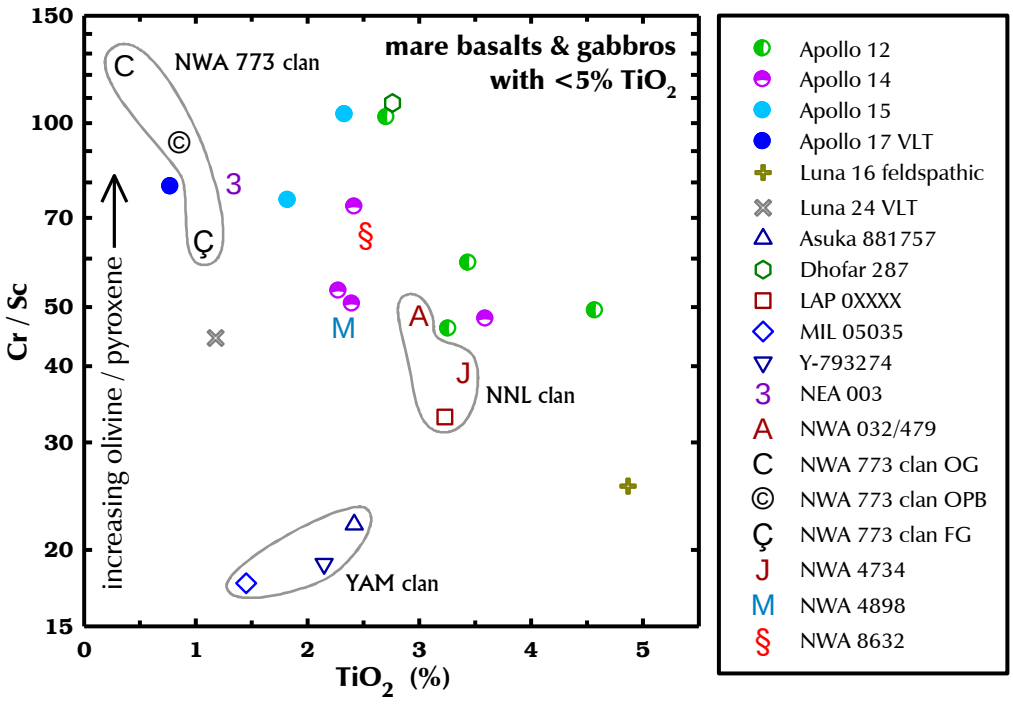

Fig. S51. Comparison of compositions of crystalline mare basalts and gabbros among the lunar meteorites with low-Ti and VLT (very-low Ti) to basalts in the Apollo and Luna collections. The high-Ti basalts of Apollos 11 and 17 plot off scale at 8–13% TiO_2; no lunar meteorites are high-Ti basalts but the basalt component of breccias NWA 6687 and NWA 11886 are likely high-Ti basalts. Cr/Sc is a proxy for olivine/pyroxene (Fig. 4). Each point represents the mean for a chemical class of basalts (Neal and Taylor, 1992: Apollo 12 olivine, pigeonite, ilmenite, and feldspathic, Apollo 14 aluminous (three subgroups of Neal and Kramer (2006) and high-K), Apollo 15 quartz and olivine, Apollo 17 VLT, Luna 16 aluminous, and Luna 24 VLT). The "NNL clan" and "YAM clan" each comprise launch pairs (e.g., Korotev and Zeigler, 2014). For the NWA 773 clan (Fig. S53), the three points represent the olivine gabbro (OG), olivine-phyric basalt (OPB), and the ferrogabbro (FG; Kuehner et al., 2012a; North-Valencia et al., 2014; Valencia et al., 2019). TiO_2 data are not available for other NWA 773 clan igneous lithologies. Data from this work, Cohen et al., 2019; Haloda et al., 2009; Jolliff et al., 1993; Joy et al., 2008; Koeberl et al., 1993; Korotev and Zeigler (2015), Valencia et al. (2019); Warren and Kallemeyn (1993), and Yanai and Kojima (1991).

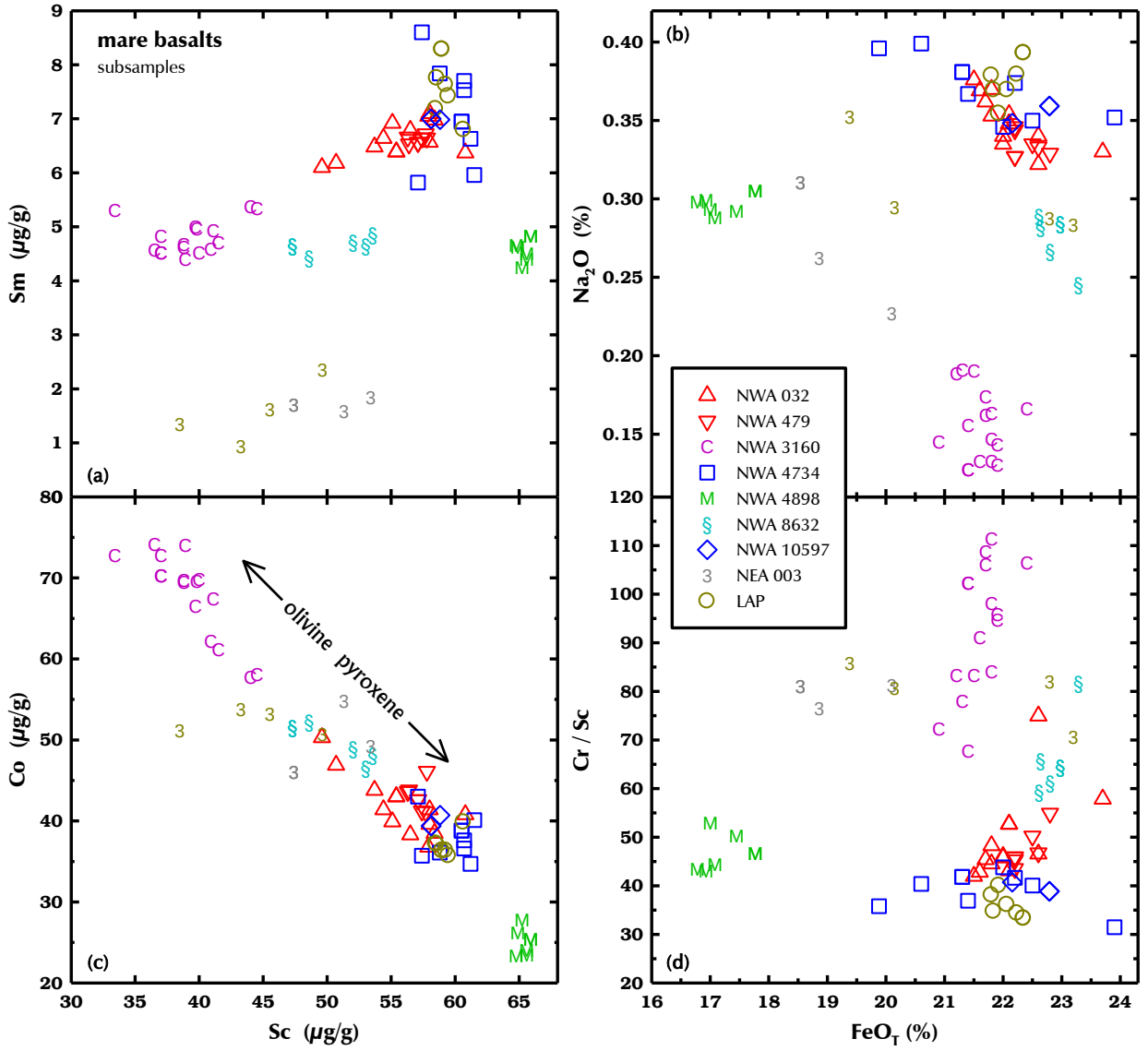

Fig. S52. Subsample data for mare basalts among the lunar meteorites from northern Africa. For comparison, the 6 LAP points each represent a stone mean for the paired stones (LaPaz Icefield (Antarctica) stones 02205, 02224, 02226, 02436, 03632, and 04841; Zeigler et al., 2005; Korotev and Zeigler, 2014). NWA 4734 and NWA 10597 are indistinguishable from each other, thus we assume that they are paired. Together, NWA 4734/10597 is indistinguishable from the 6 LAP basalts, thus we assume that they are launch paired. NWA 479 is indistinguishable in composition from NWA 032 and NWA 10597 is indistinguishable in composition from NWA 4734, thus we assume terrestrial pairing. None of the other meteorites in the figure appear to be paired with others, although NWA 8632 is most similar to NWA 032/479 and may be an olivine-rich variant (see text). Aluminous NWA 4898 (11.7% Al_2O_3, Table S2) is distinct in having high Sc (a,c) and low FeO_T (c,d). The "NWA 3160" points represent 8 subsamples from NWA 3160, 3 from NWA 3333, 2 from Anoual, and 1 from NWA 2727 that are dominated by olivine-phyric basalt; these are all stones of the NWA 773 clan (Valencia et al., 2019).

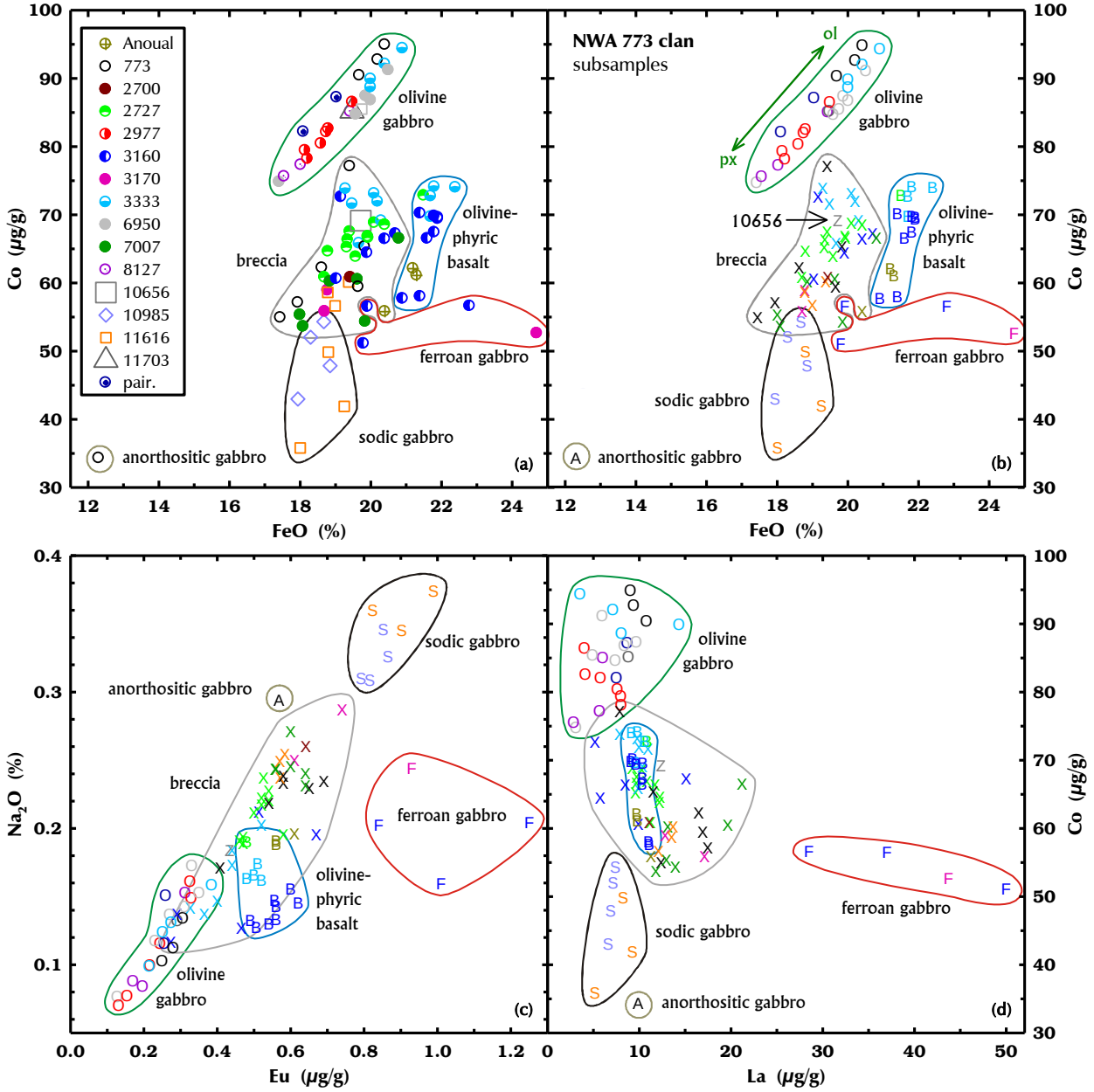

Fig. S53. Data for 98 subsamples of 16 stones of the NWA 773 clan (11.9 kg; updated from Fig. 2.16 of Valencia et al., 2019). In (a), the large triangle in the olivine gabbro field represents a 29-mg INAA subsample of pulverized saw cutting "dust" from two saw passes through NWA 11703. Consequently, it plots in the center of the distribution of small-chip subsamples. The large square represents a 20-mg subsample from 262.5 mg of pulverized NWA 10656, an "olivine diabase" (A. Irving and S. Kuehner in MetBull) or "olivine gabbro" (Valencia et al., 2019) that plots with the fragmental breccias for all elements measured. NWA 10985 is an olivine-bearing "gabbro" (C. Agee in MetBull) that is distinctly more sodic than the other NWA-773-clan igneous lithologies (c). The breccia lithology of NWA 11616 plots with the other NWA-773-clan breccias whereas the "olivine gabbro" lithology of NWA 11616 (Irving et al., MetBull) is distinct from the NWA 773 olivine gabbro but identical to the sodic gabbro of NWA 10985.

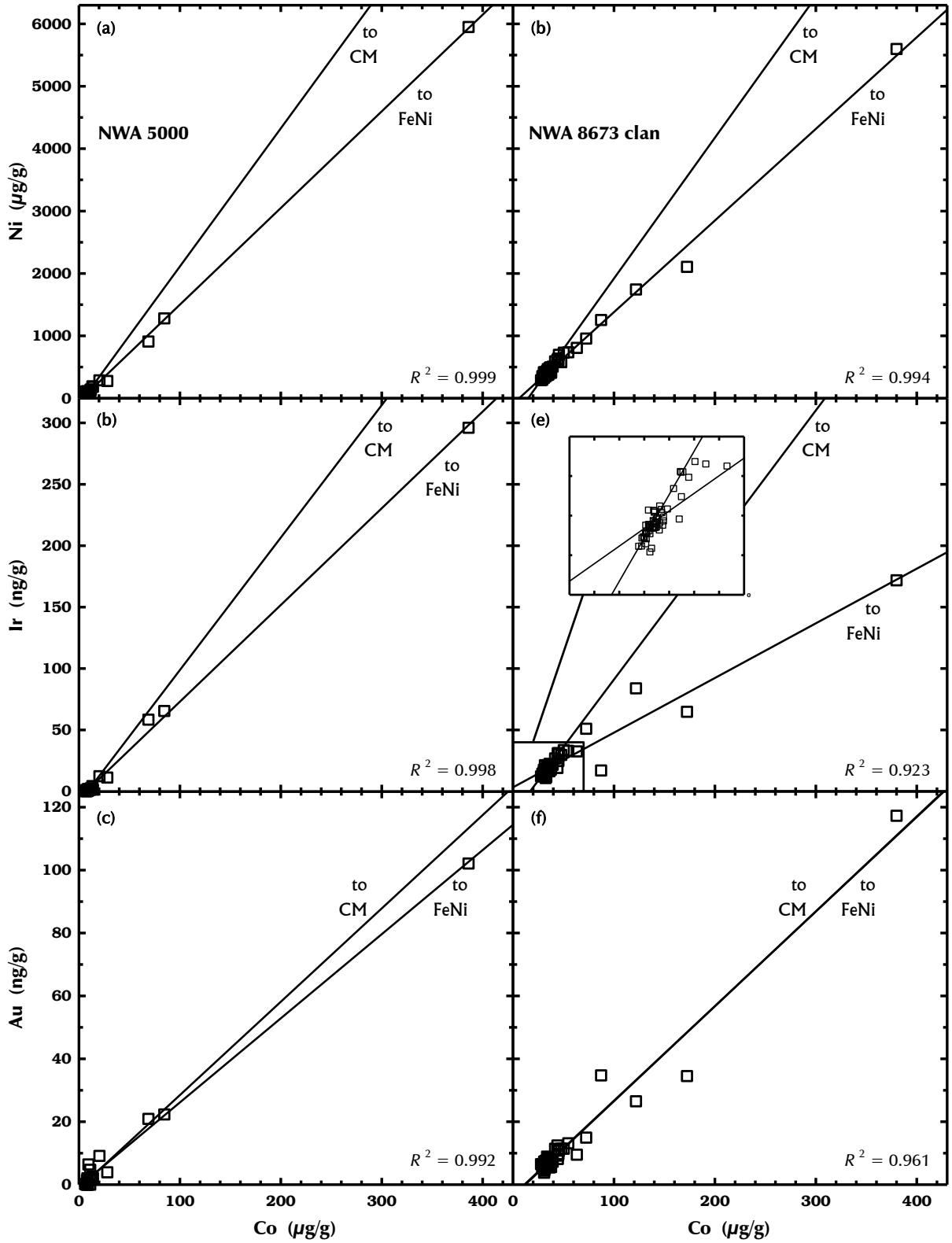
(a)
NWA 5000
to CM
to FeNi
R^2 = 0.999
(b)
NWA 8673 clan
to CM
to FeNi
R^2 = 0.994
(b)
to CM
to FeNi
R^2 = 0.998
(e)
to CM
to FeNi
R^2 = 0.923
(c)
to CM
to FeNi
R^2 = 0.992
(f)
to CM
to FeNi
R^2 = 0.961
Ni (μg/g)
Ir (ng/g)
Au (ng/g)
Co (μg/g)
Co (μg/g)

Fig. S54. Variation of Ni, Ir, and Au against Co (the most precisely determined of the four elements) for (a-c) 20 subsamples of NWA 5000 and (d-f) 65 subsamples of the NWA 8673 clan. The lines labeled “to CM” are defined by (1) the mean of the low-Co points and (2) CM chondrites (Lodders and Fegley, 1988). Subsamples with high siderophile element concentrations contain grains or nuggets of Fe-Ni metal (e.g., Figs. S1c, S27, and S28). The diagonal lines labeled “to FeNi” are simple least-squares regressions to the subsample data. The ratios and concentrations of Table S6 were calculated by extrapolating the lines of this figure to 5000 μg/g Co, a typical value for extralunar metal in lunar rocks (Gooley et al., 1973; Goldstein et al., 1974; Hewins and Goldstein, 1975; Hewins et al., 1976). Because the lines nearly pass through the origin, it makes no significant difference whether we choose 2000 μg/g, 5000, or 10,000 μg/g for the ratios of Table S6. This technique makes no assumptions regarding the intrinsic concentrations of siderophile elements in the lunar minerals. Note in panel (e, inset) that the variation in Co and Ir in the low-Co samples is consistent with a CM chondrite component, i.e., micrometeorites may dominate siderophile elements in the metal-poor samples. The fact that there are two meteorite components with different Ir/Co largely accounts for the positive Ir intercept (3.4±2.1 ng/g Ir at 0 μg/g Co; 95% confidence level) of the regression line. Assuming 6% Ni in the metal, the highest-Ni subsample (31 mg) contains 3.0 mg of metal.

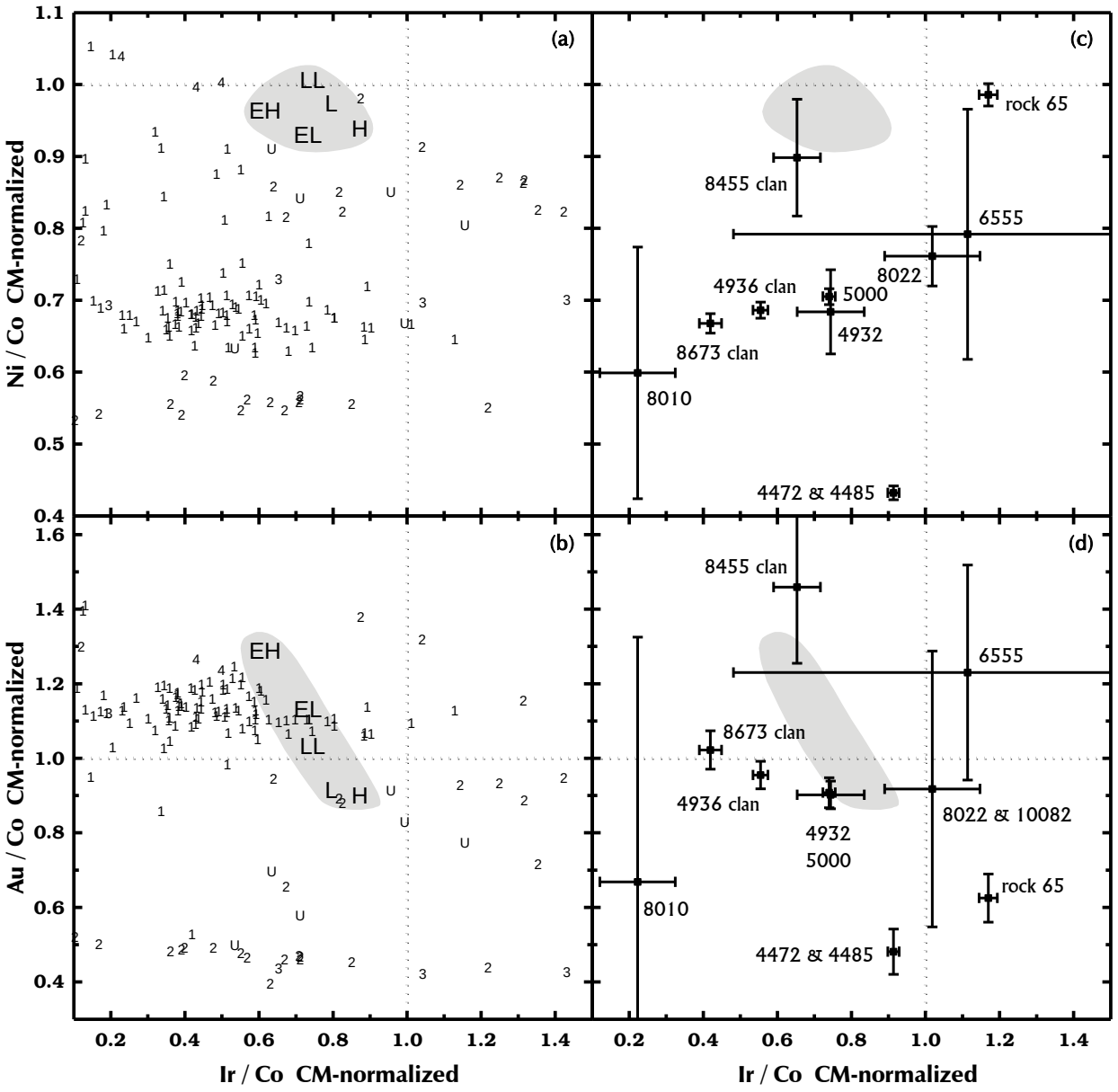

Fig. S55. (a,b) CM-chondrite-normalized Ni/Co, Ir/Co, and Au/Co in ordinary chondrites (gray fields, data of Lodders and Fegley, 1998) and iron meteorites (data of Wasson and Wang, 1986; Wasson et al., 1989, 2007; Wasson and Kallemeyn, 2002). 1= Group IAB, 2 = Groups IIAB, IID, and IIE, 3 = Group IIIAB, 4 = Group IVA, U = ungrouped. (c,d) The same ratios in the Fe-Ni metal components of some metal-rich brecciated lunar meteorites and rock 65, as inferred from the regressions such as those of Fig. S54. The error bars are 95% confidence limits based on the regression statistics (Table S6). Metal in metal-rich lunar meteorites is largely not consistent with metal in ordinary chondrites but is in the range of iron meteorites.

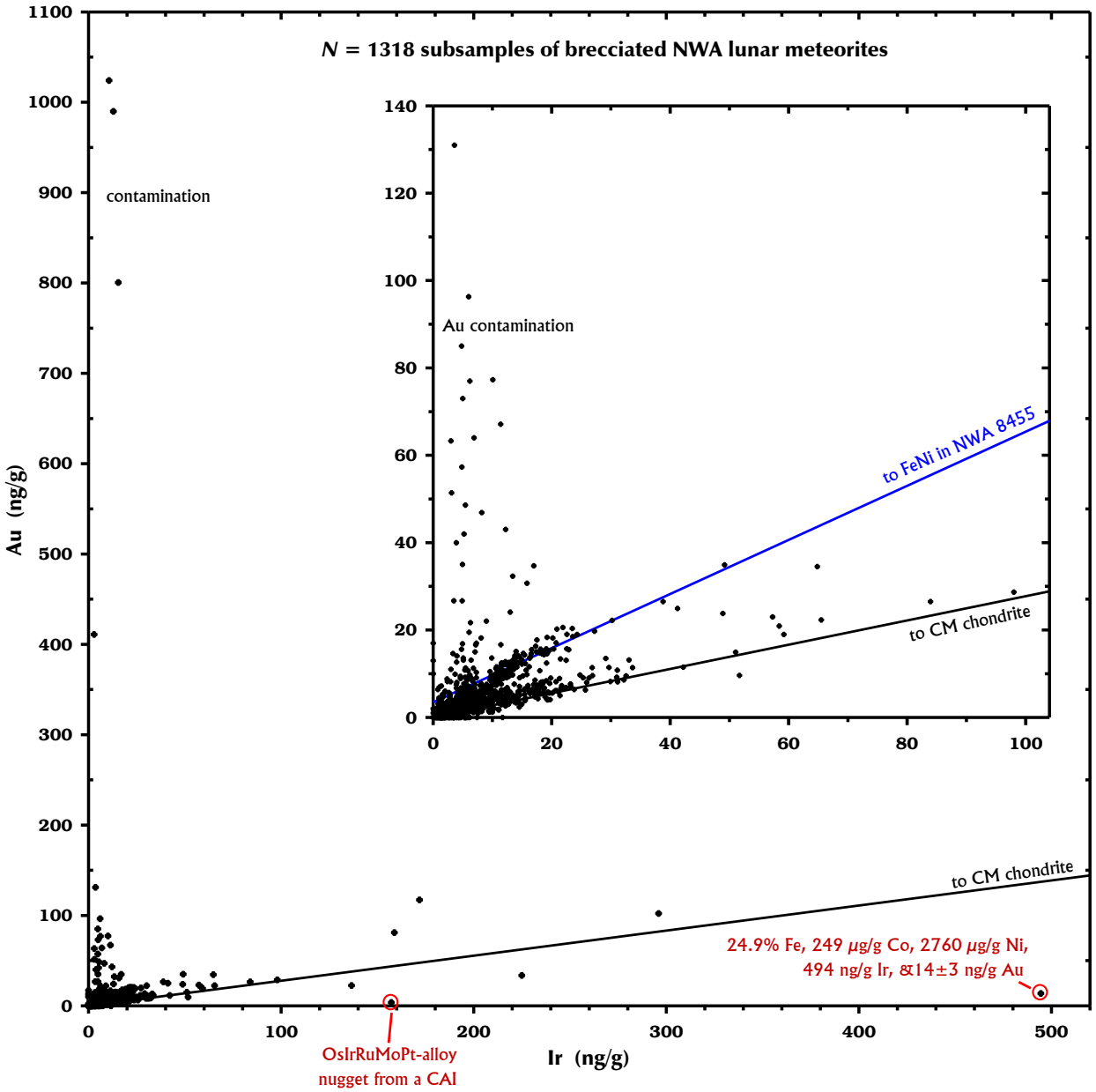

Fig. S56. Ir and Au in meteorite subsamples. Several lunar meteorites from northern Africa are contaminated with terrestrial gold (Table S2). Points lying along the "to FeNi in NWA 8455" line mostly represent subsamples of the NWA 4936 (Au/Ir/CM = 2.9) and NWA 8455 clans (Au/Ir/CM = 3.0) that contain FeNi metal with nonchondritic siderophile-element ratios (Fig. 15c). The sample (NWA 8673 pair) with the highest Ir concentration contains a large FeNi metal grain that has lost nearly all its gold to terrestrial processes such as those described by Wasson (2019). The low-Au/Ir point at 157 ng/g Ir is from the NWA 6252 subsample mentioned in Fig. S36.

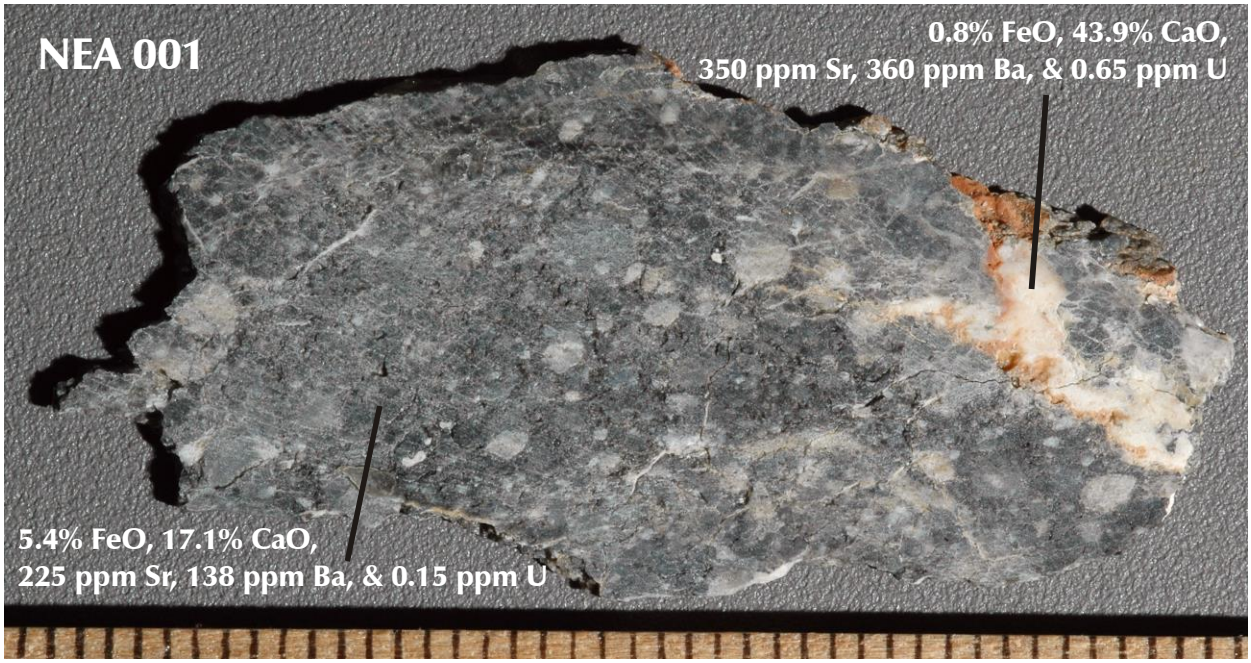

Fig. S57. NEA 001 is one of the most weathered lunar meteorites that we have analyzed. One of the subsamples from a slice of the type specimen (6.1 mg, pinkish-white material at upper right) contains 43.9 % CaO, 0.83% FeO, 0.074 % Na_2O, 352 µg/g Sr and 359 µg/g Ba. The CaO concentration corresponds to a mixture of 48% calcite and 52% gypsum. We do not include this subsample in the mass-weighted mean composition (Table S3). Millimeter ticks for scale.

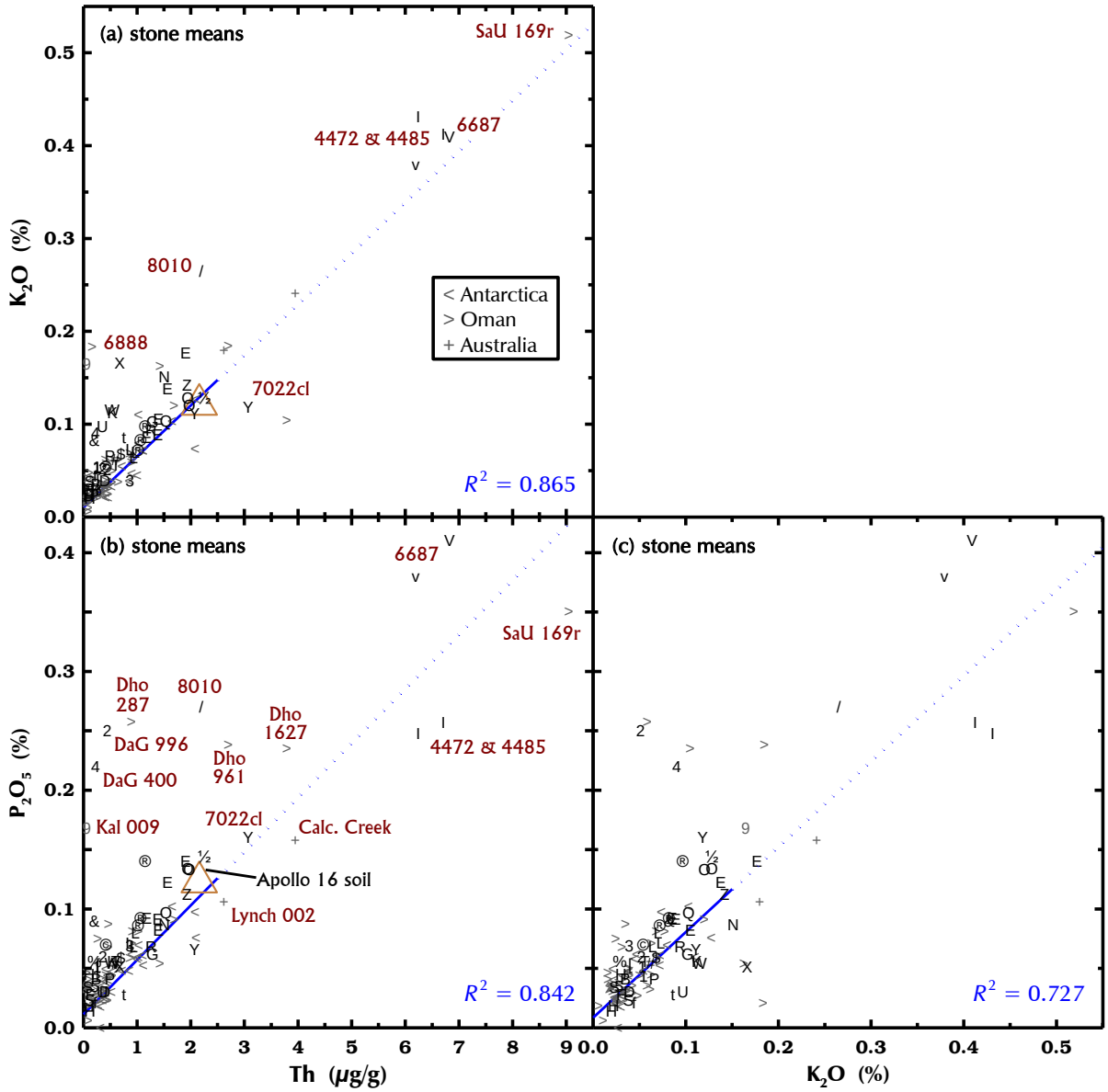

Fig. S58. Phosphorous and potassium concentrations in some lunar meteorites. Note that NWA 8632 (basalt) is the highest numbered NWA meteorite for which we have major-element data. The blue lines are simple linear regressions to the (largely obscured) Antarctic data (mare basalts not included) and the Apollo-16-soil point (large triangle). The coefficients of determination (R^2) apply to the data of these lines. (a) As a result of terrestrial alteration, most of the African meteorites (and many from Oman) have greater concentrations of K_2O than do Antarctic meteorite of similar Th concentration. The effect is most severe in DaG 400 (symbol 4), Kalahari 008 and 009 (8,9), NWA 2995 and 2996 (E), NWA 4819 (N), NWA 4932 (K), NWA 6578 (U), NWA 6721 (W), NWA 6888 (X), NWA 7274 (Z), NWA 8010 (/), and NWA 8055 (&). (b) Similarly, P_2O_5 is enriched in some of the African meteorites, with the effect most severe in DaG 262 and 996 (2), DaG 400 (4), Kalahari 009 (9), NWA 2995 and 2996 (E), NWA 7834 (®), NWA 7959 (©), NWA 8010 (/), NWA 8055 (&), and NWA 8182 (½). (c) In nonmare Apollo lunar rocks and soils and lunar meteorites from Africa absolute concentrations of K_2O and P_2O_5 are often nearly identical. Meteorites enriched in terrestrial P_2O_5 are not necessarily enriched in terrestrial K_2O, and conversely. See Table S1 for symbol key.

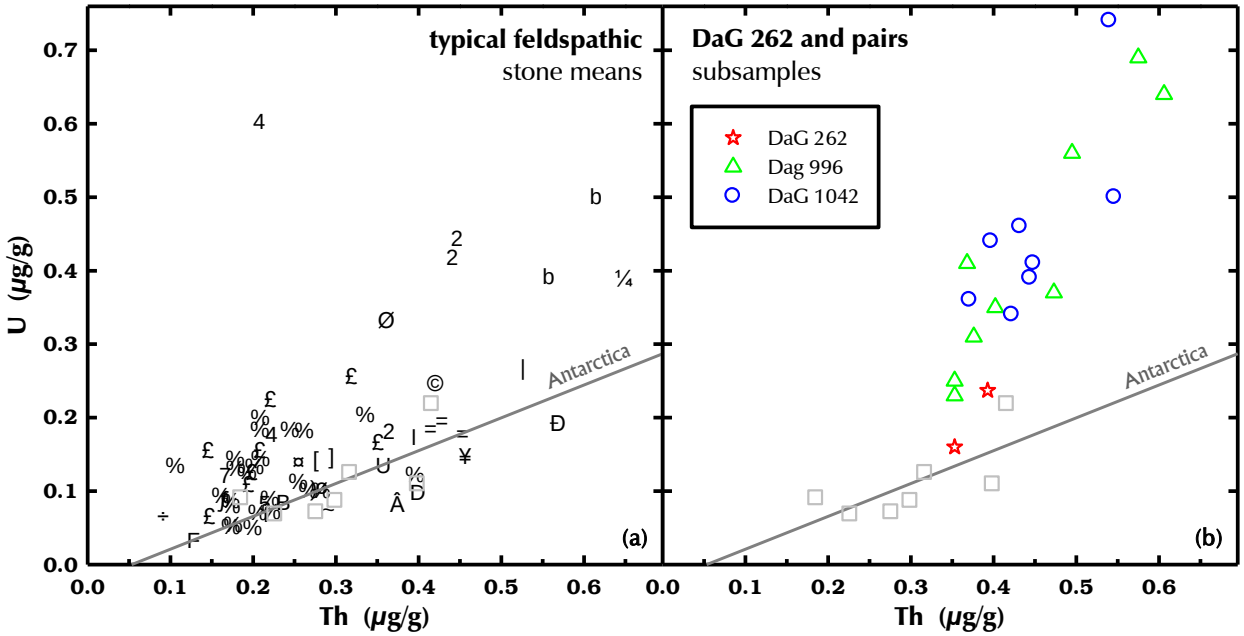

Fig. S59. (a) Many lunar meteorites from northern Africa are contaminated with terrestrial uranium from chemical weathering. The effect is most apparent among the typical feldspathic lunar meteorites in which U concentrations are intrinsically low. The diagonal line is a simple linear regression through the typical feldspathic meteorites from Antarctica (squares), which are uncontaminated. The most severely contaminated meteorites are DaG 1058 (symbol 4, but not its pair, the 4 symbol at 0.18 μg/g U), DaG 996 (2), DaG 1042 (2), NWA 10073 and pair (b), NWA 8586 (¼), NWA 10665 (Ø), the NWA 8222 (£) clan, and some but not all of the NWA 8046 clan (%). See Table S1 for symbol key. (b) Even among subsamples of a single stone contamination levels vary considerably.

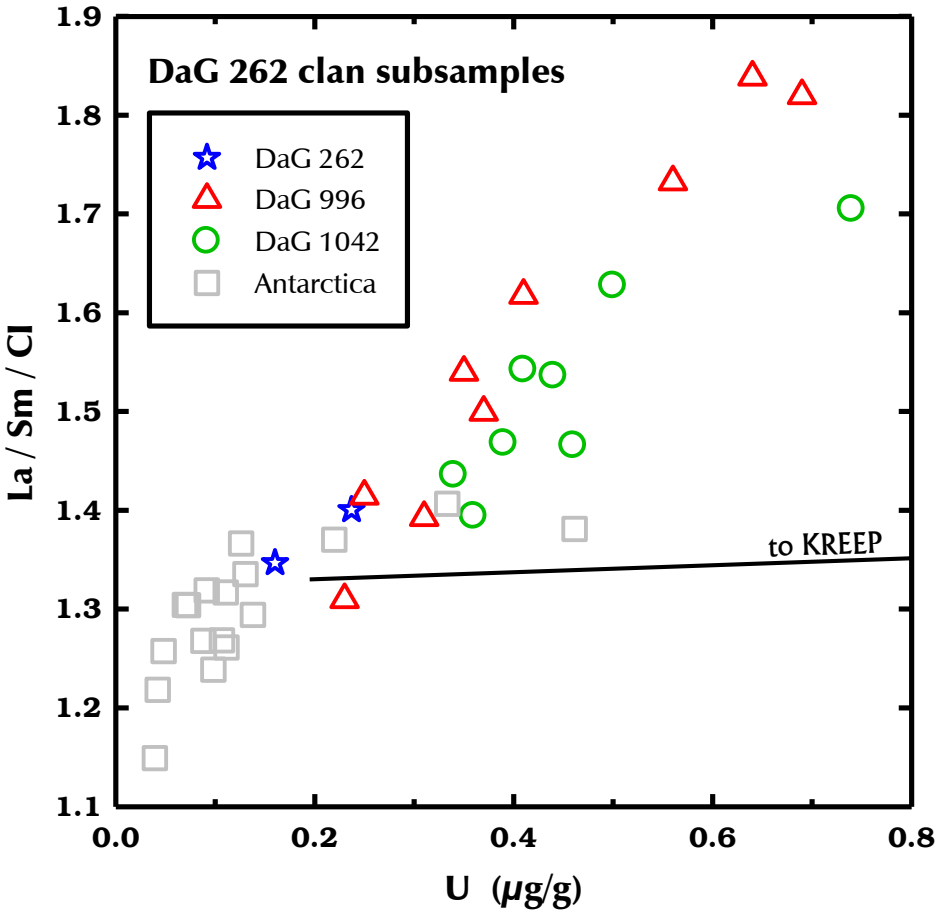

Fig. S60. La/Sm among subsamples of the DaG 262 clan (1.33 kg) exceeds that in feldspathic lunar meteorites from Antarctica. The variation in La/Sm is not due to varying proportions of a KREEP component but correlates (R^2=0.826) with the U excess from terrestrial alteration (Fig. S59b). As noted by Crozaz and Wadhwa (2001), "weathering effects in hot desert meteorites can vary on the cm-scale." The DaG-262-clan subsamples of this plot average 25 mg in mass, thus the effects vary on the millimeter scale.

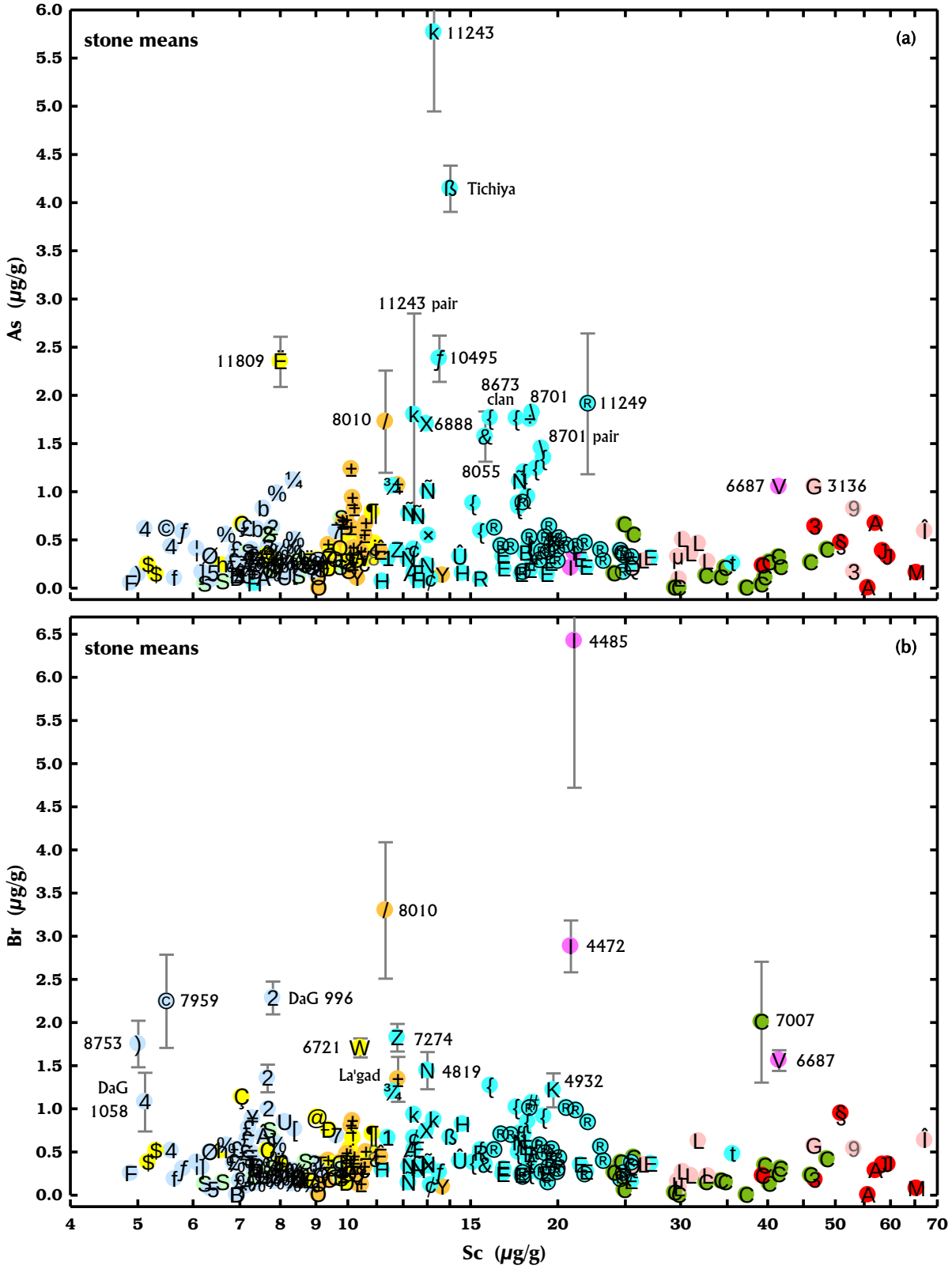

Fig. S61. As and Br concentrations in lunar meteorites from northern Africa. The error bars are 95% confidence limits. Concentrations of these two elements in feldspathic lunar meteorites from Antarctica are below our detection limits, 0.05–0.25 μg/g for As and 0.2–0.5 μg/g for Br. See Table S1 or Fig. S4 for symbol key and color coding.

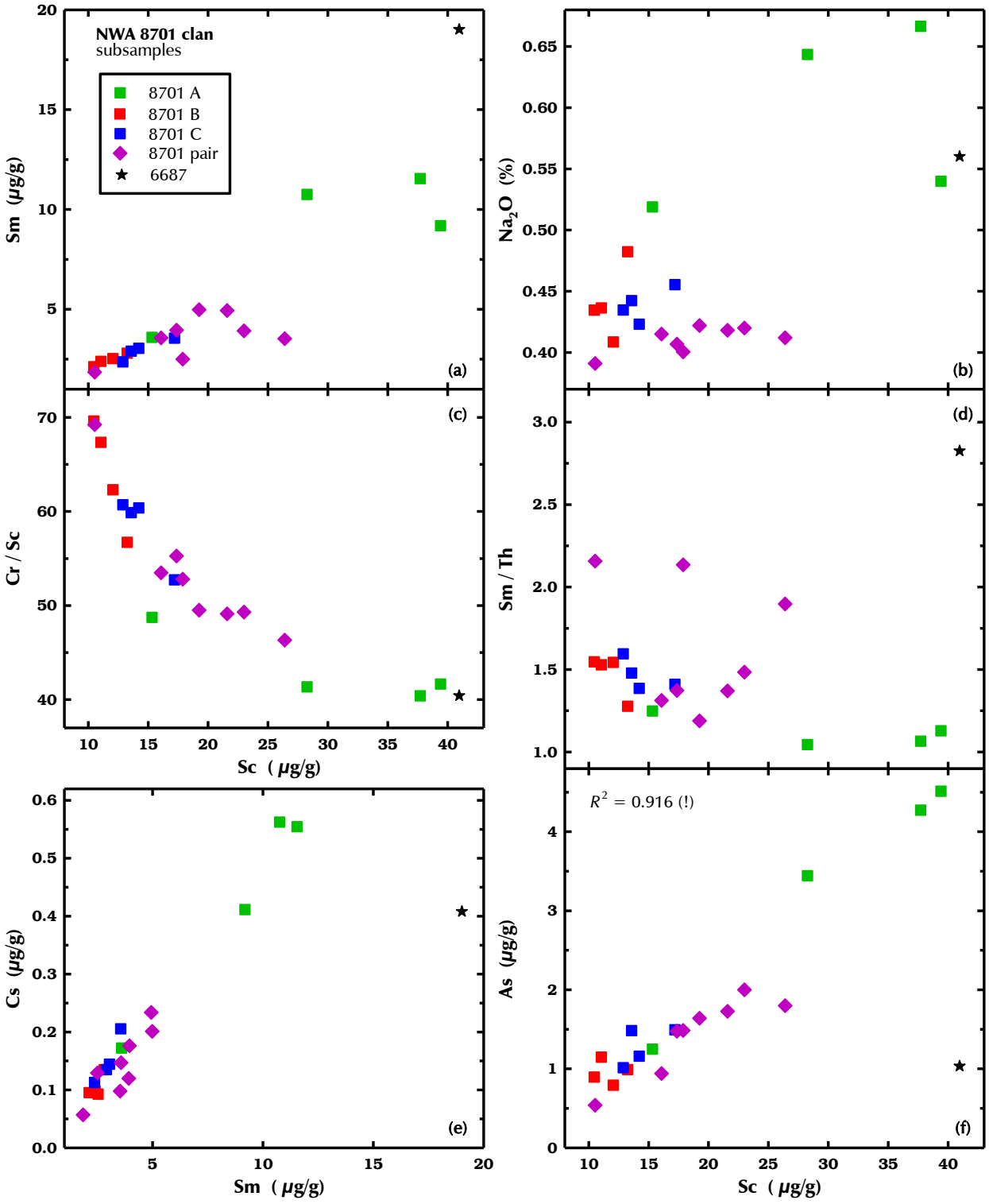

Fig. S62. We analyzed three different samples of NWA 8701 (72 g) and a stone that appears to be a pair. Three of four subsamples of stone A are rich are a mare component that bears some resemblance to NWA 6687, that is, they rich in incompatible elements (a), rich in alkali elements (b,e), and low Cr/Sr (c). (f) NWA 8701 has one of the greatest concentrations of presumably terrestrial arsenic that we have observed but we do not know why As correlates so strongly with Sc (pyroxene).

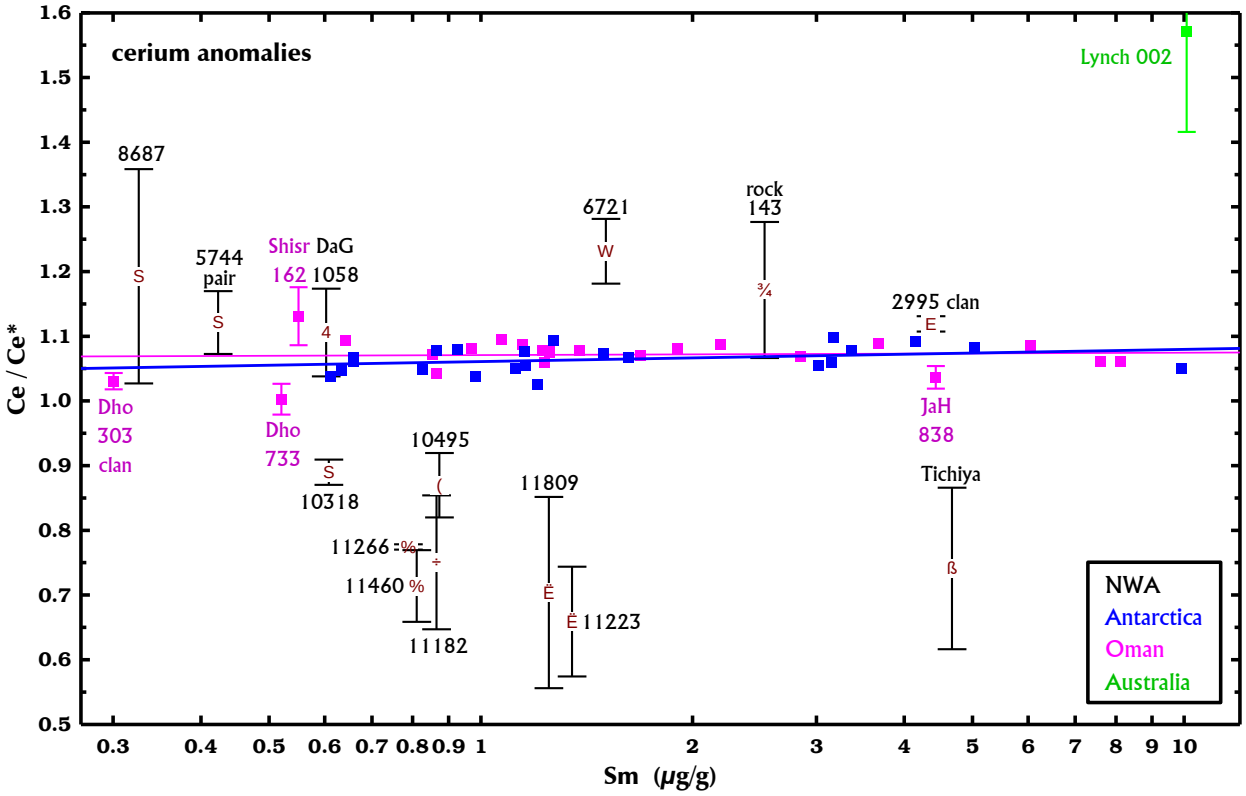

Fig. S63. Magnitude of Ce anomalies in NWA lunar meteorites having significant anomalies. The anomaly is calculated as Ce/Ce* = {[Ce]/C_{Ce}}/{10^(4*log([La]/C_{La})+1*log([Sm]/C_{Sm}))/5} where [Ce], [La], and [Sm] are the concentrations of the three elements in the meteorite stones (Table S3) and C_{Ce}, C_{La}, and C_{Sm} are the concentrations of the three elements in CI chondrites (Anders and Grevesse, 1989). The error bars are 95% confidence limits. Data for Antarctic and Omani meteorites are presented for comparison; the lines are simple least-squares fits to the Antarctic and Omani sets. Four Omani meteorites have Ce anomalies, both positive and negative but none are as severe as some of those from northern Africa. Three of the anomalous meteorites (symbol S) are from the troctolitic NWA 5744 clan, the troctolitic Dhofar 303 clan, and troctolitic Dhofar 773/1766 from Oman. Only meteorites with <15% FeO_T, <35 μg/g Sc, and <11 μg/g Sm are plotted. Note that three of the NWA meteorites with negative Ce anomalies here are also those with anomalously high La/Sm in Fig. S7 (NWA 10318, NWA 11266, NWA 11460).

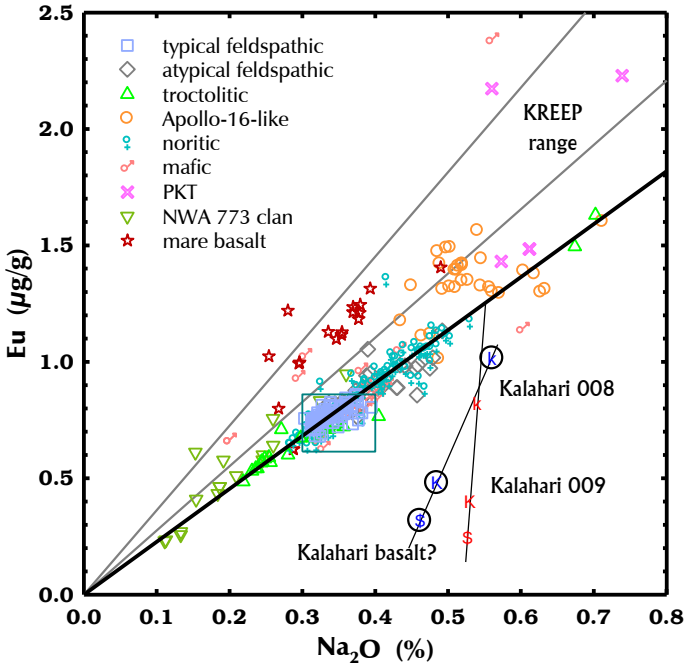

Fig. S64. Comparison of Kalahari 008 (585 g) and Kalahari 009 (13.5 kg) to other lunar meteorites in Na-Eu space. Both Kalahari stones have distinctly lower Eu/Na than other feldspathic and basaltic lunar meteorites. For reference, the heavy diagonal line is defined by the origin and the mean concentrations of the typical feldspathic lunar meteorites (near center of large rectangle). For the k and K (Kalahari) points, the circled blue points are the data of Korotev et al. (2009) and the uncircled red points are the data of Sokol et al. (2008). The $ points represent the model composition of the basalt component from the model described in the text. This figure and Fig. S65 provide some of the strongest compositional evidence that Kalahari 008 and Kalahari 009 are, in fact, paired.

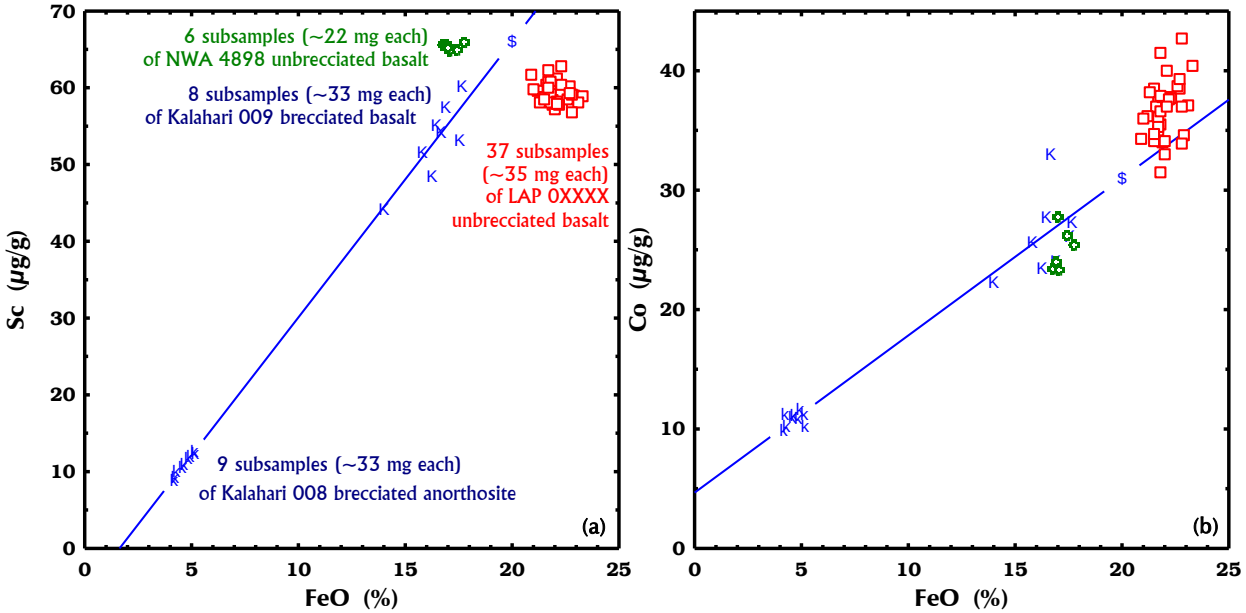

Fig. S65. Kalahari 008 and 009 subsamples lie along the same trend lines in FeO-Sc and FeO-Co space, suggesting that each is a mixture containing a component of the other. For reference, the diagonal lines are defined by the mean concentrations of the Kalahari 008 (k) and Kalahari 009 (K) points. The $ point represents the model basalt component of Kalahari 009 described in the text. (a) Note that the data for the unbrecciated mare basalts do not trend as do the data for Kalahari 009. (b) The mixing trend is less obvious for Co. Subsample data for the 6 LAP (LaPaz Icefield) meteorites are presented in Table S2.

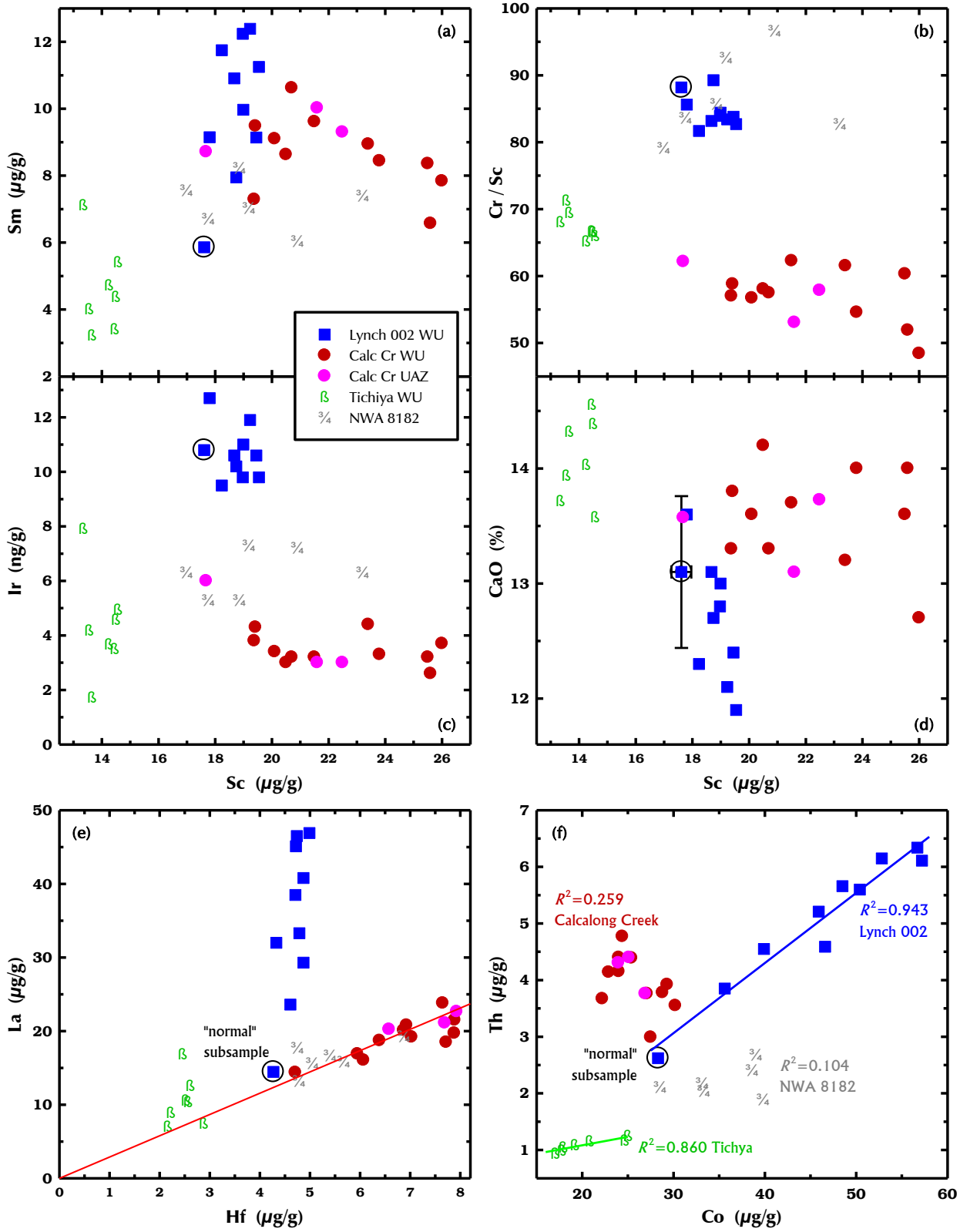
(a)
(b)
(c)
(d)
(e)
(f)
Sm (μg/g)
Cr / Sc
Ir (ng/g)
CaO (%)
Sc (μg/g)
Sc (μg/g)
La (μg/g)
Hf (μg/g)
Th (μg/g)
Co (μg/g)
Lynch 002 WU
Calc Cr WU
Calc Cr UAZ
Tichiya WU
NWA 8182
"normal" subsample
"normal" subsample
R²=0.259
Calcalong Creek
R²=0.943
Lynch 002
R²=0.104
NWA 8182
R²=0.860 Tichya

Fig. S66. Subsample data for Lynch 002. (a) In Sc-Sm space, Lynch 002 (36.5 g) is similar to Calcalong Creek (19 g), the only other lunar meteorite from Australia. Both are similar to NWA 8182. Compositionally, all three are breccias composed of feldspathic, basaltic, and KREEP lithologies, decreasing in that order, an observation consistent with the petrography (Hill and Boynton, 2003; Smith et al., 2012; Robinson et al., 2016). (b,c) The two meteorites from Australia are distinct from each other in Cr/Sc and Ir, however, largely dismissing any compositional argument that they are paired. (d) CaO is the least precisely determined element or ratio plotted here. The error bar represents typical 2σ analytical uncertainties. Nevertheless, Lynch 002 varies considerably in CaO concentration, an apparent loss with weathering compared to the other meteorites and the "normal" subsample of Fig. 19. (e) The diagonal red line is defined by the origin and the mean of the Calcalong Creek points (UAZ data from Hill and Boynton, 2003). The La/Hf ratio of Calcalong Creek, 2.8, is essentially that of KREEP. As a result of some terrestrial weathering process, all but the "normal" Lynch 002 subsample of Fig. 19 are variably enriched (up to 3×) in La compared to the pre-terrestrial concentrations inferred from the Hf concentration and the La concentration of the normal subsample. (f) A geochemically unlikely pair, Co and Th are also enriched in the high-La subsamples. Tichiya (NWA, 9.35 kg), with a negative Ce anomaly (Fig. 19), shows some of the same properties, La enrichment (e) and correlation of Th with Co.

Figures Cited Only Here

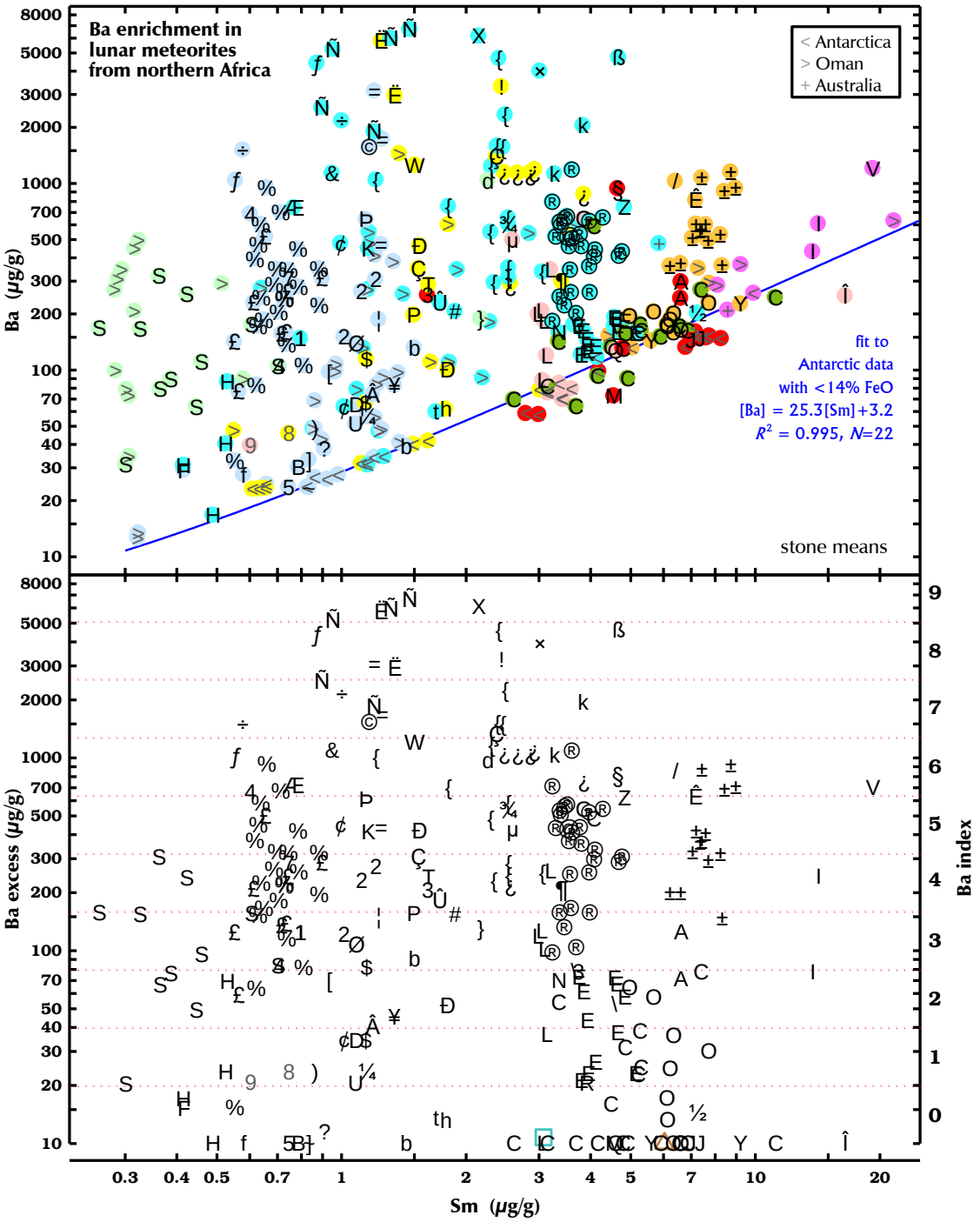

Fig. S67. (a) Nearly all lunar meteorites from northern Africa are contaminated with terrestrial Ba to varying degrees. On the Moon, represented here by the lunar meteorites from Antarctica, Ba correlates with Sm in the feldspathic highlands. The blue line is a fit to the Antarctic data. (b) Ba excess (contamination) calculated simply as the greater of 10 ug/g or the concentration value of (a) minus the Ba concentration of the blue line of (a) at the same Sm concentration. The Ba index (BaI) of Table S1 is the range represented on the right-hand axis. See Table S1 or Fig. S4 for symbol key and color coding.

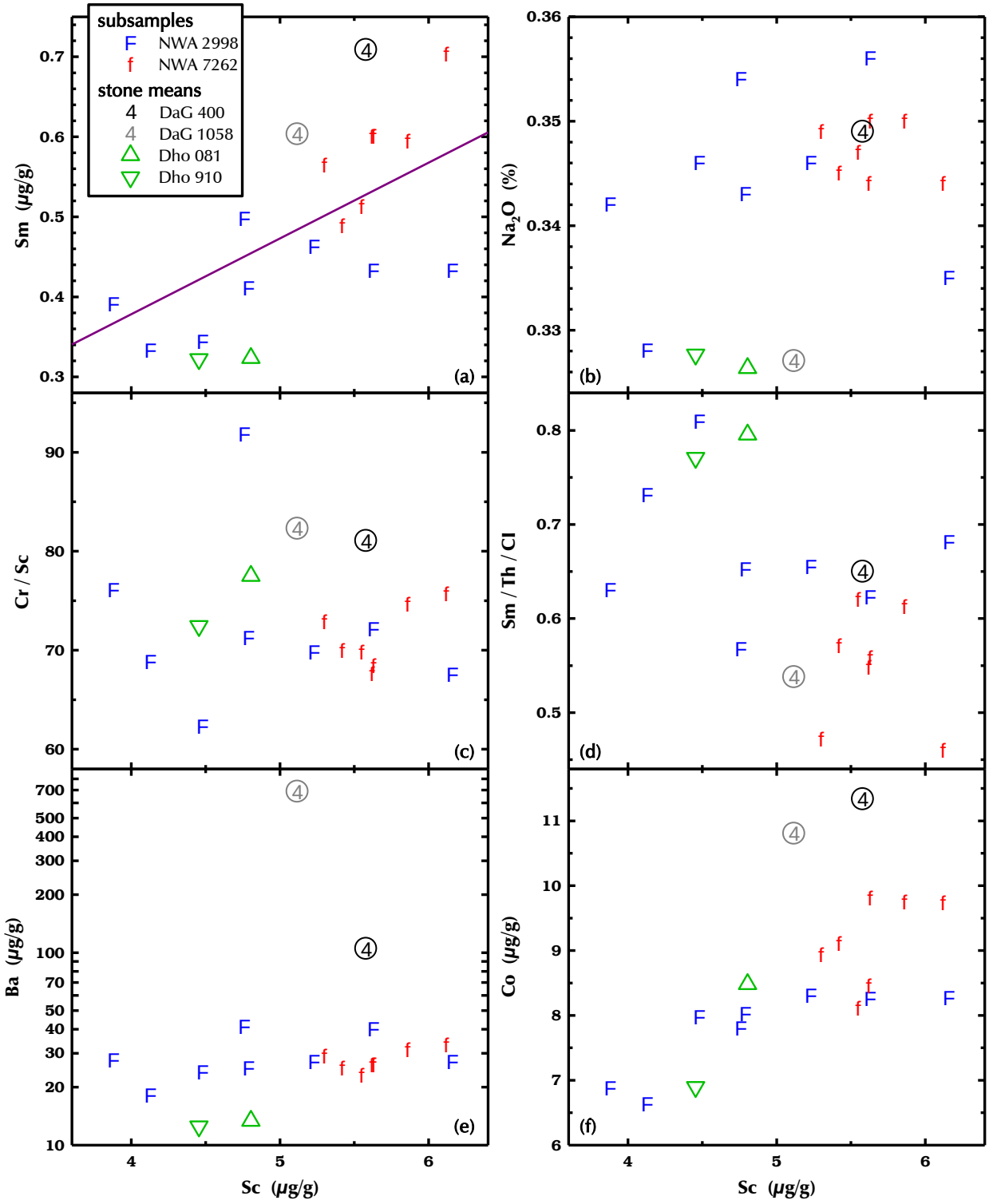

Fig. S68. NWA 2998 (163 g) is the most feldspathic (lowest Sc) of the meteorites of this study (symbol F on Fig. 6). NWA 7262 (413 g) is slightly more mafic on average but overlaps in composition with NWA 2998 for all elements, thus we assume that NWA 2998 and NWA 7262 are terrestrial or launch pairs. (a) For reference, the diagonal line is defined by the origin and the mass-weighted mean of the NWA 2998 and NWA 7262 subsamples. Paired stones DaG 400 and DaG 1058 and paired stones Dhofar 081 and Dhofar 910 (Korotev, 2012; stone means plotted) are the only other lunar meteorites that plot in the field of this plot. (c) The DaG stones have greater Cr/Sc than the NWA stones, however, so we assume that they are not launch paired with NWA 2998/7262. (d) The NWA stones have greater Sm/Th than the DaG Stones, so we assume the two meteorites are also not launch

paired. (e,f) NWA 2998 and NWA 7262 have among the lowest concentrations of Ba and Ni of feldspathic meteorites from Northwest Africa (Figs. 14 and 16). The low Ba and the fact that both stones retain their fusion crusts suggest a relatively short terrestrial age. (a), (b), and (d) together suggest that the Dhofar stones are not likely launch paired with the NWA stones. Also, the textures are very different with the NWA stones being largely fragmental whereas the Dhofar stones have abundant schlieren and vesicles.

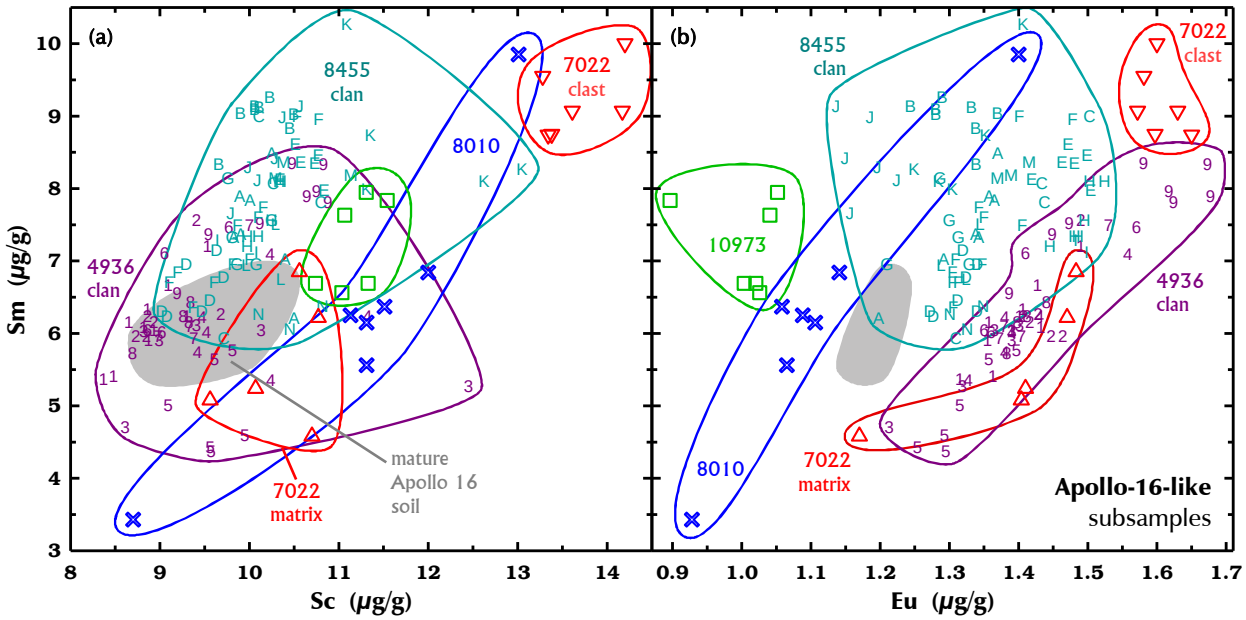

1	**4936**	A	**8455**
2	5406	B	8609
3	6221	C	8651
4	6355	D	8668
5	6470	E	8727
6	6570	F	8783
7	7190	G	10130
8	7986	H	10228
9	8181	I	10621
		J	10953
		K	La'gad
		M	pair
		N	pair

Fig. S69. Subsample data for the meteorites of Fig. S35 (Apollo-16-like). The gray fields represent the range of mature and submature soils from Apollo 16 (Korotev, 1997). (a) Although mean compositions of NWA 8010 and NWA 10973 are similar (Fig. S35), the subsample data for NWA 10793 clusters while that for NWA 8010 trends. (b) Sm/Eu is distinctly greater in NWA 8454 than NWA 4936. Table below: For 19 well-behaved elements, the percentage of subsamples (column mean) for each lunar meteorite that lie within the compositional range of submature and mature soils from Apollo 16 (bottom two rows, Korotev, 1997). For example, at one extreme, concentrations of Na_2O in none of the 18 subsamples of Dhofar 1627/1980 lie within the range of Apollo 16 soils; all are much greater (Fig. S35b). At the other extreme, all of the subsamples of Dhofar 1627/1980 have concentrations of Co, Ni, Ir, and Au that lie within the range of Apollo 16 soils (Fig. S35e). Of the 9 meteorites, NWA 4936 is most similar and MIL 090036 is least similar to Apollo 16 soils.

Eight "Apollo-16-like" lunar meteorites in decreasing order of "likeness."

	N	Na_2O	Sc	Cr	FeO	Co	Ni	La	Ce	Nd	Sm	Eu	Tb	Yb	Lu	Hf	Ta	Ir	Au	Th	mean
NWA 4936	54	37	91	85	67	93	91	80	83	85	80	4	89	91	87	81	80	93	93	96	79
JaH 838	5	20	100	100	100	40	40	100	100	80	80	0	80	100	100	100	100	80	80	80	78
NWA 7022	5	20	80	100	100	40	20	100	100	100	100	20	100	80	80	100	100	80	20	100	76
NWA 10973	6	83	0	0	33	100	100	50	50	50	50	0	50	83	100	100	100	100	100	100	66
NWA 8010	7	57	14	57	71	86	86	71	71	71	71	14	71	71	71	57	86	43	86	71	65
Dho 1627 & 1980	18	0	94	78	78	100	100	22	28	67	28	11	56	56	67	44	67	100	100	56	61
NWA 8455	76	54	84	61	29	96	75	28	39	39	32	13	42	45	49	33	54	82	83	53	52
MIL 090036	16	0	63	63	75	25	13	44	56	50	44	25	38	31	31	44	38	38	13	25	38
mean	187	34	66	68	69	72	65	62	66	68	61	11	66	70	73	70	78	77	72	73	64
Apollo 16		%	μg/g	μg/g	%	μg/g	μg/g	μg/g	μg/g	μg/g	μg/g	μg/g	μg/g	μg/g	μg/g	μg/g	μg/g	ng/g	ng/g	μg/g	
min		0.45	7.6	590	4.4	19	250	9.0	23	14	4.2	1.13	0.9	3.0	0.43	3.1	0.38	7	5	1.5	
max		0.51	10.7	865	6.0	54	265	15.5	41	26	7.2	1.26	1.5	5.2	0.72	5.6	0.70	20	19	2.7	

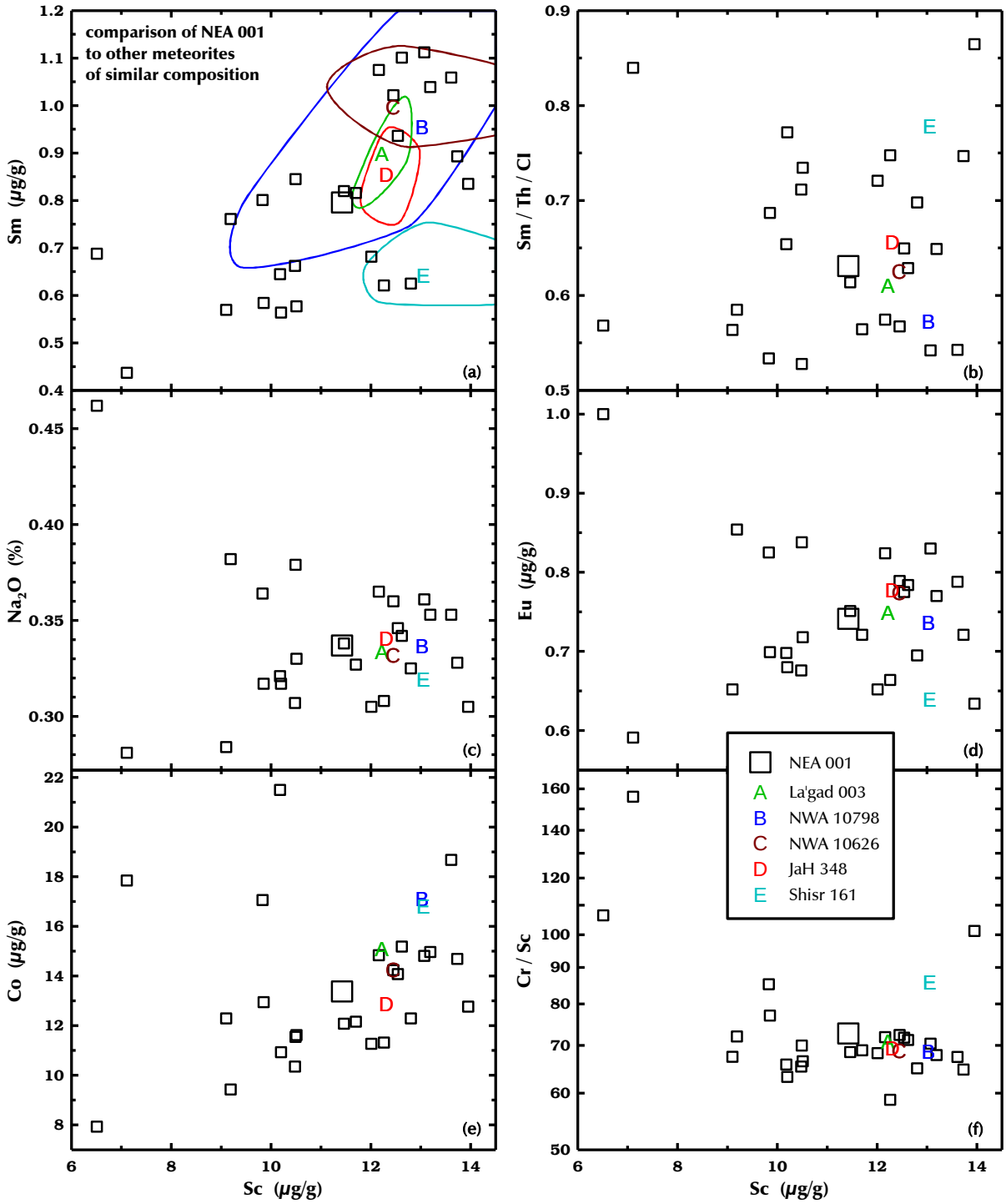

Fig. S70. Comparison of NEA 001 (262 g) subsamples (small squares) to mass-weighted means of other stones of similar composition (symbols A–E). The large square represents the mass-weighted mean of NEA 001. The other 5 stones of the figure are all meteorites for which the mass-weighted means plot within the ranges of the NEA 001 subsamples for all 6 panels of the figure and for which Sc is >9 μg/g. (a) The ranges of the subsample data for the 5 similar stones are shown. NWA 10626 (*N*=8), JaH (Jiddat al Harasis) 348 (*N*=8), and, to a lesser extent, NWA 10798 (*N*=6) are unlikely launch paired with NEA 001 because the compositional range for subsamples of these stones are much less than for NEA 001 and there are no highly feldspathic subsamples, as with NEA 001. There is little overlap between NEA 001 and Shişr 161. La'gad 003 (*N*=19 subsamples), which is likely paired with NWA 10798 (Fig. S73), is the most similar to NEA 001 but is not as feldspathic on average. Jah 348 and Shişr 161 data from Korotev (2012, 2017).

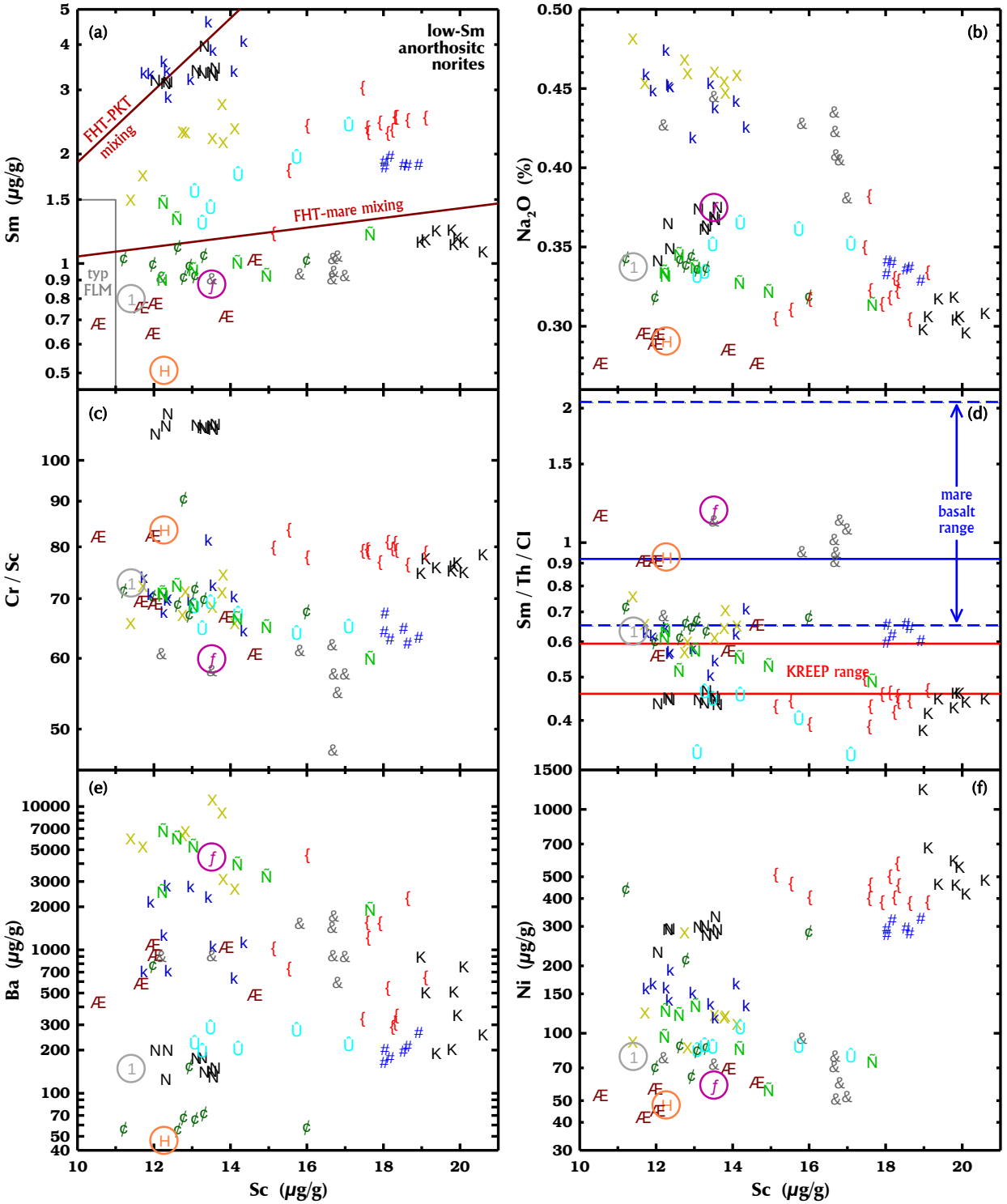

Fig. S71. Mostly-subsample data for low-Sc, low-Sm meteorites of anorthositic-norite composition, i.e., those meteorites that are slightly more mafic than the typical feldspathic lunar meteorites (panel a) and that plot below or near the FHT-mare join of the triangle of Fig. 6 (i.e., minimal PKT component). Subsample data for NEA 001 (Fig. S70), the NWA 3163 clan (Fig. S45), and NWA 10495 (Fig. S72) are heterogeneous, so for clarity only the mass-weighted means are plotted here (circled). The NWA 10509 clan is also heterogeneous (Fig. S73), so stone means are plotted (*N*=6). In (a), the diagonal lines are the mixing triangle of Fig. 6. In (d), the blue lines represent the range and geometric mean of the 11 mare basalts among lunar meteorites and the red lines delineate the KREEP range (Fig. S15).

Some meteorites of the figure are self-evidently compositionally distinct and presumably unpaired with any others, e.g., NWA 4819 (symbol N) in panel (c). Other are clearly unpaired with others when more than one panel is considered, e.g., NWA 7931 (#) in (a,c,d). From these self-evident data we conclude that:

1. NEA 001 (1) is more heterogeneous (Fig. S70) than any of the meteorites plotted here and is not likely launch paired with any NWA stone.
2. The NWA 3163 clan (H) is not paired (a, e, and Fig. S45) with any other meteorite of this plot. (d) The NWA 3163 clan plots within the mare basalt range despite that it likely contains negligible mare basalt.
3. NWA 4819 (N) is not paired (b,f).
4. NWA 4932 (K) is not paired (a–f).
5. NWA 6888 (X) is not paired (a,b, and table below).
6. NWA 7931 (#) is not paired (a–f).
7. NWA 8055 (&) is unpaired (a,b,d) and has the lowest Cr/Sc (c) and low *Mg*' (60, Table S4), consistent with a component of mare basalt.
8. The NWA 8673 clan ({) is not paired (see also Fig. S46).
9. NWA 11243 (k) is not paired (a,b,f).

Some compositionally heterogeneous meteorites are not self-evidently distinct from other meteorites of the figure. For those we have used the *t*-test on all subsamples to determine which elements are different in composition. Conclusions:

10. The NWA 10495 clan (ƒ) is not paired (a ,d, and Fig. S71).
11. The NWA-10509-clan data differs significantly from the 10626 clan mainly for terrestrial contamination elements (CaO, As, Sr, and Ba) suggesting possible launch pairing (Fig. S80).
12. The NWA 10509 clan is unpaired with other meteorites of the figure (a,b,f).
13. Rabt Sbayta 008 (Æ) is unique (b,f).

plot symbol	meteorite or clan	When taken together, it is self-evident from the panels that the meteorite is compositionally unique.	Or, for the two meteorites, the mean concentrations of these elements significantly differ from each other (Welch's t-test @ 99% confidence).
1 & *ƒ*	NEA 001 & 10495	Fig. S70	Co, Ni, As, Br, Cs, *Ba*, Ta, Ir, Th, U, Sm/Th
1 & Ñ	NEA 001 & 10509	Fig. S70	*Ca*, Sc, Fe, Co, *As*, *Br*, *Cs*, *Ba*, REE, Hf, Th
1 & ¢	NEA 001 & 10626	Fig. S70	*Ca*, Sr, HREE, Hf, Th, U
H	3163 clan	a, e, & Fig. S45	
N	4819	b & f	
K	4932	a, b, c, d, & f	
X & N	6888 & 4819	a, b, & e	Na, Cr, Fe, Co, Ni, *As*, *Br*, *Sr*, *Ba*, REE, Hf, Ta, Th, U, Cr/Sc, Sm/Th
X & Û	6888 & 11127		Na, Ca, *As*, *Br*, Rb, *Sr*, Cs, *Ba*, Eu, Sm/Th
X & k	6888 & 11243		Sr, Cs, *Ba*, REE, Hf, Ta, Th, U
#	7931	a, c, d, e, & f	
&	8055	a, b, c, d, e, & f	mare basalt?
{	8673 clan	a, c, d, & f	
ƒ & Ñ	10495 & 10509		*Ca*, Cr, Fe, Co, Ni, *As*, REE, Hf, Ta, Ir, Th, Sm/Th
ƒ & ¢	10495 & 10626		Cr, *As*, Rb, Sr, *Ba*, Hf, Ta, Ir, Th, Sm/Th
Ñ & ¢	10509 & 10626		*Ca*, *As*, *Sr*, *Ba*, La, & Th
Û	11127	a, b, d, & e	
k	11243	a, b, e	
Æ & H	RaSb 008 & 3163	a, e	*Ca*, Cr, Co, *Sr*, *Ba*, *LREE*, Ir; significant different in texture

Elements in italics may differ because of variable degrees of terrestrial weathering.

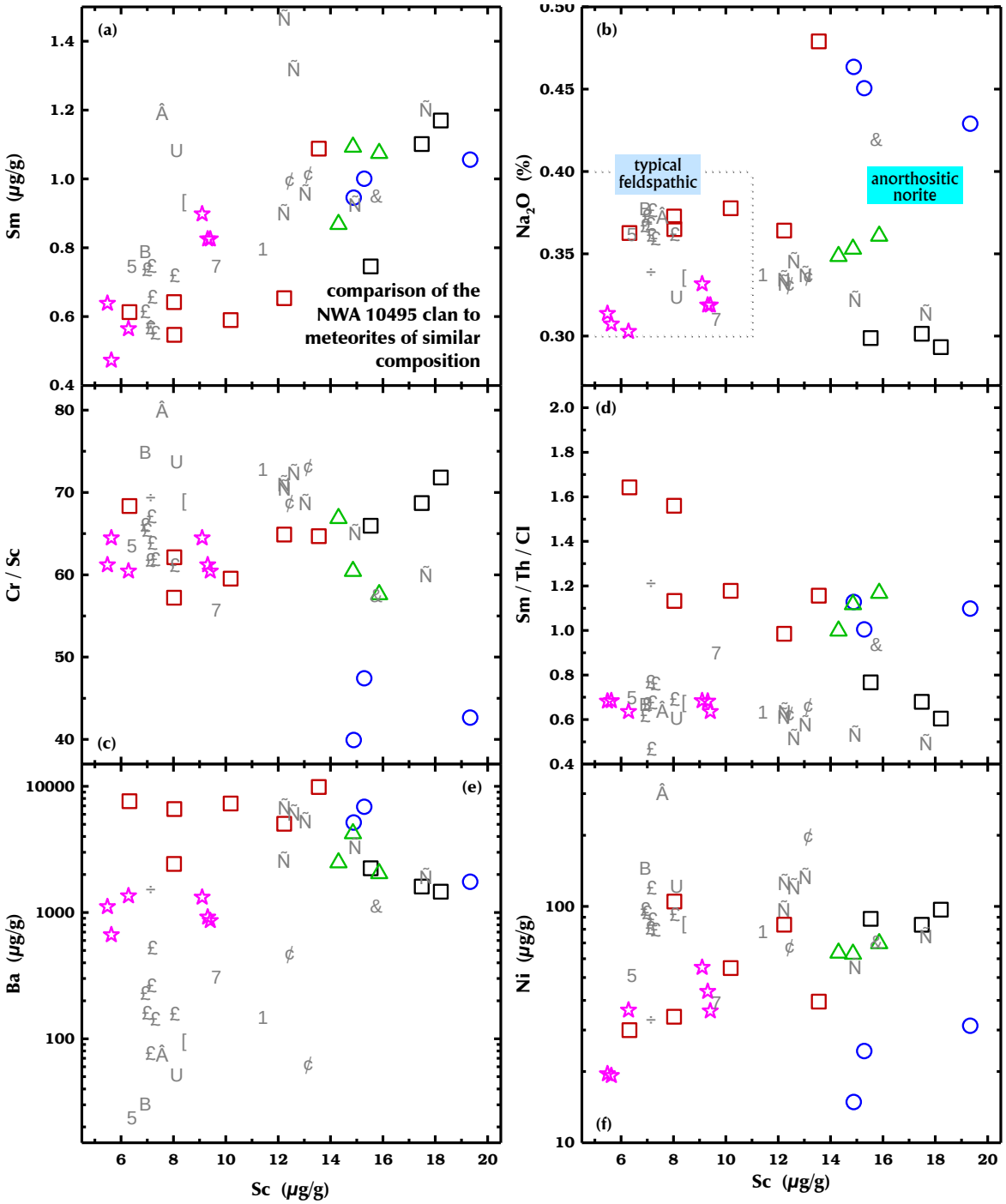

NWA 10495	□□○△	NWA 8055	&
Sueilila 005	☆	NWA 8222 clan	£
NWA 10509 clan	Ñ	NWA 10626 clan	¢
NEA 001	1	NWA 11182	÷
NWA 482	B	NWA 11352	Â
NWA 6578	U	OA 001	5
NWA 7493	[		

Fig. S72. The NWA 10495 clan consists of NWA 10495 ("several" pieces [MetBull] totaling 15.6 kg) and Sueilila 005 (1 piece, 282 g). All were found together in 2015, but the name NWA 10495 was approved in 2016 while the Sueilila 005 name was not approved until 2019. The subsample data plotted here are from 3 different pieces of NWA 10495: 2 different samples of the "B" piece (□ 3 and □6 subsamples each), and 1 each sample of the "C" piece (○, 3 subsamples), and the "D" piece (△, 3 subsamples). The Sueilila 005 data derive from 2 different samples (symbol ☆, 3 subsamples each, low- and high-Sc). Compositionally, the NWA 10495 clan is very heterogeneous. Panels (b) and (d) suggest that Sueilila 005 is not paired with NWA 10495, but panel (e) is consistent with them both being found in the same area. The 3 different pieces of NWA 10495 largely do not overlap in composition. One of the piece "B" samples (6 subsamples) largely plots in the field of typical FLMs while all the others are richer in Sc and plot in the anorthositic norite field. Sc concentrations vary by a factor of 3.5 among subsamples of the NWA 10495 clan and are consistent with FHT-mare mixing if, in fact, the pieces are all paired. Panels (d) and (e) provide the strongest evidence that the 3 NWA 10495 pieces are paired. The other meteorites of the figure (stone means) are all those that plot in the ranges of panel (a–d). Taken together, this figure allows that only NWA 8055 (&) and NWA 11182 (÷) are paired with NWA 10495. We reject the NWA 8055 pairing hypothesis, however, because of the uniformity of the NWA 8055 data in Fig. S71 compared with scatter of the NWA 10495 data here. We reject the NWA 11182 pairing hypothesis because mean concentrations of Sc, Co, Ni, trivalent REE, Hf, Ta, and Th are significant at the 99% confidence level.

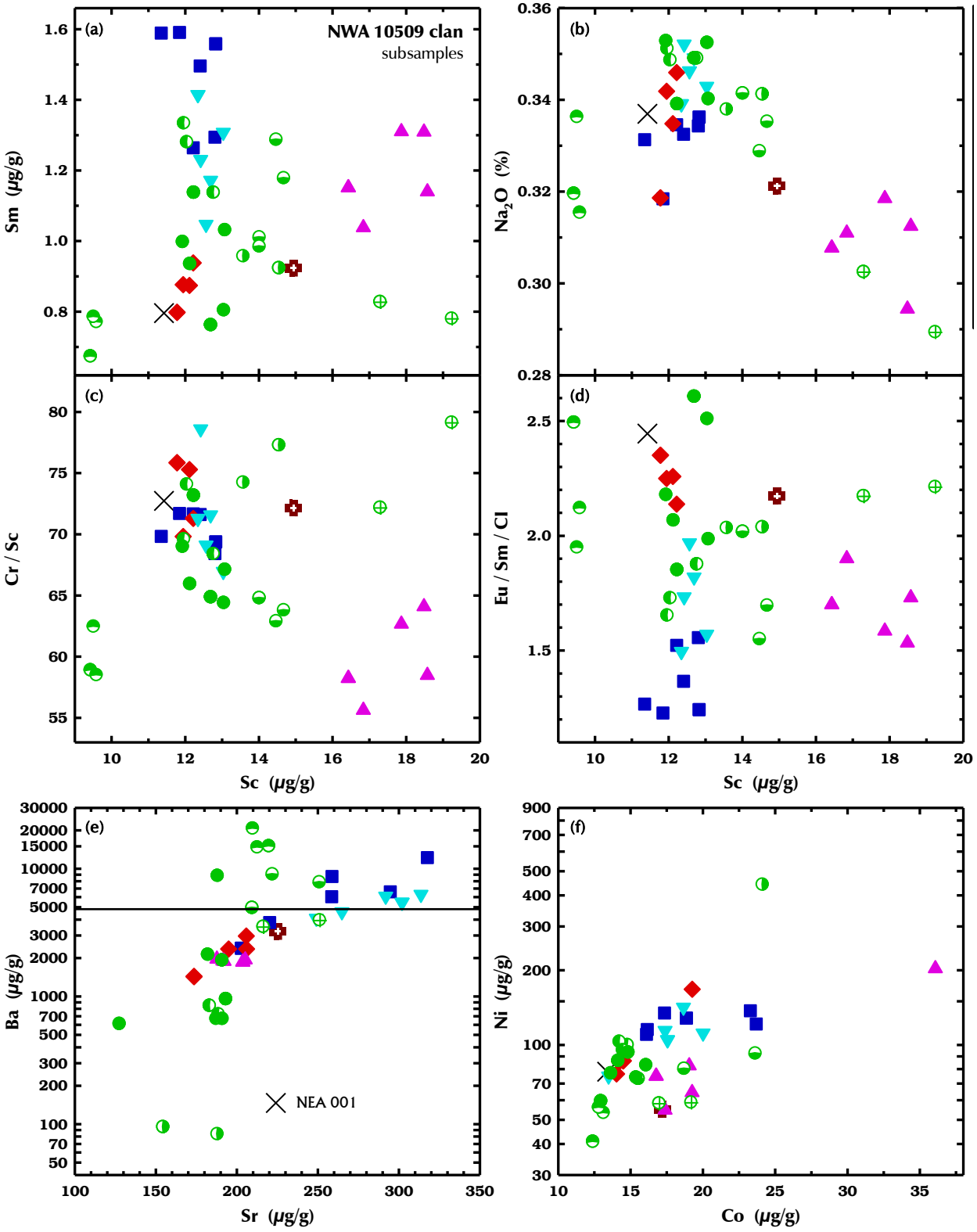
(a)
NWA 10509 clan
subsamples
Sm (μg/g)
(b)
Na2O (%)
(c)
Cr / Sc
Sc (μg/g)
(d)
Eu / Sm / CI
Sc (μg/g)
(e)
Ba (μg/g)
NEA 001
Sr (μg/g)
(f)
Ni (μg/g)
Co (μg/g)

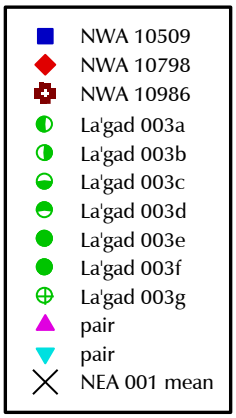

Fig. S73. Except for NEA 001 (Sudan), we assume that all the meteorites of this figure are paired. NWA 10798 (319 g, many pieces) has 0.6–0.7× concentrations of incompatible elements compared to those of NWA 10509 (660 g, 1 piece) but other elements and ratios are similar. La'gad 003 (27 kg, many pieces) is also a Sm-poor anorthositic norite in composition (Fig. 6). We analyzed subsamples of 7 pieces of the large La'gad 003 meteorite, which is compositionally heterogeneous. There is little compositional overlap of La'gad 003 subsamples with the NWA 10509 subsamples but there is overlap with NWA 10798. The single point for NWA 10986 (108 g, several pieces) is the mean of the data of Roberts at al. (2019) and it is upon the basis of this figure that we assume that it is paired with NWA 10509. (e) Together these stones have among the highest Ba concentrations that we observe in NWA lunar meteorites (Ñ symbols of Figs. 16 and S67), which is one of the strongest arguments that they are all paired. The NWA 10509 clan may simply be very heterogeneous. For reference, the large × represents the mass-weighted mean of another heterogeneous meteorite of similar composition, NEA 001 (Fig. S70). We do not suspect launch pairing with the NWA 10509, however, because differences in several mean concentrations and ratios (Sc, Fe, Co, all trivalent REE, Hf, Th, Na/Sm, and Sm/Eu) are significantly different at the 99% confidence level (Welch's *t*-test; Welch, 1947). Clan mass: 28.2 kg.

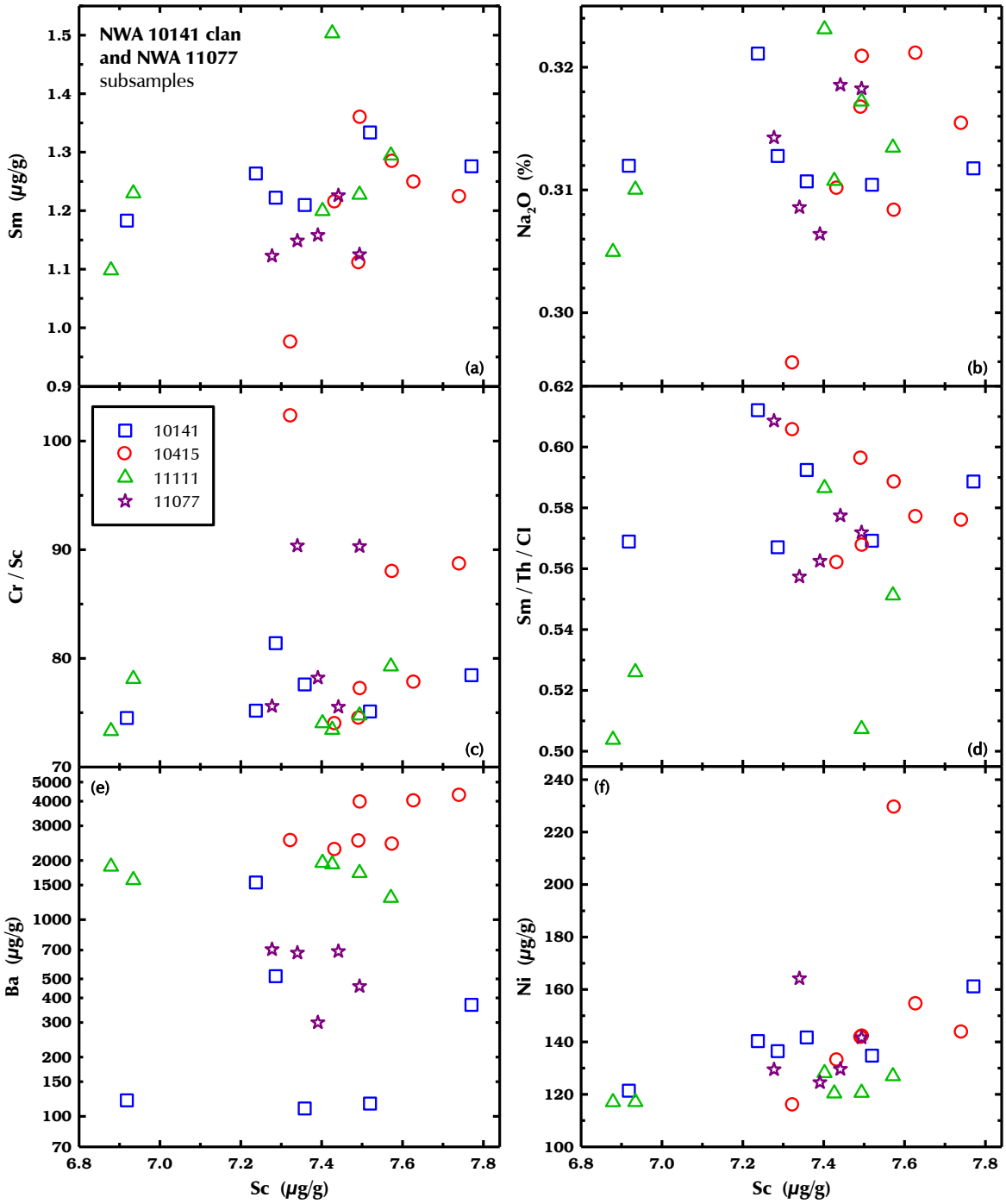

Fig. S74a. Except for Ba, data for subsamples of NWA 10141, 10415, and NWA 11111 overlap for all elements and we assume that the stones are paired. NWA 11077 is similar, but concentrations of Sr (0.68×), Ba (0.35×), and the light REE (La, Ce, Nd, and Sm: (0.87–0.93×) are significantly lower (Welch's t-test, 99% confidence level) in the mass-weighted mean of the 7 subsamples of NWA 11077 than the 24 subsamples of the NWA 10141 clan. A lower degree of terrestrial weathering in NWA 11077 can account for all these differences. NWA 11077, however, has a very different texture (Fig. S74b), so our working hypothesis is that it might be a launch pair of the NWA 10141 clan.

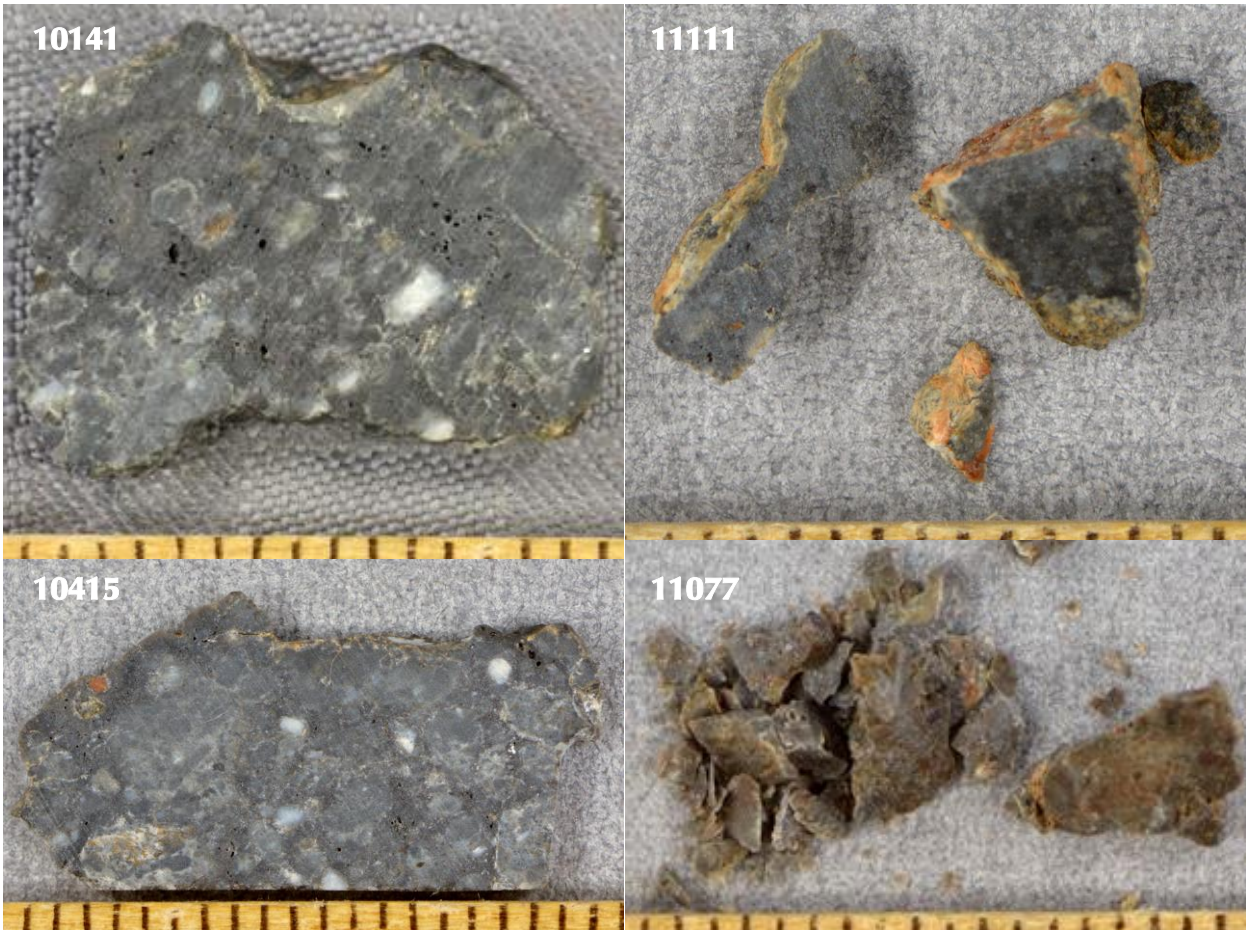

Fig. S74b. Photos of the samples of the 4 stones of Fig. S74a; millimeter ticks for scale. NWA 10141 and NWA 10415 have clasts (up to 7 mm in size on the basis of online photos) and vesicular shock melt (C. Agee in MetBull). NWA 11111 is described as "Fine-grained mineral (plagioclase, low-Ca pyroxene and olivine) clasts and anorthositic rock debris (0.01–0.6 mm) are set in the very fine-grained recrystallized matrix… Minor unrecrystallized shock melt veins (~50 μm) are also present" (Li Y. in MetBull). NWA 11077 differs significantly: "Extremely fine-grained breccia consisting mainly of very tiny mineral grains plus devitrified glass (some with swirly texture visible in thin section) plus sparse lithic clasts, which are themselves melt rocks with intersertal texture and sparse relict clasts" (A. Irving and S. Kuehner in MetBull).

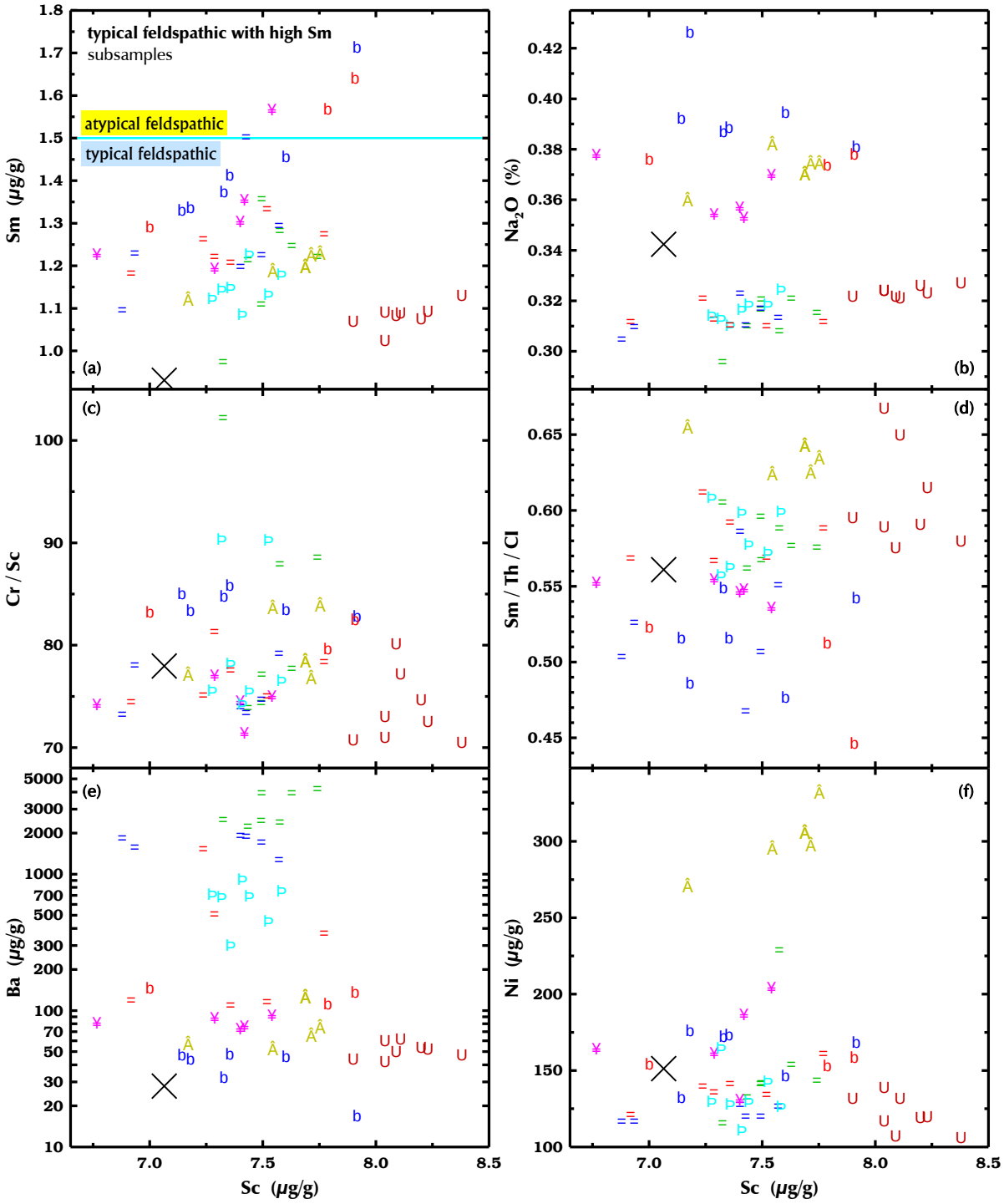

U	6578
b	10073
=	10141
=	10415
=	11111
Þ	11077
Â	11352
¥	rock 87
×	typFLM

Fig. S75. Meteorites at the high-Sm end of the range of typical feldspathic lunar meteorites (Fig. S17). Data for NWA 10141, NWA 10415, NWA 11111, and NWA 11077 are the same as those of Fig. S74a. Subsamples of NWA 10073 define a linear mixing trends in (a), (c), and (e), unlike any of the other meteorites, so we assume that it is unpaired. NWA 6578 is distinct. NWA 11352 overlaps with the NWA 10141 clan in (a) and (c) but not in (b) and (d). The large × represents the mean composition of typical feldspathic lunar meteorites (Table S5).

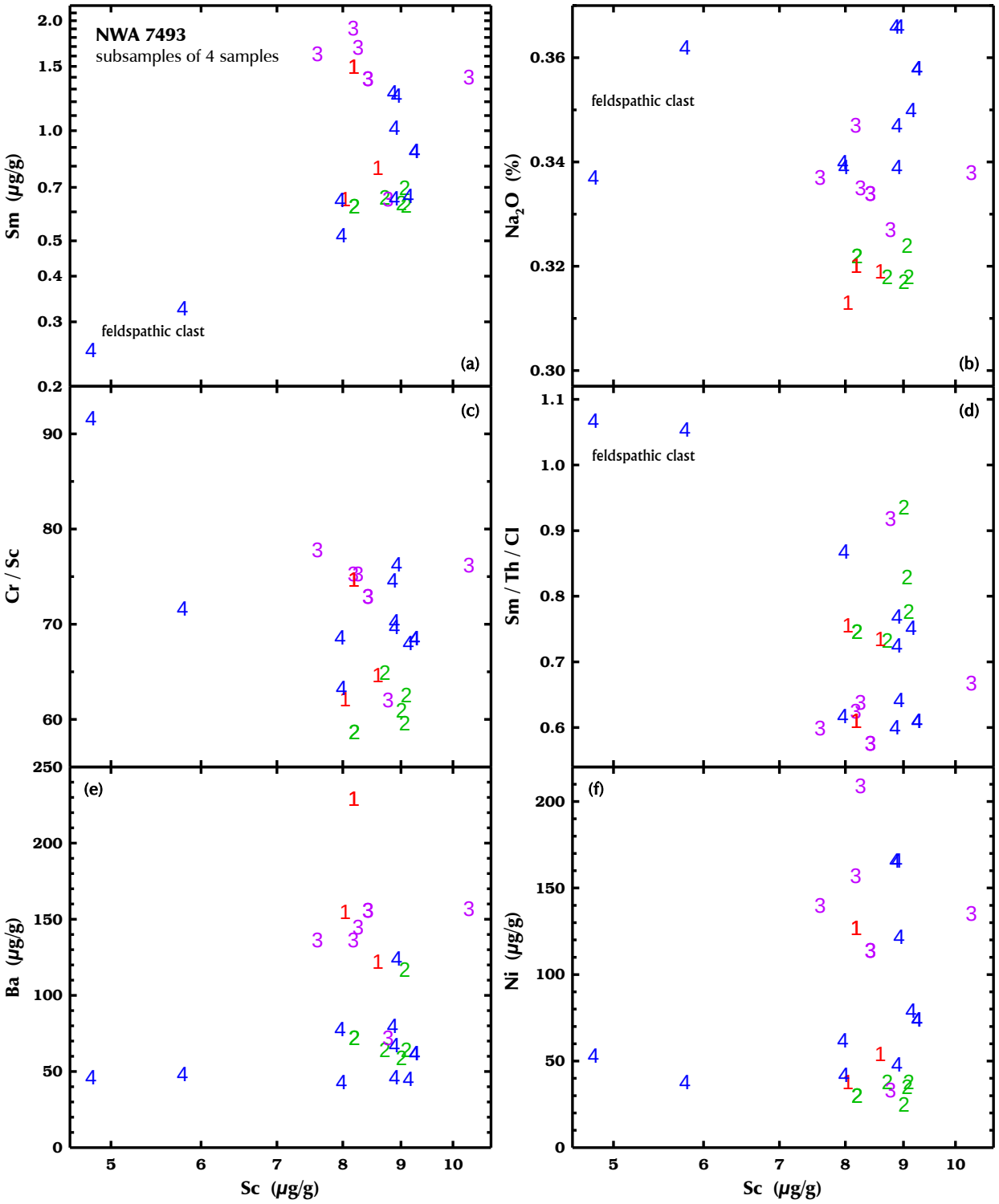

Fig. S76. NWA 7493 (503 g) is a typical feldspathic lunar meteorite (6 pieces totaling 503 g). We analyzed subsamples of 4 different samples (Table S2). Samples 1, 2, and 4 are from a 146-g piece and sample 3 is from a 341-g piece. (a) The latter is slightly richer in Sm (a). The meteorite is one of the most heterogeneous in composition of feldspathic lunar meteorites (Figs. S17–S21), with piece 4 having two subsamples containing fragments of a feldspathic clast (photo: Fig. S1f).

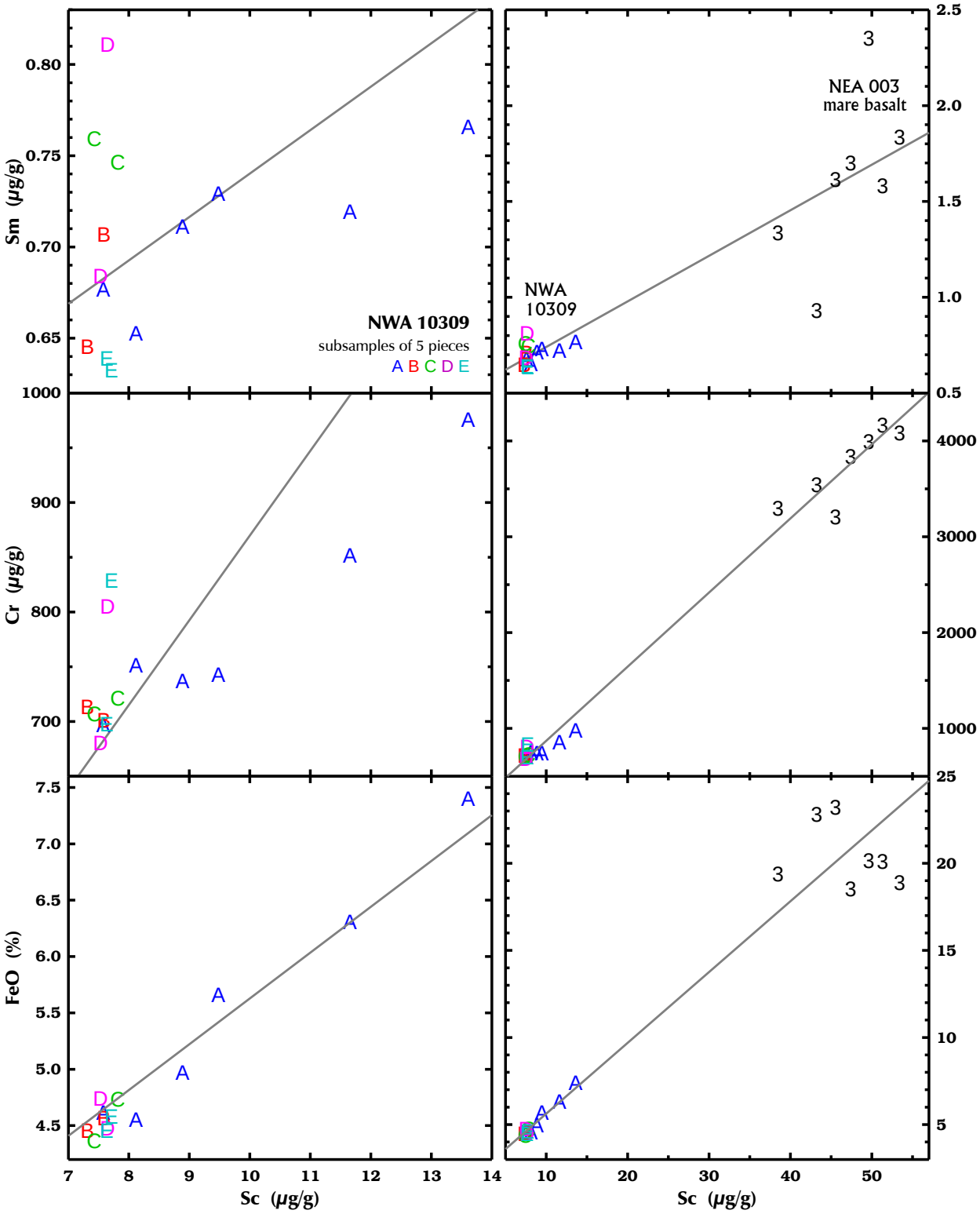

Fig. S77. (left) Subsample data for five (A–E) of the "several" (MetBull) pieces of NWA 10309 (16.5 kg total). NWA 10309 is one of the NWA 8046-clan stones (Fig. S24). The data for pieces B–D overlap with each other but 5 of the 6 A-pieces subsamples are richer in Sc. (right) The trend of the NWA 10309 A-stone subsamples extrapolates toward mare basalt with a composition like that of NEA 003. For reference, in all panels the lines are defined by the points corresponding to the mass-weighted means of the NWA 10309 and NEA 003 subsamples.

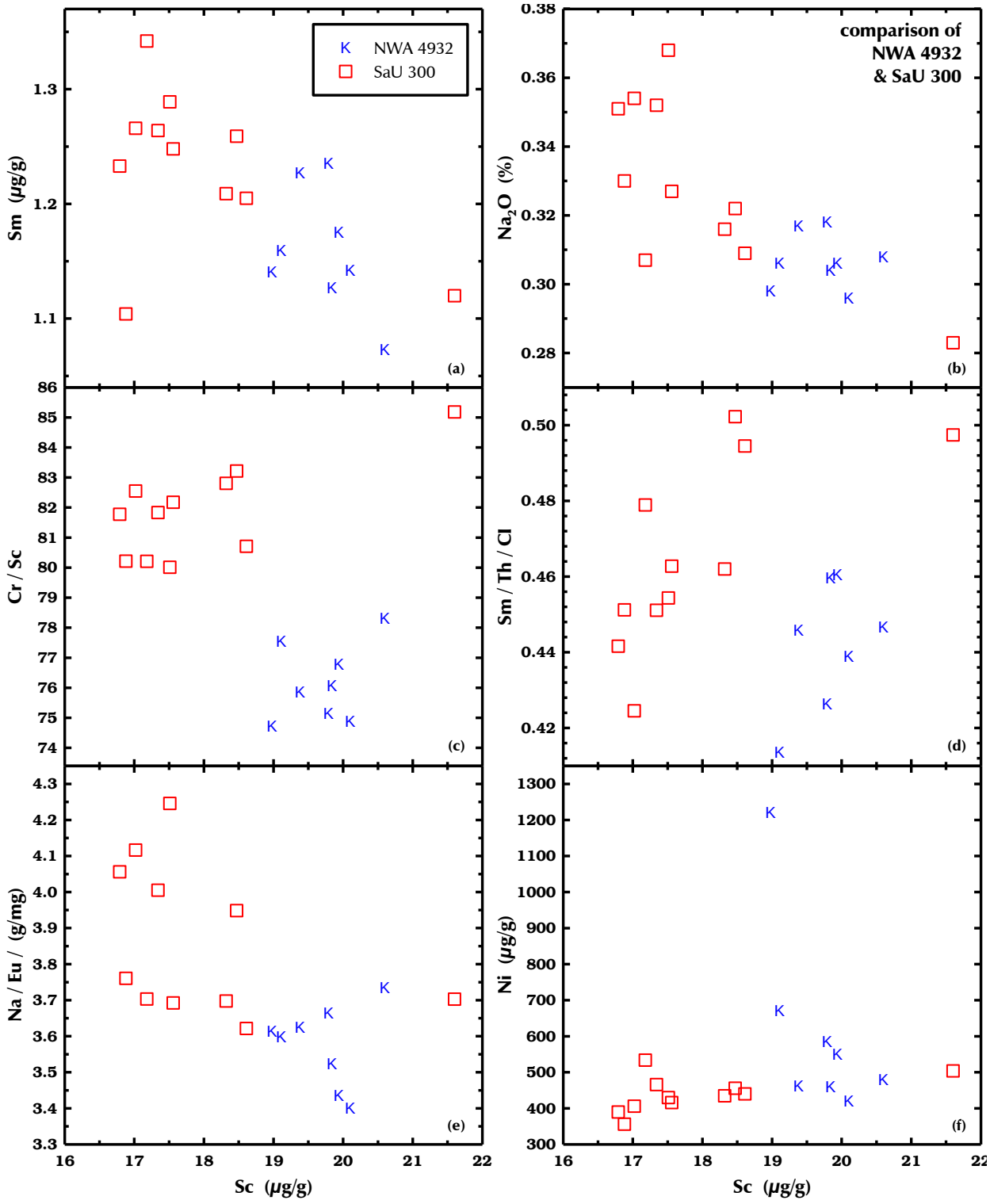

Fig. S78. Comparison of subsample data for NWA 4932 (93 g) and SaU 300 (Oman; 153 g). We previously suggested that these two meteorites may be launch paired (Korotev et al., 2009) but on the basis of this figure, we reject that hypothesis now. These are the only 2 lunar meteorites for which the stone means plot in all 6 panels of the figure. Mean concentrations or ratios of Sc, Cr/Sc, and Na/Eu are significantly different at the 99% confidence level (Welch's *t*-test).

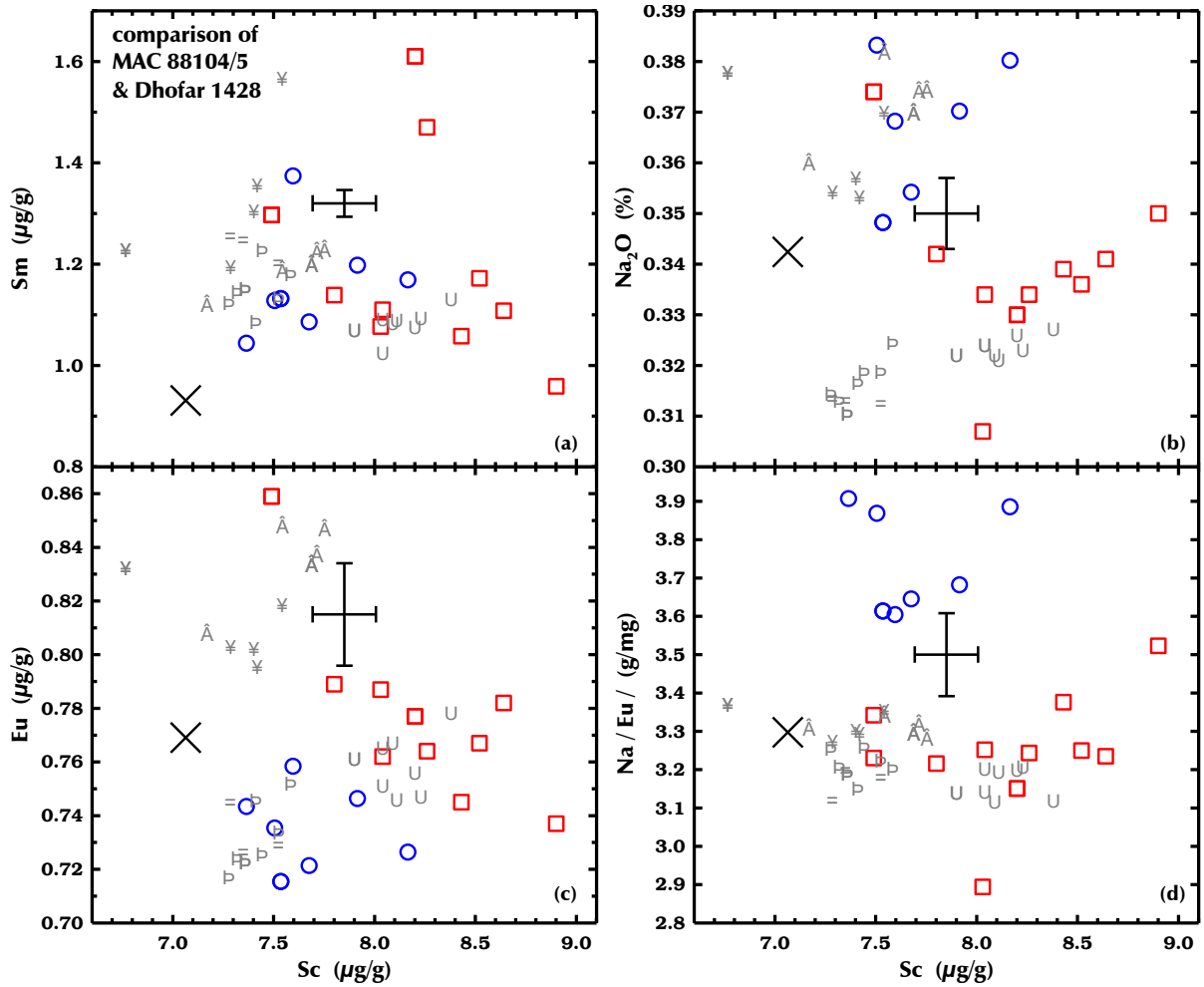

Fig. S79. Like Fig. S75, but with addition of subsample data for MAC 88104/5 (MacAlpine Hills, Antarctica) and Dhofar 1428 (Oman). We previously suggested that these two meteorites may be launch paired because of their similar compositions (Korotev and Zeigler, 2005) but, on the basis of this figure, we now reject that hypothesis. Mean concentrations or ratios of Na, Eu, and Na/Eu are significantly different at the 99% confidence level (Welch's *t*-test). Subsample data for NWA meteorites of similar composition are also shown except that for the NWA 10141 clan, stone means of the three stone are plotted (see Fig. S74). (d) Dhofar 1428 is not likely launch paired with any of the other meteorites of the figure. (b) MAC 88104/5 is distinct from NWA 11077, NWA 11352, and the NWA 10141 clan. Statistically, panel (b) eliminates NWA 6578 from being a likely launch pair to MAC 88104/5 (99% confidence level). Also, NWA 6578 is a granulitic breccia of uniform composition (Fig. 7) whereas as MAC 88104/5 is a regolith breccia of less uniform composition (several clast-rich subsamples of MAC 88104/5 plot off the scale of these plots). The large × represents the mean composition of typical feldspathic lunar meteorites (Table S5). MAC 88104/5 data are from Table S2 (those chip subsamples >10 mg in mass but excluding several clast-rich subsamples). The error bars represent typical 2s analytical uncertainties.

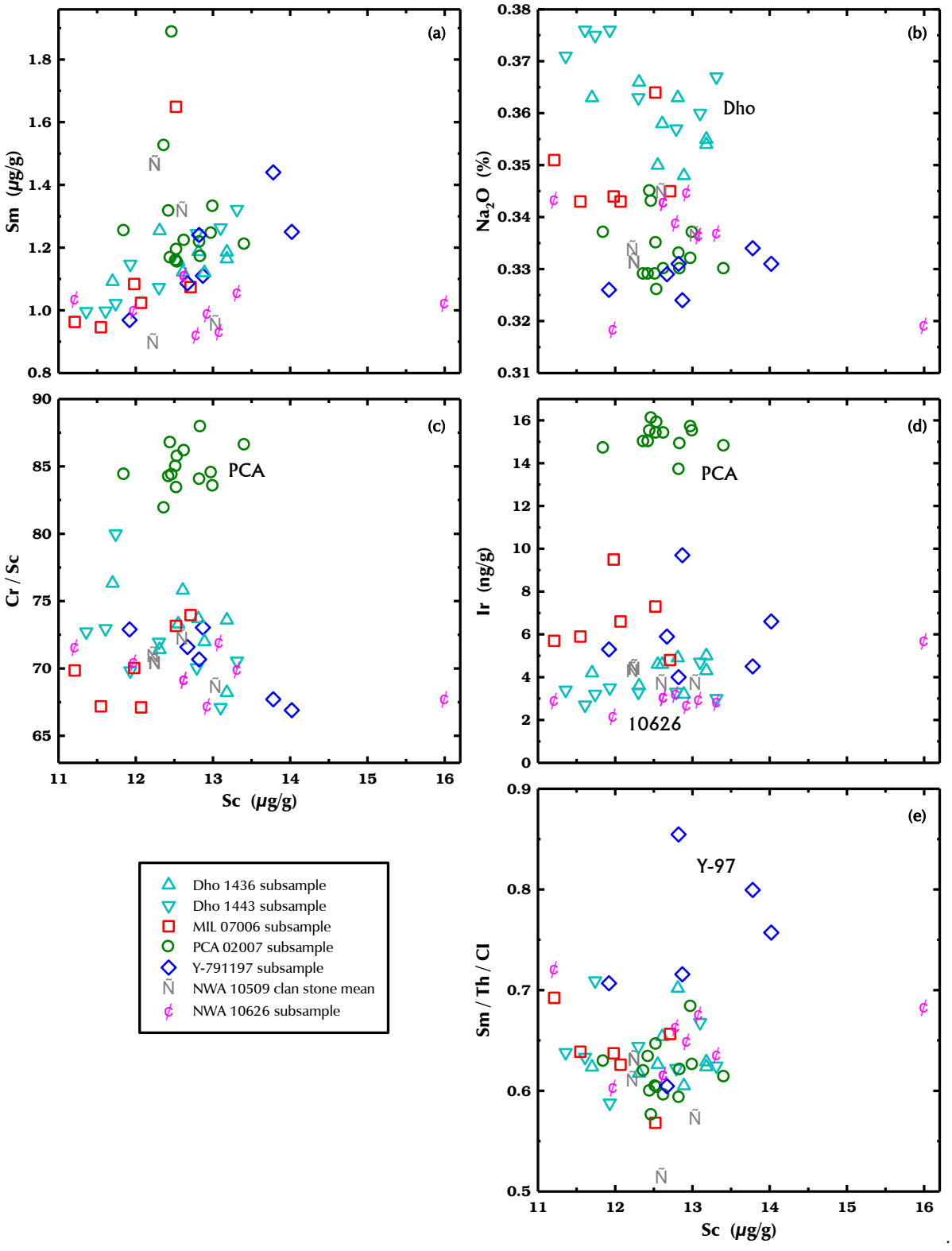
(a)
Sm (μg/g)
(b)
Na2O (%)
Dho
(c)
Cr / Sc
PCA
Sc (μg/g)
(d)
Ir (ng/g)
PCA
10626
(e)
Sm / Th / Cl
Y-97
Sc (μg/g)
Dho 1436 subsample
Dho 1443 subsample
MIL 07006 subsample
PCA 02007 subsample
Y-791197 subsample
NWA 10509 clan stone mean
NWA 10626 subsample

Fig. S80. Like Fig. S71, but including non-African meteorites: lunar meteorites with slightly greater Sc (>11 μg/g) but similar Sm (<1.5 μg/g Sm, Fig. S17) to typical feldspathic lunar meteorites. We previously suggested "Compositionally, MIL 07006 is similar to PCA 02007 and Yamato 791197 from Antarctica, but it is much more similar to Dhofar 1436/1443 [paired, Korotev, 2012] from Oman." This figure shows that this speculation is not accurate.

Lunar meteorite pairs		Elements for which the differences in mean concentrations are significant at 99% confidence limit (Welch's *t*-test)	
LM 1	LM 2	well behaved	contamination
Dho 1436/1443	MIL 07006	Na, Ni, Eu, Ni/Co	As, Br, Sr, Ba
Dho 1436/1443	NWA 10509 clan	Na, Ni, Eu, Ni/Co	As, Br, Sr, Ba
Dho 1436/1443	NWA 10626 clan	Na, REE, Eu, Hf, Th	Sr, U
Dho 1436/1443	PCA 01007	Na, Cr, Fe, Co, Ni, Eu, HREE, Hf, Ta, Ir, Cr/Sc, Na/Sm, Sm/Eu, Ni/Co	Ca, As, Sr, Ba, U
Dho 1436/1443	Y-791197	Na, Co, Ni, Eu, Ni/Co	As, Sr, Ba, U
MIL 07006	NWA 10509 clan	Na, Sc, Eu, Ir, Ni/Co	Ca, As, Br, Sr, Ba
MIL 07006	NWA 10626 clan	Eu, Ir	
MIL 07006	PCA 01007	Na, Ca, Cr, Fe, Co, Ni, Eu, Ir, Cr/Sc	
MIL 07006	Y-791197	Na, Eu	
NWA 10509 clan	NWA 10626 clan	Th, Sm/Th	Ca, As, Sr, Ba, La
NWA 10509 clan	PCA 01007	Cr, Fe, Co, Ni, HREE, Hf, Ta, Ir, Cr/Sc, Na/Sm, Sc/Eu	Ca, As, Sr, Ba
NWA 10509 clan	Y-791197	Th, Sm/Th, Ni/Co	Ca, As, Sr, Ba
NWA 10626 clan	PCA 01007	Ni, REE, Hf, Ta, Th, Cr/Sc, Na/Sm, Sm/Eu	Ca
NWA 10626 clan	Y-791197	Ir	
PCA 01007	Y-791197	Cr, Co, Ni, Ir, Th, Cr/Sc, Sm/Th, Ni/Co	

The data show that:

1) There is no evidence that Dho 1436/1443 (terrestrially paired) and PCA 02007 are launch paired with any of the other meteorites of the figure.
2) Na and Eu concentrations are greater by 1.06× in MIL 07006 than Y-791197, but other than that the compositions are identical the meteorites are possible launch pairs. Preliminary cosmic-ray exposure data appear to exclude launch pairing, however (Nishiizumi et al. 1991. Nishiizumi and Caffee, 2013).
3) The NWA 10509 and NWA 10626 clans may be launch paired. The NWA 10509 clan has much greater concentrations of elements associated with terrestrial contamination (Figs. S71 and S73), suggesting a different find location.
4) Y-791197 is allowably launch paired with NWA 10626 clan but less likely with the NWA 10509 clan.

INAA Procedures and Uncertainties

Procedures

For the meteorites from northern Africa, we acquired the data presented or summarized here following 53 different neutron irradiations from February 1999 through June 2018. INAA procedures are those described in Korotev et al. (2009) except for two major differences. First, in January 2013, we replaced the ancient analog gamma-ray spectrometry electronics (multichannel analyzer) with four Lynx® digital signal analyzers (Canberra Industries Inc.). This upgrade led to a distinct improvement in photopeak resolution which in turn results in more accurate concentration data for some elements (Ce, Nd, Zn) obtained from gamma-ray spectra acquired over the last 22 neutron irradiations (starting with irradiation #377, Table S2). Second, in November 2014, we replaced the TEABAGS data-reduction software (FORTRAN code) of Lindstrom and Korotev (1982) with GENIE-2000® basic spectroscopy and interactive peak-fit software (Canberra Industries Inc.). Although more tedious to use, the proprietary software has led to some improvements in data quality for elements at or near detection limits for data obtained from the last 17 irradiations (starting with irradiation #382 in Table S2). We convert the peak-area data obtained from the GENIE system to concentration values with Microsoft Excel®.

NWA 5000 Sawdust and INAA Uncertainty and Error

We obtained from Adam Hupé ~1 g of sawdust from the cutting of 11.5-kg NWA 5000. This material provides a better average composition of the course-grained meteorite (Fig. S27) than do the subsample data (Fig. S29). It also provides a means of addressing systematic error and assessing the batch-to-batch precision of our INAA procedure. We have included one (sometimes two) sample of the sawdust in each batch of samples irradiated between May of 2008 and September of 2016 (Table S8), during which time 56% of the northern-Africa-subsample data presented here were obtained.

Systematic Error from Nonuniform Neutron Flux

Concentrations of incompatible elements in the sawdust (Table S8) are about 1.5× that of the mass-weighted mean of the 20 chips of NWA 5000 that we analyzed (Table S3). Almost certainly, this difference is simply a sampling issue (Fig. S29). Concentrations of Ni, Zn, Ag, Sb, and Au are greater in the sawdust, however, as a result of contamination from the diamond band-saw blade used to cut the rock.

In the 27 sawdust samples (Table 8), Na and Eu have the lowest relative standard deviations, 1.2% each (Table 8). From the sampling perspective, it is reasonable that concentrations of these two elements are most constant because both elements are carried mainly by plagioclase and the rock is 75% plagioclase by mass. (The relative standard deviation for CaO is 1.5%.)

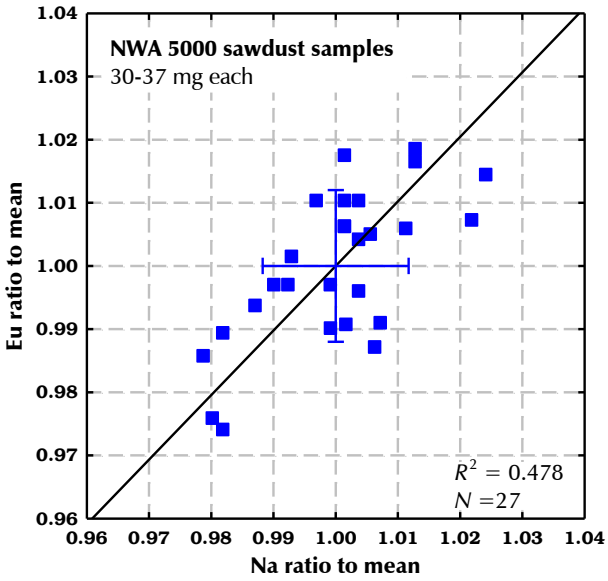

Fig. S81. Eu and Na concentrations in samples of NWA 5000 sawdust are moderately well correlated. The error bars represent standard deviations, 1.2% each. The line is a least-squares fit to the data with both Na and Eu concentrations weighted by 1.2%.

Concentrations of Na and Eu are correlated among the samples, with the trend extrapolating to the origin (Fig. S81). This behavior is what we would expect from small variations among the samples in the ratio of plagioclase to all other phases, mainly pyroxene. Such variation is not the cause of the trend, however. The relative standard deviation for Sc, carried mainly by pyroxene, is only slightly larger than that for Na and Eu, 1.5% but Sc correlates weakly, but positively, with Na and Eu (Fig. S82 a,b). If the correlation were due to variable plagioclase/pyroxene, then Sc would decrease with increasing Na or Eu.

We expect that much of the scatter for precisely determined elements is, instead, the result of systematic analytical error that affects all elements to the same degree. In INAA, possible sources of such error are imprecision in sample mass determination, nonuniformity in thermal neutron flux between a sample and standard(s), and variation in sample-to-detector geometry during radioassay. We believe that most of the systematic variation of Fig. S81 is due to inhomogeneous neutron flux (Korotev, 1996). For example, three different samples of the Na and Eu standard (a synthetic glass) are used in each irradiation and it is common (but frustrating) to see that one such sample has, for example, ~1% lower concentrations of all precisely determined elements than another. If for each sample we (1) calculate the ratio of the concentration of each element to the mean concentration of all samples ("ratio to mean"), (2) average the ratio-to-mean for Na and Eu for each sample, and (3) divide all concentration values for each sample by this mean ratio, we can effectively factor out the effects of flux variation. This procedure reduces the relative standard deviations in Na concentration from 1.17% to 0.47% and that for Eu from 1.20%& to 0.47%. It also removes the correlation between Sc and Na or Eu (Fig. S82c,d).

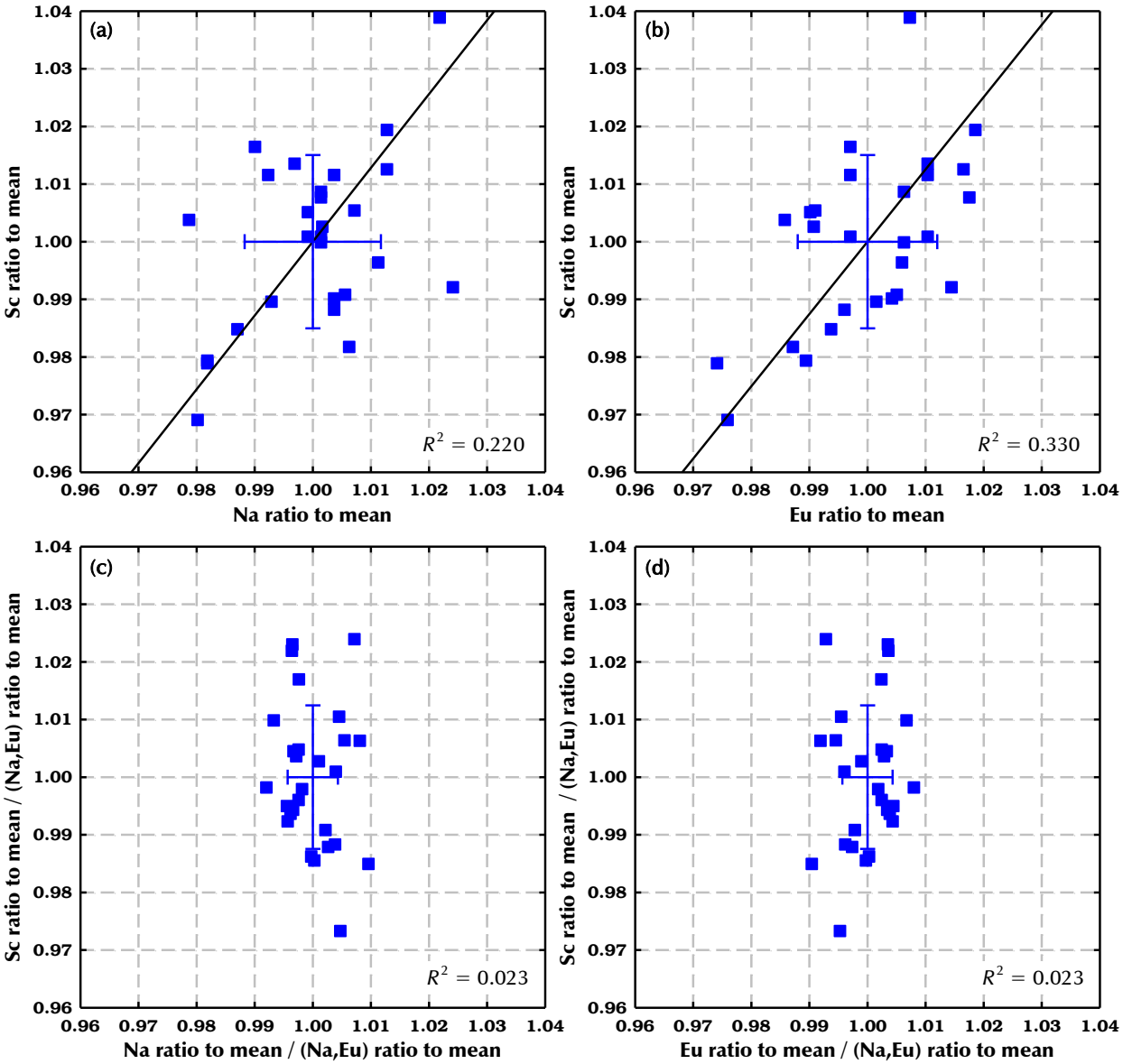

Fig. S82 (a,b) Sc correlates positively with Na and Eu, which is not consistent with variation in the plagioclase to pyroxene ratios among the samples. The error bar represents ± 1 standard deviation. (c,d) Normalizing the data as described in the text removes the correlation.

In summary, all data presented here are subject to a component of systematic error from nonuniform neutron flux experienced by the ~60 sample tubes of a sample pack in each irradiation. The effect is to cause all concentration values in a given sample to be up to 2.5% low or high (i.e., max/min values of 1.05 for Na_2O and Eu, Table S8) compared to the mean of many such analyses. The standard deviation of this effect is about 1%. Thus, the 2-σ analytical uncertainties in Table S2 are calculated as $\sigma^2 = \sigma_f^2 + \sigma_c^2$, where σ_f is 1% of the concentration value and σ_c is the standard deviation calculate from counting statistics. (The value σ_c is much less than 1% for Na, Sc, Cr, Fe, Co, La, Sm, and Eu for all samples.)

Table S8. Results of INAA for NWA 5000 sawdust

sample	Na_2O	CaO	Sc	Cr	FeO_T	Co	Ni	Zn	As	Br	Rb	Sr	Zr	Ag	Sb	Cs	Ba
	%	%	μg/g	μg/g	%	μg/g	μg/g	μg/g	μg/g	μg/g	μg/g	μg/g	μg/g	μg/g	μg/g	μg/g	μg/g
364.40	0.439	15.3	10.40	788	5.83	30.8	755	101	0.35	0.27	1.3	187	65	96	0.12	0.043	128
364.41	0.441	15.2	10.26	775	5.70	32.4	810	105	0.34	0.32	1.2	192	63	103	0.11	0.040	126
365.47	0.441	15.0	10.34	783	5.71	27.7	671	105	0.40	0.22	3.5	184	61	106	0.13	0.042	119
366.28	0.437	14.7	10.38	788	5.85	34.9	849	86	0.25	0.25	1.1	194	61	112	0.12	0.050	119
370.24	0.442	14.9	10.16	769	5.62	29.1	690	n.a.	0.29	0.29	n.a.	186	68	108	0.10	0.052	124
371.33	0.440	15.0	10.27	773	5.67	29.4	771	112	0.34	0.26	n.a.	191	78	111	0.10	0.041	121
372.44	0.450	15.4	10.66	809	5.90	31.2	771	95	0.28	0.26	2.6	189	66	106	0.11	0.056	121
373.20	0.436	14.9	10.43	792	5.85	31.4	775	96	0.29	0.20	1.3	190	66	104	0.09	0.030	125
374.14	0.431	14.8	10.30	773	5.75	32.3	799	103	0.35	0.30	2.6	192	64	105	0.13	0.048	124
375.23	0.446	15.3	10.39	798	5.76	28.7	699	100	0.39	0.30	3.1	189	76	111	0.10	0.050	123
376.30	0.446	15.4	10.46	793	5.81	30.6	763	101	0.30	0.26	2.5	187	79	106	0.10	0.045	121
377.48	0.441	15.1	10.35	778	5.78	31.2	816	106	0.35	0.27	2.6	186	71	102	0.80	0.050	125
378.52	0.441	14.3	10.27	764	5.66	29.1	748	104	0.33	0.26	1.5	172	70	104	0.13	0.041	115
379.52	0.451	14.4	10.18	751	5.59	28.0	720	104	0.23	0.28	1.7	213	66	104	0.10	0.036	117
380.54	0.442	14.7	10.14	756	5.69	30.5	745	106	0.29	0.44	1.9	173	61	109	0.13	0.038	102
381.46	0.442	15.0	10.38	775	5.79	32.2	733	110	0.45	0.25	1.3	176	62	117	0.11	0.035	112
382.47	0.445	14.6	10.22	763	5.77	32.7	789	98	0.46	0.29	2.4	187	84	106	0.09	0.044	122
383.32	0.432	14.3	10.04	743	5.54	28.5	728	97	0.36	0.48	1.8	165	80	134	0.10	0.041	117
384.53	0.437	14.6	10.15	760	5.64	28.1	691	97	0.50	0.34	1.9	181	80	99	0.13	0.070	111
385.51	0.435	14.4	10.11	757	5.58	28.0	717	101	0.19	0.30	1.4	175	83	104	0.12	0.050	141
386.52	0.443	14.9	10.17	762	5.59	28.6	724	101	0.33	0.31	1.7	158	91	106	0.12	0.044	123
387.53	0.432	14.5	10.05	754	5.59	28.3	709	113	0.37	0.28	1.4	214	107	116	0.12	0.040	117
388.51	0.432	14.4	9.94	742	5.49	27.7	671	126	0.42	0.34	1.7	181	99	105	0.13	0.045	117
388.52	0.444	14.5	10.32	768	5.77	31.0	781	94	0.41	0.16	1.8	173	81	117	0.14	0.044	112
389.52	0.441	14.8	10.29	779	5.80	32.4	805	86	0.64	0.16	2.0	197	83	113	0.14	0.034	113
390.53	0.440	14.4	10.31	780	5.74	29.4	1349	2798	0.83	0.34	1.4	289	87	142	0.96	0.038	115
391.53	0.443	14.6	10.07	760	5.57	28.7	729	80	0.68	0.17	1.5	181	59	114	0.14	0.037	123
$\bar{x}_{mw}$	0.440	14.8	10.26	772	5.70	30.1	748	97	0.39	0.28	1.7	189	74	108	0.12	0.044	120
$\bar{x}$	0.440	14.8	10.26	772	5.71	30.1	748	101	0.39	0.28	1.9	189	74	108	0.12	0.044	120
s	0.005	0.3	0.15	17	0.11	1.9	47	9	0.14	0.07	0.6	23	12	7	0.02	0.008	7
$s/\bar{x}$, %	1.2	2.3	1.5	2.2	1.9	6.4	6.3	9	36	25	33	12	17	7	14	18	6
min	0.431	14.3	9.94	742	5.49	27.7	671	80	0.19	0.16	1.1	158	59	96	0.09	0.030	102
max	0.451	15.4	10.66	809	5.90	34.9	849	126	0.83	0.48	3.5	289	107	134	0.14	0.070	141
max/min	1.05	1.08	1.07	1.09	1.07	1.26	1.27	1.56	4.4	3.0	3.2	1.83	1.81	1.39	1.60	2.35	1.38
$\sigma_{anal.}$	0.004	0.2	0.10	8	0.06	0.3	10	1	0.08	0.07	0.6	7	7	1.1	0.007	0.015	3
$s/\sigma_{anal.}$	1.17	1.7	1.53	2.16	1.90	6.4	4.6	7.4	1.87	1.08	0.98	3.4	1.68	6.9	2.47	0.53	2.33
N	27	27	27	27	27	27	26	25	27	27	25	27	27	26	25	27	27
$\bar{x}_{mw}$, chips	0.411	15.3	9.94	861	5.76	37.2	530	4	0.57	0.38	n.a.	181	42	<1	0.01	0.028	197
dust/chips	1.07	0.97	1.03	0.90	0.99	0.81	1.41	23.1	0.68	0.75	n.a.	1.04	1.78	>500	17	1.57	0.61

Table 8, continued.

sample	La µg/g	Ce µg/g	Nd µg/g	Sm µg/g	Eu µg/g	Tb µg/g	Yb µg/g	Lu µg/g	Hf µg/g	Ta µg/g	Ir ng/g	Au ng/g	Th µg/g	U µg/g	mass mg	DR
364.40	4.92	12.8	7.0	2.21	0.986	0.444	1.602	0.225	1.70	0.204	18.8	31.8	0.700	0.240	35.21	T
364.41	4.81	12.4	7.6	2.21	0.982	0.450	1.581	0.221	1.69	0.202	17.9	35.6	0.690	0.240	35.40	T
365.47	4.89	12.8	6.8	2.20	0.993	0.437	1.601	0.221	1.70	0.199	16.4	26.4	0.726	0.253	30.49	T
366.28	4.84	12.5	7.6	2.21	0.973	0.436	1.596	0.222	1.68	0.197	20.5	27.5	0.732	0.210	30.99	T
370.24	4.85	12.8	8.3	2.28	0.980	0.447	1.622	0.223	1.59	0.206	16.6	28.2	0.730	0.240	34.20	T
371.33	4.77	12.2	6.8	2.21	0.973	0.426	1.569	0.219	1.68	0.197	17.6	29.9	0.698	0.250	36.64	T
372.44	4.90	12.6	7.1	2.22	0.983	0.457	1.630	0.223	1.74	0.207	18.1	30.4	0.758	0.260	35.58	T
373.20	4.95	12.8	7.2	2.26	0.973	0.448	1.594	0.224	1.70	0.220	18.2	27.6	0.720	0.220	33.67	T
374.14	4.77	12.6	7.1	2.19	0.962	0.445	1.580	0.220	1.67	0.207	19.8	26.3	0.709	0.210	33.76	T
375.23	4.80	12.5	5.9	2.22	0.992	0.443	1.602	0.221	1.69	0.199	16.9	24.3	0.730	0.210	31.54	T
376.30	4.97	12.9	7.4	2.24	0.994	0.443	1.611	0.230	1.76	0.214	17.3	31.1	0.704	0.250	30.30	T
377.48	5.05	13.0	7.4	2.22	0.982	0.444	1.589	0.223	1.76	0.211	19.0	30.2	0.717	0.208	31.53	T
378.52	4.88	12.6	7.6	2.23	0.986	0.441	1.604	0.219	1.74	0.186	16.0	21.2	0.702	0.165	32.64	T
379.52	4.86	12.9	5.9	2.23	0.990	0.443	1.540	0.214	1.62	0.175	17.0	25.0	0.661	0.171	30.96	T
380.54	4.88	12.4	8.7	2.18	0.972	0.434	1.565	0.218	1.63	0.192	19.5	30.3	0.646	0.200	32.43	T
381.46	4.89	12.0	7.2	2.16	0.986	0.439	1.556	0.218	1.69	0.191	19.8	27.4	0.728	0.230	34.92	T
382.47	5.26	12.8	8.4	2.26	0.982	0.451	1.545	0.217	1.60	0.185	21.0	28.8	0.690	0.279	19.91	C
383.32	5.00	12.2	7.4	2.17	0.951	0.415	1.509	0.213	1.56	0.174	16.8	28.3	0.686	0.238	35.08	C
384.53	4.82	12.0	7.3	2.21	0.977	0.436	1.537	0.215	1.63	0.190	16.4	27.6	0.678	0.222	33.42	C
385.51	5.48	13.5	8.1	2.17	0.970	0.439	1.530	0.220	1.63	0.179	16.7	26.4	0.711	0.259	32.85	C
386.52	4.89	12.7	6.8	2.23	0.981	0.428	1.554	0.223	1.73	0.200	17.2	30.0	0.711	0.208	33.63	C
387.53	4.70	12.2	7.0	2.16	0.966	0.437	1.520	0.216	1.61	0.253	18.0	30.9	0.708	0.237	33.27	C
388.51	4.79	12.2	7.2	2.19	0.952	0.426	1.515	0.215	1.68	0.217	16.5	30.6	0.709	0.228	32.52	C
388.52	4.80	12.3	7.8	2.20	0.967	0.435	1.548	0.219	1.72	0.194	19.7	20.7	0.720	0.233	31.63	C
389.52	4.81	12.2	8.5	2.20	0.967	0.428	1.534	0.218	1.69	0.193	20.3	22.4	0.735	0.276	33.33	C
390.53	4.78	11.9	6.5	2.14	0.966	0.419	1.507	0.223	1.71	0.189	17.9	46.1	0.718	0.299	35.71	C
391.53	5.39	12.8	7.4	2.20	0.963	0.415	1.538	0.221	1.67	0.188	17.8	25.1	0.711	0.267	34.01	C
$\bar{x}_{mw}$	4.91	12.5	7.3	2.21	0.976	0.437	1.566	0.220	1.68	0.199	18.0	27.9	0.709	0.233	885.62	
$\bar{x}$	4.92	12.5	7.3	2.21	0.976	0.437	1.566	0.220	1.68	0.199	18.1	27.8	0.708	0.233	32.80	
s	0.18	0.4	0.7	0.03	0.012	0.011	0.036	0.004	0.05	0.016	1.4	3.4	0.023	0.031		
$s/\bar{x}$, %	3.8	2.8	9.4	1.5	1.2	2.5	2.3	1.7	3.2	8.1	8.0	12.3	3.3	13.2		
min	4.70	11.9	5.9	2.14	0.951	0.415	1.51	0.213	1.56	0.174	16.0	20.7	0.646	0.17	19.91	
max	5.48	13.5	8.7	2.28	0.994	0.457	1.63	0.230	1.76	0.253	21.0	35.6	0.758	0.30	36.64	
max/min	1.16	1.13	1.47	1.07	1.05	1.10	1.08	1.08	1.13	1.45	1.32	1.72	1.17	1.81	1.84	
$\sigma_{anal.}$	0.05	0.2	0.6	0.02	0.010	0.007	0.016	0.002	0.02	0.011	0.5	0.7	0.012	0.021		
$s/\sigma_{anal.}$	3.4	1.76	1.25	1.49	1.12	1.64	2.29	1.64	2.80	1.52	3.1	5.2	2.04	1.46		
N	27	27	27	27	27	27	27	27	27	27	27	26	27	27	27	
$\bar{x}_{mw}$, chips	3.26	8.6	5.1	1.50	0.915	0.311	1.17	0.163	1.10	0.14	23.8	9.2	0.494	0.201	632.64	
dust/chips	1.51	1.46	1.45	1.47	1.07	1.41	1.34	1.35	1.52	1.47	0.76	3.02	1.44	1.16		

Table 8, continued. Footnotes

sample	(irradiation number).(tube number). Note that there were 2 tubes each included in irradiations 364 and 388.
FeO_T	total Fe as FeO
DR	data reduction, T = Teabags, C = Canberra; see text.
n.a.	not analyzed
$\bar{x}_{mw}$	mass-weighted mean concentration
$\bar{x}$	arithmetic mean concentration
s	sample standard deviation
$s/\bar{x}$, %	relative sample standard deviation
min	minimum concentration value
max	maximum concentration value
max/min	maximum concentration/ minimum concentration
$\sigma_{anal.}$	1-standard deviation estimate of analytical uncertainty (counting statistics)
$s/\sigma_{anal.}$	For values substantially greater than unity, sampling uncertainty exceeds analytical uncertainty
N	number of samples analyzed
$\bar{x}_{mw}$, chips	mass weighted mean concentrations of 20 chips of subsamples from Table S2.
dust/chips	ratio of mass-weighted means, sawdust/chips
italics	contamination suspected; values not included in means and standard deviation. In sample 390.53 we suspect fragment of saw blade in the sawdust.

Systematic Error with Time

The NWA 5000 sawdust data allow us to seek any systematic error with time over the 25 neutron irradiations. As noted in Chemical Analysis section, in 2014 we changed software that extracts photopeak areas from the gamma-ray spectra. For most elements there is no significant difference from changing the peak-area software. For five elements, the difference is >1% and statistically significant (Welch's t-test, 95% confidence limit), however.

(1) **Ca.** Post-change values are 0.972× the pre-change values (Fig. S83) but the difference is significant. We suspect the post-change values are better because the Canberra software deals better with the spectral interference on the 1297 keV peak of ^{47}Ca from the huge 1292 keV peak of ^{59}Fe and the 1299 keV peak of ^{152}Eu.

(2) **As.** Arsenic is imprecisely determined at 39% (2 standard deviations / mean concentration) . Post change values are 1.44× the pre-change values (not shown in Fig. S83), and the difference is significant. We suspect the post-change values are better because the Canberra software is better at extracting peak areas from peaks with high signal to noise.

(3) **Zr.** We determine Zr with poor to moderate analytical precision in NWA 5000, 20% (2 standard deviations). The post-change values are 1.32× the pre-change values, a significant difference. We don't know the cause of this difference. Hafnium is determined at high precision.

(4) **Yb.** The analytical precision for Yb is high, ~2% (2 standard deviations). The post-change data for Yb is 0.968 times the pre-change data, a significant difference (95% confidence limit). We do not know the cause of the discrepancy.

(5) **U.** We determine U with poor to moderate precision, 18% in NWA 5000. The post-change concentration values average 1.12× the pre-change values, a significant difference. Both the 228 keV and 278 keV peaks of ^{239}Np used to determine U concentrations have spectral interferences from ^{182}Ta (229 keV) and ^{133}Ba (276 keV). We suspect that the post change values are better for the same reason as for As.

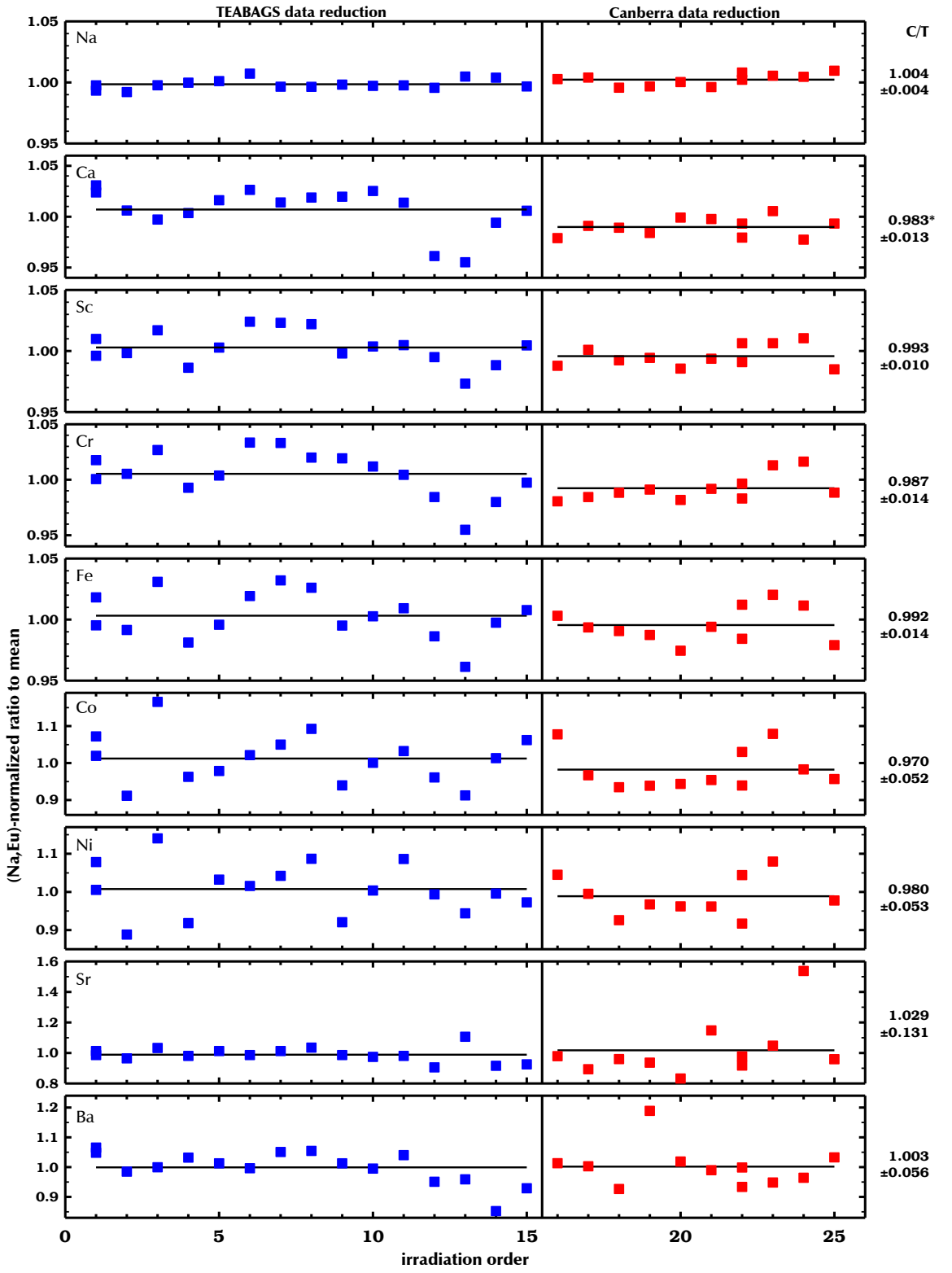

Fig. S83. NWA 5000 sawdust: Normalized ratios-to-mean (see text) as a function of irradiation (batch) order (May 2008 to October 2016). Before irradiation #15, we used the TEABAGs software of Lindstrom and Korotev (1982) to calculate photopeak areas. After that we used proprietary software of Canberra Industries (see text). The C/T data on the right is the ratio (with 95% confidence limits) of the latter means to the former means. Those ratios with asterisks (*) are significantly different from unity.

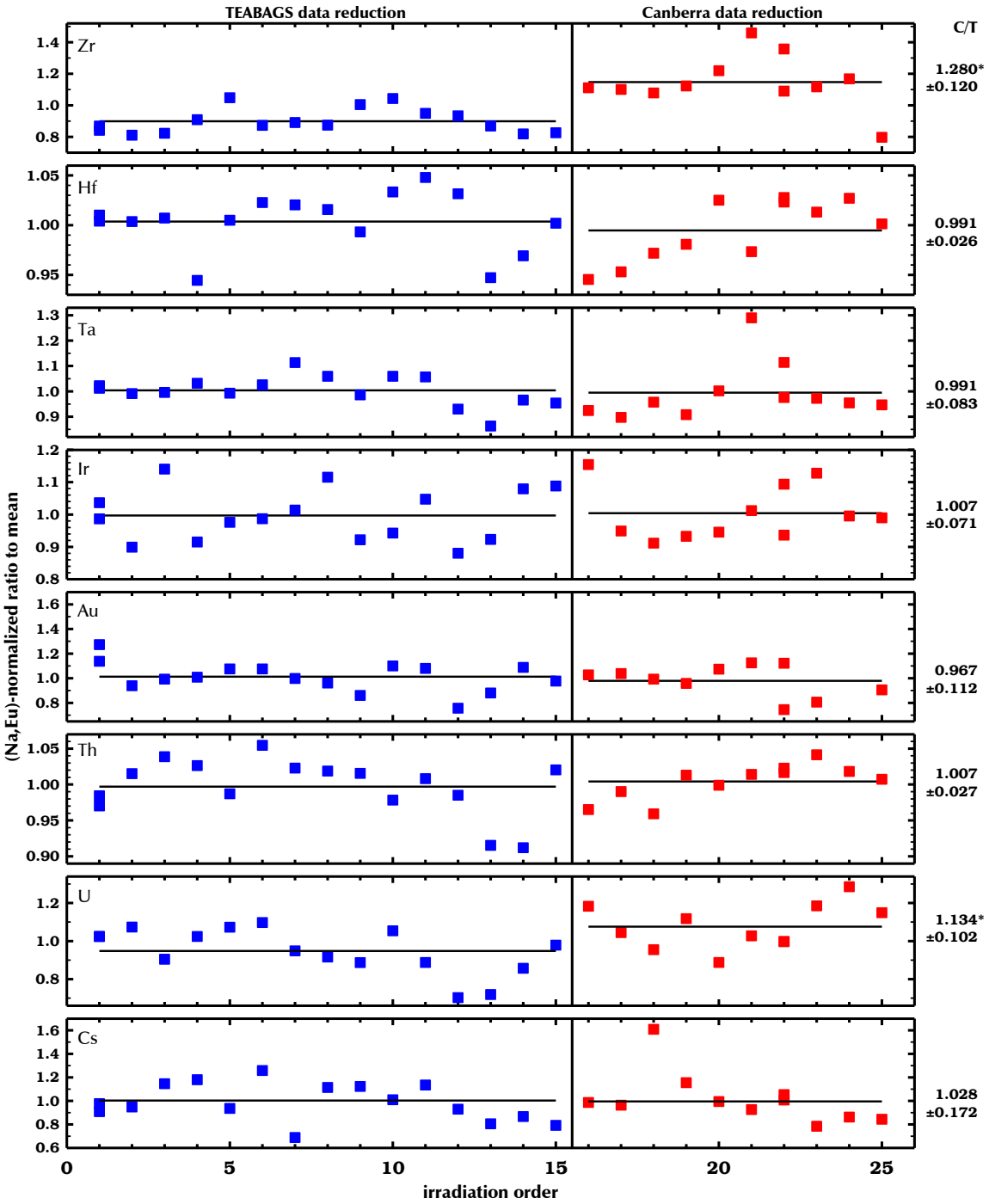

Fig. S83, continued.

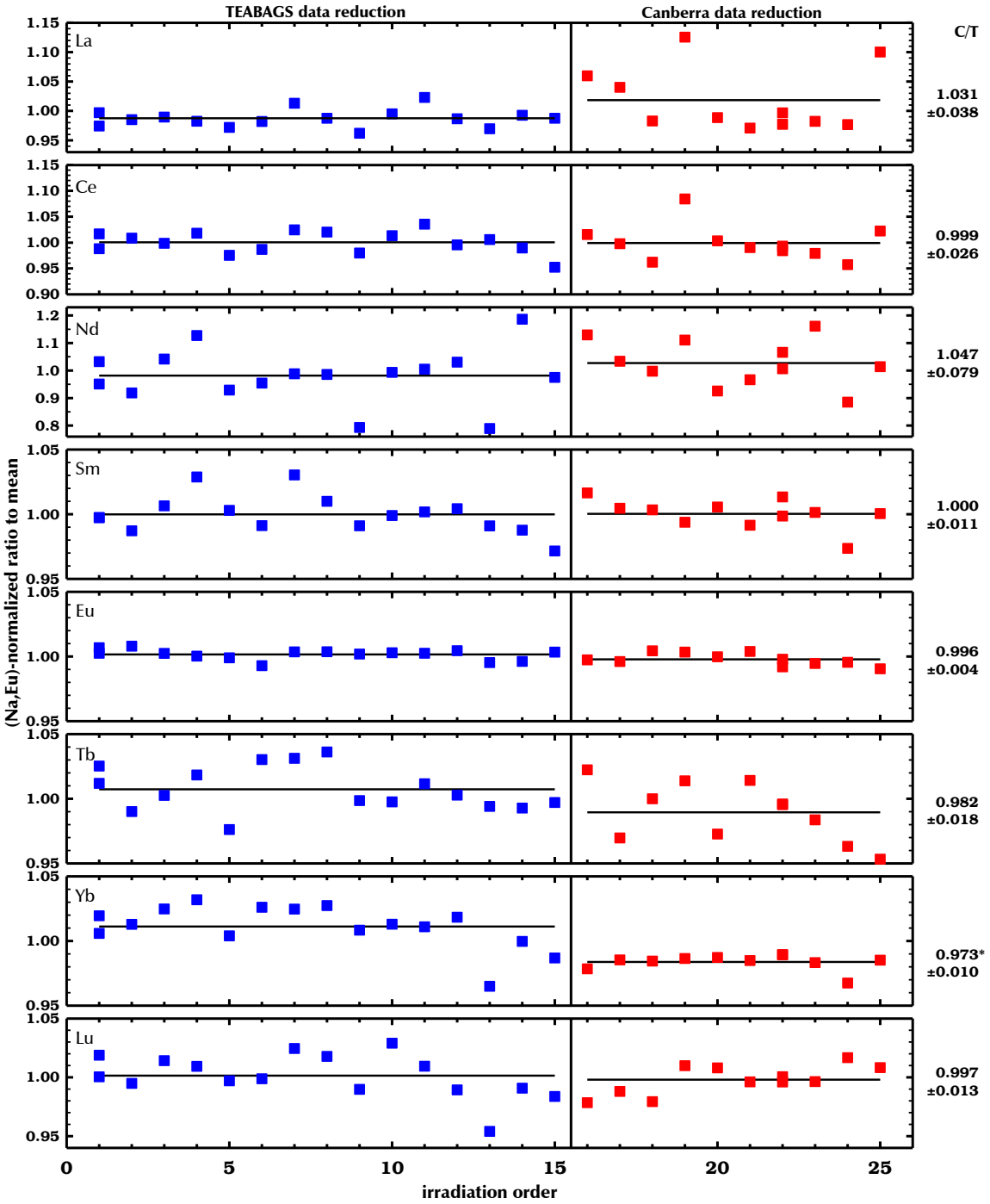

Fig. S83, continued.

Light Rare Earth Element Variability in NWA 5000 Sawdust

In the NWA 5000 sawdust, the relative standard deviations for light REE La (3.8%) and Ce (2.8%) are greater than for middle REE Sm (1.5%) and heavy REE Lu (1.5%) (Table S8; Fig. S84). Both Irving et al. (2008) and Nagurney et al. (2016) report the presence of merrillite, and the difference between the low-La and high-La subsamples corresponds to a ~0.3-ng grain of RE-merrillite, which would have negligible effect on the heavy REE (e.g., merrillite from Apollo 16 sample 65903, Table 3 of Jolliff et al., 2006). Alternatively, the variation in La/Sm may be a terrestrial weathering effect (Fig. S63).

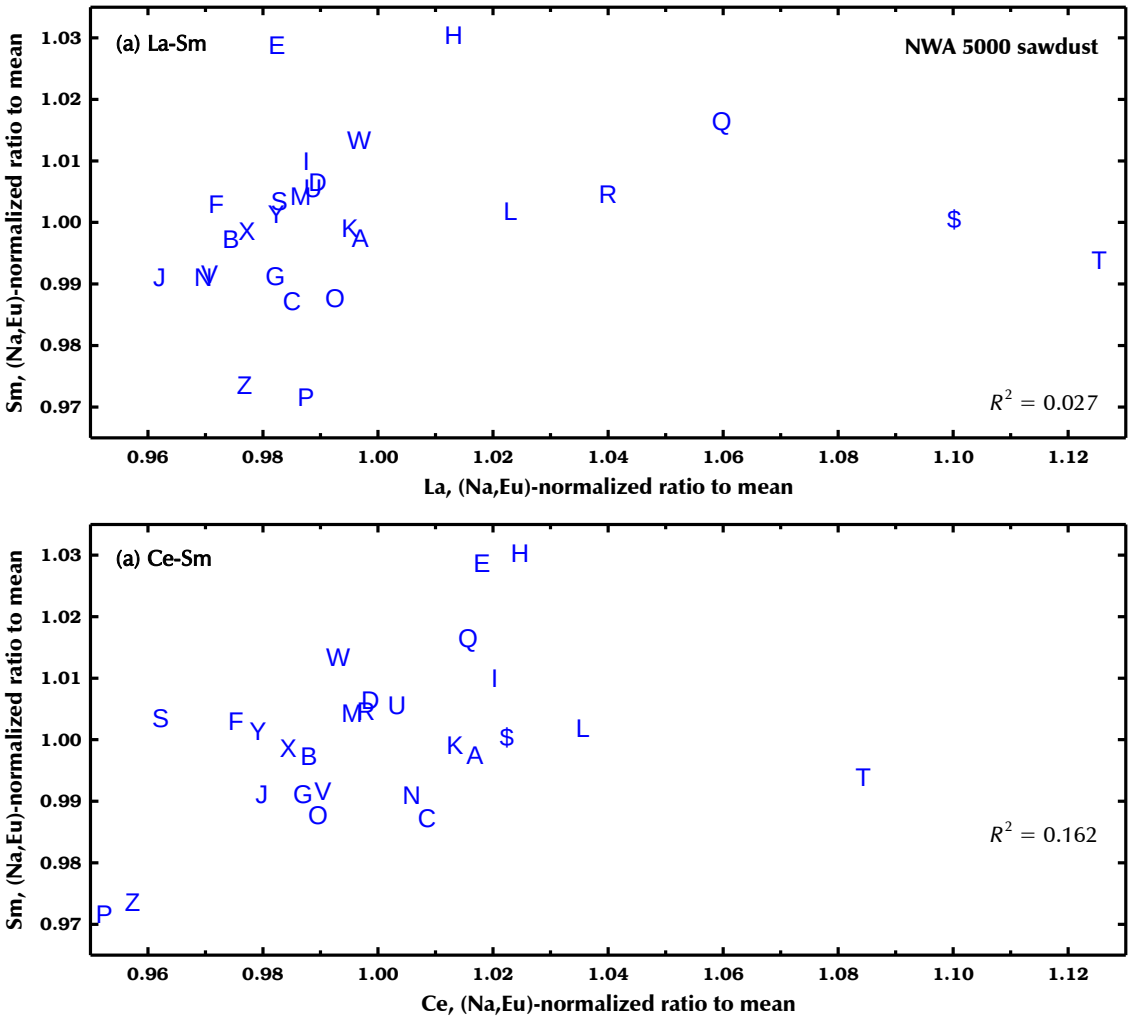

Fig. S84. Light REEs La and Ce scatter over a greater range than does middle REE Sm. The alphabetic point symbols (A–Z, $) represent the chronologic order of the irradiations (Table S8).

References

Anders E. and Grevesse N. 1989. Abundances of the elements: Meteoritic and solar. *Geochimica et Cosmochimica Acta* 53:197–214.

Arai T. and Warren P. H. 1999. Lunar meteorite Queen Alexandra Range 94281: Glass compositions and other evidence for launch pairing with Yamato 793274. *Meteoritics & Planetary Science* 34:209–234.

Arai T. Misawa K. Tomiyama T. Yoshitake M. Irving A. J. 2009. Constraints on lunar KREEP magmatism: A variety of KREEP basalt derivatives in lunar meteorite NWA 4485 (abstract #2292). 40th Lunar and Planetary Science Conference.

Arai T., Hawke B. R., Giguere T. A., Misawa K., Miyamoto M., and Kojima H. 2010. Antarctic lunar meteorites Yamato-793169, Asuka-881757, MIL 05035, and MET 01210 (YAMM): Launch pairing and possible cryptomare origin. *Geochimica et Cosmochimica Acta* 74:2231–2248.

Bischoff A., Weber D., Clayton R. N., Faestermann T., Franchi I. A., Herpers U., Knie K., Korschinek G., Kubik P. W., Mayeda T. K., Merchel S., Michel R., Neumann S., Palme H., Pillinger C. T., Schultz L., Sexton A. S., Spettel B., Verchovsky A. B., Weber H. W., Weckwerth G., and Wolf D. 1998. Petrology, chemistry, and isotopic compositions of the lunar highland regolith breccia Dar al Gani 262. *Meteoritics & Planetary Science* 33:1243–1257.

Boyle S., Gross J., and Prissel T. C. 2018. Understanding the magnesium-suite lithology and lunar highlands terrain through a detailed investigation of lunar meteorites Northwest Africa (NWA) 10291 and 11182 (abstract #2346). 49th Lunar and Planetary Science Conference.

Chou C.-L, Baedecker P. A., and Wasson J. T. 1976. Allende inclusions: volatile-element distribution and evidence for incomplete volatilization of presolar solids. *Geochimica et Cosmochimica Acta* 40:85–94.

Cohen B. A., James O. B., Taylor L. A., Nazarov M. A., and Barsukova L. D. 2004. Lunar highland meteorite Dhofar 026 and Apollo sample 15418: Two strongly shocked, partially melted, granulitic breccias. *Meteoritics & Planetary Science* 39:1419–1447.

Cohen M. E., Kuehner S. M., Tepper J. H., Burney D. C., Neal C. R., Irving A. J., Korotev R. L., and B. Hoefnagels 2019. Mineralogy and bulk composition of lunar mare basalt Northwest Africa 12008 (abstract #2508). 50th Lunar and Planetary Science Conference.

Collareta A., D'Orazio M., Gemelli M., Pack A., Folco L. 2016. High crustal diversity preserved in the lunar meteorite Mount DeWitt 12007 (Victoria Land, Antarctica). *Meteoritics & Planetary Science* 51:351–371.

Crozaz G. and Wadhwa M. (2001) The terrestrial alteration of Saharan Shergottites Dar al Gani 476 and 489: A case study of weathering in a hot desert environment. *Geochimica et Cosmochimica Acta* 65:971–978.

Demidova S. I., Nazarov M. A., Lorenz C. A., Kurat G., Brandstätter F., and Ntaflos Th. 2007. Chemical composition of lunar meteorites and the lunar crust. *Petrology* 15:386–407.

Demidova S. I. Nazarov M. A. Ivanova M. A. Lorenz K. A. Kononkova N. N. 2012. New lunar meteorite from the Sahara Desert: North West Africa 6888 (abstract #1726). 43rd Lunar and Planetary Science Conference.

Dymek R.F., Albee A.L. and Chodos A.A. 1975. Comparative petrology of lunar cumulate rocks of possible primary origin: Dunite 72415, troctolite 76535, norite 78235, and anorthosite 62237. *Proceedings of the 6th Lunar Science Conference*, 301–341.

Fukuoka T. 1990. Chemistry of Yamato-793274 lunar meteorite (abstract). In *Papers Presented to the Fifteenth Symposium on Antarctic Meteorites*, pp. 122–123.

Goldstein J. I., Hewins R. H., and Axon H. J. 1974. Metal silicate relationships in Apollo 17 soils. *Proceedings of the 5th Lunar Science Conference*, 653–671.

Gooley R. C., Brett R., and Warner J. L. 1973. Crystallization history of metal particles in Apollo 16 rake samples. *Proceedings of the 4th Lunar Science Conference*, 799–810.

Gooley R.C., Brett R., Warner J.L. and Smyth J.R. 1974. A lunar rock of deep crustal origin: Sample 76535. *Geochimica et Cosmochimica Acta* 38:1329–1339.

Grossman J. N., editor. Meteoritical Bulletin Database, 1 January 2020, https://www.lpi.usra.edu/meteor/

Haloda J., Týcová P., Jakeš P., Gabzdyl P., and Košler J. 2006. Lunar meteorite Northeast Africa 003-B: A new lunar mare basaltic breccia (abstract #2311). 37th Lunar and Planetary Science Conference. CD-ROM

Haloda J., Týcová P., Korotev R. L., Fernandes V. A., Burgess R., Thöni M., Jelenc M., Jakeš P., Gabzdyl P., and Košler J. 2009. Petrology, geochemistry, and age of low-Ti mare-basalt meteorite Northeast Africa 003-A: A possible member of the Apollo 15 mare basaltic suite. *Geochimica et Cosmochimica Acta* 73:3450–3470.

Haskin L. A., Shih C.-Y., Bansal B. M., Rhodes J. M., Wiesmann H., and Nyquist L. E. 1974. The evidence for the origin of 76535 as a cumulate. *Proceedings of the 5th Lunar Science Conference*, 1213–1225.

Hewins R. H. and Goldstein J. I. 1975. The provenance of metal in anorthositic rocks. *Proceedings of the 6th Lunar Science Conference*, 343–362.

Hewins R. H., Goldstein J. I., and Axon H. J. 1976. The relation of metal composition to rock type for clasts in Apollo 16 soil. *Proceedings of the 7th Lunar Science Conference*, 819–836.

Hidaka Y., Yamaguchi A., and Ebihara M. 2014. Lunar meteorite, Dhofar 1428: Feldspathic breccia containing KREEP and meteoritic components. *Meteoritics & Planetary Science* 49:921–928.

Hill D. H. and Boynton W. V. 2003. Chemistry of the Calcalong Creek lunar meteorite and its relationship to lunar terranes. *Meteoritics & Planetary Science* 38:595–626.

Hollocher K. T. Norm Calculation Program, 1 January 2019, https://minerva.union.edu/hollochk/c_petrology/other_files/norm4.xls

Humayun M. and Irving A. 2008. Impactor metal in gabbroic lunar meteorite Northwest Africa 5000 (abstract). *Geochimica et Cosmochimica Acta* 72:A402.

Irving A. J., Kuehner S. M., Korotev R. L., Rumble D. III, and Hupé A. C. 2008. Petrology and bulk composition of large lunar feldspathic leucogabbroic breccia Northwest Africa 5000 (abstract #2186). 39th Lunar and Planetary Science Conference. CD-ROM

Jolliff B. L., Korotev R. L., and Haskin L. A. 1993. Lunar basaltic meteorites Yamato-793169 and Asuka-881757: Samples of the same low-Ti mare-lava? In *Papers Presented to the Eighteenth Symposium on Antarctic Meteorites*, pp. 214–217.

Jolliff B. L., Rockow K. M., and Korotev R. L. 1998. Geochemistry and petrology of lunar meteorite Queen Alexandra Range 94281, a mixed mare and highland regolith breccia, with special emphasis on very-low-Ti mafic components. *Meteoritics & Planetary Science* 33:581–601.

Jolliff B. L. Hughes J. M., Freeman J. J., and Zeigler R. A. 2006. Crystal chemistry of lunar merrillite and comparison to other meteoritic and planetary suites of whitlockite and merrillite. *American Mineralogist* 91:1583–1595.

Joy K. H., Crawford I.A., Anand M., Greenwood R. C., Franchi, I. A., Russell S. S. 2008. The petrology and geochemistry of Miller Range 05035: A new lunar gabbroic meteorite. *Geochimica et Cosmochimica Acta* 72:3822–3844.

Joy K. H., Crawford I. A., Russell S. S., and Kearsley A. T. 2010. Lunar meteorite regolith breccias: An in situ study of impact melt composition using LA-ICP-MS with implications for the composition of the lunar crust. *Meteoritics & Planetary Science* 45:917–946.

Joy K. H., Burgess R., Hinton R., Fernandes V. A., Crawford I. A., Kearsley A. T., and Irving A. J. 2011. Petrogenesis and chronology of lunar meteorite Northwest Africa 4472: A KREEPy regolith breccia from the Moon. *Geochimica et Cosmochimica Acta* 75:2420–2452.

Lodders K. and Fegley B. Jr. 1998. *The Planetary Scientist's Companion*, Oxford University Press, New York, 371 pp.

Kallemeyn G. W. and Warren P. H. 1983. Compositional implications regarding the lunar origin of the ALHA81005 meteorite. *Geophysical Research Letters* 10:833–836.

Koeberl C., Kurat G., and Brandstätter F. (1991) Lunar meteorites Yamato 793274: Mixture of mare and highland components, and barringerite from the Moon. *Proceedings of the NIPR Symposium on Antarctic Meteorites, No. 4*, pp. 33–55. National Institute of Polar Research, Tokyo.

Koeberl C., Kurat G., and Brandstätter F. 1993. Gabbroic lunar mare meteorites Asuka-881757 (Asuka-31) and Yamato 793169: Geochemical and mineralogical study. *Proceedings of the NIPR Symposium on Antarctic Meteorites, Number 6*, pp. 14–34.

Korotev R. L. 1991. Geochemical stratigraphy of two regolith cores from the central highlands of the Moon. *Proceedings of Lunar and Planetary Science 21*:229–289.

Korotev R. L. 1994. Compositional variation in Apollo 16 impact-melt breccias and inferences for the geology and bombardment history of the Central Highlands of the Moon. *Geochimica et Cosmochimica Acta* 58, 3931–3969.

Korotev R. L. 1996. A self-consistent compilation of elemental concentration data for 93 geochemical reference samples. *Geostandards Newsletter* 20:217–245.

Korotev R. L. 1997. Some things we can infer about the Moon from the composition of the Apollo 16 regolith. *Meteoritics & Planetary Science* 32:447–478.

Korotev R. L. 2000. The great lunar hot spot and the composition and origin of the Apollo mafic ("LKFM") impact-melt breccias. *Journal of Geophysical Research* 105:4317–4345.

Korotev R. L. 2012. Lunar meteorites from Oman. *Meteoritics & Planetary Science* 47:1365–1402.

Korotev R. L. 2017. Update (2012–2017) on lunar meteorites from Oman. *Meteoritics & Planetary Science* 52:1251–1256.

Korotev R. L. and Morris R. V. 1993. Composition and maturity of Apollo 16 regolith core 60013/14. *Geochimica et Cosmochimica Acta* 57:4813–4826.

Korotev R. L. and Zeigler R. A. 2014. ANSMET meteorites from the Moon. In *35 Seasons of U.S. Antarctic Meteorites*, edited by Righter K., Corrigan C. M., McCoy T. J., and Harvey R. Washington, D.C.: American Geophysical Union. pp. 101–130.

Korotev R. L., Morris R. V., Jolliff B. L., and Schwarz C. 1997. Lithological variation with depth and decoupling of maturity parameters in Apollo 16 regolith core 68001/2. *Geochimica et Cosmochimica Acta* 61:2989–3002.

Korotev R. L., Jolliff B. L., Zeigler R. A., Gillis J. J., and Haskin L. A. 2003a. Feldspathic lunar meteorites and their implications for compositional remote sensing of the lunar surface and the composition of the lunar crust. *Geochimica et Cosmochimica Acta* 67:4895–4923.

Korotev R. L., Jolliff B. L., Zeigler R. A., and Haskin L. A. 2003b. Compositional constraints on the launch pairing of three brecciated lunar meteorites of basaltic composition. *Antarctic Meteorite Research* 16:152–175.

Korotev R. L, Zeigler R. A., Jolliff B. L., Irving A. J., and Bunch T. E. 2009. Compositional and lithological diversity among brecciated lunar meteorites of intermediate iron composition. *Meteoritics & Planetary Science* 44:1287–1322.

Korotev R. L., Jolliff B. L., Zeigler R. A., Seddio S. M., and Haskin L. A. 2011. Apollo 12 revisited. *Geochimica et Cosmochimica Acta* 75:1540–1573.

Kuehner S. M., Irving A. J., and Korotev R. L. 2012a. Petrology and composition of lunar mare ferroan gabbro breccia Northwest Africa 7007: New insights into the complex petrogenesis of Northwest Africa 773 and siblings (abstract #1519). 43rd Lunar and Planetary Science Conference.

Kuehner S. M., Irving A. J., and Korotev R. L. 2012b. Petrology and composition of lunar meteorite Northwest Africa 7022: An unusually sodic anorthositic gabbroic impact melt breccia with compositional similarities to Miller Range 090036 (abstract #1524). 43rd Lunar and Planetary Science Conference.

Lindstrom D. J. and Korotev R. L. 1982. TEABAGS: Computer programs for instrumental neutron activation analysis. *Journal of Radioanalytical Chemistry* 70:439–458.

Lindstrom M. M., Mittlefehldt D. W., Martinez R. R., Lipschutz M. J., and Wang M.-S. 1991. Geochemistry of Yamato-82192, -86032 and -793274 lunar meteorites. *Proceedings of the NIPR Symposium on Antarctic Meteorites, Number 4*, pp. 12–32.

Lodders K. and Fegley B. Jr. 1998. *The Planetary Scientist's Companion*. New York: Oxford University Press, 371 p.

Mercer C. N., Treiman A. H., and Joy K. H. 2013. New lunar meteorite Northwest Africa 2996: A window into farside lithologies and petrogenesis. *Meteoritics & Planetary Science* 48:289–315.

Mészáros M., Hofmann B. A., Lanari P., Korotev R. L., Gnos E., Greber N. D., Leya I., Greenwood R. C., Jull A. J. T., Al-Wagdani K., Mahjoub A., Al-Solami A. A., and Habibullah S. N. (2016) Petrology and geochemistry of feldspathic impact-melt breccia Abar al' Uj 012, the first lunar meteorite from Saudi Arabia. *Meteoritics & Planetary Science* 51:1830–1848.

MetBull: Grossman J. N., editor. Meteoritical Bulletin Database, 20 July 2019, https://www.lpi.usra.edu/meteor/

Moggi-Cecchi V., Caporali S., Pratesi G., and Franchi I. A., and Greenwood R.C. 2012. NWA 6687: A new lunar meteorite from northwest Africa (abstract #2710). *42nd Lunar and Planetary Science Conference*.

Nagurney A. B., Treiman A. H., and Spudis P. D. 2016. Petrology, bulk composition, and provenance of meteorite Northwest Africa 5000 (abstract #1103). 46th Lunar and Planetary Science Conference.

Neal C. R. and Kramer G. Y. 2006. The petrogenesis of the Apollo 14 high-Al mare basalts. *American Mineralogist* 91:1521–1535.

Neal C. R. and L. A. Taylor 1992. Petrogenesis of mare basalts: A record of lunar volcanism. *Geochimica et Cosmochimica Acta* 56:2177–2211.

North-Valencia S. N., Jolliff B. L., and Korotev R. L. 2014. Ferroan gabbro and leucogabbro lithologies in NWA 3170, possible petrogenetic link and comparison to NWA 2727 (abstract #2858). 45th Lunar and Planetary Science Conference.

Nishiizumi K., Arnold J. R., Klein J., Fink D., Middleton R., Kubik P. W., Sharma P., Elmore D., and Reedy R. C. (1991) Exposure histories of lunar meteorites: ALHA81005, MAC81004, MAC81005, and Y791197. *Geochimica et Cosmochimica Acta* 55:3149–3155.

Nishiizumi, K., and Caffee M. W. 2013. Relationships among six lunar meteorites from Miller Range, Antarctica based on cosmogenic radionuclides (abstract #2715). 44th Lunar and Planetary Science Conference.

Palme H., Spettel B., Weckwerth G., and Wänke H. 1983. Antarctic meteorite ALHA 81005, a piece from the ancient lunar crust. *Geophysical Research Letters* 10:817–820.

Roberts S. E., McCanta M. C., Jean M. M., and Taylor L. A. 2019). New lunar meteorite NWA 10986: A mingled impact melt breccia from the highlands—A complete cross section of the lunar crust. *Meteoritics & Planetary Science* 54:3018–3035.

Robinson K. L., Smith C. L., Kearsley A. T., Bevan A. W. R., and Anand M. 2016. The Lynch 002 lunar meteorite revisited (abstract #1470). 46th Lunar and Planetary Science Conference.

Sipiera P. P., Irving A. J., Kuehner S. M., Korotev R. L., and Debienne A. 2014. Petrology and composition of unpaired 5.9 gram lunar feldspathic regolithic breccia meteorite Northwest Africa 7931 (abstract #5198). 77th Annual Meeting of the Meteoritical Society.

Smith C. L., Kearsley A. T., Bermingham K. R., Deacon G. L., Kurahashi E., Franchi I. A., and Bevan A. W. R. (2012) Lynch 002: A new lunar meteorite from the Nullarbor Desert, Western Australia (abstract #5137). 75th Annual Meeting of the Meteoritical Society.

Sokol A. K., Fernandes V. A., Schulz T., Bischoff A., Burgess R., R Clayton. N., Münker C., Nishiizumi K., H Palme., Schultz L., G Weckwerth., Mezger K., and Horstmannaan M. 2008. Geochemistry, petrology and ages of the lunar meteorites Kalahari 008 and 009: New constraints on early lunar evolution. *Geochimica et Cosmochimica Acta* 72:4845–4873.

Stephant A., Anand M., Ashcroft H. O., Zhao X., Hu S., Korotev R. L., Strekopytov S., Greenwood R.C., Humphreys-Williams E., Liu Y., Tang G., Li Q., and Franchi I. A. 2019. An ancient reservoir of volatiles in the Moon sampled by lunar meteorite Northwest Africa 10989. *Geochimica et Cosmochimica Acta* 266:163–183.

Taylor L. A., Nazarov M. A., Cohen B. A., Warren P. H., Barsukova L. D., Clayton R. N., and Mayeda T. K. 2001. Bulk chemistry and oxygen isotopic compositions of lunar meteorites Dhofar 025 and Dhofar 026: A second-generation impact melt (abstract #1985). 32nd Lunar and Planetary Science Conference. CD-ROM.

Valencia S. N., Jolliff B. L., and Korotev R. L. 2019. Petrography, relationships, and petrogenesis of the gabbroic lithologies in Northwest Africa 773 clan members Northwest Africa 773, 2727, 3160, 3170, 7007, and 10656. *Meteoritics & Planetary Science* 54:2083–2115.

Wark D. A. 1987. Plagioclase-rich inclusions in carbonaceous chondrite meteorites: Liquid condensates? *Geochimica et Cosmochimica Acta* 51:221–242.

Warren P. H. and Kallemeyn G. W. 1991a. The MacAlpine Hills lunar meteorite and implications of the lunar meteorites collectively for the composition and origin of the Moon. *Geochimica et Cosmochimica Acta* 55:3123–3138.

Warren P. H. and Kallemeyn G. W. 1991b. Geochemical investigations of five lunar meteorites: Implications for the composition, origin and evolution of the lunar crust. *Proceedings of the NIPR Symposium on Antarctic Meteorites, Number 4*: pp. 91–117.

Warren P. H and Kallemeyn G. W. 1993. Geochemical investigations of two lunar mare meteorites: Yamato-793169 and Asuka-881757. *Proceedings of the NIPR Symposium on Antarctic Meteorites, Number 6*, pp. 35–57. National Institute of Polar Research, Tokyo.

Warren P. H. and Wasson J. T. 1977. Pristine nonmare rocks and the nature of the lunar crust. *Proceedings of the 8th Lunar Planetary Science Conference*, 2215–2235.

Warren P. H., Ulff-Møller F., and Kallemeyn G. W. 2005. "New" lunar meteorites: Implications for composition of the global lunar surface, lunar crust, and the bulk Moon. *Meteoritics and Planetary Science* 40:477–506.

Wasson J. T. 2019. Campo del Cielo: A Campo by any other name. *Meteoritics & Planetary Science* 54:280–289.

Wasson J. T. and Kallemeyn G. W. 2002. The IAB iron-meteorite complex: A group, five subgroups, numerous grouplets, closely related, mainly formed by crystal segregation in rapidly cooled melts, *Geochimica et Cosmochimica Acta* 66:2445–2473.

Wasson J. T. and Wang J. 1986. A nonmagmatic origin of group-IIE iron meteorites. *Geochimica et Cosmochimica Acta* 50:725–732.

Wasson J. T., Boynton W. V., Chou C.-L. and Baedecker P. A. 1975. Compositional evidence regarding the influx of interplanetary materials onto the lunar surface. *The Moon* 13:121–141.

Wasson J. T., Ouyang X., Wang J., and Jerde E. 1989. Chemical classification of iron meteorites: XI. Multi-element studies of 38 new irons and the high abundance of ungrouped irons from Antarctica. *Geochimica et Cosmochimica Acta* 53:735–744.

Wasson J. T., Huber H., and Malvin D. J. 2007. Formation of IIAB iron meteorites. *Geochimica et Cosmochimica Acta* 71:760–781.

Welch, B. L. 1947. The generalization of "Student's" problem when several different population variances are involved." *Biometrika*:34, 28–35.

Wittmann A., Korotev R. L., Jolliff B. L, Nishiizumi K., Jull A. J. T., Caffee M. W., Zanetti M., and Irving A. J. 2019. Petrogenesis of lunar impact melt rock meteorite Oued Awlitis 001. *Meteoritics & Planetary Science* 54:2167–2188.

Yanai K. and Kojima H. 1991. Varieties of lunar meteorites recovered from Antarctica. *Proceedings of the NIPR Symposium on Antarctic Meteorites, Number 4*. p. 70–90.

Zeigler R. A., Korotev R. L., Jolliff B. L., and Haskin L. A. 2005. Petrology and geochemistry of the LaPaz icefield basaltic lunar meteorite and source-crater pairing with Northwest Africa 032. *Meteoritics & Planetary Science* 40:1073–1102.

Zeigler R. A., Korotev R. L., Haskin L. A., Jolliff B. L., and Gillis J. J. 2006. Petrology and geochemistry of five new Apollo 16 mare basalts and evidence for post-basin deposition of basaltic material at the site. *Meteoritics & Planetary Science* 41:263–284.

Zeng X., Joy K. H., Li S., Pernet-Fisher J., Li X., Martin D. J. P., Li Y., and Wang S. (2018) Multiple lithic clasts in lunar breccia Northwest Africa 7948 and implication for the lithologic components of lunar crust. *Meteoritics and Planetary Science* 53:1030–1050.

Zipfel J., Spettel B., Palme H., Wolf D., Franchi I., Sexton A. S., Pillinger C. T., and Bischoff A. 1998. Dar al Gani 400: Chemistry and petrology of the largest lunar meteorite (abstract). *Meteoritics & Planetary Science* 33:A171.

Figure order

1 @Hist
2 @FeTh
3 @ScPyx
4 @ScCrMgFe
5 @MgFeNorm
6 @ScSm
7 @trends
8 @PyPlagOl
9 @A16FeSm
10 @AlMgFe
11 @CrScSmNa
12 @ScIr
13 @MB
14 @NiCo
15 @IrNiCM
16 @BaSr
17 @REE_Ce
18 @CaAlTi
19 @LynchREE